ZooKeys 846: 1–18 (2019)
doi: 10.3897/zookeys.846.31497
http://zookeys.pensoft.net

RESEARCH ARTICLE

A peer-reviewed open-access journal
ZooKeys
Launched to accelerate biodiversity research

A new species of *Bestiolina* (Crustacea, Copepoda, Calanoida, Paracalanidae) from coastal waters of the Colombian Pacific, including a worldwide key for the identification of the species

John Dorado-Roncancio[1], Santiago Gaviria[2], Luis Bernal-De La Torre[3], Michael J. Ahrens[1]

1 *Universidad de Bogota Jorge Tadeo Lozano, Facultad de Ciencias Naturales e Ingeniería, Programa de Ciencias Biológicas y Ambientales, Laboratorio de Limnología, Cra 4 No 22-61, Módulo 5, Piso 8, Bogotá, Colombia* **2** *University of Vienna, Dept of Limnology and Bio-Oceanography and Technisches Büro für Biologie, Fred-Raymond-Gasse 19/2/4, A-1220, Vienna, Austria* **3** *Pontificia Universidad Javeriana, Facultad de estudios ambientales y rurales. Transversal 4° No 42-00, Bogotá, Colombia*

Corresponding author: *John Dorado-Roncancio* (johnh.dorador@utadeo.edu.co)

Academic editor: *D. Defaye* | Received 9 November 2018 | Accepted 6 February 2019 | Published 16 May 2019

http://zoobank.org/E665C532-92E3-4482-B8AD-436953D4133F

Citation: Dorado-Roncancio J, Gaviria S, Bernal-De La Torre L, Ahrens MJ (2019) A new species of *Bestiolina* (Crustacea, Copepoda, Calanoida, Paracalanidae) from coastal waters of the Colombian Pacific, including a worldwide key for the identification of the species. ZooKeys 846: 1–18. https://doi.org/10.3897/zookeys.846.31497

Abstract

Plankton samples obtained from estuarine waters of the Colombian Pacific yielded adults specimens of an undescribed species of a paracalanid copepod of the genus *Bestiolina*. It most closely resembles two Asian species; *B. sinica* (Shen & Lee, 1966) from China and *B. arabica* (Ali, Al-Yamani & Prusova, 2007) from the Arabian Gulf. These three species share the absence of spinules on the posterior surfaces of exopod segments of legs 2, 3 and 4. *Bestiolina sarae* Dorado-Roncancio & Gaviria, **sp. n.** can be easily separated from *B. sinica* by the number of spinules on the anterior surface of endopod 2 of legs 2 and 3, and by the absence of spinules on the posterior surface of second endopod of leg 4. It can be distinguished from *B. arabica* by the presence of spinules on the posterior surface of endopod 2 of same legs (absent in *B. arabica*), and the size of spinules on the anterior surface of the same segments. The only other species known from

Copyright *J. Dorado-Roncancio et al.* This is an open access article distributed under the terms of the Creative Commons Attribution License (CC BY 4.0), which permits unrestricted use, distribution, and reproduction in any medium, provided the original author and source are credited.

the Americas, *B. mexicana* (Suárez-Morales & Almeyda-Artigas, 2016), can be distinguished from *Bestiolina sarae* Dorado-Roncancio & Gaviria, **sp. n.** by the presence of spinules on the posterior surface of the leg 2 first exopodal segment and the morphology of the mandible blade. The morphological and meristic differences to the eight known species of the genus are presented. An identification key to the species of *Bestiolina* is provided.

Keywords
Coastal zone, crustaceans, estuaries, taxonomy, tropical zooplankton

Introduction

The family Paracalanidae is represented by seven genera (Razouls et al. 2018; Walter and Boxshall 2018) and are among the common estuarine and coastal planktonic copepods of tropical and subtropical latitudes (Suárez-Morales and Almeyda-Artigas 2016). The paracalanid genus *Bestiolina* (Andronov 1991) currently includes eight species and was originally named *Bestiola* (Andronov 1972). It was subsequently renamed because *Bestiola* was preoccupied by an insect generic name (Nikolskaya 1963). It can be considered as a relatively recently described genus in relation to the first descriptions of marine planktonic copepod species done at the middle of the 19th century (i.e., Dana 1852; Claus 1863; Boeck 1865; Brady 1899). Most species of *Bestiolina* were described in the last 20 years (Mulyadi 2004; Ali et al. 2007; Moon et al. 2010; Suárez-Morales and Almeyda-Artigas 2016). The poor knowledge of the diversity and distributional patterns of the genus could be explained by their small size (670–1008 μm), inappropriate sampling techniques (nets with mesh size > 200 μm) and confusion with copepodite stages of other paracalanid species. The lack of information about *Bestiolina* in the tropical eastern Pacific could also be explained by the few faunal surveys done in coastal waters of the region.

Bestiolina can be characterized as a coastal-neritic copepod genus that lives in shallow waters near the coastal areas (Bradford-Grieve 1994; Boxshall and Hasley 2004). Species of *Bestiolina* are concentrated in tropical latitudes of different oceans, and its origin has been speculated to be Indo-Malayan (Ali et al. 2007). Except for the record of *Bestiolina mexicana* in the Gulf of Mexico (Suárez-Morales and Almeyda-Artigas 2016), no other species of *Bestiolina* have been hitherto recorded in coastal waters of the Americas.

During the development of a project to evaluate marine bioinvasions in the Colombian Pacific and their relation with marine traffic, zooplankton samples were collected in three different coastal areas. Specimens of *Bestiolina* present in several samples could not be assigned to any known species of the genus and was thus deemed as new. Based on several adult female and male specimens available, the species is described and illustrated herein.

Methods

Zooplankton samples were collected only once in six localities from three major port areas of the Colombian Pacific coast (Fig. 1) between September/October 2016 and May/June 2017 as follows:

1) Bahia Solano, Departamento del Chocó (6°14'N, 77°24'W)
2) Huina, Departamento del Chocó (6°16'N, 77°27'W)
3) Buenaventura, Departamento del Valle del Cauca (3°53'N, 77°03'W)
4) Bahia de Málaga-Juanchaco, Departamento del Valle del Cauca (3°55'N, 77°20'W)
5) Tumaco Port, Departamento de Nariño (1°48'N, 78°45'W)
6) Tumaco City, Departamento de Nariño (1°49'N, 78°45'W)

Samples were obtained via surface trawls using a standard zooplankton net with 150 µm mesh size hauled for 2 minutes from a boat travelling at approximately 2 knots. Zooplankton was narcotized with $MgCl_2$ (Suther and Rissik 2009) prior to fixation and preservation in ethanol 80% at a 1:3 ratio.

Dissection techniques followed Björnberg (1981). Specimens were dissected in glycerine using sharpened tungsten needles. Specimens were then mounted in Entellan (J. Dorado) and lactophenol (S. Gaviria) and sealed with varnish. Animals were studied using a Zeiss Ax10 Scope A1 (J. Dorado) and a Nikon Ellypse 200 (S. Gaviria). Drawings were performed based on images obtained with a Zeiss Ax10 Scope equipped with a digital camera.

Type specimens were deposited at the Museo de Historia Natural Marina de Colombia, Santa Marta, Colombia (MAKURIWA) of the Instituto de Investigaciones Marinas y Costeras INVEMAR, and at the Naturhistorisches Museum Wien (NHMW) in Vienna, Austria.

The descriptive terminology follows Huys and Boxshall (1991) and Ferrari and Ivanenko (2008).

Environmental parameters were measured *in situ* with a multiparametric probe (Hach-HQ40d) and water transparency was determined with a Secchi disk. At each site, 200 ml water was filtered through glass fibre filters (Whatman GFC) for chlorophyll-*a* analysis (*ex situ* using spectrophotometry). Water temperature, salinity, dissolved oxygen, Secchi depth and chlorophyll-*a* data, together with standard deviation (SD) were as follows: surface water temperature $\bar{x}$ = 28.7 °C (SD 1.0 °C, *n* = 18) in 2016 and $\bar{x}$ = 28.8 °C (SD 1.1 °C, *n* = 14) in 2017; salinity $\bar{x}$ = 23.0 (SD 6.1, *n* = 18) in 2016 and $\bar{x}$ = 23.9 (SD 1.1, *n* = 14) in 2017; dissolved oxygen $\bar{x}$ = 6.4 mg/L (SD 0.6 mg/L, *n* = 18) in 2016 and $\bar{x}$ = 6.7 mg/L (SD 0.5 mg/L, *n* = 14) in 2017. Secchi depth was $\bar{x}$ = 3.6 m (SD 3.5 m, *n* = 18) in 2016 and $\bar{x}$ = 4.8 m (SD 3.9 m, *n* = 14) in 2017. Chlorophyll-*a* concentration was $\bar{x}$ = 3.0 µg/L (SD 4.3 µg/L, *n* = 17) in 2016 and $\bar{x}$= 2.8 µg/L (SD 4.1 µg/L, *n* = 19) in 2017.

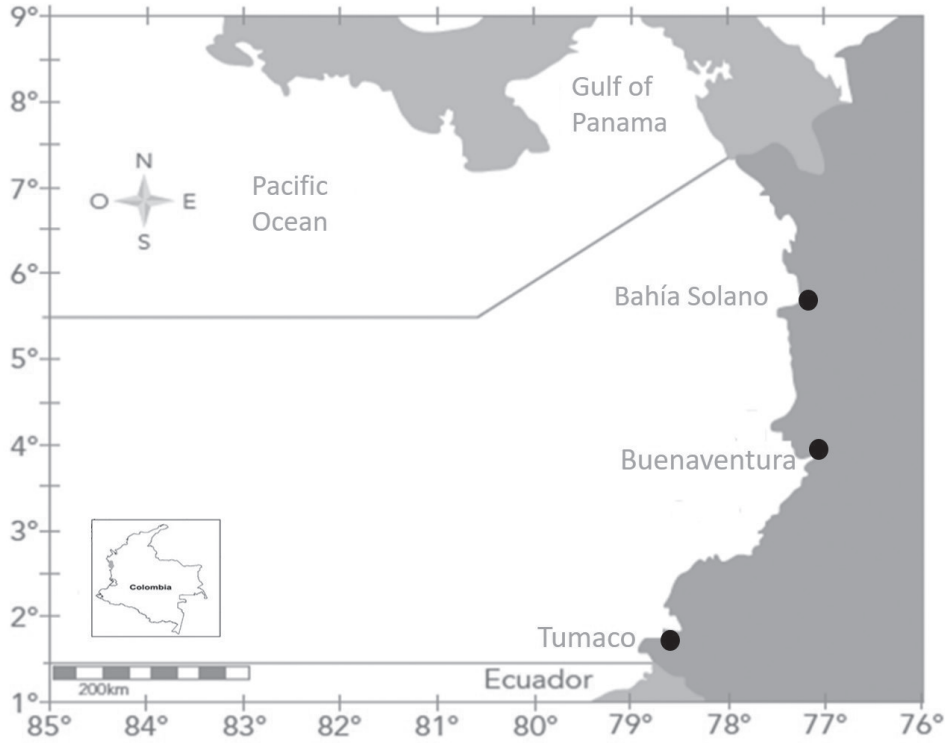

Figure 1. Sampling locations (modified from Dorado Roncancio 2018).

Results

Taxonomy

Class Hexanauplia Oakley, Wolfe, Lindgren & Zaharof, 2013
Subclass Copepoda Milne Edwards, 1840
Order Calanoida G.O. Sars, 1903
Family Paracalanidae Giesbrecht, 1893
Genus *Bestiolina* Andronov, 1991

***Bestiolina sarae* Dorado-Roncancio & Gaviria, sp. n.**
http://zoobank.org/E0A2340A-31B3-42B2-BB70-418C4DFBA9A4

Material examined. Holotype: Adult female (MAKURIWA INV-CRU8991) dissected on a slide, mounted in Entellan. Allotype: male dissected on a slide (MAKURIWA INV-CRU8992), mounted in Entellan. Paratypes: two females (NHMW 26309 and 26310), each one dissected on three slides and mounted in lactophenol, one female (NHMW 26311) dissected and mounted in one slide; six females (NHMW 26312) undissected and preserved in ethanol; one female and two males undissected, preserved

in ethanol+glycerine (MAKURIWA INV-CRU8993 y 8994). Material was collected by L. Bernal, M. Ahrens and J. Dorado-Roncancio, as follows: holotype and allotype on 30/09/2016 near Buenaventura harbor (03°53'49.054"N, 077°03'44.3"W), paratypes on 26/07/2017 in the Bahía Málaga (03°55'30.759"N, 077°20'56.48"W).

Etymology. The new species is named in honour of Sara Dorado, an important member of the family of the first author, who passed away one year before the discovery of the species. The name of the species is a feminine noun in genitive singular.

Type locality. Near Buenaventura harbor (03°53'49.054"N; 077°03'44.3"W) (Fig. 1), Eastern Pacific Ocean, Colombia. At the type locality, the waters are characterized as coastal and estuarine. The type locality belongs to the Buenaventura natural ecoregion of the Colombian Pacific according to the classification of Diaz and Acero (2003). The area is characterized by bays, with an average depth between 12 m and 15 m, and tectonic estuaries, which include a wide variety of habitats such as sandy and rocky beaches, mudflats, large areas of high-productivity mangroves, sandstone cliffs and soft-sediment floodplains. Many rivers and streams empty into the sea, bringing high amounts of sediments and causing variations in the physical and chemical conditions of the waters (Lazarus-Agudelo et al. 2007, Betancourt and Portela et al. 2011). Precipitation in the region is very high (> 5000 mm/y) (Dimar 2002). Water chemistry can be characterized as follows: surface temperature ranges between 26.6 °C and 29.7 °C; salinity between 1.3 and 30 psu; relative humidity close to 90%. Precipitation for the area ranges between 5000–7000 mm per year, semidiurnal tides with an average range of 4.1 m (Cantera and Blanco 2001).

Differential diagnosis. *Bestiolina* of small size (female 0.64–0.73 mm, male 0.63–0.75 mm), with body divided in prosome and slender urosome. Cephalic dorsal hump present in male. Rostrum short and stout divided in acute points. First pedigerous somite fused with cephalothorax, fifth pedigerous somite separated from preceding somite. Posterolateral margins of fifth pedigerous somite rounded and ornamented with small spinules. Genital double-somite with ventral protuberance in adult females. Exopods of legs 2–4 with anterior and posterior surfaces of all segments without spinules. Endopod 2 of legs 2 and 3 with anterior surface mostly with 3 small spinules and posterior surface mostly with 4 large spinules. Leg 5 of female rudimentary, unsegmented, consisting of a pair of rounded lobes, lobes with smooth margin. Leg 5 of male asymmetrical, right leg as in female, left leg long, 5-segmented, last segment with long distal spine.

Description of holotype female. (Fig. 2A) Length of specimen measured from tip of rostrum to posterior margin of caudal rami: 0.70 mm. Body robust, widest section at second somite, anterior part of cephalosome rounded. Rostrum short and stout, divided into acute points (Fig. 2B). First pedigerous somite completely fused with cephalosome. Second, thirth and fourth pedigerous somites free. Fifth pedigerous somite completely separated from fourth, with posterolateral margins rounded and bearing small spinules (Fig. 2C).

Urosome, 4-segmented. First and second urosomites fused forming a ventrally expanded genital-double somite. Anal somite slightly longer than second and third urosomites together (Fig. 2D). Caudal rami not divergent, shorter than anal somite, armed with 5 setae. Dorsal setae (VII) strongly reduced, setae I and II lacking (Huys and Boxshall 1991). Without setae on the inner and outer sides of rami (Fig. 2E).

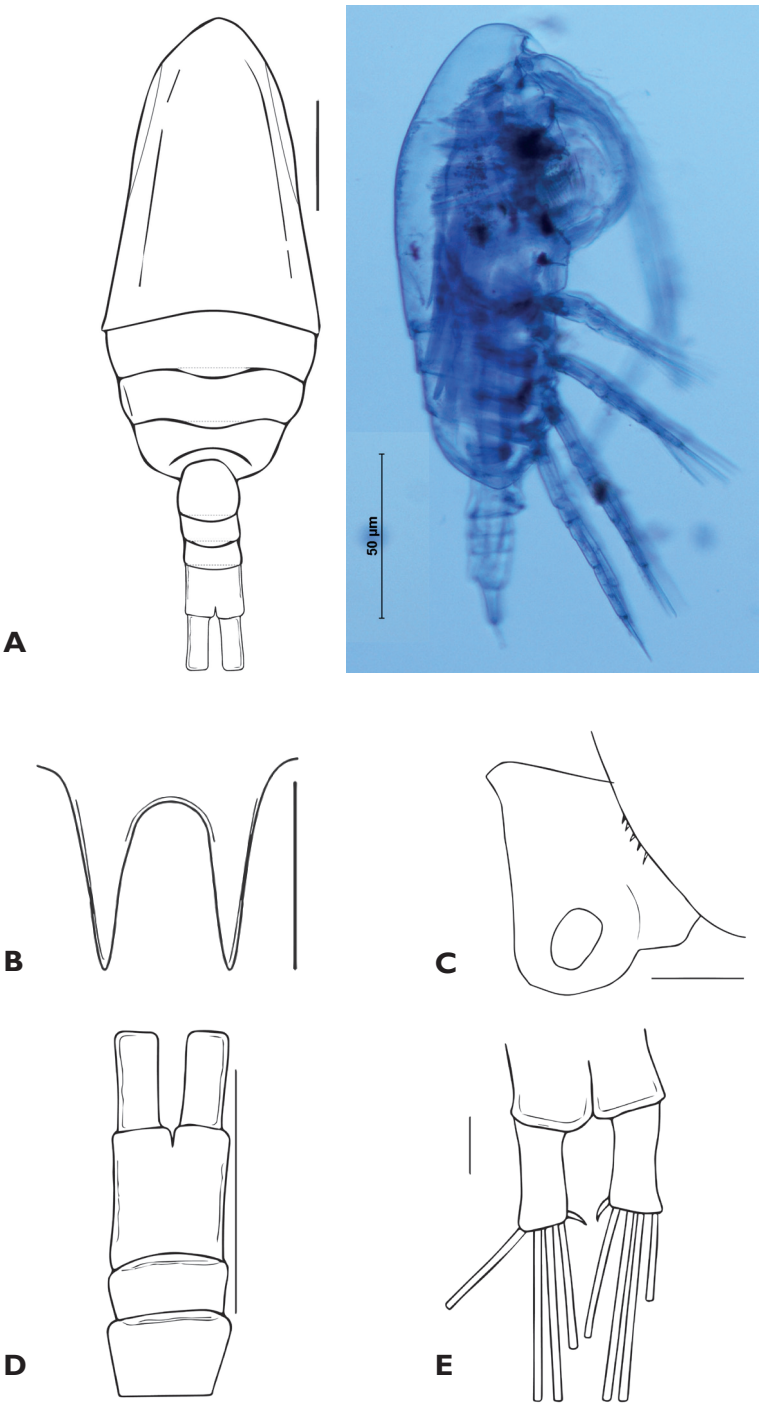

Figure 2. Female Holotype of *Bestiolina sarae* sp. n. **A** habitus, dorsal view and digital photograph **B** rostrum **C** posterolateral margins of fifth pedigerous somite, lateral view **D** second and third urosomites and anal somite with caudal rami **E** caudal rami and setae. Scales bar: 0.1 mm (**A**, **D**); 0.01 mm (**B**, **E**); 0.05 mm (**C**).

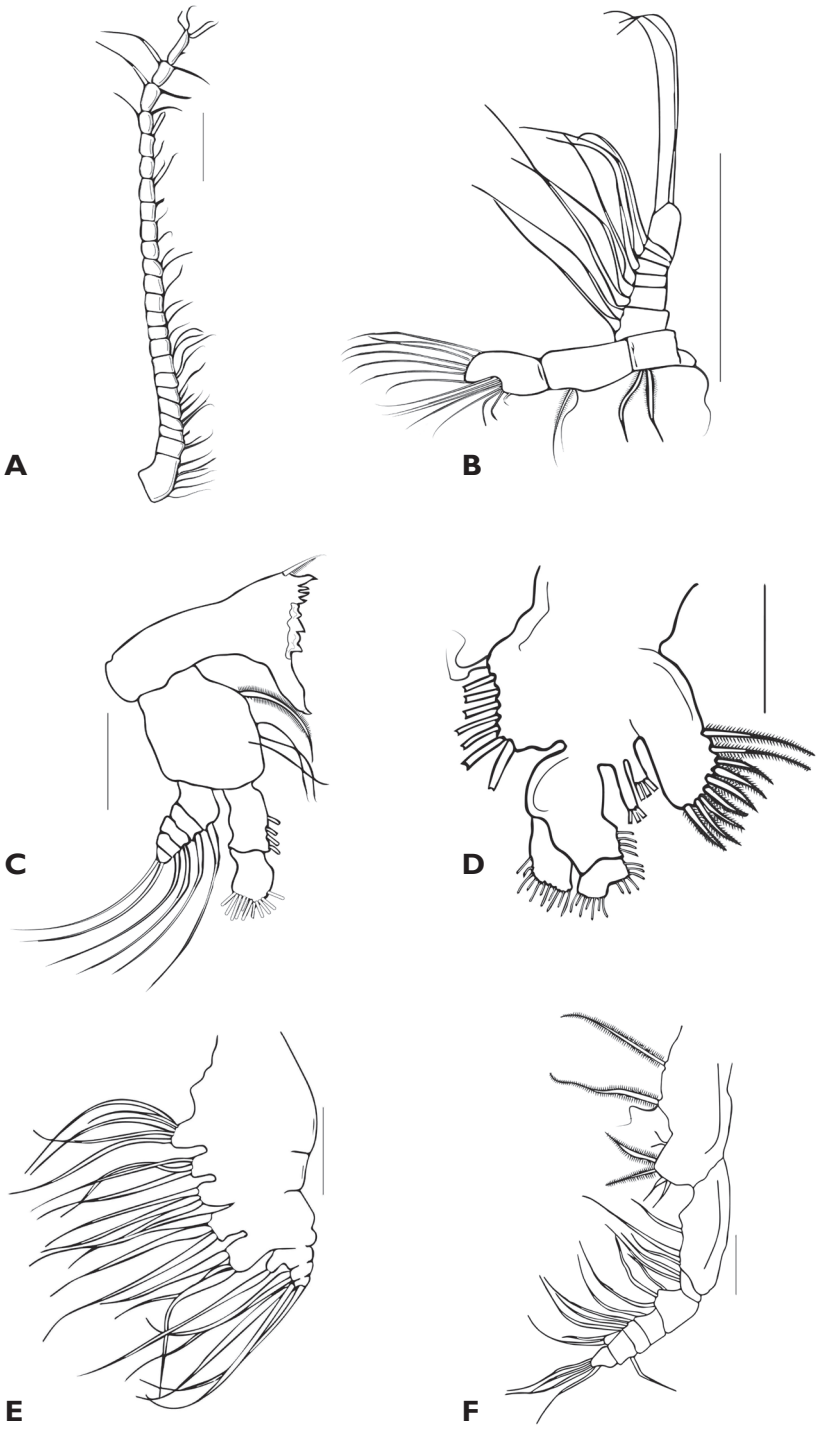

Figure 3. Female Holotype of *Bestiolina sarae* sp. n. **A** antennule **B** antenna **C** mandible **D** maxillule **E** maxilla **F** maxilliped. Scales bars: 0.1 mm (**A**); 0.05 mm (**B–F**).

Antennule 24-segmented (Fig. 3A). Ancestral segments (Huys and Boxshall 1991) I – IV and XXVII–XXVIII fused. Armature formula with current segments designated with Arabic numerals (s = seta, sp = spine, ae = aesthetask): 1:6s, 2:2s, 3:1s, 4:2s, 5:1s, 6–8:2s, 9–12:1s, 13:0s, 14:2s, 15:1s, 16:1s, 17:1ae, 18:2s, 19:1s, 20:1ae, 21 to 23:2s, 24:4s+1sp.

Antenna (Fig. 3B) biramous. Coxa small, partially fused with basis, with 1 seta. Basis with 2 long distal seate. Endopod 2-segmented, first segment with 2 subdistal setae, second segment bilobated, subterminal lobe with 8 setae, terminal lobe with 7 setae. Exopod 7-segmented, first and second segments fused, each with 2 setae, segments 3–6 each with 1 seta, terminal segment with 3 setae.

Mandible (Fig. 3C) with thick gnathobase armed with 3 medial teeth, 4 dorsal teeth, 1 large anterior tooth separated from main cuting edge by a diastemma, and a short dorsal seta. Palp basis with 4 subequal setae; endopod 2-segmented, first segment with 4 distal setae, second segment with 11 subequal setae; exopod short, 5-segmented, each segment with 1 seta except distal segment with 2.

The maxillule, maxilla and maxilliped are described according to Ferrari and Ivanenko (2008).

Maxillule (Fig. 3D) with precoxal endite bearing 9 thick spiniform setae. Coxa with 2 endites, each endite with 3 setae, exite with 9 setae. Basis with 4 setae on inner margin; distal endite bilobated with 6 setae on short lobe and 7 setae on long lobe. Exopod with 11 setae.

Maxilla (Fig. 3E), precoxal endite of syncoxa armed with 5 setae. Three coxal endites each with 3 setae. Basis with 3 setae. Endopod 3-segmented, first segment with endite bearing 1 seta, second segment with 2 setae, third segment with 3 setae.

Maxilliped (Fig. 3F) long. Coxa armed with 4 groups of elements: proximal endite of praecoxa reduced to 1 thick seta, middle endite of praecoxa represented by 1 thick and 1 thin seta, distal endite of praecoxa consists of 2 thin setae, endite of coxa represented by 4 subequal setae. Distal endite of basis with 3 setae. Endopod 6-segmented, setal formula of first 4 segments 2, 3, 1, 3, fifth segment bilobated with 1 and 2 setae on each lobe (each side), distal segment with 4 setae.

Leg 1 (Fig. 4A): coxa with row of short setae on inner margin, and 2 setae on outer margin. Basis with 1 seta on inner margin. Exopod 3-segmented; first segment with 1 spine distally on outer margin, inner margin with 1 seta; second segment, outer margin naked, inner margin with 1 seta; third segment outer margin with 2 setae, distal margin with 1 seta, inner margin with 4 setae. Endopod 2-segmented; first segment, inner margin with 1 seta; second segment, outer margin with 1 seta, distal margin and inner margins each with 2 setae. Anterior and posterior surfaces of all segments without spinules.

Legs 2 to 4 (Fig. 4B–D): coxa with 1 seta on inner margin. Basis without marginal seta. Legs with 3-segmented exopod and endopod. Exopod, first and second segments, outer margin with 1 short and thick distal spine, first segment inner margin with 1 seta (leg 2) or without seta (leg 3 and 4); third segment, outer margin with 3 short and thick spines, 1 inserted medially, 2 inserted subapically, distal margin with 1 long spine, inner margin with 5 setae. Long spine of distal margin thicker on leg 3 and 4.

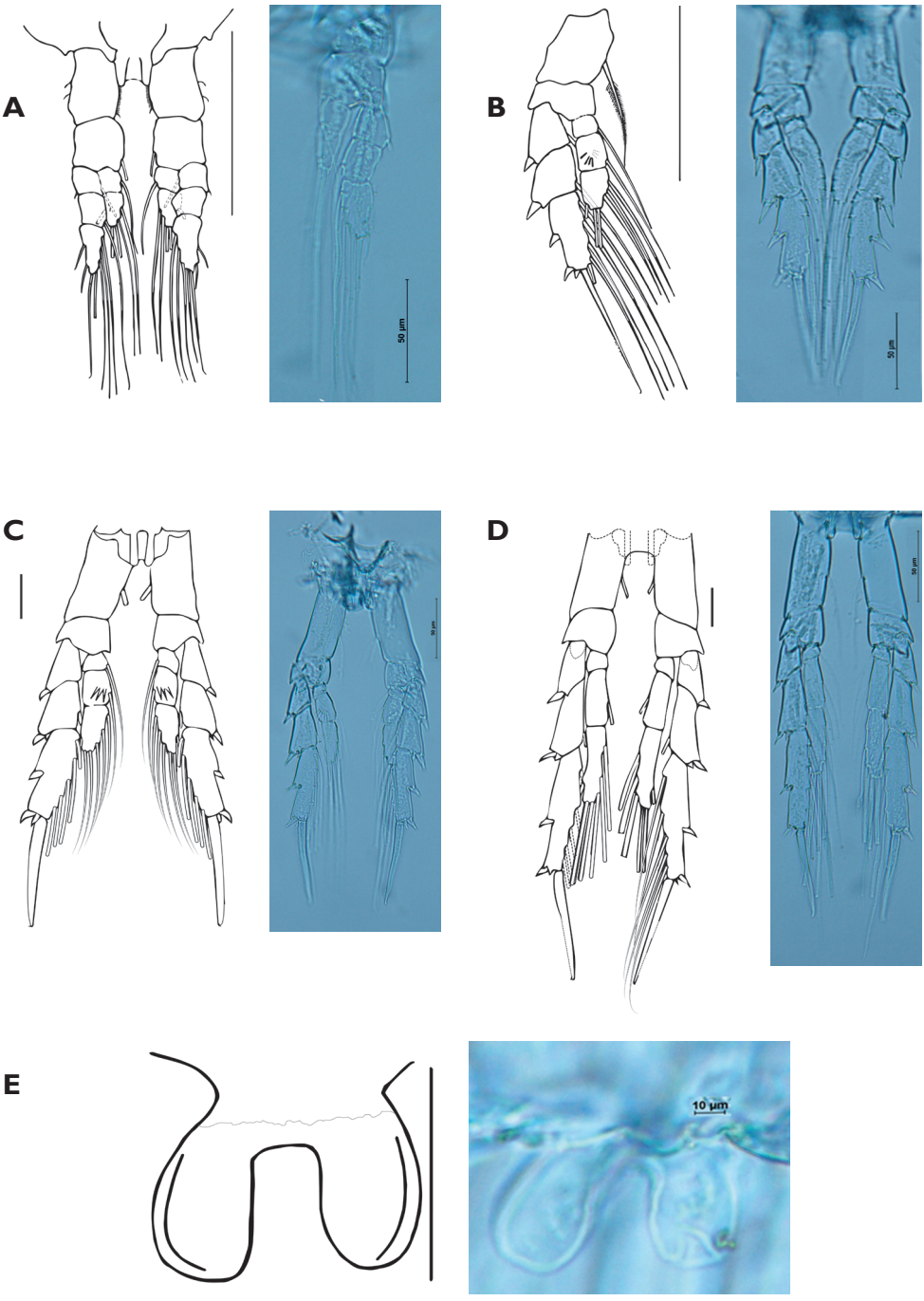

Figure 4. Female of *Bestiolina sarae* sp. n. **A** Leg 1, anterior view, Leg 1 and digital photograph **B** leg 2, posterior view and digital photograph **C** leg 3, anterior view (spinules on posterior surface not indicated in contrast with leg 2) and digital photograph **D** leg 4, anterior view and digital photograph **E** leg 5 and digital photograph. Scales bars: 0.05 mm (**A–D**); 0.01 mm (**E**).

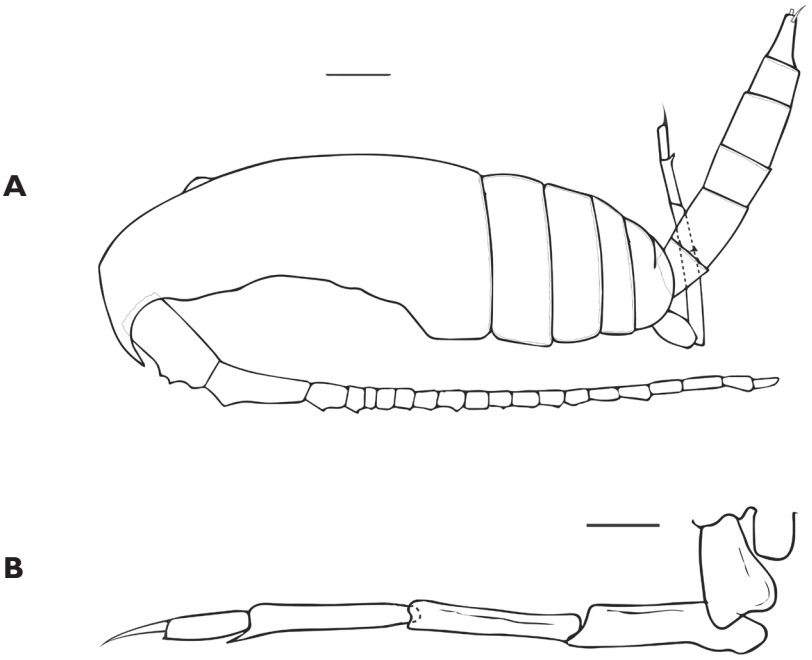

Figure 5. Male of *Bestiolina sarae* sp. n. **A** Habitus, lateral view **B** leg 5. Scales bars: 0.1 mm (**A**); 0.01 mm (**B**).

Leg 2 (Fig. 4B): exopod, anterior and posterior surfaces of all 3 segments without spinules. Endopod, anterior and posterior surfaces of first and third segment without spinules, second segment, anterior surface with 3 short spinules, posterior surface with 4 long spinules.

Leg 3 (Fig. 4C): number and size of spinules of anterior and posterior surfaces like leg 2. Distal segment of endopods of legs 3 and 4 with 6 setae.

Leg 4 (Fig. 4D): exopod and endopod, anterior and posterior surfaces of all segments without spinules.

Leg 5 (Fig. 4E): reduced in size, represented by symmetrical lobes with smooth margins.

Spine (Roman numerals) and setal (Arabic numerals) formula of legs 1–4 as follows:

Leg	Coxa	Basis	Exopod	Endopod
1	0–0	0–1	0–1; 0–1; 2,1,4	0–1; 1,2,2
2	0–1	0–0	I–1; I–1; III,I,5	0–1; 0–1; 1,2,3
3	0–1	0–0	I–0; I–1; III,I,5	0–1; 0–1; 1,2,3
4	0–1	0–0	I–0; I–1; III,I,5	0–0; 0–1; 1,2,3

Description of male (Fig. 5A): length of allotype measured from tip of rostrum to tip of caudal rami: 0.70 mm. Body more slender and slightly longer than in female. Cephalothorax with dorsal hump. Antennule 20-segmented, setation patterns of ancestral segments (indicated with Arabic numerals, s = seta), as follow: 1:3s, 2:1s, 3:1s, 4:1s, 5 and 8:0s, 9:1s, 10 and 12:0s, 13:1s, 14 and 15:0s, 16:1s, 17:0s, 18:1s, 19:1s, 20:4s.

Table 1. Number of spinules on anterior and posterior surface of endopod 2 of leg 2 and leg 3 of females of *Bestiolina sarae* sp. n. (holotype and four paratypes). Spinules of anterior surface are small, spinules of posterior surface are large and strong. n/o means spinules not observed (segment lost during dissection).

Character		Holotype MAKURIWA INV-CRU8991	Paratype MAKURIWA INV-CRU8993	Paratype NHMW 26309	Paratype NHMW 26310	Paratype NHMW 26311
Number of spinules anterior + posterior surface	Leg 2 left	3+4	4+5	4+4	3+4	3+4
	Leg 2 right	3+4	4+5	4+4	4+4	3+5
	Leg 3 left	3+4	4+5	3+5	3+4	n/o+n/o
	Leg 3 right	3+4	4+5	3+4	3+4	n/o+n/o

First to fifth pedigerous somites and swimming legs like in female. Urosome 5-segmented. Leg 5 (Fig. 5B) typical for the family, right leg consisting of a rounded lobe as in female, left leg elongate, 5-segmented, distal segment with apical spine.

Variability (Table 1): Females (n = 13): morphological variability in body length $\bar{x}$ = 0.70 ± 0.03 (0.64–0.73 mm) and in ornamentation pattern (number of spinules) of endopod 2 of legs 2 and 3.

Leg 2, endopod 2: holotype and 1 paratype (NHMW 26311) with 3 short spinules on anterior surface and 4 long spinules on posterior surface of left and right legs, one paratype (NHMW 26310) shows an additional spinule on anterior surface (4 instead of 3) of right leg, one paratype (NHMW 26311) shows an additional spinule on posterior surface of same leg. Two paratypes (MAKURIWA INV-CRU8993, NHMW 26309) show a different combination of spinules: one additional spinule on the anterior surface of both legs (left and right) (4 instead 3) and 1 additional spinule on posterior surface of left and right legs (5 instead of 4) MAKURIWA (Table 1).

Leg 3, endopod 2: variability of the ornamentation pattern was also noted on this leg but less accentuated than in leg 2 (Table 1). Anterior surface with 3 short spinules on anterior surface and 4 long spinules on posterior surface (holotype and paratype NHMW 26310) on both left and right legs; one paratype (MAKURIWA INV-CRU8993) shows 1 additional spinule on both legs on anterior and posterior surfaces (4+5 instead of 3+4). One paratype (NHMW 26309) shows 1 additional spinule on posterior surface (total 3+5) of left leg. In general, the most common spinulation pattern of second endopods in legs 2 and 3 is 3 spinules on anterior surface and 4 on posterior surface.

Males (n = 3) show variability on body length $\bar{x}$ = 0.70 ± 0.06 (0.63–0.75 mm). No variability was noted on spinulation pattern of the 3 studied specimens.

Discussion

Specimens from the Colombian Pacific were identified as belonging to the genus *Bestiolina* based on the diagnostic characters of the genus (Bradford-Grieve 1994): relatively short rostrum, presence of one seta on the inner margin of basis of leg 1, outer margin of exopo-

dal segments 2 and 3 of legs 2–4 without teeth, and distal segment of endopods of legs 3 and 4 with 6 setae. The typically reduced female fifth leg, with a bilobated form in female, the dorsal hump of cephalothorax and the asymmetrical legs 5 with long left leg and bilobated right leg in male, constitute the most discriminative characteristics of *Bestiolina*.

Adult members of genus *Bestiolina* can be confused with juvenile stages of other Paracalanidae due to the size of the anal segment (slightly longer than urosomites 2 and 3 together). Copepodites V of the other Paracalanidae have the same pattern and only the adult stages show an anal segment as long as urosomite 3. Additionally, the morphology of female leg 5 in immature stages of *Acrocalanus* and *Parvocalanus* is similar to adult stages of females of *Bestiolina*.

Specimens of Colombian *Bestiolina* were compared with the eight known species of the genus (Tables 2, 3).

Bestiolina sarae sp. n. can be distinguished from the other species by a combination of morphological characters related to body length, the number of segments of the antennule, the relationship of first pedigerous somite to cephalosome, and ornamentation of fifth pedigerous somite (Table 2). The three species, *Bestiolina zeylonica* (Andronov, 1972), *Bestiolina mexicana* (Suárez-Morales & Almeyda-Artigas, 2016) and *Bestiolina sarae* sp. n., are the smallest of the genus. The number of segments of the antennule is 25 in *Bestiolina coreana* (Moon, Lee & Soh, 2010) and *Bestiolina similis* (Sewell, 1914), 24 in *Bestiolina amoyensis* (Li & Huang, 1984) and *Bestiolina sarae* sp. n., and 23 in the remaining species; no information of this character is available for *Bestiolina sinica* (Shen & Lee, 1966). The cephalosome and the first pedigerous somite are fused in *B. coreana*, *B. similis*, *B. amoyensis*, *Bestiolina arabica* (Ali, Al-Yamani & Prusova, 2007), *B. sinica*, *B. zeylonica* (Andronov, 1972) and *Bestiolina sarae* sp. n. (Fig. 2A), while they are separate in *B. inermis* (Sewell, 1912) and *B. mexicana*. Three species *B. similis*, *B. arabica* and *B. inermis* have no spinules on the distal margin of the fifth pedigerous somite, while spinules are present in the other species and in *Bestiolina sarae* sp. n. (Fig. 2D).

In *Bestiolina,* the ornamentation of endopods and exopods of legs 2–4 is important to distinguish the species (Table 3). *Bestiolina sarae* sp. n. shares with *B. sinica* and *B. arabica* the absence of spinules on anterior and posterior surfaces on exopod segments of legs 2–4, but females of *B. sinica* are longer ($\bar{x}$ = 0.94 mm) than *Bestiolina sarae* sp. n. ($\bar{x}$ = 0.70 mm, Table 2), and have 4 and 5 spinules on the anterior surface of endopod 2 of legs 2 and 3, respectively (vs 3 and 3, respectively, in *Bestiolina sarae* sp. n.; Table 3). The new species also shares with *B. arabica* the number of spinules (3) on the anterior surface of endopod 2 of legs 2 and 3, but this species lacks spinules on the posterior surface of the same segments (vs 4 in *Bestiolina sarae* sp. n.). Additionally, spinules of the anterior surface of this segment in *B. arabica* are large while those of *Bestiolina sarae* sp. n. of the same surface are small.

The most relevant character to distinguish species of *Bestiolina* is the spinulation pattern on the anterior and posterior surfaces of endopod 2 of legs 2 and 3. *B. sarae* sp. n. bears 3 (anterior surface) and 4 (posterior surface) spinules, where as all other species have a different combination pattern: 4+3 in *B. coreana*, 0+5 in *B. similis*, 0+4 (leg 2) and 0+5 (leg 3) in *B. amoyensis*, 3+0 in *B. arabica*, 4+4 (leg 2) and 4+5 (leg 3) in *B. sinica*, 4+0 (leg 2) and 4+3 (leg 3) in *B. zeylonica*, 2+4 (leg 2) and 2+0 (leg 3) in

Table 2. Distribution and comparison of female morphological traits related to habitus, antennules, cephalosome and prosome of *Bestiolina* species. n/a no information available.

	***B. coreana* (Moon et al., 2016)**	***B. similis* (Sewell, 1914)**	***B. amoyensis* (Li & Huang, 1984)**	***B. arabica* (Ali et al., 2007)**	***B. inermis* (Sewell, 1912)**	***B. sinica* (Shen & Lee, 1966)**	***B. zeylonica* (Andronov, 1972)**	***B. mexicana* (Suárez-Morales & Almeida-Artigas, 2016)**	***B. sarae* sp. n.**
Distribution	Yellow Sea and Southern waters of Korea	Pacific and Indian Oceans, tropical / subtropical	South China Sea	Arabian Gulf	Pacific and Indian Oceans, tropical / subtropical	South China Sea	Sri Lanka	Gulf of Mexico	Pacific Coast of Colombia
Body, mean length (mm)	0.94	1.08	0.93	0.85	1.08	0.99	0.69	0.67	0.70
Antennule, # of segments	25	25	24	23	23	n/a	23	23	24
Cephalosome and first pedigerous segment	fused	fused	fused	fused	separate	fused	fused	separate	fused
Fifth pedigerous somite, distal margin with spinules	yes	no	yes	no	no	yes	yes	yes	yes

Table 3. Comparison of female morphological traits of *Bestiolina* species relatively to ornamentation of exopod (segments 1–3) and endopod (segment 2) of leg 2–4. n/a no information available.

Character	**Leg**	***B. coreana***	***B. similis***	***B. amoyensis***	***B. arabica***	***B. inermis***	***B. sinica***	***B. zeylonica***	***B. mexicana***	***B. sarae* sp. n.**
Exopod, number of spinules on posterior surface of segments 1–3	leg 2 leg 3 leg 4	0,6,3 0,4,0 0,3,0	0,0,3 0,0,3 absent	2,1,1 1,1,2 1,2,1	absent absent absent	0,3,0 n/a n/a	absent absent absent	3,3,2 0,3,2 absent	3,0,0 absent absent	absent absent absent
Endopod 2, number of spinules on anterior and posterior surface of segments 1–3	leg 2 leg 3 leg 4	4+3 4+3 0+4	0+5 0+5 absent	0+5 0+4 0+small spinules	3+0 3+0 absent	4 n/a n/a	4+4 5+4 0+4	4 4+3 0+small spinules	2+4 2+0 3+0	3+4 3+4 absent

B. mexicana. Although no information is available for leg 3 of *B. inermis* and that it is not specified if the four spinules of leg 2 are inserted at the anterior or posterior surface, other characters like the presence of 3 spinules on the posterior surface of exopod 2 distinguish it from *Bestiolina sarae* sp. n. (no spinules on exopodal segments).

Differences with *B. mexicana* are the form of the rostrum, which is short and stout in *Bestiolina sarae* sp. n. and long and with slender filaments in *B. mexicana*, and the morphology of the cutting edge of the mandible (two dorsal teeth in *B. mexicana*, one in *Bestiolina sarae* sp. n.). Additionally, *B. mexicana* bears spinules on the posterior surface of first exopod segment of leg 2, while this surface is naked in *Bestiolina sarae* sp. n. (Table 2).

Although a high variability on the spinulation pattern of the endopod 2 of legs 2 and 3 was observed in *Bestiolina sarae* sp. n. (Table 1), sometimes also differing between right and left legs of the same individual, the most common pattern is represented by 3+4 (three small spinules on the anterior surface and four large spinules on the posterior surface). Other spinulation patterns observed on the same segments are: leg 2 (4+4, 4+5) and leg 3 (3+5, 4+5). In contrast, *B. arabica* with leg 2 (3+0) and leg 3 (3+0) does not show this pattern. Although the 4+4 pattern (typical in *B. sinica*) was observed in endopod of leg 2 in two specimens of *Bestiolina sarae* sp. n. (left and right leg 2 in paratype NHMW 26309; right leg 2 in paratype 26310), *B. sinica* bears four spinules on the posterior surface of endopod 2 of leg 4, while in *Bestiolina sarae* sp. n. it is always naked.

Bestiolina sarae sp. n. is a component of plankton of tropical waters (28.7–28.8 °C). It was found in brackish waters with low salinity (23.0–23.9 pt), dissolved oxygen from 6.4 to 6.7 mg/L, and primary productivity (in terms of chorophyll-*a*) with 2.8–3.0 µg/l. Where *B. sarae* was collected, light penetration of the water was low (Secchi disk depth 3.6–4.8 m).

In the present study, *B. sarae* sp. n. showed a wide range of densities, from 3 to 624 individuals/m^3. As the species was found in all six localities, separated by up to 500 km from each other, it seems to be widely distributed in the area and could represent a typical copepod of the zooplankton of the Panama Bight. Due to the climatological and oceanographical characteristics of the study area (Dimar 2002; Fernández-Álamo and Färber-Lorda 2006), it seems likely that this species also occurs in coastal waters of the Baudó and Sanquianga ecoregions of the Colombian Pacific (Diaz and Acero 2003) and in other countries of the Eastern Tropical Pacific, such as Panama and Ecuador. It is conceivable that *B. sarae* also occurs in other regions influenced by the El Niño Southern Oscillation phenomenon as result of the tropicalization of species (Carrasco and Santander 1987).

Conclusions

With the discovery of *Bestiolina sarae* sp. n., the number of species of the genus is increased to nine, with two of them living in coastal waters of the tropical Americas. It is the first representative of the genus in the Eastern Tropical Pacific and seems to be native to the Panama Bight. It seems possible that the species is also distributed in

neighbouring coastal waters such as those of Ecuador and Panama, and it might also be expected in other areas influenced by the climatological and oceanographical El Niño Southern Oscillation.

Bestiolina sarae sp. n. was probably not detected in the past due to the paucity of surveys in the study area, the use of inappropriately sized zooplankton nets, and the confusion of adults with juvenile stages of other paracalanids. For future studies, we recommend the use of nets with mesh sizes less than 150 μm, which will allow for the collection of small copepods such as *B. sarae* sp. n. and other members of Paracalanidae.

Key to the identification of females of the genus *Bestiolina*

(Modified from Moon et al. 2010)

1 Presence of row of spinules on the distal margin of fifth pedigerous somite. **4**
– Absence of row of spinules on the distal margin of fifth pedigerous somite..... **2**
2 Leg 2: presence of spinules on posterior surface of third exopod segment..... ..... ***Bestiolina similis*** **(Sewell, 1914)**
– Leg 2: absence of spinules on posterior surface of third exopod segment..... **3**
3 Leg 2: presence of spinules on posterodistal surface of second exopod. Body size > 1 mm ..... ***B. inermis*** **(Sewell, 1912)**
– Leg 2: absence of spinules on posterodistal surface of second exopod. Body size < 1 mm ..... ***B. arabica*** **(Ali et al., 2007)**
4 Leg 2: absence of spinules on posterodistal surface of first exopod segment..... **5**
– Leg 2: presence of spinules on posterodistal surface of first exopod segment 7
5 Leg 3: presence of spinules on posterodistal surface of second exopod..... ..... ***B. coreana*** **(Moon et al., 2016)**
– Leg 3: absence of spinules on posterodistal surface of second exopod..... **6**
6 Leg 4: presence of spinules on posterodistal surface of second endopod segment. Body size almost 1 mm..... ***B. sinica*** **(Shen & Lee, 1966)**
– Leg 4: absence of spinules on posterodistal surface of second endopod segment. Body size less than 0.8 mm..... ***B. sarae*** **sp. n.**
7 Leg 4: presence of spinules on posterodistal surface of exopod. Body size > 0.9 mm..... ***B. amoyensis*** **(Li & Huang, 1984)**
– Leg 4: absence of spinules on posterodistal surface of exopod. Body size < 0.7 mm..... **8**
8 Leg 3: presence of spinules on posterodistal surface of second and third exopod. Cephalosome fused with first pedigerous somite..... ..... ***B. zeylonica*** **(Andronov, 1972)**
– Leg 3: absence of spinules on posterodistal surface of second and third exopod. Cephalosome separated from first pedigerous somite .... ***B. mexicana*** **(Suárez-Morales & Almeida-Artigas, 2016)**

Acknowledgements

We thank the members and postgraduate students of the Laboratorio de Limnología, Universidad Jorge Tadeo Lozano (UJTL), for their assistance during sample collection and transport. We also thank the research office of UJTL for funding the publication of this article.

This study was part of the research project "Evaluation of marine bioinvasions in 3 harbor zones of the Colombian Pacific and their relation with marine transport", which was supported by the Departamento Administrativo de Ciencia, Tecnología e Innovación de Colombia (contract no. 088-2016), within the project group "Proyectos de Investigación, DesarrolloTecnológico e Innovaciónen Ambiente, Océanos y Biodiversidad – 2015".

References

Andronov VN (1972) Velsonogie rachki *Bestiola* gen. n. (Copepoda, Paracalanidae). Zoologicheskii Zhurnal 51: 290–292. [In Russian, English summary]

Andronov VN (1991) Ob izmenenii nazvanii nekotorykh taksonov Calanoida (Crustacea). Zoologicheskii Zhurnal 70 (6): 133–134. [In Russian with English summary]

Ali M, Al-Yamani F, Prusova I (2007) *Bestiolina arabica* sp. nov. (Copepoda, Calanoida, Paracalanidae), a new species from the Northwestern Arabian Gulf. Crustaceana 80 (2): 195–205. https://doi.org/10.1163/156854007780121429

Betancourt Portela JM, Sánchez Díazgranados JG, Mejía-Ladino LM, Cantera Kintz JR (2011) Calidad de las aguas superficiales de Bahía Málaga, Pacífico Colombiano. Acta Biológica Colombiana 16 (2): 1751–92.

Boeck A (1865) Oversigt over de ved Norges Kyster jagttagne Copepoder, henhörende til Calanidernes, Cyclopidernes og Harpactidernes Familier. Forhandlinger I Videnskabsselskabet I Kristiania 1964: 226–282.

Boxshall GA, Hasley SH (2004) An Introduction to Copepod Diversity, Vol. 1. The Ray Society London.

Björnberg TSK (1981) Copepoda. In: Boltovskoy D (Ed.) Atlas del zooplancton del Atlántico sudoccidental y métodos de trabajo con el zooplancton marino. Instituto Nacional de Desarrollo Pesquero, Mar del Plata, 586–679.

Brady GS (1899) On the marine Copepoda of New Zealand. Transactions of the Zoological Society of London 15(2): 31–54. https://doi.org/10.1111/j.1096-3642.1899.tb00018.x

Bradford-Grieve JM (1994) The marine fauna of New Zealand: Calanoid Copepoda: Megacalanidae, Calanidae, Paracalanidae, Mecynoceridae, Eucalanidae, Spinocalanidae, Clausocalanidae. National Institute of Water Atmospheric Research, Wellington, 160 pp.

Cantera JR, Blanco JF (2001) The estuary ecosystem of Buenaventura Bay, Colombia. In: Seeliger U, Kjerfve B (Eds) Coastal Marine Ecosystems of Latin America, Ecological Studies, Vol. 144. Springer-Verlag, Berlin/Heidelberg, 265–279. https://doi.org/10.1007/978-3-662-04482-7_19

Carrasco S, Santander H (1987) The El Niño event and its influence on the zooplankton of Peru. Journal of Geophysical Research 92(C3): 14405–14410. https://doi.org/10.1029/JC092iC13p14405

Claus C (1863) Die frei lebenden Copepoden mit besonderer Berücksichtigung der Fauna Deutschlands, der Nordsee und des Mittelmeeres. Engelmann, Leipzig, 230 pp. https://doi.org/10.5962/bhl.title.58676

Dana JD (1852) Crustacea, Part II. United States Exploring Expedition during the years 1838–1842, under the command of Charles Wilkes 13: 1019–1262.

Diaz JM, Acero A (2003) Marine Biodiversity in Colombia: achievements, status of knowledge, and challenges. Gayana 67(2): 261–274. https://doi.org/10.4067/S0717-65382003000200011

Dimar-Dirección General Marítima (2002) Compilación Oceanográfica de la Cuenca Pacífica Colombiana. Centro Control Contaminación del Pacífico, Tumaco, 124 pp.

Dorado Roncancio J (2018) Variabilidad de la composición y abundancia de la subclase Copepoda en el océano Pacífico colombiano durante septiembre de 2005 y 2007. Master's thesis. Universidad Nacional de Colombia, Bogotá, 75 pp.

Fernández-Álamo MA, Färber-Lorda J (2006) Zooplankton and the oceanography of the eastern tropical Pacific: a review. Progress in Oceanography 2006(69): 318–359. https://doi.org/10.1016/j.pocean.2006.03.003

Ferrari FD, Ivanenko VN (2008) The identity of protopodal segments and the ramus of maxilla 2 of copepods (Copepoda). Crustaceana 81: 823–835. https://doi.org/10.1163/156854008784771702

Giesbrecht W (1893) Systematik und Faunistik der pelagischen Copepoden des Golfes von Neapel und der angrenzenden Meeres-Abschnitte. Fauna und Flora des Golfes von Neapel und der Angrenzenden Meeres-Abschnitte, Herausgegeben von der Zoologischen Station zu Neapel 19: 1–831. [pls 1–54]

Huys R, Boxshall GA (1991) Copepod Evolution. The Ray Society, London, 468 pp.

Lazarus-Agudelo JF, Cantera-Kintz JR (2007) Crustáceos (Crustacea: Sessilia, Stomatopoda, Isopoda, Amphipoda, Decapoda) de Bahía Málaga, Valle del Cauca (Pacífico colombiano). Biota Colombiana 8(2): 221–190.

Li SJ, Huang JQ (1984) On two new species of planktonic Copepoda from the estuary of Juilong River, Fujian, China. Journal of Xiamen University of Natural Sciences 23(3): 381–390.

Milne Edwards H (1840) Ordre des copépodes. In: Histoire naturelle des Crustacés, comprenant l'anatomie, la physiologie et la classification de ces animaux. Tome 3: 411–529. [pls 37–40]

Moon SY, Lee W, Soh HY (2010) A new species of *Bestiolina* (Crustacea: Copepoda: Calanoida) from the Yellow Sea, with notes on the zoogeography of the genus. Proceedings of the Biological Society of Washington 123: 32–46. https://doi.org/10.2988/09-12.1

Mulyadi M (2004) Calanoid Copepods in Indonesian Waters. Research Center for Biology, Indonesia Institute of Sciences, Bogor, 195 pp.

Nikolskaya MN (1963) The calcid Fauna of the USSR (Chalcidoidea). Israel Program for Scientific Translations, Jerusalem, 593 pp.

Oakley TH, Wolfe JM, Lindgren AR, Zaharoff AK (2013) Phylotranscriptomics to bring the understudied into the fold: monophyletic Ostracoda, fossil placement, and pancrustacean phylogeny. Molecular Biology and Evolution 30(1): 215–233. https://doi.org/10.1093/molbev/mss216

Razouls C, de Bovée F, Kouwenberg J, Desreumaux N (2005–2018) Diversity and Geographic Distribution of Marine Planktonic Copepods. Sorbonne Université, Centre national de la recherche scientifique, Paris. http://copepodes.obs-banyuls.fr/en [Accessed on: 2018-8-8]

Sars GO (1902) An account of the Crustacea of Norway, with short descriptions and figures of all the species: IV. Copepoda Calanoida. Bergens Museum, Bergen, 171 pp. [pls 1–102] https://doi.org/10.5962/bhl.title.1164

Sewell RBS (1912) Notes on the surface-living Copepoda of the Bay of Bengal, I and II. Records of the Indian Museum 7: 313–382. https://doi.org/10.5962/bhl.part.28239

Sewell RBS (1914) Notes on the surface Copepoda of the Gulf of Mannar. Spolia Zeylanica 9: 191–263. https://doi.org/10.5962/bhl.part.7319

Shen C, Lee F (1966) On the estuarine copepods of Chaikiang River, Kwangtung Province. Acta Zoologica Sinica 3: 215–223.

Suárez-Morales E, Almeyda-Artigas RJ (2016) A new species of *Bestiolina* (Copepoda: Calanoida: Paracalanidae) from the Northwestern Atlantic with comments on the distribution of the genus. Revista Mexicana de Biodiversidad 87: 301–310. https://doi.org/10.1016/j.rmb.2016.05.002

Suthers IM, Rissik D (2009) Plankton: A Guide to their Ecology and Monitoring for Water Quality. CSIRO Publishing, Collinwood, 256 pp. https://doi.org/10.1093/plankt/fbp102

Walter TC, Boxshall G (2018) World of Copepods Database. http://www.marinespecies.org/copepoda [Accessed on: 2018-8-8]

ZooKeys 846: 19–30 (2019)
doi: 10.3897/zookeys.846.34372
http://zookeys.pensoft.net

RESEARCH ARTICLE

A peer-reviewed open-access journal
ZooKeys
Launched to accelerate biodiversity research

A new semislug of the genus *Laocaia* (Gastropoda, Pulmonata, Helicarionidae) from Vietnam

Ivaylo Dedov[1], Ulrich Schneppat[2], Manh Quang Vu[3], Nguyen Quoc Huy[4]

1 *Institute of Biodiversity and Ecosystem Research, Bulgarian Academy of Sciences, 2 Gagarin Street, 1113 Sofia, Bulgaria* **2** *CH-7074 Churwalden-Malix, Sennereiweg 8, Switzerland* **3** *Ho Chi Minh City University of Food Industry, 140 Le Trong Tan St., Tan Phu, Ho Chi Minh City; c/o Hanoi National University of Education (HNUE), 136 Xuan Thuy Rd., DHSP Cau Giay, Hanoi, Vietnam* **4** *Institute of Ecology and Works protection, 267 Rd. Chua Boc, Dong Đa, Hanoi, Vietnam*

Corresponding author: *Ivaylo Dedov* (idedov@gmail.com)

Academic editor: *Eike Neubert* | Received 7 March 2019 | Accepted 10 April 2019 | Published 16 May 2019

http://zoobank.org/F7A4EB59-8816-4792-924E-24C99170110C

Citation: Dedov I, Schneppat U, Vu MQ, Huy NQ (2019) A new semislug of the genus *Laocaia* (Gastropoda, Pulmonata, Helicarionidae) from Vietnam. ZooKeys 846: 19–30. https://doi.org/10.3897/zookeys.846.34372

Abstract

A new species of the genus *Laocaia* Kuzminykh, 1999, *Laocaia simovi* Dedov & Schneppat, **sp. nov.**, is described, which was collected from a single locality in northern Vietnam. Color pictures of living specimens are provided. For the first time, information on the ecology and biology of a representative of the genus *Laocaia* is presented.

Keywords

Helicarionidae, *Laocaia*, new species, Vietnam

Introduction

The genus *Laocaia* was described by Kuzminykh (1999) and contains two species – *Laocaia attenuata* Kuzminykh, 1999 and *L. obesa* Kuzminykh, 1999 – from the area of the Fansipan Mountain massive, northern Vietnam. Both species were recorded from relatively high altitudes between 1800–2000 m in the forest zone in the vicinity of Fansipan. The habitats for both species were not explicitly described by Kuzminykh

Copyright *Ivaylo Dedov et al.* This is an open access article distributed under the terms of the Creative Commons Attribution License (CC BY 4.0), which permits unrestricted use, distribution, and reproduction in any medium, provided the original author and source are credited.

(1999), and the type localities were not georeferenced. Until recently, no additional information on other species or the biology of members of the genus were published (Schileyko 2011).

Our finding of a third species strongly suggests that the genus has evolved in the ecological niches of the high altitudes of the Fansipan Mountain tops, and records of further new species of the genus can be expected in the future. The potential type locality of *L. attenuata* is situated only 3.5 km eastwards, and that of *L. obesa* can be found about 4.8 km in a southeast direction of the type locality of *Laocaia simovi* Dedov & Schneppat, sp. nov., on the same mountain massive. This indicates a high degree of endemism in a comparatively small area, which is in urgent need of further research. According to Páll-Gergely et al. (2015), the molluscan fauna of the border region of Sơn La and Yen Bái Provinces (Phan Xi Păng = "Fansipan" Mountain and its vicinity) is nearly unknown. This may be due to the high abundance of limestone-free bedrock causing a relatively depleted richness and diversity of land molluscs.

Material and methods

The specimens were collected with an entomological standard sweep net from elevated branches of a leaf bearing tree of unknown species in the forest, on the eastern slope of the top of Fansipan Mountain (Fig. 1).

The treatment of the specimens followed Nitz et al. (2009: 280), directly after collecting in the evening of the same day. One specimen was photographically documented alive prior to killing and preservation, using a digital camera Panasonic, Lumix DMC-TZ31. Because of the delicateness of the preserved specimens these were soaked for some minutes in a 1% NaCl-solution to relax them and to prevent desiccation and malformation during the measuring process under the stereo microscope. All measurements have been taken from preserved animals. The measurements were taken under a stereo-microscope with a scaled ocular and transformed into millimeters.

Abbreviations: **IBER-BAN** – Institute of Biodiversity and Ecosystem Research, Bulgarian Academy of Sciences; **NMNHS** – National Museum of Natural History, Sofia, Bulgaria.

Morphological studies

All measurements given are from specimens preserved in ethanol 75%. The total length and body width, mantle length and mantle width, length of free mantle flap, sole length and sole width, height and width of genital pore of the three adults of the series were measured. Maturity was determined prior to dissection by examining the genital pore under a binocular microscope. The general method of dissecting follows Wiktor (2000: 383–384).

Figure 1. *Laocaia simovi* Dedov & Schneppat, sp. nov. habitat picture, from the type locality near the peak of Fansipan. The black arrow points towards the epiphytic plants, in which the new species was found.

Results

Family Helicarionidae Bourguignat, 1877
Subfamily Helicarioninae Bourguignat, 1877

Genus *Laocaia* Kuzminykh, 1999

Type species. *Laocaia attenuata* Kuzminykh, 1999.

Diagnosis. small slugs with non-coiled visceral hump, rounded posteriorly, lying in V- shaped body groove; body cavity not extending into tail; shell very thin, non-spiral, internal, hemispheric, completely covering visceral hump, with small calcified part; penis short, bulbous, with large stimulator inside; epiphallus and flagellum absent; spermatheca entering atrium between vagina and penis (amended after Kuzminykh 1999).

Remarks. for the systematic position of the genus *Laocaia*, we here follow MolluscaBase (2018). The genus was originally placed in the family Ariophantidae by Kuzminykh (1999), which was followed by Bouchet et al. (2017). However, Schileyko (2002, 2011) transferred it to the family Helicarionidae.

Laocaia simovi Dedov & Schneppat, sp. nov.

http://zoobank.org/5106D544-8BDC-4BBF-B04D-EEB763616827
Figs 2–8

Holotype. VIETNAM: Lao Cai Province, Fansipan Mountain below peak, in monsoon influenced leaf-bearing mountain forest with dense undergrowth of bamboo, ca 2990 m; 22.30560°N, 103.77625°E; 21 Sep 2018; I. Dedov, N. Simov, R. Bekchiev, P. Beron leg.; NMNHS 10805, ex. coll. IBER-BAN 40339/1-A.

Paratypes. 2 adults and 2 juveniles, same data as for holotype: NMNHS 10806, ex. coll. IBER-BAN 40339/1-E; coll. IBER-BAN, 40339/1: B, C, D.

The paratype IBER-BAN 40339/1-C is shown in the photos of the living semislug, as well as in all photos of the preserved animal and its anatomy.

Measurements of holotype. Holotype: total length 24.12 mm, body width 6.72 mm, mantle length 15.96 mm, mantle width 6.72 mm, free mantle flap length 4.08 mm, sole length 24 mm, sole width 3.36 mm, tale length 8.28, tale width 2.52 mm, tale “horn” length 1.3 mm, tale “horn” width 1 mm, genital pore length 1.05 mm, genital pore width 0.25 mm (Fig. 2).

Differential diagnosis. Externally, *L. simovi* Dedov & Schneppat, sp. nov. differs from *L. attenuata* and *L. obesa* by its coloration. The anterior body of *L. attenuata* is yellow, and its head and neck show three indistinct stripes, while the mantle is marbled with irregularly arranged black spots. The posterior part of the foot is uniformly grayish. In contrast, the body of *L. obesa* is whitish-grayish colored and covered with numerous white spots. On the visceral hump, the mantle of this species displays a pattern of irregularly arranged black spots (Kuzminykh 1999).

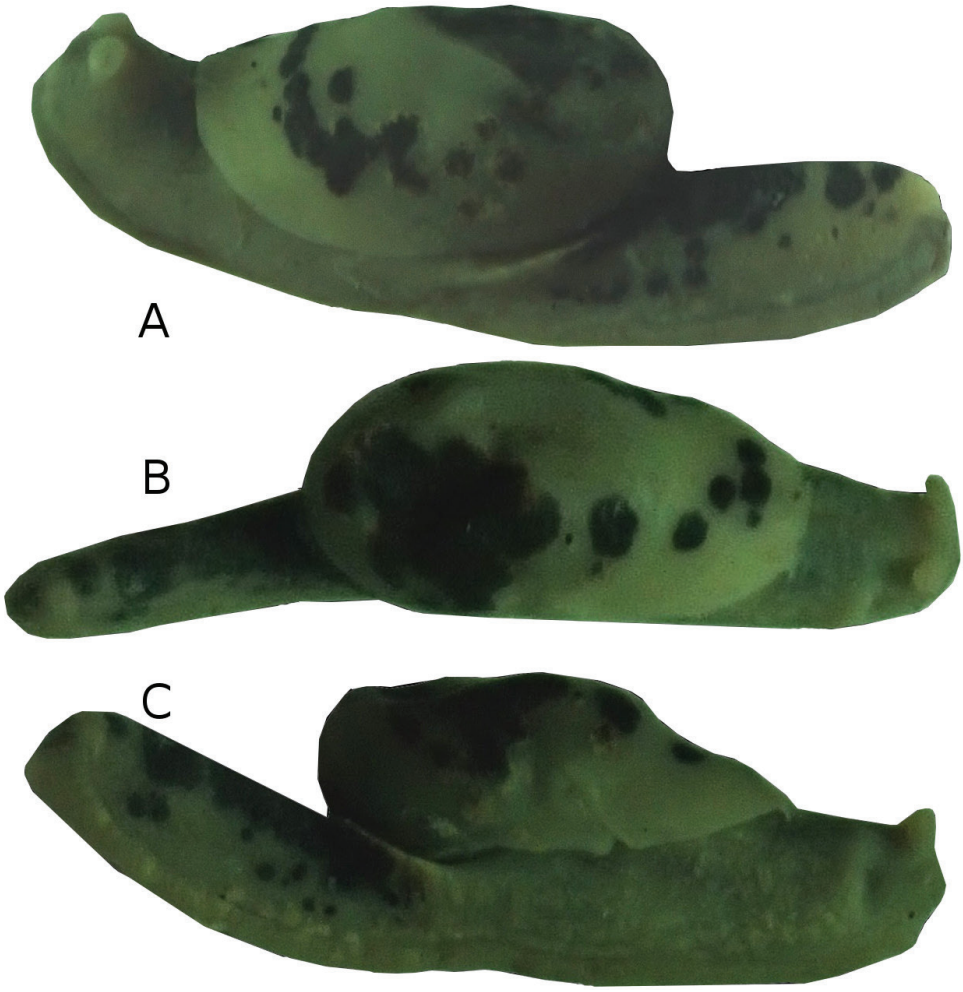

Figure 2. *Laocaia simovi* Dedov & Schneppat, sp. nov. holotype specimen in lateral left (**A**), dorsal (**B**), and lateral right (**C**) views.

Anatomically, *L. simovi* sp. nov. differs from *L. attenuata* by the narrower base of the penis, as well as by its much more globular sarcobelum with a pointed, cone-shaped apical tip. The sarcobelum is not covered with numerous distinct papillae, but it shows very fine longitudinal striae. The striation is not well visible even under high magnification.

Laocaia simovi sp. nov. differs from *L. obesa* by its less voluminous penis and the narrower base of the penis. The inner wall of the penis is not covered with papillae, but with almost invisible, very fine granules. The bursa copulatrix of *L. simovi* sp. nov. is of almost globular shape, the pedunculus is long, slender and of the same diameter all along its length; its bursa copulatrix is more voluminous than the penis.

Description. *Coloration*: The primary color of the anterior body is light-ocher-brownish. The head, including the ommatophores, is of a grayish-ocher color. The

Figure 3. *Laocaia simovi* Dedov & Schneppat, sp. nov. coloration of the body with the visceral hump and U-shaped dorsal groove.

black eye spot on top of the ommatophores is contrasting and well visible. The "tale", e.g. the posterior part of the foot is of a deep brick red color. This coloration continues anteriorly until the lower sides of the head, where it fades. The whole body shows a pattern of irregularly dispersed, white-yellowish and brownish-blackish spots and markings, which are also irregular in size, shape and placement between specimens. The brownish-blackish spots are missing on the neck and lower frontal sides of the body. The well pronounced dorsal edge of the "U" shaped dorsal groove behind the visceral hump is yellowish (Fig. 3). The sole in living specimens is subdivided in two reddish lateral sole fields and a central creamy-yellowish field (Fig. 4A). In preserved animals, the complete sole loses its differentiating pigmentation (Fig. 4B), which is also the case for all other body-parts of the specimens. All colorful pigments (besides melanin) are dissolved in ethanol during the preservation process (Fig. 5A, B). On the entire body, the slime is thin, transparent and colorless (see Fig. 6B). There was no defensive slime of different color or consistence observed in living specimens.

Body: The body (n = 3, adult specimens) is slender, elongated, and of comparatively small size and fits the known body dimensions of species within the genus *Laocaia*. The total length of preserved adult specimens is 21.12–26.40 mm. The body width is 5.76–6.72 mm. The visceral hump length is 11.52–15.96 mm. The visceral hump width is equal to the body width. The free mantle flap is 3.60–4.08 mm. In living animals,

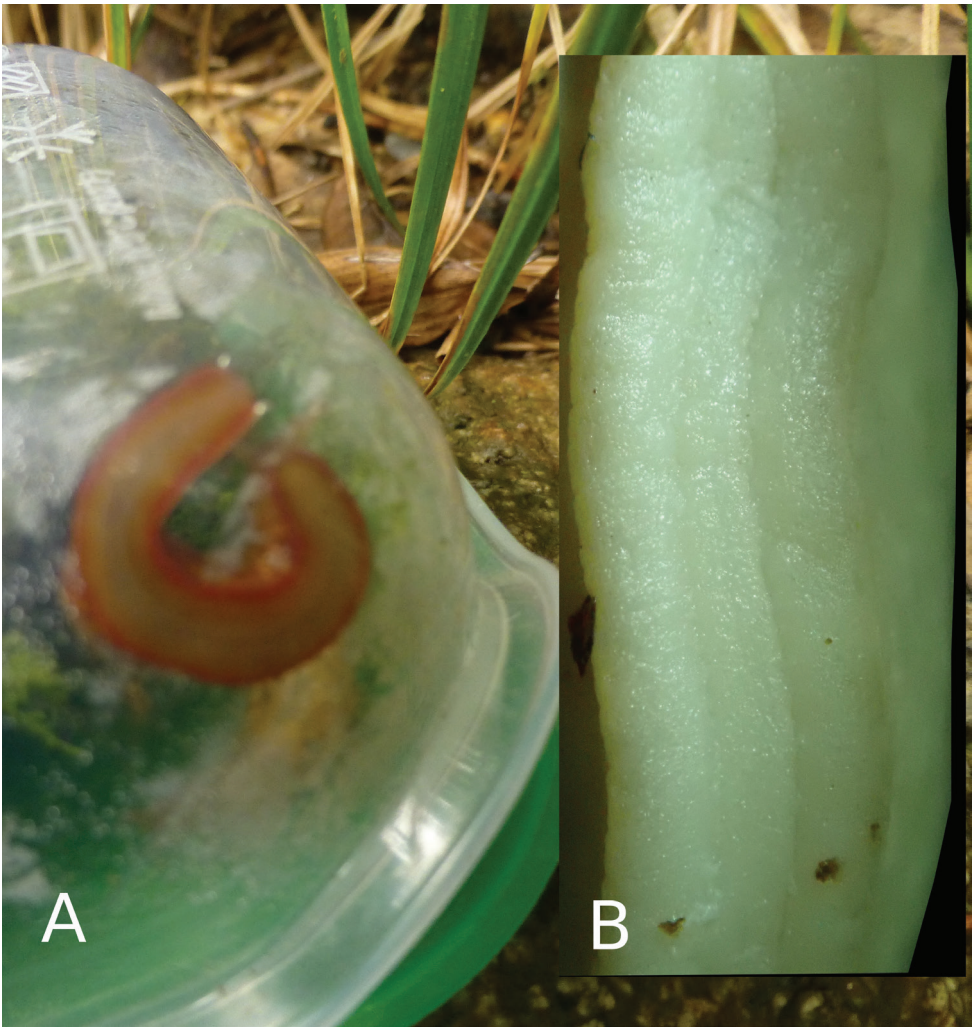

Figure 4. *Laocaia simovi* Dedov & Schneppat, sp. nov. sole coloration and sole zones in a living specimen (**A**) picture was taken in situ in the field, when the first animal was collected in the box, and sole of preserved animal (**B**).

the integument of the anterior part of the body, including the mantle over the visceral hump, is very finely granulated, but looks smooth on the photo of a living specimen (Fig. 3). However, the integument of the posterior part of the foot, as well as of the body flanks, is visibly roughly sculptured with big and well-rounded granules, which appear almost like the wrinkle rows in other slugs. This sculpture of the integument disappeared in all specimens during preservation, and not even the grooves between the sculptural elements remained (Fig. 5A, B). The posterior part of the foot is laterally depressed and formed like a steep roof. Observed with the naked eye, it resembles a keel structure, but there is no real keel like in Limacidae, for example. The length

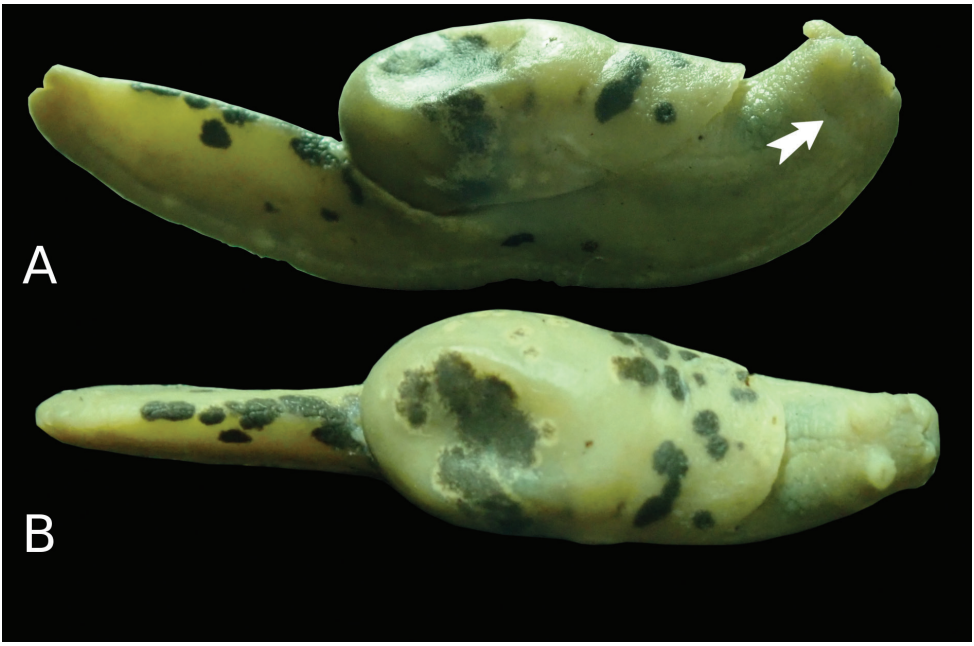

Figure 5. *Laocaia simovi* Dedov & Schneppat, sp. nov. preserved specimen, paratype IBER-BAN 40339/1-C, lateral right (**A**) and dorsal (**B**) view. The white arrow points to the genital pore.

of the posterior part of the foot is 7.08–9.48 mm; the width is 2.40–2.64 mm. The dorsum has a little hornlike prolongation at its posterior end. The posterior horn length is 1.30–1.32 mm; the posterior prolongation width is 0.72–1.00 mm. The posterior prolongation is slightly longer than the foot in living animals (see Fig. 6A). The posterior prolongation is separated from the dorsum with a slit and lays on it (observed in preserved specimens). The enlarged and bubble-shaped visceral hump with the entity of the visceral mass is lying in the body cavity. The mantle fully covers the shell, also in the juvenile specimens, and no slit was observed. The body cavity is not enlarged into the posterior part of the foot, which is fully muscular. The sole is narrow, only about a third of the body width, divided in three longitudinally fields, equally finely sculptured resembling small blisters (see Fig. 4B). The sole length is 21.26–26.04 mm, sole width 3.00–3.36 mm, the lateral zones 1.08–1.2 mm, and the central zone 0.84–0.96 mm. The pneumostome is located more or less centrally of the right of the mantle. The wide and deep dorsal U-shaped groove behind the visceral hump, as well as the lack of organs, except muscles in the posterior part of the foot, allows *Laocaia simovi* sp. nov. to move its raised "tale" very fast from side to side (refer to biological and ecological observations). In mature animals, the genital pore is well visible, about 2.1–2.6 mm posterior to the front on the right side of the neck, a little below the base of the right ommatophore. The length of the genital pore is 1.05–1.10 mm; the width is 0.25–0.30 mm (Fig. 5A).

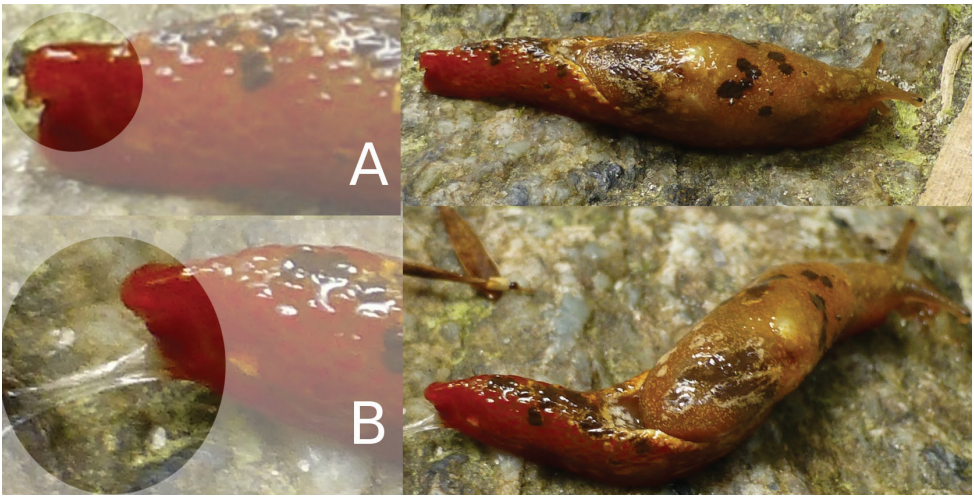

Figure 6. *Laocaia simovi* Dedov & Schneppat, sp. nov. pointed posterior end of the dorsum with the horn-like structure (**A**) and the coloration of the slime (**B**).

Shell: The vestigial shell is placed on the anterior roof of the visceral hump. The more calcified apical part of it is situated on the anterior part of the shell. The whole shell is found somewhat central right from the body axis. In other known vestigial shells, the small calcified part is situated apically. The thin seam of periostracum is posterior to the hard plate, rather than anterior to it in other *Laocaia* species. The apex is well distinguished and positioned almost centrally. The whole vestigial shell is completely covered with the mantle. It is difficult to extract it out of the shell-bed without damage. The shell is very thin and transparent. Under high magnification it is grainy, calcareous from ventral, except the much harder, triangulate, more massive calcified plate of creamy-white opaque color. The shell is without any remains of a helicoid apex, more like those, usually found in Limacidae, Agriolimacidae or Milacidae (Fig. 7A–C). The periostracum is somewhat glossy and of pale-yellow color.

Anatomy of genital organs (Fig. 8A–E): ♂-parts: the penis (p) is relatively short, widened in its middle section and generally fusiform, narrow in its basal part – length: 2.80 mm, width – base: 1.08 mm, – middle section: 1.56 mm. The walls of the penis are muscular, its interior walls are very finely granulated. Inside the penis, at its posterior end, a globular sarcobelum (sb), with a pointed, cone-shaped apical tip. Its surface is fine longitudinally striated, but the striation is not well visible even under high magnification (Fig. 7D, E). Below the sarcobelum, there is the simple opening of the vas deferens. The musculus retractor penis (mrp) is short and thick. Its length is 0.84 mm, width is 0.33–0.66 mm. The musculus retractor penis is attached almost apically to the posterior end of the penis. The vas deferens (vd) is short and thinner than the penis. It attaches to the outer wall of the penis and inserts at the penis aside the mrp. The vas deferens is wrapped tightly with connective tissue around the penis (Fig. 8B). An epiphallus or a flagellum is absent.

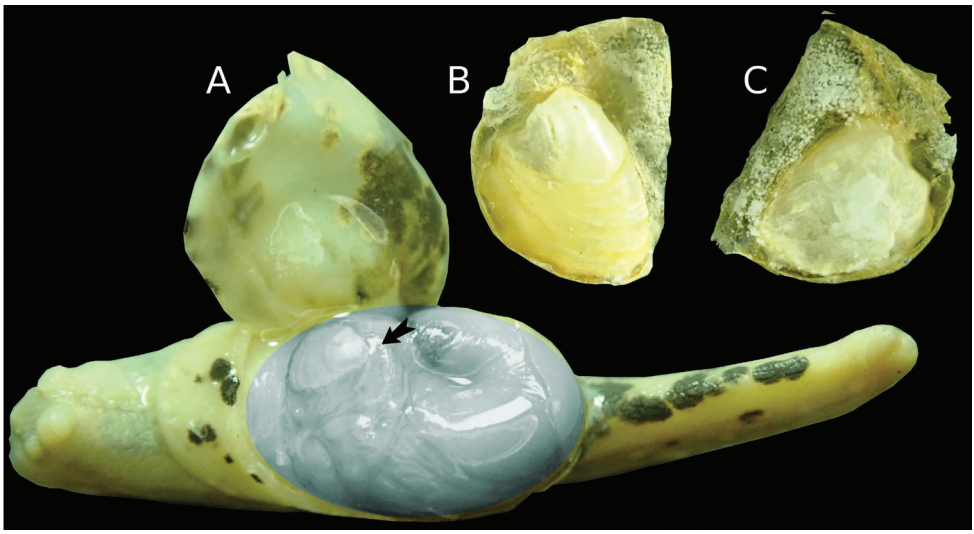

Figure 7. *Laocaia simovi* Dedov & Schneppat, sp. nov. vestigial shell (**A**) position of its calcified part on anterior roof of the visceral hump indicated by black arrow, the visceral hump indicated by grayish ellipse; dorsal view of the shell (**B**) ventral view of the shell (**C**).

♀-parts: Bursa copulatrix (bc) is big, almost spherical – length: 3.09 mm, width: 2.40 mm, with a relatively long pedunculus (pd) – length: 4.62 mm, width: 0.93 mm over its complete length. A spermatophore was not found in the pedunculus or bursa copulatrix. The albumen gland (ag) is very large and pale yellowish-white – length: 4.14 mm, width: 2.55–2.76 mm. The free oviduct (fod) is basally conical and then twisted and folded with approximate length of 3.7 mm and a width of 0.9–1.1 mm. It inserts to the atrium at almost the same position as the penis.

♂♀-parts: The atrium (at) is short and tubular. The hermaphroditic gland (hg) is big, relatively globular with a length of 3.6 mm and a width of 2.4 mm, gray-brownish and covered with a dense blackish, irregular connective tissue. The hermaphroditic duct (hd) is short, twisted and folded all along its length with a width of 0.54–0.6 mm. The spermoviduct (sod) is of 1.11–1.14 mm width.

Biological and ecological observations: Up to now, the species was found in epiphytic plant-groups, on elevated branches, in the tree crowns in the forests just below the Fansipan peak. If the animal is touched, it first tries to escape very fast, but if caught, the semislug takes a position with the head inverted and starts to wag its raised "tail" very fast from one side to the other, probably imitating land leeches (Hirudinea). This behavior can be interpreted to be a protective measure against predators, but also to flip itself down from twigs or leaves to the forest floor in order to escape a potential predator. Similar observations of rapid "tail movement" are published by Wiktor (2002) for the semislug species *Cryptaustenia saltatoria* Wiktor, 2002 and *Cryptaustenia obesa* Wiktor, 2002 (Helicarionidae) in New Guinea.

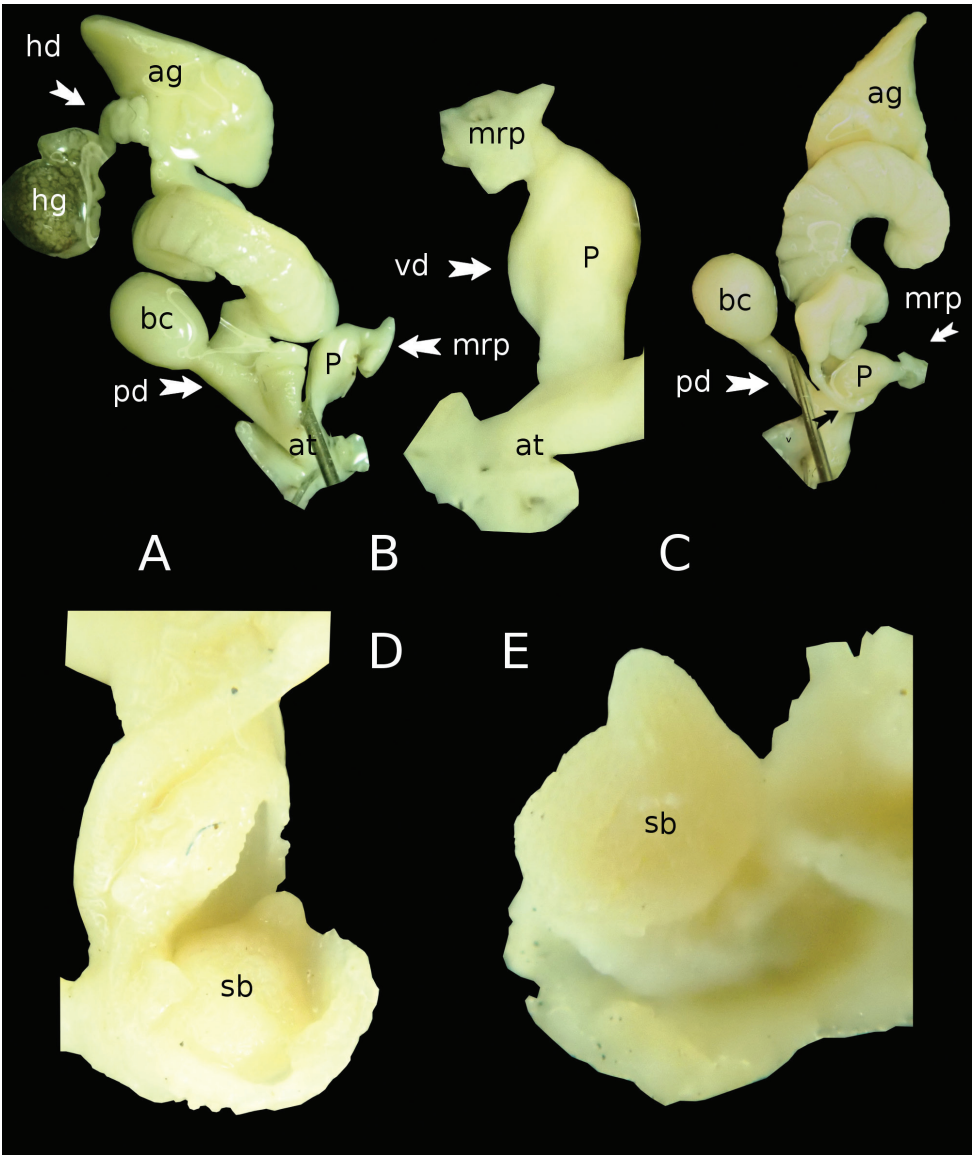

Figure 8. *Laocaia simovi* Dedov & Schneppat, sp. nov. genital anatomy, the whole sexual system (**A**), male part of the sexual system (**B**), sexual system, opposite view (**C**), position of the sarcobelum inside of the penis (**D**), and inverted (**E**). Abbreviations: **p** – penis; **sb** – sarcobelum, **mrp** – musculus retractor penis, **vd** – vas deferens, **at** – atrium, **bc** – bursa copulatrix, **pd** – pedunculus, **ag** – albumen gland, **hg** – hermaphroditic gland, **hd** – hermaphroditic duct.

Distribution. Up to now this species is known only from its type locality.

Derivatio nominis. This new species is named after our friend and biologist Dr. Nikolay Simov, NMNHS, Sofia, Bulgaria, who found the first specimen of the species.

Acknowledgements

This study was financially supported by scientific and technological research authorities of the Ministry of Education and Training, Vietnam, Code: B2016- SPH-24. The authors would like to thank to the editor Dr. Eike Neubert and the reviewer Dr. Barna Páll-Gergely for their helpful remarks.

References

Bouchet P, Rocroi JP, Hausdorf B, Kaim A, Kano Y, Nützel A, Parkhaev P, Schrödl M, Strong EE (2017) Revised classification, nomenclator and typification of gastropod and monoplacophoran families. Malacologia 61(1–2): 1–526. https://doi.org/10.4002/040.061.0201

Kuzminykh AA (1999) A new genus and two new species of land snails of the family Ariophantidae from North Vietnam. Ruthenica 9 (1): 47–50.

MolluscaBase (2018) *Laocaia* Kuzminykh, 1999. http://www.molluscabase.org/aphia.php?p=taxdetails&id=1322011 [2019-04-10]

Nitz B, Heim R, Schneppat UE, Hyman I, Haszprunar G (2009) Towards a new standard in slug species descriptions: the case of *Limax sarnensis* Heim & Nitz n. sp. (Pulmonata: Limacidae) from the Western Central Alps. Journal of Molluscan Studies 75: 279–294. https://doi.org/10.1093/mollus/eyp030

Páll-Gergely B, Hunyadi A, Ablett J, Lương HV, Naggs F, Asami T (2015) Systematics of the family Plectopylidae in Vietnam with additional information on Chinese taxa (Gastropoda, Pulmonata, Stylommatophora). ZooKeys 473: 1–118. https://doi.org/10.3897/zookeys.473.8659

Schileyko AA (2002) Treatise on recent terrestrial pulmonate molluscs Part 9. Helicarionidae, Gymnarionidae, Rhysotinidae, Ariophantidae. Rhuthenica Supplement 2: 1165–1307.

Schileyko AA (2011) Check-list of land pulmonate molluscs of Vietnam (Gastropoda: Stylommatophora). Ruthenica 21 (1): 1–68. https://biotaxa.org/Ruthenica/article/view/3603

Wiktor A (2000) Agriolimacidae (Gastropoda: Pulmonata) – a systematic monograph. Annales Zoologici 49 (4): 347–590.

Wiktor A (2002) Terrestrial Gastropods of the Province of Madang in Papua New Guinea. Part II. Two species of *Cryptaustenia* Cockerell, 1898 (Pulmonata: Helicarionidae) new to the science. Folia Malacologica 10(4): 225–231.https://doi.org/10.12657/folmal.010.014

ZooKeys 846: 31–41 (2019)
doi: 10.3897/zookeys.846.35028
http://zookeys.pensoft.net

RESEARCH ARTICLE

A peer-reviewed open-access journal
ZooKeys
Launched to accelerate biodiversity research

A new and cryptic species of *Lissodesmus* Chamberlin, 1920 (Diplopoda, Polydesmida, Dalodesmidae) from Tasmania, Australia

Robert Mesibov[1]

1 *West Ulverstone, Tasmania 7315, Australia*

Corresponding author: *Robert Mesibov* (robert.mesibov@gmail.com)

Academic editor: *D. V.anden Spiegel* | Received 31 March 2019 | Accepted 18 April 2019 | Published 16 May 2019

http://zoobank.org/94EF21BF-BB65-4298-818A-322BED06068D

Citation: Mesibov R (2019) A new and cryptic species of *Lissodesmus* Chamberlin, 1920 (Diplopoda, Polydesmida, Dalodesmidae) from Tasmania, Australia. ZooKeys 846: 31–41. https://doi.org/10.3897/zookeys.846.35028

Abstract

Lissodesmus piscator **sp. nov.** differs from the 30 previously described *Lissodesmus* species in the form of the femoral process of the gonopod telopodite, which is tripartite with an erect distal branch and two posteromedially curving basal branches. Despite careful searching, the new species has only been collected by pitfall trapping and may have a very small range in the northwest corner of the Central Plateau in Tasmania, Australia.

Keywords

Australia, Dalodesmidae, Diplopoda, Polydesmida, Tasmania

Introduction

The genus *Lissodesmus* Chamberlin, 1920 currently includes 19 species in Tasmania and 11 species in Victoria; see Mesibov (2018) for a genus synonymy and list of species. Although the Tasmanian *Lissodesmus* fauna has been well sampled over many years (Fig. 1A), a narrow-range alpine species was only first collected in 2017 (Mesibov 2018) and additional narrow-range species probably remain to be discovered.

The new *Lissodesmus* species described in this paper might represent another category of undescribed Tasmanian millipedes: possibly more widely distributed, but unusually cryptic. It was pitfall-trapped at a single location in the summers of 2017, 2018 and 2019, but has not yet been collected by hand in the pitfall area, despite careful searching.

Copyright *Robert Mesibov*. This is an open access article distributed under the terms of the Creative Commons Attribution License (CC BY 4.0), which permits unrestricted use, distribution, and reproduction in any medium, provided the original author and source are credited.

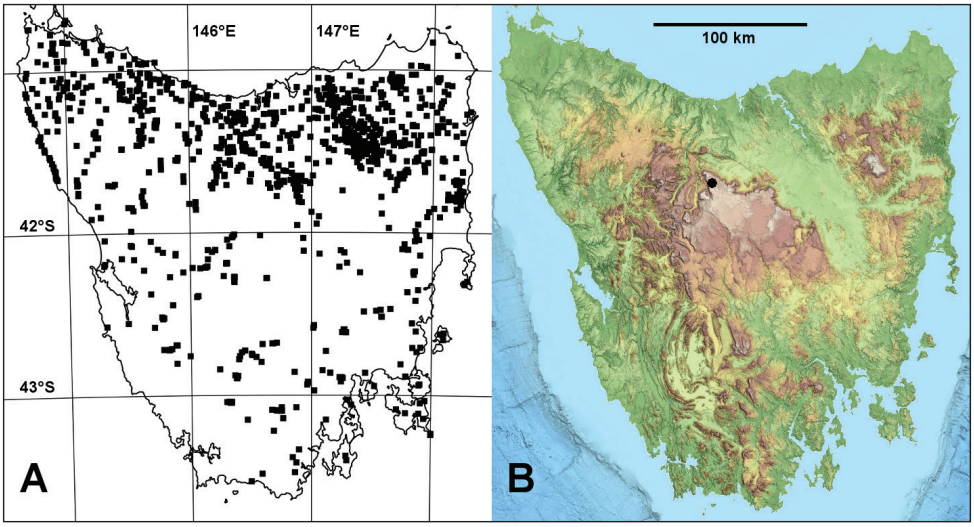

Figure 1. *Lissodesmus* localities in Tasmania (excluding Bass Strait islands) **A** localities for *Lissodesmus* specimens identified to species (black squares) from *Atlas of Living Australia* (https://collections.ala.org.au/public/show/dr444, accessed 10 January 2019) **B** locality for *L. piscator* sp. nov. (black circle) on coloured relief map from *theLIST* (https://maps.thelist.tas.gov.au/listmap/app/list/map) State of Tasmania. Mercator projections.

Materials and methods

Pitfall trapping

Pitfall traps were set and emptied by Michael Driessen of the Department of Primary Industries, Parks, Water and Environment (DPIPWE), Tasmania. The trapping was part of a wildfire recovery study following a fire that burned from January to March 2016 and covered ca. 26,000 ha south and west of Lake Mackenzie, a hydroelectric impoundment at the northwest corner of Tasmania's Central Plateau (Natural Values Conservation Branch 2017). Post-fire monitoring studies of flora and fauna were initiated shortly after the fire had been brought under control.

The pitfall traps were set on Ritters Plain (Fig. 2), ca. 2.5 km west of Lake Mackenzie and ca. 1 km south of the Fisher River gorge. Each trap was a 225 ml plastic cup placed with its rim flush with the ground surface in a short section of 75 mm PVC pipe fitted snugly in a hole drilled with an auger. The traps were placed in each of three burn categories: unburned vegetation and unburned peat, burned vegetation and unburned peat (lightly burned) and burned vegetation and burned peat (deeply burned). Ten traps were irregularly placed a minimum of 5 m apart in each category, reflecting the patchy nature of the burn. Each trap cup was filled with 100 ml of 70% ethanol over a few ml of glycerol, covered with a rain shield and left for 14 days in the late austral summer: 20 February – 6 March 2017, 22 February – 8 March 2018 and 20 February – 6 March 2019.

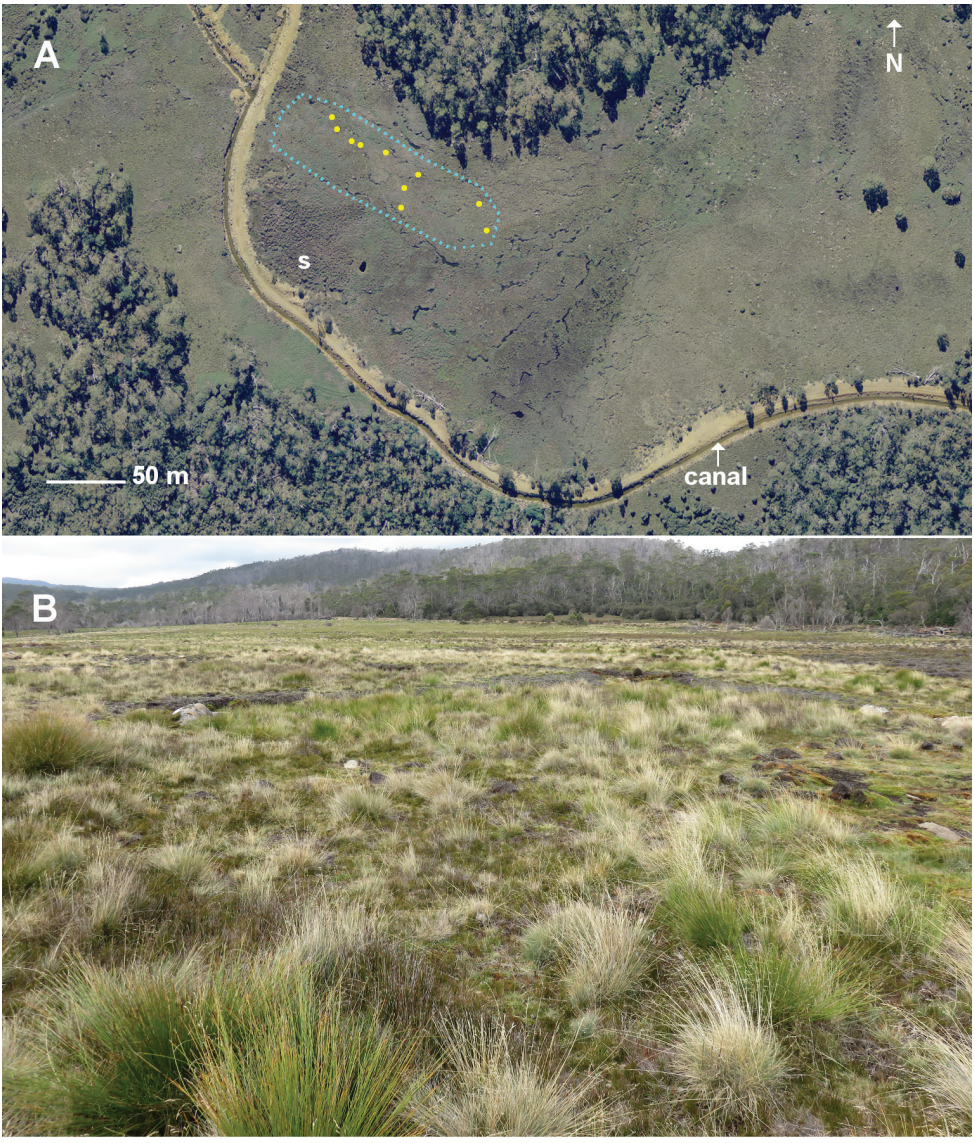

Figure 2. Ritters Plain pitfall area and surrounds **A** pre-fire aerial photo (14 April 2014) showing the pitfall area (blue dotted line), locations of pitfall traps with *Lissodesmus piscator* sp. nov. (yellow dots), a dense shrubbery of *Richea scoparia* (**s**) and the canal draining this portion of the Plain **B** view to the southeast on 28 March 2019 from a point near the western end of the pitfall area.

Millipedes and other invertebrates in the traps were sorted for DPIPWE by Kevin Bonham, who sent specimens of an unfamiliar *Lissodesmus* to the author for identification in May 2018.

Millipede searches

I searched the Ritters Plain pitfall area and the nearby grassy sedgeland and subalpine forest unsuccessfully for fresh material of the new *Lissodesmus* on 8 December 2018 and on 20 February, 11 March and 28 March 2019, for a total of ca. 8.5 hours over ca. 20 ha. I collected representative specimens of other millipede species on each visit. Microhabitats examined included woody litter, bark litter, leaf litter, grass and sedge turf, and the spaces under stones and under prostrate (rock-hugging) shrubs. I also excavated small deposits of peaty soil underlying elevated *Sphagnum* moss mounds on the south side of the Plain.

Specimen preparation

All specimens of the new *Lissodesmus* species are stored in 80% ethanol in the Queen Victoria Museum and Art Gallery. The paratype male was briefly treated with vinegar to reduce its stiffness. Specimens were examined and measured using a Nikon SMZ800 binocular dissecting microscope. Focus-stacks of colour images were manually generated using a Canon EOS 1000D digital SLR camera mounted on the Nikon SMZ800 fitted with a beam splitter, then processed with Zerene Stacker 1.04 software. The gonopods of a male from 2018 pitfall trapping were cleared in 80% lactic acid, temporarily mounted in a 1:1 glycerol:water mixture and imaged using an eyepiece video camera mounted on an Amscope binocular microscope. Preliminary drawings were traced from printed copies of the images, then corrected by reference to the actual gonopods. Figures were composed using GIMP 2.8 and the map in Fig. 1A with QGIS 2.14.

Specimen locality data are provided in Supplement material 1 in Darwin Core format. Pitfall trap locations were provided by Michael Driessen as a site map based on a georegistered aerial photograph (see Fig. 2A). Locations of the 10 traps yielding the new *Lissodesmus* species have been spatially summarised as -41.6824 146.3524 ±75 m (WGS84 datum).

The terminology of gonopod telopodite parts follows Mesibov (2006).

Repositories, institutional acronyms, or institutional abbreviations: **QVMAG,** Queen Victoria Museum and Art Gallery, Launceston, Tasmania.

Results

Pitfall trapping

Twelve specimens of a new *Lissodesmus* species (described below) were found in five 2017 traps, five 2018 traps, and one 2019 trap (Fig. 2A). Four of the traps were in lightly burned ground and six in unburned ground; one unburned-ground trap location had a single specimen in each of 2017 and 2018. In three trapping seasons, the traps also yielded eight specimens of *Paredrodesmus monticolus* Mesibov, 2003 (Poly-

desmida, suborder Dalodesmidea), two of *Australeuma simile* Golovatch, 1986 (Chordeumatida, Metopidiotrichidae), and one each of *Amastigogonus fossuliger* Verhoeff, 1944 (Spirostreptida, Iulomorphidae) and *Atrophotergum montanum* Mesibov, 2004 (Polydesmida, Dalodesmidae).

Millipede searches

As mentioned in the Materials and methods section, I found no *Lissodesmus* specimens in or near the pitfall area. However, I had little difficulty finding the four other trapped species, as well as four more: *Gasterogramma psi* Jeekel, 1982 and "M20" (both Polydesmida: Dalodesmidae, the latter undescribed but recorded elsewhere in northwest Tasmania), an unidentified *Procyliosoma* sp. (Sphaerotheriida, Procyliosomatidae) and the undescribed but well-recorded siphonotid "AcuMes" (Polyzoniida: Siphonotidae).

Order Polydesmida Pocock, 1887
Suborder Dalodesmidea Hoffman, 1980
Family Dalodesmidae Cook, 1896

***Lissodesmus piscator* sp. nov.**
http://zoobank.org/50E0322D-8436-4443-A613-8E644A695995
Figs 3, 4

Holotype. AUSTRALIA • male; Tasmania, Central Plateau, Ritters Plain; [41.6824°S 146.3524°E]; 1080 m a.s.l.; 6 Mar. 2019; M. Driessen leg.; pitfall PU9 20 Feb.–6 Mar. 2019; coordinates are center of cluster of pitfall traps yielding *L. piscator* sp. nov. in 2017, 2018, 2019; coordinate uncertainty 75 m; QVMAG: QVM:2019:23:0015.

Paratype. AUSTRALIA • male; same data as for holotype; dissected; QVMAG: QVM:2019:23:0016.

Other material. 5 males, 4 females and 1 stadium 7 female, same locality as holotype; see Supplement material 1 for details.

Diagnosis. Distinguished from all other known *Lissodesmus* species by the form of the femoral process on the gonopod telopodite: the process has an erect, flattened, bluntly toothed distal branch and two large basal branches curving posteromedially across the posterior face of the telopodite.

Description. Male/female approximate measurements: length 15/20 mm, midbody vertical diameter 1.3/1.6 mm, midbody width across paranota 1.7/1.7 mm. Colour in alcohol almost uniformly pale, antennae roseate (Fig. 3A).

Male with clypeus and frons moderately setose, vertex sparsely setose. Antennal sockets separated by ca. 2.5X socket diameter. Antenna short, just reaching ring 3 when manipulated backwards; relative length of antennomeres 6 > (2,3) > (4,5), antennomere 6 widest. Head approx. as wide as tergite 4, cardines in dorsal view

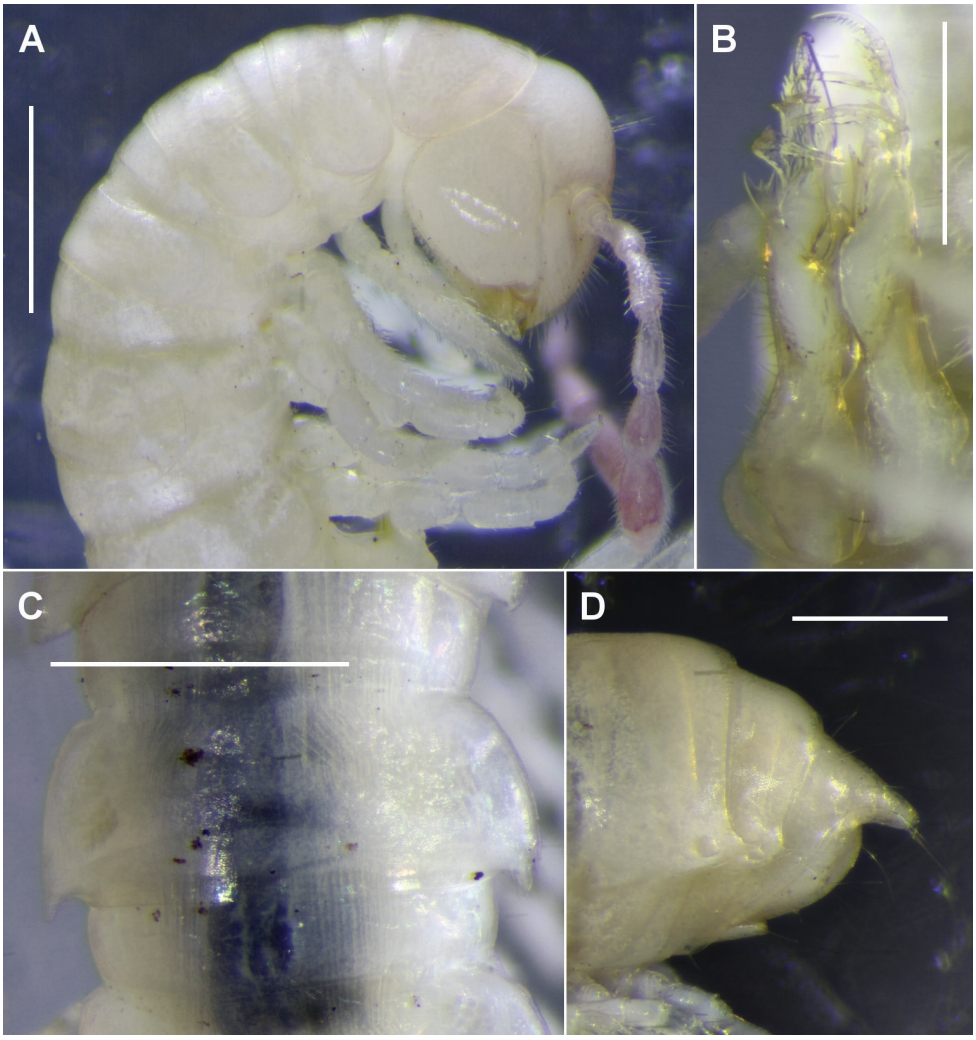

Figure 3. *Lissodesmus piscator* sp. nov., holotype (**A, D**) and paratype (**B, C**) **A** right lateral view of head and anterior rings **B** ventral and slightly left-lateral view of gonopods in situ **C** dorsal view of midbody rings **D** left lateral view of telson. Scale bars 1.0 mm (**A, C**); 0.5 mm (**B, D**).

quadrate in outline; collum narrower than head and tergite 2; anterior collum margin gently convex, curvature extending smoothly to slightly convex lateral margin; posterior margin more or less straight; corners bluntly pointed. Tergite width increasing gradually from rings 2–6, then subequal, then decreasing 17–19. Waist pronounced (Fig. 3C), with faint longitudinal striations. Prozonites and metazonites with faint cellular sculpturing; limbus composed of narrow, distally tapered tabs. Paranota (Fig. 3C) smooth, narrow (ratio of overall width to prozonite width ca. 1.2 on midbody ring); anterior shoulder gently curving into slightly convex lateral mar-

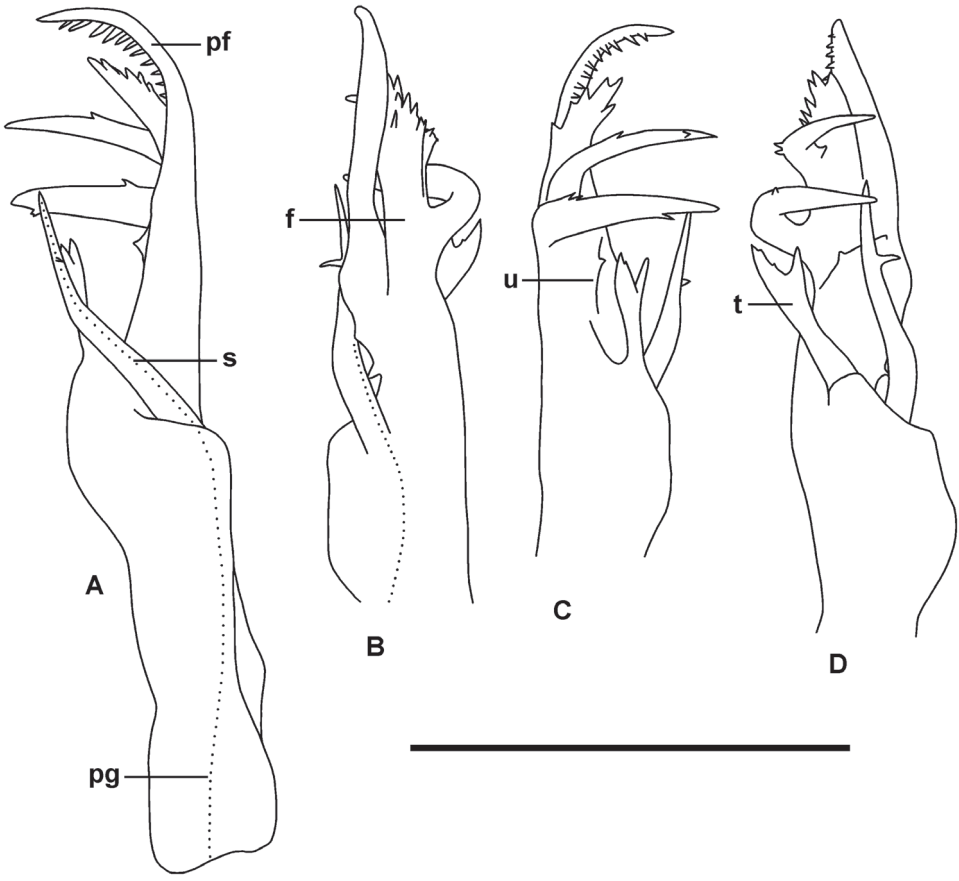

Figure 4. *Lissodesmus piscator* sp. nov., QVM:2018:23:0053. Right gonopod telopodite in medial (**A**) anterior (**B**) lateral (**C**) and posterior (**D**) views. Abbreviations: f = femoral process, pf = prefemoral process, pg (dotted line) = prostatic groove, s = solenomere, t = tibiotarsus, u = uncus. Setation not shown. Scale bar 0.5 mm.

gin, the latter with a small notch posteriorly and with short seta on anterior corner of notch; posterior corner upturned, extending just past posterior metatergite margin on most rings, usually with small subterminal seta; posterior corner seta prominent, erect (broken off on some rings). Ozopore small, round, opening dorsally close to paranotal margin and anterior to posterior corner; pore formula 5, 7, 9, 10, 12, 13, 15–19. Spiracles on diplosegments small, round, not emergent; rims slightly raised above pleural surface; posterior spiracle approx. midway between leg bases. Sternites approx. as long as wide, with short, sparse setae; transverse impression more pronounced than longitudinal. Legs short, ca. 0.9x as long as maximum ring diameter at midbody; legpairs 3–9 with prefemur slightly swollen dorsally; relative podomere lengths tarsus > (femur, prefemur) > (postfemur, tibia) on midbody legs;

tarsus straight, ca. 1.3x as long as femur. From legpair 3, sphaerotrichomes on femur, postfemur, tibia and tarsus, densest on tibia and tarsus; sphaerotrichome numbers rapidly diminishing posteriorly but with a few sphaerotrichomes on tibia and tarsus of posterior legs; no sphaerotrichomes on last two legpairs; each sphaerotrichome hemispherical with tapering, blunt-tipped seta inclined distoventrally. Dense brush setae with slightly expanded tips on prefemur and femur of anterior legs; brush setae disappearing posteriorly. Pre-anal ring (Fig. 3D) with sparse, long setae; hypoproct trapezoidal, dorsal margin straight; epiproct extending past anal valves, tapering to truncate tip ca. 1/10 maximum width of ring 19; spinnerets in square array in shallow cavity just ventral to epiproct tip.

Gonopore small, opening mediodistally on only slightly enlarged leg 2 coxa. Bases of legs 6 and 7 well-separated by shallowly concave sternite, bases of legs 5 closer; brushes of sparse, long setae on sternites just medial to coxae of legs 5, 6, 7. Aperture ovoid, wider than long, ca. 1/2 width of ring 7 prozonite, rim slightly raised laterally and posteriorly.

Gonopods: Gonocoxae truncate-conical, lightly joined distomedially. Telopodite (Figs 3B, 4) slender, erect, extending to leg 5 bases when retracted; moderately setose on posterolateral surface from base to level of tibiotarsus origin. Solenomere (Fig. 4, s) slender, tapering, arising anteromedially at 1/3-1/2 telopodite height and terminating at ca. 3/4 telopodite height; directed posterodistally, slightly bent laterally at ca. 2/3 solenomere height, with small, medially directed, subapical tooth. Prostatic groove (Fig. 4, pg) running on anteromedial surface of telopodite to solenomere base, opening at solenomere tip. Tibiotarsus (Fig. 4, t) arising at ca. 1/2 telopodite height in large, anteromedial flange on telopodite; directed distolaterally above thickening on telopodite surface, slightly flattened anteroposteriorly, terminating in wide "Y" at level of subapical tooth on solenomere. Prefemoral process (Fig. 4, pf) tapering distally to bluntly rounded, posteriorly curved tip; subapically with posteroventral comb of 10-12 strong, well-spaced teeth; uncus (Fig. 4, u) at ca. 1/2 prefemoral process height, oblique, with small medial tooth; a small, sharp tooth on mediobasal surface of prefemoral process. Femoral process (Fig. 4, f) arising on anterolateral surface of prefemoral process, closely appressed to distal portion of latter; divided into erect distal branch, slightly expanded distally with small, blunt, marginal and submarginal teeth, the branch terminating just below level of prefemoral process tip; and 2 stout, well-separated basal branches curving posteriorly and medially, the most basal branch reaching and almost touching the solenomere tip, both branches with a few small teeth.

Female closely resembling male but stouter. Genital aperture with posterior margin gently convex medially; cyphopods not examined.

Name. Latin *piscator*, fisherman, noun in apposition, for the type locality in the Fisher River catchment.

Distribution. So far known only from Ritters Plain near Lake Mackenzie in northwest Tasmania (Figs 1B, 2). The Plain has a habitat area of ca. 100 ha and a known occupied area of less than 1 ha.

Discussion

In what microhabitats are *L. piscator* sp. nov. living?

Ritters Plain is almost entirely treeless (Fig. 2). Most of the Plain is covered by a tightly intergrown turf of grass and sedge species overlying a dense, fibrous, anaerobic peat, mixed with patches of slightly elevated *Sphagnum* bog (Department of Primary Industries, Parks, Water & Environment 2016, Natural Values Conservation Branch 2017). Annual rainfall at nearby Lake Mackenzie is ca. 2100 mm and snow lies on the Plain during the winter months. For much of the year the soil is saturated with water. The pitfall area was probably even wetter before a canal (Fig. 2A) was constructed in the 1960s on the uphill side of the Plain to capture additional water for the Fisher River hydroelectric project.

There are no above-ground shelters near the pitfall traps in which *L. piscator* sp. nov. was found, so the population is probably living underground, either in crevices in the root-filled turf or in cavities among the periglacially shattered rock fragments that cover much of this portion of the Central Plateau and underlie the peaty soil. Adults might be expected to come to the surface to mate and disperse during late summer — when the pitfall trapping was carried out — and 11 of the 12 specimens trapped were adults.

The densest populations of millipedes I found by searching on Ritters Plain were in surface peat associated with elevated *Sphagnum* moss mounds, such as the ones surrounding the lower parts of *Richea scoparia* stems just to the southwest of the pitfall area (s in Fig. 2A). The foliage and fine branches of the *Richea* were burned in the 2016 fire, but many of the lower stems buried in moss were still alive in 2019. The moss mounds themselves, with and without *Richea*, were largely unburned. In the peat close to the moss I frequently found *G. psi* and *Procyliosoma* sp., and occasionally small groups of *P. monticolus* and *A. fossuliger*. I was surprised not to find *L. piscator* sp. nov. in the peat as well, since *Lissodesmus* spp. cohabit with *Gasterogramma* spp. elsewhere in Tasmania.

Does *L. piscator* sp. nov. have a very narrow range, or is it unusually cryptic, or both?

I collected repeatedly above ca. 1000 m in the Lake Mackenzie area in the period 1985-2007, finding the polydesmidans *A. montanum*, *G. psi*, *P. monticolus* and *Bromodesmus rufus* Mesibov, 2004 (Dalodesmidae), but no *Lissodesmus* species. The only previous *Lissodesmus* records from the catchments of the Fisher River and its tributary the Little Fisher River are for the common northwest Tasmanian species *L. perporosus* Jeekel, 1984 at somewhat lower elevations (to 920 m; records in *Atlas of Living Australia*, https://collections.ala.org.au/public/show/dr444; accessed 10 January 2019). The nearest high-elevation *L. perporosus* locality is ca. 12 km to the east of Ritters Plain, at ca. 1150 m (higher than Ritters Plain) in the headwaters of Western Creek.

If *L. piscator* sp. nov. is largely a subterranean species, the fact that it has not yet been hand-collected is not surprising. It is unlikely that it only occurs in the small

portion of Ritters Plain that coincidentally was sampled with pitfalls in the post-fire recovery study. I suspect that it also occurs nearby in the voids in the periglacial scree deposits that cover slopes with boulder-sized rocks in the northwest corner of the Central Plateau. Sampling in the screes would be even more difficult than setting pitfall traps over a wide area, and the true distribution and conservation status of *L. piscator* sp. nov. are likely to remain indeterminate.

Acknowledgements

I thank Michael Driessen (Department of Primary Industries, Parks, Water and Environment, Tasmania) and Kevin Bonham (Hobart, Tasmania) for the specimens of *L. piscator* sp. nov. and for answering many questions about the pitfall study. Many thanks also to Sergei Golovatch and Zoltán Korsós for reviewing a draft of the manuscript.

References

Department of Primary Industries, Parks, Water & Environment (2016) Lake Mackenzie Alpine Fire Impacts Workshop, 8 June 2016. Nature Conservation Report Series 16/2. https://dpipwe.tas.gov.au/Documents/Lake%20Mackenzie%20Fire%20Workshop%20Final%20161010.pdf [accessed 31 January 2019]

Mesibov R (2006) The millipede genus *Lissodesmus* Chamberlin, 1920 (Diplopoda: Polydesmida: Dalodesmidae) from Tasmania and Victoria, with descriptions of a new genus and 24 new species. Memoirs of Museum Victoria 62(2): 103–146. https://doi.org/10.24199/j.mmv.2005.62.4

Mesibov R (2018) A new, alpine species of *Lissodesmus* Chamberlin, 1920 from Tasmania, Australia (Diplopoda, Polydesmida, Dalodesmidae). ZooKeys 754: 103–111. https://doi.org/10.3897/zookeys.754.25704

Natural Values Conservation Branch (2017) Assessment of the ecological impacts of the 2016 Mersey Forest Fire Complex, Nature Conservation Report no 17/5. Department of Primary Industries, Parks, Water & Environment, Hobart. http://dpipwe.tas.gov.au/Documents/Mersey_Forest_Fire_Impact_Report_Final_170802.pdf [accessed 31 January 2019]

Supplementary material 1

Specimen data for *Lissodesmus piscator* sp. nov.

Authors: Robert Mesibov

Data type: occurrence

Explanation note: Data file Specimen_data_Lissodesmus_piscator_2019.tsv for 12 specimen lots of Lissodesmus piscator sp. nov. in the Queen Victoria Museum and Art Gallery, Launceston, Tasmania, Australia. The file is a tab-separated table in UTF-8 encoding with the following Darwin Core fields: institutionCode, catalogNumber, phylum, class, order, family, genus, specificEpithet, scientificName, typeStatus, organismRemarks, locality, country, stateProvince, decimalLatitude, decimalLongitude, geodeticDatum, coordinateUncertaintyInMeters, georeferenceSources, georeferencedBy, georeferenceRemarks, minimumElevationInMeters, recordedBy, eventRemarks and eventDate.

Copyright notice: This dataset is made available under the Open Database License (http://opendatacommons.org/licenses/odbl/1.0/). The Open Database License (ODbL) is a license agreement intended to allow users to freely share, modify, and use this Dataset while maintaining this same freedom for others, provided that the original source and author(s) are credited.

Link: https://doi.org/10.3897/zookeys.846.35028.suppl1

ZooKeys 846: 43–53 (2019)
doi: 10.3897/zookeys.846.34003
http://zookeys.pensoft.net

RESEARCH ARTICLE

A peer-reviewed open-access journal
ZooKeys
Launched to accelerate biodiversity research

Three new species in the leafhopper tribe Drabescini (Hemiptera, Cicadellidae, Deltocephalinae) from southern China

Zhou Yu[1], Mick Webb[2], Ren-huai Dai[1], Mao-fa Yang[1]

1 *Institute of Entomology, Guizhou University; The Provincial Key Laboratory for Agricultural Pest Management Mountainous Region, Guiyang, Guizhou 550025, China* **2** *Department of Entomology, The Natural History Museum, Cromwell Road, London SW7 5 BD, UK*

Corresponding author: *Ren-huai Dai* (rhdai69@163.com)

Academic editor: *James Zahniser* | Received 20 February 2019 | Accepted 27 March 2019 | Published 16 May 2019

http://zoobank.org/9874E631-5AAE-4E34-815B-100217FEA356

Citation: Yu Z, Webb M, Dai R-h, Yang M-h (2019) Three new species in the leafhopper tribe Drabescini (Hemiptera, Cicadellidae, Deltocephalinae) from southern China. ZooKeys 846: 43–53. https://doi.org/10.3897/zookeys.846.34003

Abstract

Three new species of the leafhopper tribe Drabescini: *Drabescus bilaminatus* **sp. n.**, *Drabescus multipunctatus* **sp. n.**, and *Parabolopona robustipenis* **sp. n.** are described and illustrated from southern China. A key and checklist to the species of *Parabolopona* are also provided.

Keywords

China, Drabescini, morphology, taxonomy

Introduction

In a review of the largest leafhopper subfamily, Deltocephalinae, Zahniser and Dietrich (2013) partly followed Dmitriev (2004) and included two groups previously included in Selenocephalinae, i.e., Drabescina and Paraboloponina as subtribes of Drabescini. Both groups have nymphs with long appendages on the pygofer (that do not persist into the adult stage). However, Drabescina are large, robust, the body mainly black or grey, antennal ledges are very strong, and frontoclypeus has a striate or rugose texture

Copyright *Zhou Yu et al.* This is an open access article distributed under the terms of the Creative Commons Attribution License (CC BY 4.0), which permits unrestricted use, distribution, and reproduction in any medium, provided the original author and source are credited.

(that persists into the adult stage). Therefore, in the adult stage these characters are the main features to separate the two groups while the transverse striations or carinae on the fore margin of the head distinguish the two groups from most other leafhoppers. Since a revision of the two groups by Zhang and Webb (1996) several new taxa have been described, mainly from China. In the current work a further two new species of *Drabescus* Stål and one new species of *Parabolopona* Matsumura, from China, are described and illustrated.

Materials and methods

Specimens were collected by sweep net. The external morphology was illustrated and described under a stereo microscope of Olympus SZX7. The images of adults were taken with a system of KEYENCE VHX-1000. Genitalia were drawn with Adobe Illustrator CS6 and Adobe Photoshop CS6.

Male genitalia were prepared by placing in the boiling solution of 8–10% NaOH for 1–2 min or in the cold solution for 12 hr, rinsed 1–2 times in the fresh water, then transferred into glycerine on glass slides for examination and dissection under an Olympus SZX7 stereo microscope. The structures of genitalia and abdomen were placed into fresh glycerine and stored in micro vials along with the specimens for the further examination.

The specimens studied are deposited in the Institute of Entomology, Guizhou University, Guiyang, Guizhou, China (**GUGC**) except where indicated.

Taxonomy

Drabescus Stål, 1870

Type species. *Bythoscopus remotus* Walker, 1851

Diagnosis. Overall coloration brown to black often with contrasting yellow marking on head and thorax. Body more or less robust, wedge-shaped. Crown short and broad, with transverse ridge on front, the latter slightly arched forward. Ocelli marginal, distant from eye. Face with antenna situated above midline of eye, moderately long (very long in immature); antennal ledge strong; anteclypeus nearly triangular, broad at base; laterofrontal sutures extended to corresponding ocellus. Hind femur with apical setae 2+1, 2+1+1, or 2+2+1. Male pygofer side with or without macrosetae and with or without a posterior process or marginal serrations. Connective usually Y-shaped. Subgenital plate triangular or elongate with digitate apex, usually with short fine setae marginally on ventral surface. Aedeagus with or without basal processes; gonopore apical on ventral surface.

Remarks. *Drabescus* is the largest genus in the subtribe Drabescina containing 60 species in the Old World tropics of which 34 species are from China (mainly southern China).

***Drabescus bilaminatus* sp. n.**
http://zoobank.org/660BE687-C6E3-453A-9647-A4ECBC39A452
Figs 1–9

Diagnosis. Overall colour yellowish brown with numerous dark spots on the forewings. Subgenital plate wrinkled at apex. Aedeagal shaft with large flange on each side of ventral surface extending sub-basally to near apex.

Description. Vertex approximately 1.3x as long medially than next to eyes. Ocelli separated by ca. 4 x own diameter from adjacent eye. Hind femur with apical setae 2+2+1.

Male genitalia. Pygofer side nearly quadrilateral with long stout serrated ventral process directed dorsally; without macrosetae (Fig. 4). Valve triangular, nearly 2 x as wide as medial length. Subgenital plate elongate triangular with very short, wrinkled at apex; with short fine setae marginally on ventral surface (Fig. 5). Connective with stem short, 1/2 long as arms (Fig. 9). Style slender throughout length, without distinct lateral lobe (Fig. 6). Aedeagal shaft elongate, cylindrical, evenly curved dorsally, with large flange on each side of ventral surface extending sub-basally to near apex; dorsal surface with few fine teeth (Figs 7, 8).

Length (including tegmen). ♂, 11.6 mm.

Material examined. Holotype: ♂, CHINA: Guangxi province, Huaping National Nature Reserve, 18.V.2012, Zhi-hua Fan leg. Paratype: 1 ♂, data same as holotype.

Remarks. This new species is similar to *D. ineffectus* (Walker) but can be distinguished by its larger lateral flanges of the aedeagus, narrower style and shorter stem of the connective.

Etymology. The new species name is an adjective derived from a combination of the Latin words *bi* and *lamina*, referring to the laminate (thin) flanges on the aedeagus.

Distribution. China (Guangxi Province).

***Drabescus multipunctatus* sp. n.**
http://zoobank.org/662F3FA6-93BC-4F7F-8EF5-B2AC246BF1E7
Figs 10–18

Diagnosis. Overall colour yellowish brown with numerous fine dark spots; costal area of forewing yellow (Fig. 10). Pygofer side with long stout serrated ventral process directed dorsally. Aedeagal shaft with a long single crest-like dorsomedial flange on the dorsal surface (Figs 16, 17).

Description. Vertex approximately as long as next to eyes. Ocelli marginal, situated between two transverse ridges, separated by ca. 3 x own diameter from adjacent eye (Fig. 10). Hind femur with apical setae 2+2+1.

Male genitalia. Pygofer side slightly longer than wide; apically evenly rounded except for long stout serrated ventral process directed dorsally; without macrosetae (Fig. 13). Valve semicircular, approximately 2 x as wide as medial length. Subgenital plate elongate, triangular with short digitate apex, with short fine setae marginally on ven-

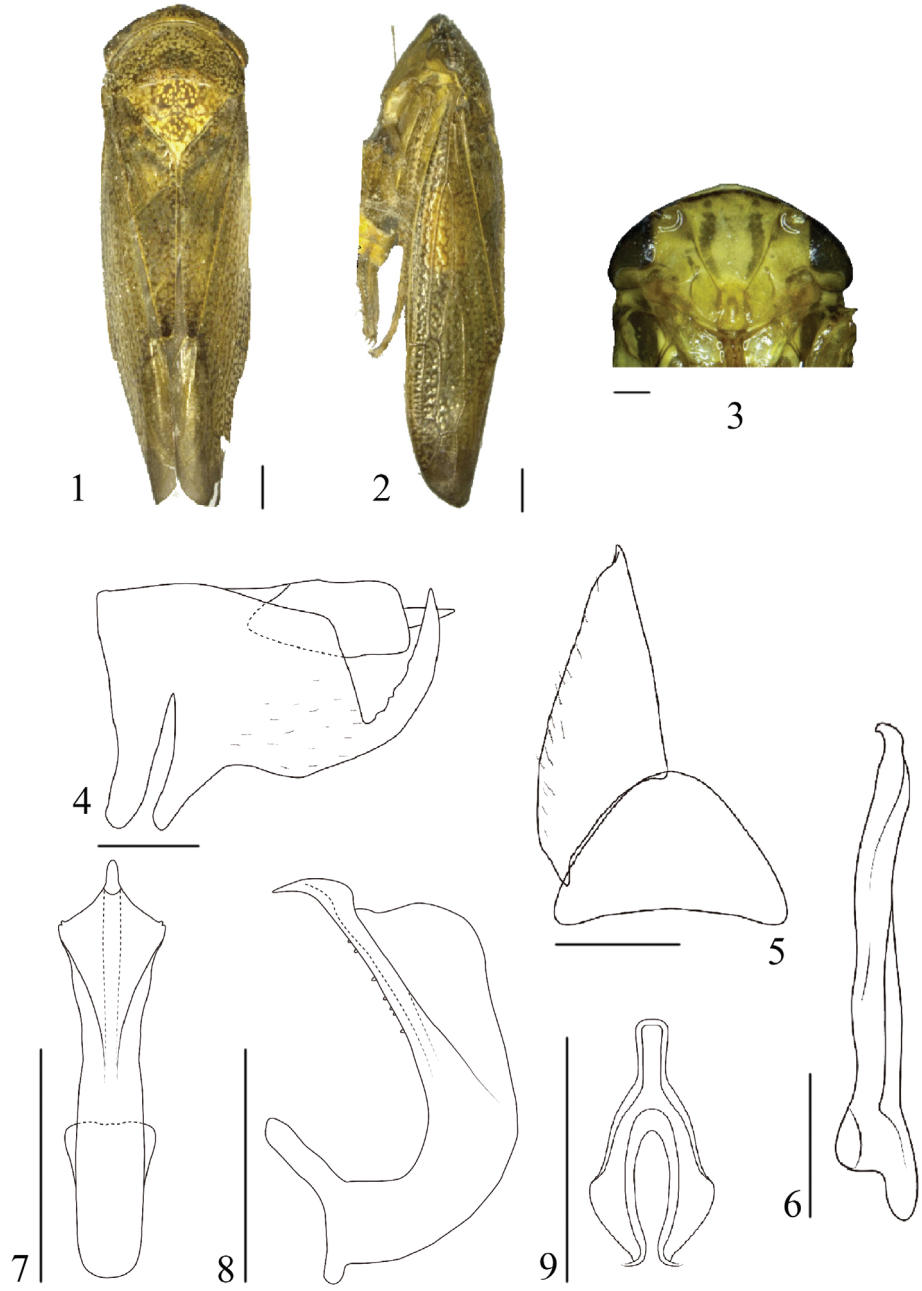

Figures 1–9. *Drabescus bilaminatus* sp. n. holotype **1** dorsal view **2** lateral view **3** face **4** pygofer, lateral view **5** valve and subgenital plate, ventral view **6** style, ventral view **7** aedeagus, ventral view **8** aedeagus, lateral view **9** connective, ventral view. Scale bars: 1.0 mm (**1, 2**); 0.5 mm (**3–9**).

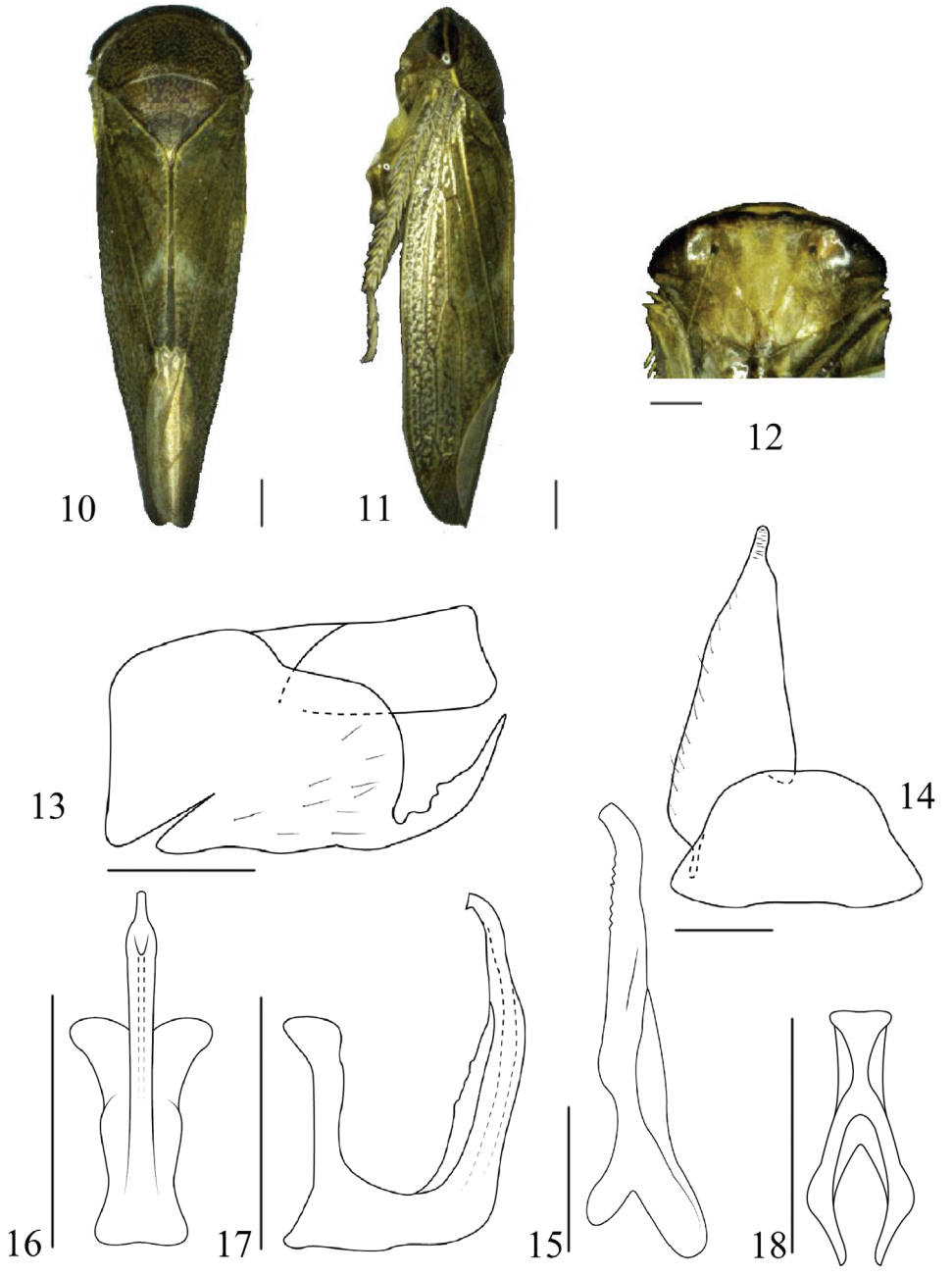

Figures 10–18. *Drabescus multipunctatus* sp. n. holotype **10** dorsal view **11** lateral view **12** face **13** pygofer, lateral view **14** valve and subgenital plate, ventral view **15** style, ventral view **16** aedeagus, ventral view **17** aedeagus, lateral view **18** connective, ventral view. Scale bars: 1.0 mm (**10, 11**); 0.5 mm (**12–18**).

tral surface (Fig. 14). Connective with stem as long as arms (Fig. 18). Style relatively slender throughout length, lateral lobe absent, apex curved inward with few serrations subapically on inner surface (Fig. 15). Aedeagal shaft elongate, cylindrical, sharply turned dorsally sub-basally, dorsal surface with a long single crest-like dorsomedial flange (Figs 16, 17).

Body length (including tegmina). ♂, 10.7mm.

Material examined. Holotype: ♂, CHINA: Hainan Province, Jianfeng ridge, Nanwang forest, 22.IV.2014, Wei-cheng Yang leg.

Remarks. The new species can be distinguished by the shape of the aedeagus with abruptly angled shaft sub-basally and with a long single crest-like dorsomedial flange.

Etymology. The new species name is an adjective derived from the Latin words *multi* and *punctatum* referring to the many fine dark spots on the body.

Distribution. China (Hainan Province).

Parabolopona Matsumura, 1912

Parabolopona Matsumura, 1912: 288; Webb, 1981: 41; Zhang and Webb 1996: 19; Cai and Shen 1999: 28; Shang and Zhang 2007: 430; Dai et al. 2016: 394.

Type species. *Parabolopona guttata* Uhler, 1896

Diagnosis. Body yellow to yellowish green, with or without pair of orange bands on vertex and pronotum; forewings with few small brown spots. Head with anterior margin rim-like; vertex approximately twice as long medially than next to eyes with fore margin obliquely rounded, shagreen. Face with antenna situated near upper corner of eye; antennal ledge strong, antennal pits encroaching onto postclypeus; latero-frontal sutures extended to corresponding ocellus; anteclypeus rectangular. Pronotum as wide as crown with many fine transverse striations. Hind femur with apical setae 2+2+1. Male pygofer without processes. Valve nearly triangular. Subgenital plate triangular or semicircular with fine ventral setae. Connective Y-shaped with strongly produced stem apex; separated from aedeagus by membrane. Aedeagus with or without basal apodeme; shaft relatively short with or without processes, gonopore apical on ventral surface. Second valvulae with very fine dorsal teeth.

Remarks. *Parabolopona* is one of several genera in the subtribe Paraboloponina. The genus contains eleven species, of which ten have been recorded from China (see checklist below).

Checklist of genus *Parabolopona*

P. basispina Dai, Qu & Yang, 2016: 394. Figs 19, 20. China (Hainan).
P. robustipenis sp. n. Figs 21, 22. China (Hainan).

P. chinensis Webb, 1981: 45. Figs 23, 24. China (Hubei, Sichuan, Shanxi).
P. cygnea Cai & Shen, 1999: 28. Figs 25, 26. China (Henan, Guizhou, Shanxi).
P. guttata (Uhler, 1896: 291). Figs 27, 28. Japan, Philippines, China (Taiwan).
P. ishihari Webb, 1981: 45. Figs 29, 30. Japan, China (Shanxi, Yunnan, Hubei).
P. luzonensis Webb, 1981: 46. Figs 31, 32. Philippines, China (Zhejiang, Guizhou).
P. mutabilis Ohara & Kogure, 2012: 205. Figs 10, 14. Japan.
P. quadrispinosa Shang & Zhang, 2006: 33. Figs 33, 34. China (Yunnan, Guangxi).
P. webbi Zahniser & Dietrich, 2013: 181. Figs 35, 36. China (Taiwan).
P. yangi Zhang, Chen & Shen, 1995: 11. Figs 37, 38. China (Guangdong).
P. zhangi Meshram, Shashank & Srinivasa, 2016: 184, 185. Figs 2–22. India.

Key to species of *Parabolopona* (males)

1 Aedeagus without processes (Figs 37, 38) ..... ***P. yangi***
– Aedeagus with processes **2**
2 Aedeagal shaft very short and robust in both lateral and ventral view (Figs 21, 22) ..... ***P. robustipenis* sp. n.**
– Aedeagal shaft not very short and robust in both lateral and ventral view **3**
3 Aedeagal shaft with two pairs of processes (Figs 33, 34) ..... ***P. quadrispinosa***
– Aedeagal shaft with one pair of processes **4**
4 Aedaegal processes very long, arising from base of shaft **5**
– Aedaegal processes short to moderately long, arising ventrally from base of shaft or midlength **6**
5 Aedeagal shaft broad distally in lateral view (Figs 19, 20) ..... ***P. basispina***
– Aedeagal shaft narrow distally in lateral view ..... ***P. zhangi***
6 Aedeagal with processes arising near midlength, closely attached to each other ..... ***P. mutabilis***
– Aedeagal processes divergent, arising from base of shaft 7
7 Aedaegal shaft broadened apically in lateral view (Figs 31, 32) .. ***P. luzonensis***
– Aedaegal shaft not broadened apically in lateral view **8**
8 Apex of aedaegal shaft branched **9**
– Apex of aedaegal shaft unbranched **11**
9 Aedeagal shaft straight in lateral view (Figs 35, 36) ..... ***P. webbi***
– Aedeagal shaft evenly curved in lateral **10**
10 Connective straight and narrow apically (Figs 23, 24) ..... ***P. chinensis***
– Connective expanded apically (Figs 27, 28) ..... ***P. guttata***
11 Aedeagal shaft with a pair of lateral triangular flanges in ventral view (Figs 25, 26) ..... ***P. cygnea***
– Aedeagal shaft without flanges (Figs 29, 30) ..... ***P. ishihari***

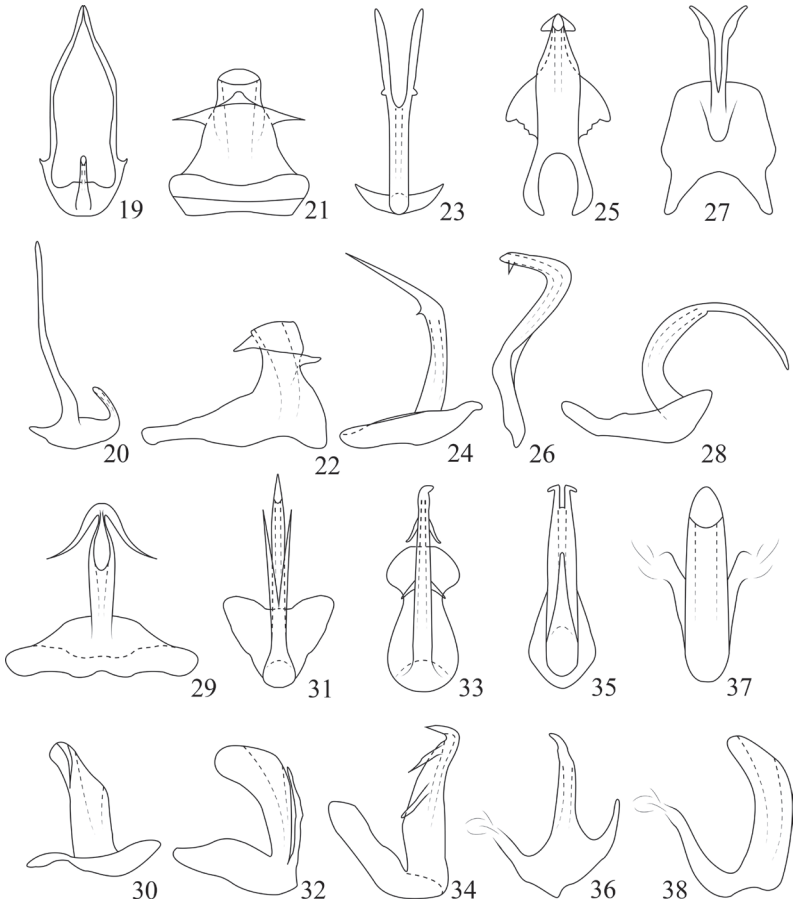

Figures 19–38. *Parabolopona* species **19, 20** *P. basispina*, aedeagus, ventral and lateral view **21, 22** *P. robustipenis* sp. nov., aedeagus, ventral and lateral view **23, 24** *P. chinensis*, aedeagus, ventral and lateral view **25, 26** *P. cygnea*, aedeagus, ventral and lateral view **27, 28** *P. guttata*, aedeagus, ventral and lateral view **29, 30** *P. ishihari*, aedeagus, ventral and lateral view **31, 32** *P. luzonensis*, aedeagus, ventral and lateral view **33, 34** *P. quadrispinosa*, aedeagus, ventral and lateral view **35, 36** *P. webbi*, aedeagus, ventral and lateral view **37, 38** *P. yangi*, aedeagus, ventral and lateral view.

Parabolopona robustipenis sp. n.

http://zoobank.org/80A10A6D-B4FB-491F-91C7-FA7E1B97EE0E
Figs 39–48

Diagnosis. Body yellowish green. Vertex and pronotum with a pair of orange longitudinal bands. Forewing with few small dark brown spots. Connective with stem about four times longer than arms, with strong dorsal keel, apical extension long. Aedeagus with shaft very short and robust (Fig. 45).

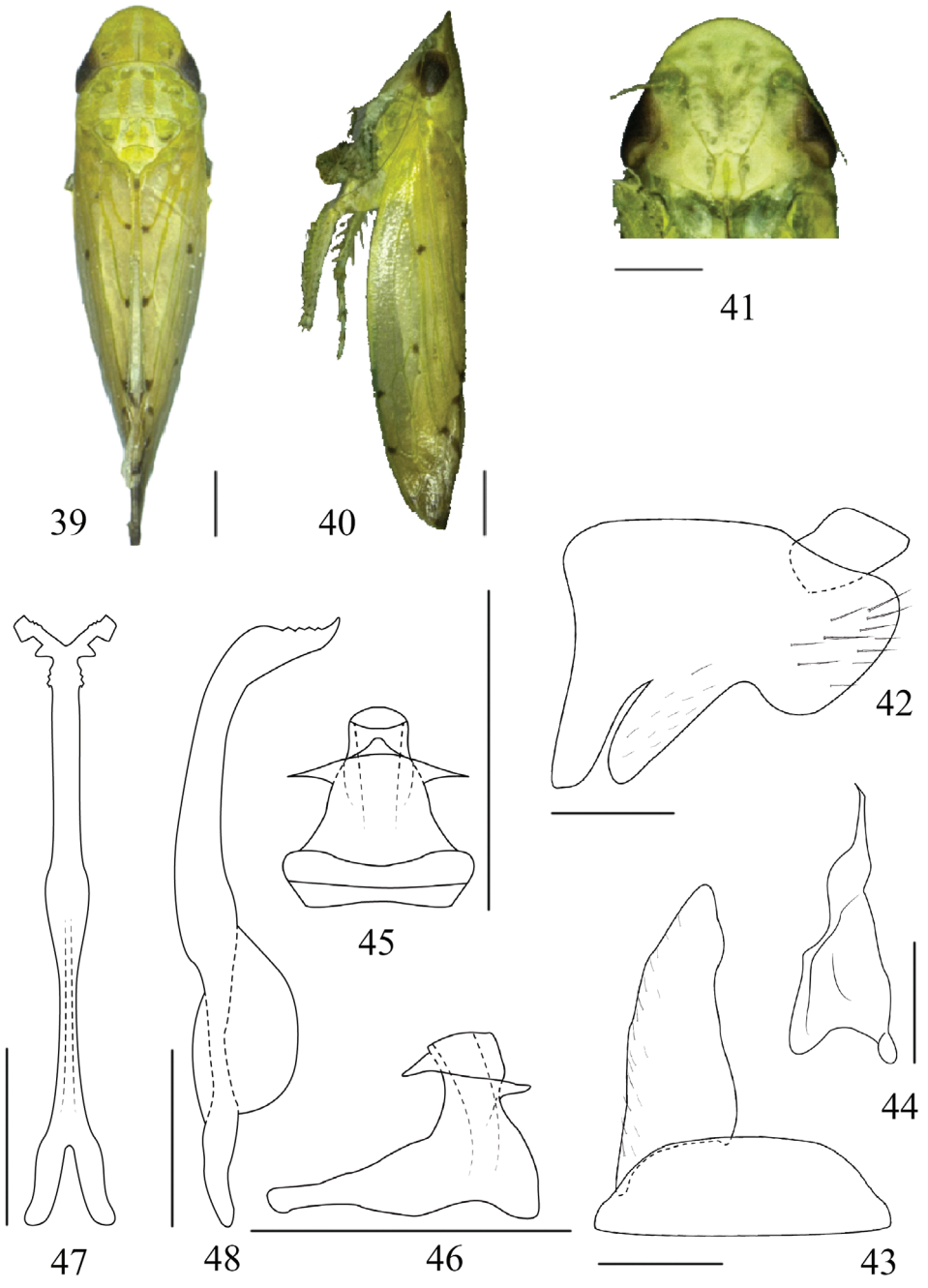

Figures 39–48. *Parabolopona robustipenis* sp. n. holotype **39** male dorsal view **40** male lateral view **41** male face **42–48** male genitalia **42** pygofer, lateral view **43** valve and subgenital plate, ventral view **44** style, ventral view **45** aedeagus, ventral view **46** aedeagus, ventral view **47** connective, ventral view **48** connective, lateral view. Scale bars: 1.0 mm (**39, 40**); 0.5 mm (**41–48**).

Description. Vertex approximately 2 x as long medially than next to eyes (Fig. 39). Ocelli marginal, separated by ca. 2 x own diameter from adjacent eye. Hind femur with apical setae 2+2+1.

Male genitalia. Pygofer side with ventral margin strongly indented; with several fine setae distally (Fig. 42). Valve semicircular, approximately 3 x as wide as medial length. Subgenital plate elongate triangular with inner margin sinuate (Fig. 43). Connective with stem about four times longer than arms, with strong dorsal keel, apical extension long, bifurcate apically with upturned serrated branches (Figs 47, 48). Style apical process very slender, tapered to acute apex; lateral lobe prominent (Fig. 44). Aedeagus with shaft very short and robust (Fig. 45), with a short triangular shaped process subapically on dorsal surface and a lamellate processes on each side subapically, gonopore apical (Fig. 46).

Length (including tegmen). ♂, 8.4 mm; ♀, 8.2–8.6 mm.

Material examined. Holotype: ♂, CHINA: Hainan Province, Donger station, Bawang ridge, 15.IV.2014, collected by Jian-kun Long and Hai-yan Sun. Paratypes: 3 ♂♂, data same as holotype; 16 ♂♂ 2♀♀, Donger station, Bawang ridge, Hainan province, 22.IV.2014, Wei-cheng Yang, Hai-yan Sun leg. (GUGC and The Natural History Museum, London).

Remarks. The new species differs from other species of the genus in the shape of the male genitalia, particularly the very short and broad aedeagal shaft with a short triangular shaped process subapically on dorsal surface and a lamellate processes on each side subapically.

Etymology. The new species name is a noun derived from the Latin words *robustus* and *penis* referring to the robust aedeagus in this species.

Distribution. China (Hainan province).

Acknowledgements

We are grateful to Ling Qu, Zhi-hua Fan, Wei-cheng Yang, Jian-kun Long, and Hai-yan Sun (Institute of Entomology, Guizhou University, Guiyang, China) for their kindly offering the materials examined in this study. The project supported by Science and Technology Foundation of Guizhou Province (J-[2015] 2041), The Program of Excellent Innovation Talents, Guizhou Province, China (No. 20164022).

References

Cai P, Jiang JF (2002) A new species of *Drabescus* Stål from Henan Province, China (Homoptera: Cicadelloidea: Selenocephalinae). In: Shen XC, Zhou Y (Eds) Insects of the Mountains Taihang and Tongbai Regions. China Agricultural Science and Technology Press, Beijing, 18–19.

Cai P, Shen XC (2002) Homoptera: Cicadellidae. In: Shen XC, Zhou Y (Eds) Insects of the Mountains Taihang and Tongbai Regions. China Agricultural Sci-Tech Press, Beijing, 269–279.

Dai RH, Qu L, Yang MF (2016) A new leafhopper species of *Parabolopona* and a new record for *Favintiga camphorae* from China (Hemiptera: Auchenorrhyncha: Cicadellidae: Deltocephalinae: Drabescini). Entomologica Americana 122(3): 393–397. https://doi.org/10.1664/1947-5144-122.3.393

Kuoh CL (1992) Homoptera: Cicadellidae. Insects of the Hengduan mountains region, Vol. 1. Science Press, Beijing, 865 pp.

Kuoh CL (1985) New species of *Drabescus* and a new allied genus (Homoptera: Iassidae). Acta Zoologica Sinica 31(4): 377–383.

Li ZZ (1992) Agriculture and Forestry Insect Fauna of Guizhou Vol.1 (Homoptera: cicadellidae). Guizhou People Press, Guiyang, 284–286.

Li ZZ, Wang LM (2005) Cicadellidae: Hecalinae, Coediinae, Iassinae, Typhlocybinae Euscelinae, Nirvaninae and Evacanthinae. In: Jin DC, Li ZZ (Eds) Landscape insects of Xishui. Guizhou Science Press, Guiyang, 159–190.

Meshram NM, Shashank PR, Srinivasa N (2016) New records of the genus *Parabolopona* Matsumara (Hemiptera: Cicadellidae: Deltocephalinae), with description of a new species from India. Zootaxa 4114(2): 182–188. https://doi.org/10.11646/zootaxa.4114.2.7

Ohara N, Kogure K (2012) A new species of the genus *Parabolopona* (Hemiptera: Cicadellidae: Deltocephalinae: Drabescini) from the Central Ryukyus, Japan. Japanese Journal of Systematic Entomology 18(2): 203–208.

Shang SQ, Zhang YL (2012) Review of leafhopper genus *Drabescus* with description of a new species from China (Hemiptera: Selenocephalinae). Chinese Science Paper Online, 641 pp.

Shang SQ, Webb MD, Zhang YL (2014) Key to Chinese species of the leafhopper genus *Drabescus* (Hemiptera: Cicadellidae: Deltocephalinae) with description of a new species. Zootaxa 3852(1): 141–146. https://doi.org/10.11646/zootaxa.3852.1.7

Wang JJ, Qu L, Xing JC, Dai RH (2016) Three new species of the leafhopper genus *Drabescus* Stål (Hemiptera: Cicadellidae: Deltocephalinae) from China. Zootaxa 4132(1): 118–126. https://doi.org/10.11646/zootaxa.4132.1.10

Zahniser JN, Dietrich C (2013) A review of the tribes of Deltocephalinae (Hemiptera: Auchenorrhyncha: Cicadellidae). European Journal of Taxonomy 45: 1–211. https://doi.org/10.5852/ejt.2013.45

Zhang YL, Zhang WZ, Chen B (1997) New species of Subfamily Selenocephalinae of Funiushan from Henan Province. Entomotaxonomia 19(4): 235–245.

Zhang YL, Zhang WZ, Chen B (1997) Selenocephaline leafhoppers (Homoptera: Cicadellidae) from Mt. Funiushan in Henan Province. Entomotaxonomia 19(4): 235–245.

Zhang YL, Webb MD (1996) A revised classification of the Asian and Pacific Selenocephaline Leafhoppers (Homoptera: Cicadellidae). Bulletin of the Natural History Museum (Entomology) 65(1): 1–103.

ZooKeys 846: 55–64 (2019)
doi: 10.3897/zookeys.846.32568
http://zookeys.pensoft.net

RESEARCH ARTICLE

A peer-reviewed open-access journal
ZooKeys
Launched to accelerate biodiversity research

New species and new records of the genus *Deinopteroloma* Jansson, 1946 (Coleoptera, Staphylinidae, Omaliinae) from China

Zhi-Fei Cheng[1], Liang Tang[1], Li-Zhen Li[1], Zhong Peng[1]

1 *Department of Biology, College of Life Sciences, Shanghai Normal University, Shanghai, 200234, P. R. China*

Corresponding author: *Zhong Peng* (pz0617@163.com)

Academic editor: *J. Klimaszewski* | Received 20 December 2018 | Accepted 4 February 2019 | Published 16 May 2019

http://zoobank.org/7779F153-75E1-4493-9727-A7FB402BC829

Citation: Cheng Z-F, Tang T, Li L-Z, Zhong Peng Z (2019) New species and new records of the genus *Deinopteroloma* Jansson, 1946 (Coleoptera, Staphylinidae, Omaliinae) from China. ZooKeys 846: 55–64. https://doi.org/10.3897/zookeys.846.32568

Abstract

New morphological, taxonomic and faunistic data of the genus *Deinopteroloma* Jansson, 1946 from China are provided. Two species are described and illustrated: *D. songi* Peng & L.-Z. Li, **sp. n.** (Xizang: Pailong) and *D. spinigerum* Peng & L.-Z. Li, **sp. n.** (Hunan: Mangshan). New provincial records are provided for *D. hamatum* Smetana, 1996 from Anhui, Zhejiang and Jiangxi, *D. obtortum* Assing, 2015 from Sichuan, and *D. tricuspidatum* Smetana, 1996 from Zhejiang.

Keywords

Coleoptera, Staphylinidae, Omaliinae, *Deinopteroloma*, China, taxonomy, new species, new records

Introduction

New morphological, taxonomic and faunistic data on the genus *Deinopteroloma* Jansson, 1946 includes 26 species distributed in Palaearctic and Oriental regions, with 12 of them known from China. The *Deinopteroloma* fauna of Sichuan with eight described species is currently the most diverse of all Chinese provinces (Assing 2015; Shavrin and Smetana 2016).

In recent years, we obtained numerous *Deinopteroloma* specimens collected during several field trips. Five species were identified, two of which are described and illustrated in the present study.

Copyright *Zhi-Fei Cheng et al.* This is an open access article distributed under the terms of the Creative Commons Attribution License (CC BY 4.0), which permits unrestricted use, distribution, and reproduction in any medium, provided the original author and source are credited.

Material and methods

The examined material is deposited in the following public collections:

SNUC Insect Collection of Shanghai Normal University, Shanghai, China
CNC Canadian National Collection of Insects, Ottawa, Canada

The genitalia and other dissected parts were mounted on plastic slides and attached to the same pin as the respective specimens. Photographs were taken with a Canon EOS 7D camera with a MP-E 65 mm macro lens or with a Canon G9 camera mounted on an Olympus CX31 microscope.

The following abbreviations were used in the text, with all measurements in millimeters:

BL Body length: length of body from apices of mandibles to abdominal apex.
FL Forebody length: length of forebody from the anterior margin of the mandibles to the posterior margin of the elytra.
HL Head length: length of head from anterior margin of frons to posterior constriction of head.
HW Head width: maximum width of head.
AnL Antenna length: length of antenna from base of antennomere I to apex of antennomere XI.
PL Pronotum length: length of pronotum along midline.
PW Pronotum width: maximum width of pronotum.
EL Elytral length: length at suture from apex of scutellum to posterior margin of elytra.
EW Elytral width: combined width of elytra.
AL Length of aedeagus: length of aedeagus from apex of longer paramere to base of aedeagal capsule.

The type labels were cited with the original spelling; different labels are separated by slashes.

Results

***Deinopteroloma hamatum* Smetana, 1996**
(Figs 1, 2A–D, 5)

Deinopteroloma hamatum Smetana, 1996: 79.
Deinopteroloma hamatum: Smetana 2001: 57, Shavrin and Smetana, 2016: 227.

Type material examined. Paratype ♂ [teneral]: "KUATUN FUKIEN, China 21.4.46, (TSCHUNG SEN.) / PARATYPUS, *Deinopteroloma hamatum*, A. Smetana 1995 [yellow label]" (CNC).

Additional material examined. (9 ♂♂, 6 ♀♀). **China: Anhui:** 2 ♂♂, 2 ♀♀, Huang Shan, Jiulongpu, 30°06'N, 118°12'E, 460–910 m, 26.XI.2011, Zhong Peng leg. (SNUC); 1 ♂, 1 ♀, Guniujiang, 360–420 m, 30.IV.2005, Tang & Hu leg. (SNUC); 2 ♂♂, Guniujiang, 950–1050 m, 28.IV.2005, Tang & Hu leg. (SNUC). **Zhejiang:** 1 ♂, Anji, Longwang Shan, 950–1200 m, 25.VI.2004, Tang & Hu leg. (SNUC); 1 ♀, Anji, Longwang Shan, 350–550 m, 24.VI.2006, Jin-Wen Li leg. (SNUC); 1 ♂, Anji, Longwang Shan, Qianmutian, 1450 m, 30°23'N, 119°26'E, 14.V.2013, Li & Zheng leg. (SNUC); 1 ♂, 1 ♀, Zhuji, Dongbai Shan, 300 m, 31.III.2013, Tie-Xiong Zhao leg. (SNUC); 1 ♂, Qingyuan County, Baishanzu, 1700 m, 27°45'25"N, 119°12'06"E, 2.V.2014, Zhong Peng leg. (SNUC); **Jiangxi:** 1 ♀, Sanqing Shan, 800 m, 4.V.2005, Tang & Hu leg. (SNUC).

Comparative notes. The original description was based on three type specimens from Guadun, Fujian (Smetana 1996). Considerable interspecific variability of *D. hamatum* was observed not only in external characters such as body size, coloration, punctation, and shapes of head, pronotum and elytra (Fig. 1), but also in the shape of parameres and internal structures of aedeagus (Fig. 2A, B). The shape of the posterior margin of the male tergite VIII is constant (Fig. 2D). It is recorded here from Anhui, Zhejiang and Jiangxi for the first time. Some specimens were sifted from wet leaves and moss on the rocks near a stream at altitudes from about 460 to 910 m (Fig. 5).

Deinopteroloma obtortum Assing, 2015

(Figs 2E, 6)

Deinopteroloma obtortum Assing, 2015: 1225.
Deinopteroloma obtortum: Shavrin and Smetana, 2016: 228.

Material studied. China: Sichuan: 1 ♂, Xiaojin County, Jiajin Shan, 30°48'49"N, 102°42'55"E, 2490 m, 30.VII.2016, Zhou, Jiang, Liu & Gao leg. (SNUC).

Comment. The original description was based on two type specimens from Min Shan, Gansu (Assing 2015). It is recorded from Sichuan for the first time. For illustrations of *D. obtortum* see figure 2E and figures 7–8, 15–18, 23–25 in Assing (2015). The specimen was sifted from leaf litter near the mountain track in mixed deciduous forests at an altitude of 2490 m (Fig. 6).

Deinopteroloma songi Peng & L.-Z. Li, sp. n.

http://zoobank.org/E941914F-A912-4E89-9C78-C125CC234D4D
(Figs 3, 7)

Type material. Holotype ♂: China: Xizang Prov., Linzhi County, Pailong, 30°02'N, 95°00'E, 13.IV.2017 2100 m, Xiao-Bin Song leg. / Holotypus ♂ *Deinopteroloma songi* sp. n., det. Peng & Li. 2018 (SNUC). Paratypes: 6 ♂♂, 10 ♀♀: same label data as holotype / PARATYPE (yellow), *D. songi* sp. nov., det. Peng & Li, 2019 (SNUC).

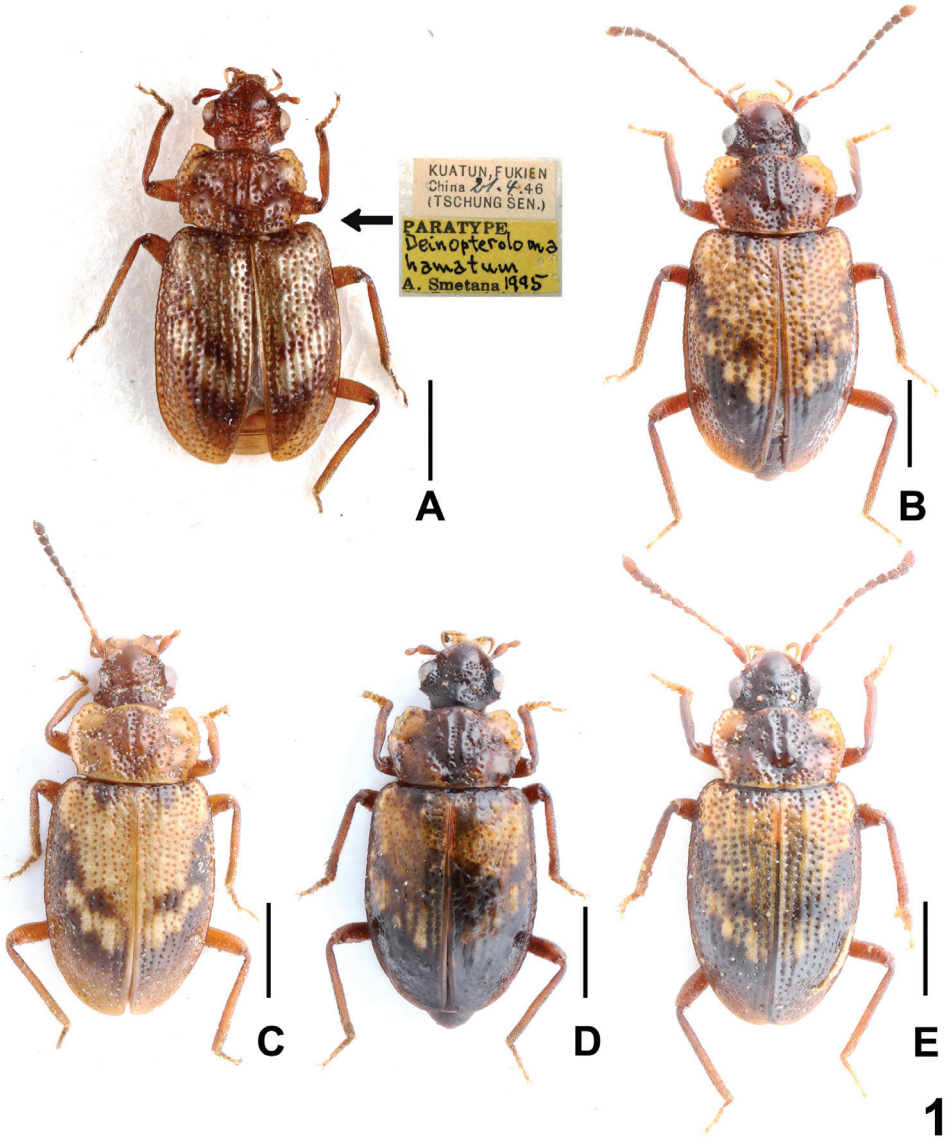

Figure 1. Habitus of *Deinopteroloma hamatum*: **A** paratype, with type labels, **B–E** male (**B** Anhui; **C–E** Zhejiang). Scale bars: 1.0 mm.

Description. Measurements (in mm) and ratios: BL 3.50–3.73, FL 3.44–3.65, HL 0.59–0.67, HW 0.78–0.83, AnL 1.68–1.78, PL 0.83–0.93, PW 1.30–1.47, EL 1.92–2.09, EW 1.50–1.67, AL 0.98–1.08, HL/HW 0.76–0.87, HW/PW 0.56–0.64, HL/PL 0.71–0.77, PL/PW 0.63–0.68, EL/EW 1.25–1.29.

Habitus as in Fig. 3A. Coloration: Body dark-brown; pronotum with broadly dark-yellowish lateral margins; each elytron with 3 or 4 yellowish brown tubercles;

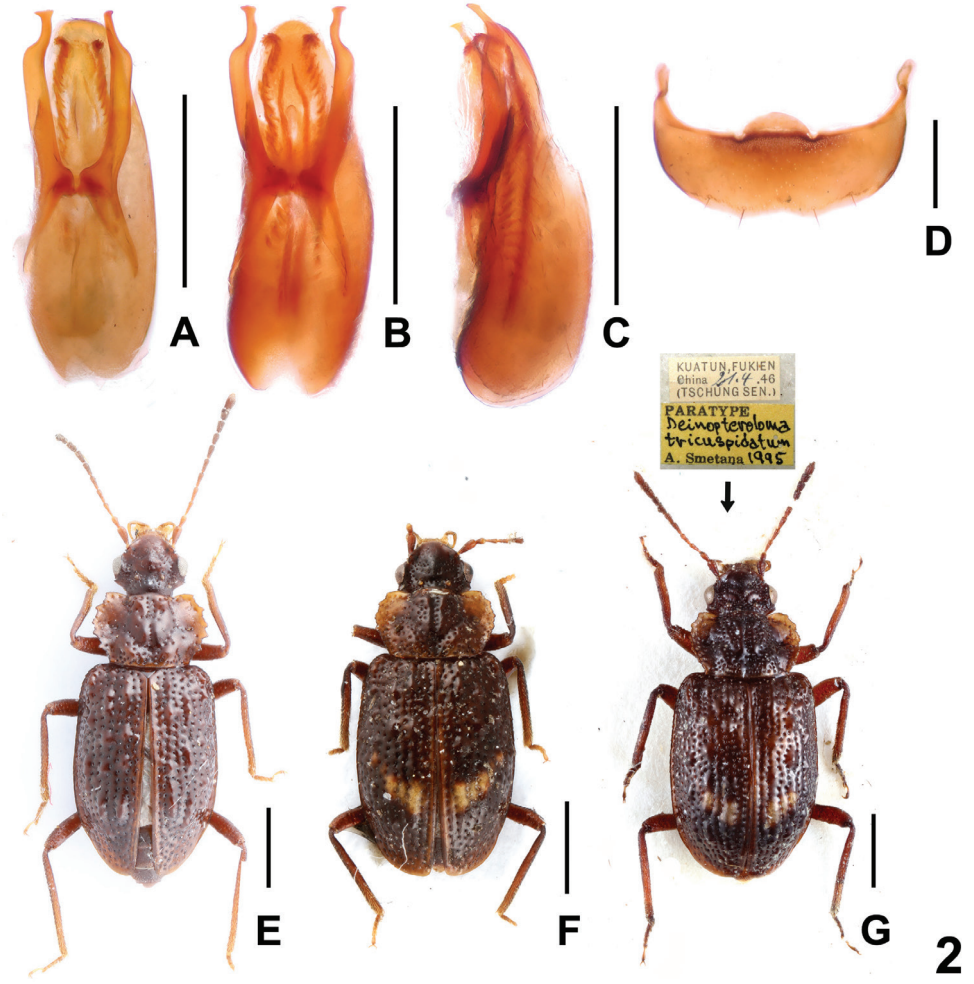

Figure 2. *Deinopteroloma hamatum* (**A–D**): **A–B** aedeagus in ventral view, **C** aedeagus in lateral view, **D** male sternite VIII. Habitus of *Deinopteroloma* spp (**E–G**): **E** *D. obtortum*, **F** *D. tricuspidatum*, **G** paratype of *D. tricuspidatum*, with type labels. Scale bars: 0.5 mm(**A–D**), 1.0 mm (**E–G**).

antenna with antennomeres I–IV yellowish and V–VIII gradually more infuscate apically, VIII–XI blackish-brown; maxillary palpi dark-yellowish.

Head transverse; posterior part of clypeus and vertex distinctly elevated, with indistinct lateral impressions in middle part and semicircular deep impression in front of ocelli, infraorbital ridges slightly impressed; eyes large and convex; small acute postocular ridge situated away from posterior margin of eye; ocelli large; frons smooth and glossy. All antennomeres longer than broad; measurements of antennomeres (length): I: 0.22; II: 0.14; III–VII: 0.16; VIII: 0.13; IX–X: 0.11; XI: 0.19.

Pronotum distinctly transverse; lateral margins finely crenulate and with somewhat regular outline; lateral portions strongly impressed; disc of pronotum with wide,

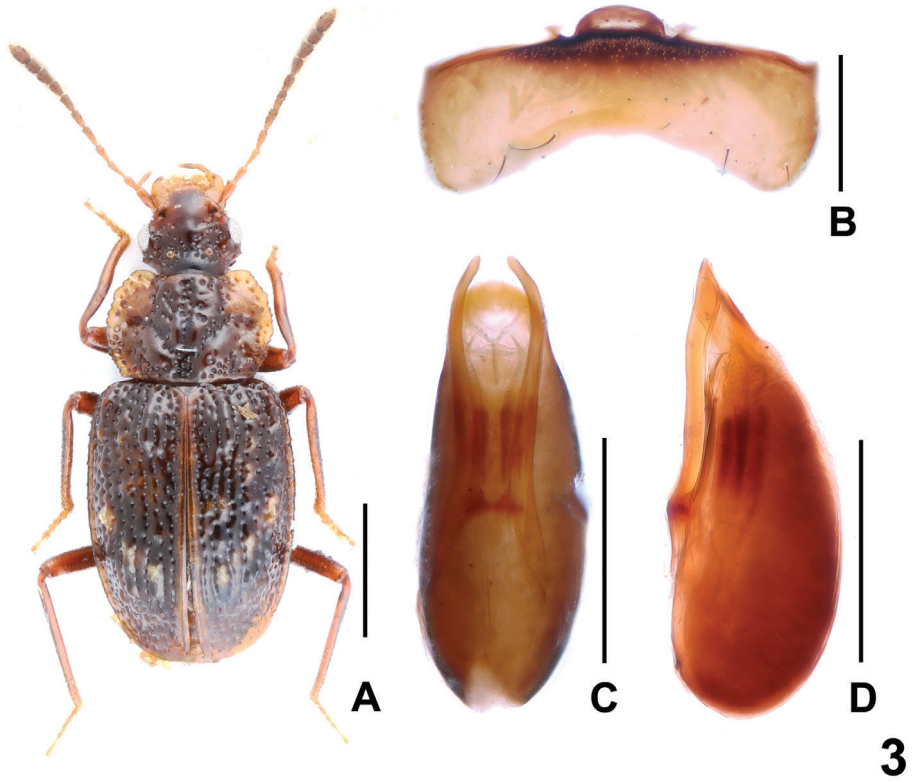

Figure 3. *Deinopteroloma songi* sp. n. **A** Habitus of paratype, **B** male sternite VIII, **C** aedeagus in ventral view, **D** aedeagus in lateral view. Scale bars: 1.0 mm (**A**), 0.5 mm (**B–D**).

very convex middle elevation and with distinct longitudinal impression; punctation coarse, rather dense in posteromedian portions, sparser in anteromedian and lateral portions, and very irregular and scattered in median portion.

Elytra without distinct longitudinal ridges; suture elevated in posterior two thirds; punctation coarse and arranged in partly irregular series (except in posterior portion of elytra); each elytron with approximately 3 or 4 smooth tubercles. Hind wings present.

Male. Protarsomeres I–IV very weakly dilated; sternites III–VII unmodified; sternite VIII (Fig. 3B) distinctly transverse, posterior margin broadly concave in middle; aedeagus as in Fig. 3C, D, both parameres slender and slightly curved in ventral view, distinctly extending apex of median lobe; internal sac with pair of sclerotized spines.

Female. Protarsomeres I–IV not dilated. Abdominal sternite VIII without posterior excision. Otherwise similar to male.

Comparative notes. Based on the coloration of the body, 6–8 smooth tubercles of the elytra, the presence of pronounced elevations on the pronotum and elytra, as well as the morphology of the aedeagus, the new species is most similar to *D. sextuberculatum* Shavrin & Smetana, 2016, from which it can be distinguished by the darker coloration, the smaller size (*D. sextuberculatum*: 4.25–4.92 mm), the

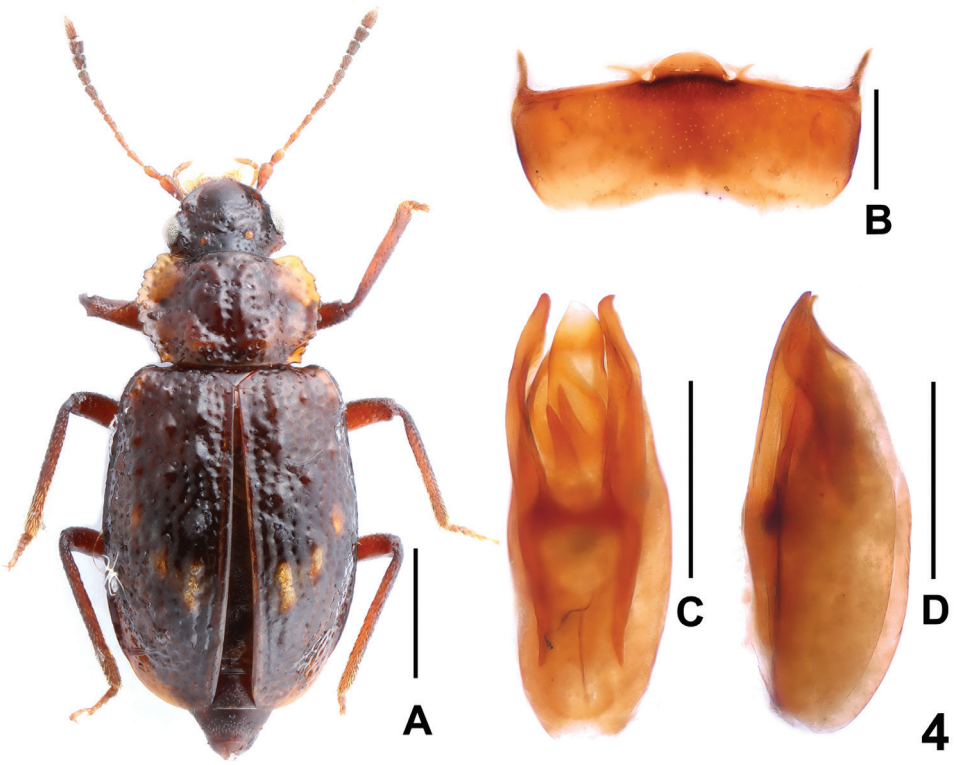

Figure 4. *Deinopteroloma spinigerum* sp. n. **A** Habitus of holotype, **B** male sternite VIII, **C** aedeagus in ventral view, **D** aedeagus in lateral view. Scale bars: 1.0 mm (**A**), 0.5 mm (**B–D**).

shape of the pronotum, the deeper posterior excision of the male sternite VIII and the stouter median lobe of the aedeagus. For illustrations of *D. sextuberculatum* see Shavrin and Smetana (2016).

Distribution and natural history. The type locality is situated in Pailong to the northeast of Linzhi, southern Xizang. The specimens were sifted from leaf litter, moss and mushrooms in broad-leaved forests at an altitude of 2100 m (Fig. 7).

Etymology. Patronymic, named after Xiao-Bin Song, who collected some of the type specimens.

***Deinopteroloma spinigerum* Peng & L.-Z. Li, sp. n.**
http://zoobank.org/AF763E24-11A8-46D2-A04E-DF95595FD2C6
(Figs 4, 8)

Type material. Holotype ♂: China: Hunan Prov., Yizhang County Mangshan N. R., 24°56'26"N, 112°59'18"E, 26.IV.2017 1400 m, Peng, Tu & Zhou leg. / Holotypus ♂ *Deinopteroloma spinigerum* sp. n., det. Peng & Li, 2019 (SNUC).

Figures 5–8. Habitats of *Deinopteroloma* in China: **5** Huang Shan, alt. 460–910 m (*Deinopteroloma hamatum*); **6** Sheng-Nan Liu (right) and De-Yao Zhou (left) collecting *Deinopteroloma obtortum* at Jiajin Shan, Sichuan; **7** Pailong, alt. 2100 m (type locality of *Deinopteroloma songi* sp. n.); **8** Ye-Yue Tu collecting *Deinopteroloma spinigerum* sp. n. at Mangshan, Hunan.

Description. Measurements (in mm) and ratios: BL 4.39, FL 3.89, HL 0.57, HW 0.91, AnL 1.61, PL 0.89, PW 1.33, EL 2.34, EW 1.81, AL 1.13, HL/HW 0.63, HW/PW 0.68, HL/PL 0.64, PL/PW 0.67, EL/EW 1.29.

Habitus as in Fig. 4A. Coloration: Body dark-brown; pronotum with broadly dark-yellowish lateral margins; each elytron with three yellowish-brown tubercles; antenna with antennomeres I–IV light-brown and V–VI gradually more infuscate apically, VII–XI blackish brown; maxillary palpi dark-yellowish.

Head transverse; posterior part of clypeus and vertex moderately elevated, with indistinct lateral impressions in middle part and weak impression in front of ocelli, infraorbital ridges impressed; eyes large and convex; small acute postocular ridge situated away from posterior margin of eye; ocelli large; frons smooth and glossy; antennomeres I–VIII and XI longer than broad; antennomeres IX–X as long as broad; measurements of antennomeres (length): I: 0.17; II: 0.10; III: 0.12; IV–V: 0.11; VI: 0.07; VII: 0.10; VIII–X: 0.08; XI: 0.14.

Pronotum distinctly transverse; lateral margins finely crenulate and with somewhat irregular outline; lateral portions indistinctly impressed; disc of pronotum with wide, very convex middle elevation and with distinct longitudinal impression; punctation

coarse, dense in posteromedian portions, rather sparser in anteromedian and lateral portions, and irregular and scattered in median portion.

Elytra without distinct longitudinal ridges; punctation coarse and arranged in partly irregular series (except in posterior portion of elytra); each elytron with approximately three smooth tubercles. Hind wings probably present.

Male. Abdominal sternites III–VII unmodified; sternite VIII (Fig. 4B) distinctly transverse, posterior margin weakly concave in the middle; aedeagus as in Fig. 4C, D, both parameres with small hook-shaped apex, weakly asymmetric and slender, slightly extending apex of median lobe; internal sac with three sclerotized spines.

Female. Unknown.

Comparative notes. As can be inferred from the similar morphology of the aedeagus, the new species is allied to *D. tricuspidatum* Smetana, 1996 (Fujian: Guadun), from which it differs by the finer punctation of the body, by the presence of three yellowish-brown tubercles on each elytron and the shape of sclerotized spines of the internal sac.

Distribution and natural history. The type locality is situated in Mangshan to the south of Yizhang, southern Hunan. The specimens were sifted from leaf litter in mixed deciduous forests at an altitude of 1400 m (Fig. 8).

Etymology. The specific epithet (Latin, adjective: with spines) alludes to the presence of sclerotized spines in the internal sac of the aedeagus.

Deinopteroloma tricuspidatum Smetana, 1996

(Fig. 2F, G)

Deinopteroloma tricuspidatum Smetana, 1996: 77.
Deinopteroloma tricuspidatum: Smetana 2001: 57, Shavrin and Smetana, 2016: 227.

Type material examined. Paratype ♀: "KUATUN FUKIEN, China 21.4.46, (TSCHUNG SEN.) / PARATYPUS, *Deinopteroloma tricuspidatum*, A. Smetana 1995 [yellow label]" (CNC).

Additional material examined. China: Zhejiang: 1 ♀, Qingyuan County, Baishanzu, 1200–1360 m 5.V.2004, Hu, Tang & Zhu leg. (SNUC).

Comparative notes. *Deinopteroloma tricuspidatum* was previously known from Guadun, Fujian (Smetana 1996). Considerable interspecific variability of *D. tricuspidatum* was observed in body size, punctation and the shape of pronotum (Fig. 2F, G). The shape of head and the morphology of female genital segment are constant. It is recorded from Zhejiang represents for the first time. For illustrations of *D. tricuspidatum* see Fig. 2F, G and Figs 1–3 in Smetana (1996).

Acknowledgements

We thank all collectors and colleagues mentioned in the text for making the specimens they collected available for our study. We are grateful to two anonymous reviewers

for comments on a previous version of the manuscript. The study is supported by the National Natural Science Foundation of China (No. 31201734, 31101659 and No. 31172134), the Foundation of Shanghai Municipal Education Commission (No. 12YZ077 and No. 13YZ062), the 63rd batch of China Postdoctoral Science Fund First Class Funding (No. 307E−9103−00−003094) and Shanghai Normal University (DZL125 and B-9013-11-003127).

References

Assing V (2015) Three new species of *Deinopteroloma* from Vietnam and China (Coleoptera: Staphylinidae: Omaliinae). Linzer Biologische Beiträge 47(2): 1217–1227.

Shavrin AV, Smetana A (2016) Nine new species of the genus *Deinopteroloma* Jansson, 1946 (Coleoptera: Staphylinidae: Omaliinae: Anthophagini) from China and Vietnam. Zootaxa 4196(2): 221–249. https://doi.org/10.11646/zootaxa.4196.2.3

Smetana A (1996) Two new species of *Deinopteroloma* Jansson, 1946 from China (Coleoptera: Staphylinidae: Omaliinae). Koleopterologische Rundschau 66: 77–81.

Smetana A (2001) A new species of *Deinopteroloma* Jansson, 1946 from China, with comments on *D. chiangi* Smetana, 1990 from Taiwan (Coleoptera: Staphylinidae: Omaliinae). Koleopterologische Rundschau 71: 53–57.

ZooKeys 846: 65–73 (2019)
doi: 10.3897/zookeys.846.30391
http://zookeys.pensoft.net

RESEARCH ARTICLE

A peer-reviewed open-access journal
ZooKeys
Launched to accelerate biodiversity research

First record of the genus *Empidideicus* Becker, 1907 (Diptera, Mythicomyiidae) in China and the Oriental Region, with description of a new species

Gang Yao[1], Gao Chen[2]

1 *Jinhua Polytechnic, Jinhua, Zhejiang 321007, China* **2** *Yunnan Key Laboratory for Integrative Conservation of Plant Species with Extremely Small Populations, Kunming Institute of Botany, Chinese Academy of Sciences, Kunming, 650204, Yunnan, China*

Corresponding author: *Gang Yao* (likygang@gmail.com)

Academic editor: *T. Dikow* | Received 7 October 2018 | Accepted 21 March 2019 | Published 16 May 2019

http://zoobank.org/6C6CDE5F-8A05-4DFC-8CB5-659D3F013A88

Citation: Yao G, Chen G (2019) First record of the genus *Empidideicus* Becker, 1907 (Diptera, Mythicomyiidae) in China and the Oriental Region, with description of a new species. ZooKeys 846: 65–73. https://doi.org/10.3897/zookeys.846.30391

Abstract

Empidideicus Becker, 1907 is newly recorded from China and the Oriental Region, with one new species, *E. pentagonius* **sp. n.**, described and illustrated. Observations are provided on the biology of *E. pentagonius* **sp. n.** visiting flowers of *Stemona mairei* (Levl.) Krause (Liliflorae, Stemonaceae). A key to the genera of Mythicomyiidae known to occur in China is provided.

Keywords

Empidideicus, flower visiting, new record, new species, pollinator

Introduction

Mythicomyiidae is a cosmopolitan family in the Bombylioidea with more than 330 described species in 25 extant genera from six subfamilies (Evenhuis 2002). This family has the greatest diversity in semi-arid and arid regions and is strongly associated with flowers. Hitherto, only three genera of Mythicomyiidae have been reported from China: *Mythenteles* Hall & Evenhuis, 1986, *Cephalodromia* Becker, 1914, and *Platypygus* Loew, 1844.

Copyright *Gang Yao, Gao Chen.* This is an open access article distributed under the terms of the Creative Commons Attribution License (CC BY 4.0), which permits unrestricted use, distribution, and reproduction in any medium, provided the original author and source are credited.

Empidideicus Becker, 1907 belongs to the monogeneric subfamily Empidideicinae. So far, 42 species have been described, with 20 species distributed exclusively in the Afrotropical Region and 20 species distributed exclusively in the Palaearctic Region, and two species are distributed in both Afrotropical and Palaearctic regions (Evenhuis 2002, 2007, 2009; Gharali et. al. 2010, 2011, 2015; Hakimian et. al. 2014). The tribe Empidideicini was established by Hull (1973) within the Mythicomyiinae, when he first introduced tribal-level classification into Bombyliidae. Initially four genera, *Empidideicus* Becker, 1907, *Anomaloptilus* Hesse, 1938, *Euanthobates* Hesse, 1965, and *Leylaiya* Efflatoun,1945, were included in Empidideicini. Recent studies have focussed on the Afrotropical fauna (Evenhuis 2009, 2007), and described 10 new species of *Empidideicus* in Iran (Gharali et. al. 2010, 2011, 2015; Hakimian et. al. 2014).

The genus *Empidideicus* is reported from China and Oriental Region for the first time, and a new species, *E. pentagonius* sp. n., is described. Observations are provided on the flower visiting behaviour of *E. pentagonius* in northwestern Yunnan, China. A key to the genera of Mythicomyiidae from China is presented. The distribution of the new species updates the easternmost distribution of the genus and more species might be distributed in the dry-hot valleys of the Oriental and eastern Palaearctic regions.

Material and methods

Specimens were collected by sweeping flowers of *Stemona mairei* (Levl.) Krause in June beside the Jinsha River in southwest China (28°21'18.91"N, 99°12'52.20"E). The photos of adults visiting flowers were taken with a Canon 5D digital Camera and combined into figures using Adobe Photoshop CS3 software. Photos of male genitalia were taken by KEYENCE VHX-2000. The specimens were studied and illustrated with an Olympus SZ61 stereo microscope. Preparations of genitalia were made by macerating the apical portion the abdomen in cold 10% NaOH for 12–15 h. After examination, dissected material was transferred to fresh glycerine and stored in a microvial together with the specimen. The holotype and other specimens examined are deposited in the Entomological Museum of the China Agricultural University, Beijing (CAU).

Taxonomy

Key to genera of Mythicomyiidae from China

1 Wing vein R_{2+3} absent **2**
– Wing vein R_{2+3} present **3**
2 Wing m-cu crossvein present; female spermathecae spherical with apical invagination ..... ***Empidideicus***
– Wing m-cu crossvein absent; female spermathecae reservoir conical ..... ***Mythenteles***

3 Wing cell dm open distally, not closed by crossvein ..... ***Cephalodromia***
– Wing cell dm closed distally by crossvein ..... ***Platypygus***

Genus *Empidideicus* Becker

Empidideicus Becker 1907: 97. Type species: *Empidideicus carthaginiensis* Becker, 1907, by monotypy.
Cyrtoides Engel 1933: 102 (as subgenus of *Empidideicus* Becker). Type species: *Empidideicus efflatouni* Engel, 1933, by monotypy.
Ecliptica Engel 1933: 103. Unavailable name; name proposed in synonymy with *Cyrtoides* and not made available before 1961.
Anomaloptilus Hesse 1938: 983 (as subgenus of *Empidideicus* Becker). Type species: *Empidideicus celluliferus* Hesse, 1938, by monotypy.
Aetheoptilus Hesse 1967: 112 (as subgenus of *Empidideicus* Becker). Type species: *Empidideicus zuluensis* Hesse, 1967, by original designation.

Empidideicus pentagonius sp. n.

http://zoobank.org/5BA3F89D-BC77-4EA0-A116-CAE9501157D5
Figures 5–11

Diagnosis. Head with ocellar tubercle yellowish, frons and face yellowish with a cup-shaped brown area between frons and face; thorax with two yellowish subtriangular marks anterolaterally, with a subtrapezoidal yellowish brown area posteriorly; katepisternum with upper 1/3 yellow; aedeagal apodeme base semicirclular, with acute tip in dorsal view, aedeagal apodeme arched in lateral view; epiphallus pentagonal, with narrow tip in dorsal view.

Description. Male. Body length 0.8–1.4 mm, wing length 1.1–1.4 mm.

Head black and yellowish, eyes red, bare; ocellar tubercle black, ocelli yellowish; eyes dichoptic, 2 × width of ocellar tubercle, frons and face bare, yellowish, except a cup-shaped brown area between frons and face; occiput black. Antenna (Fig. 11) yellowish brown, scape semicircular nearly twice wider than long; pedicel trapezoidal, slight wider than long; first flagellomere ovoid, nearly 1.7 × longer than wide; second flagellomere about 1/3 length of first flagellomere, cylindrical, about 3 × longer than wide, with minute apical style. Antennal ratio: 1:2:8. Proboscis brown except base with a yellowish quadrilateral area laterally, nearly 2 × length of head.

Thorax (Fig. 10) black and yellowish, mesonotum mostly black except edge yellowish, postpronotal lobe yellowish, anterior with two yellowish subtriangular marks laterally, and a subtrapezoidal yellowish brown area posteriorly, mesonotum with three brown prealar bristles, anepisternum and anepimeron mostly yellow except edge of front and bottom black, katepisternum mostly black except upper 1/3 yellow.

Scutellum yellowish brown. Legs yellow except femora and tarsi brown. Legs with short brown hairs; tibiae with short black hairs and bristles, tarsi with short black hairs.

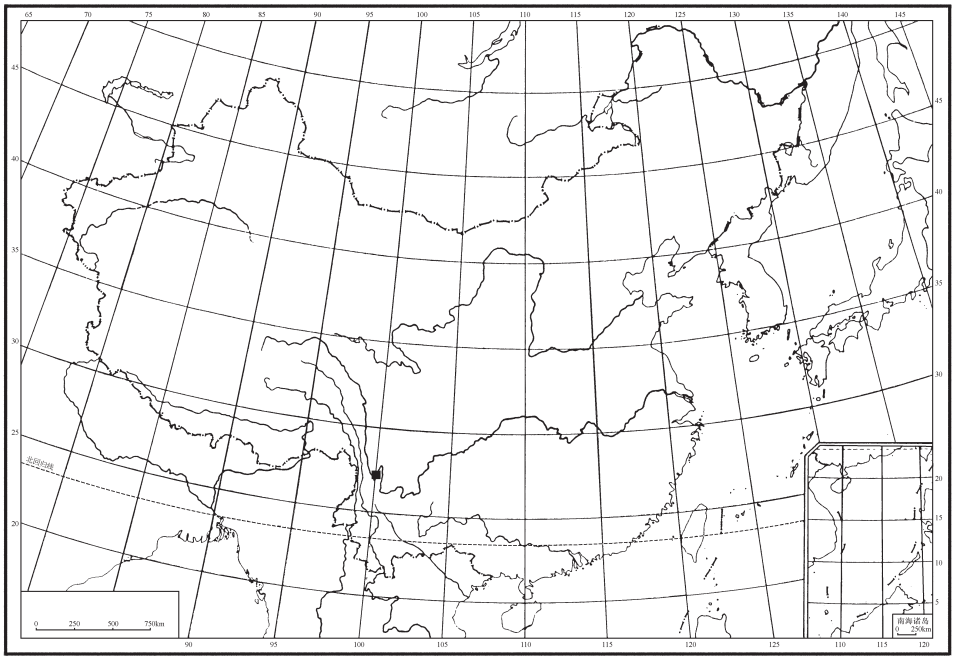

Figure 1. The location of the specimens of *Empididеicus pentagonius* sp. n. collected.

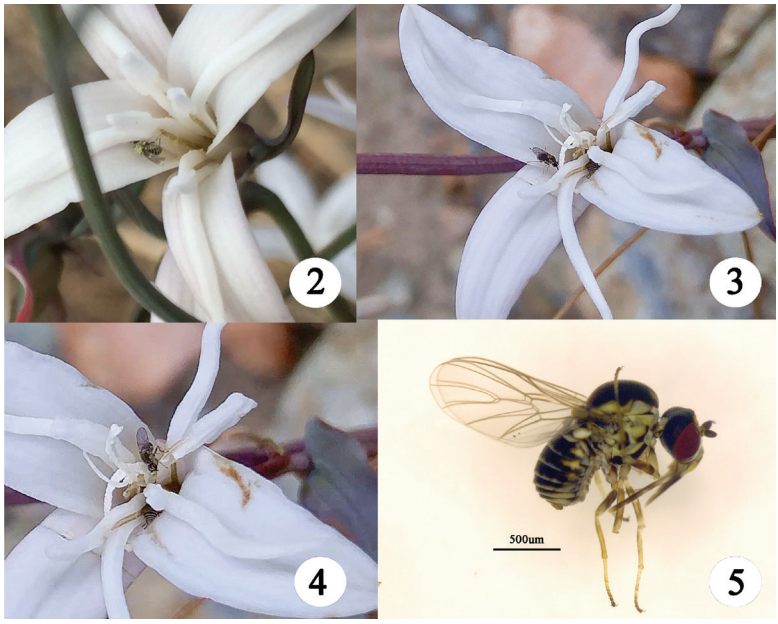

Figures 2–5. 2–4 Photographs of *Empididеicus pentagonius* sp. n. visiting *Stemona mairei* **5** adult of *Empididеicus pentagonius* sp. n. Photographs in nature by Yan Qin.

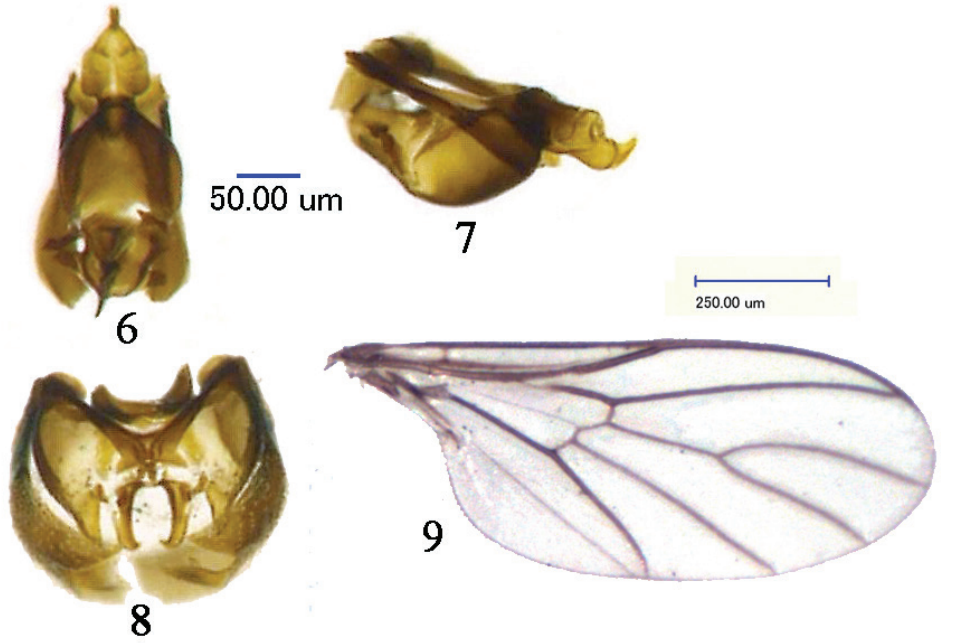

Figures 6–9. Photographs of male genitalia and wing of *Empidideicus pentagonius* sp. n. **6** phallus and gonocoxa, dorsal view **7** phallus and gonocoxa, lateral view **8** epandrium, ventral view **9** wing.

Wing (Fig. 9) hyaline, except veins brown. Wing length 2.3 × width, wing with veins R_1, R_{4+5}, M_1, M_2, M_{1+2}, CuA and Cup present, Sc incomplete; Costa, Sc, R_{4+5} and CuA_2 strongly sclerotized, vein M_1, M_2, M_{1+2} and CuA_1 less sclerotized; vein R_1 ending nearly in middle of costa, R_{4+5} slightly curved anteriorly, M_1 and M_2 form an acute angle, crossvein r-m at bottom of cell dm. Wing with tiny hairs at margin. Halteres yellowish, except edge of tip brown.

Abdomen with all tergites dark brown, except posterior margin with narrow pale brown band, and with yellow posterolaterally. Sternites yellowish mostly, except yellowish brown centrally, and pale laterally.

Male genitalia brown and black (Figs 6–8). Epandrium brown except edge black, nearly as long as wide, cercus well exposed, narrow and long, tip acutely in ventral view; gonocoxa L-shaped, nearly 2 × longer than wide, with acute tip, gonostylus triangular with acute tip in lateral view; aedeagal apodeme base semicircle, extremely long, and narrowly apically, with acute tip in dorsal view, aedeagal apodeme arch in lateral view; epiphallus pentagonal, with narrow tip in dorsal view, epiphallus tip sickle-shaped in laterally view.

Female. Body length 1.2–1.7 mm, wing length 1–1.2 mm. Female genitalia (Figs 12, 13) furca subtriangular, 1.7 higher than wide, with concavity at middle of bottom; spermathecal bulb subglobular when viewed on edge, nearly rectangular in lateral view, invaginated apically, subquadrate in form, slightly wider than deep in lateral view.

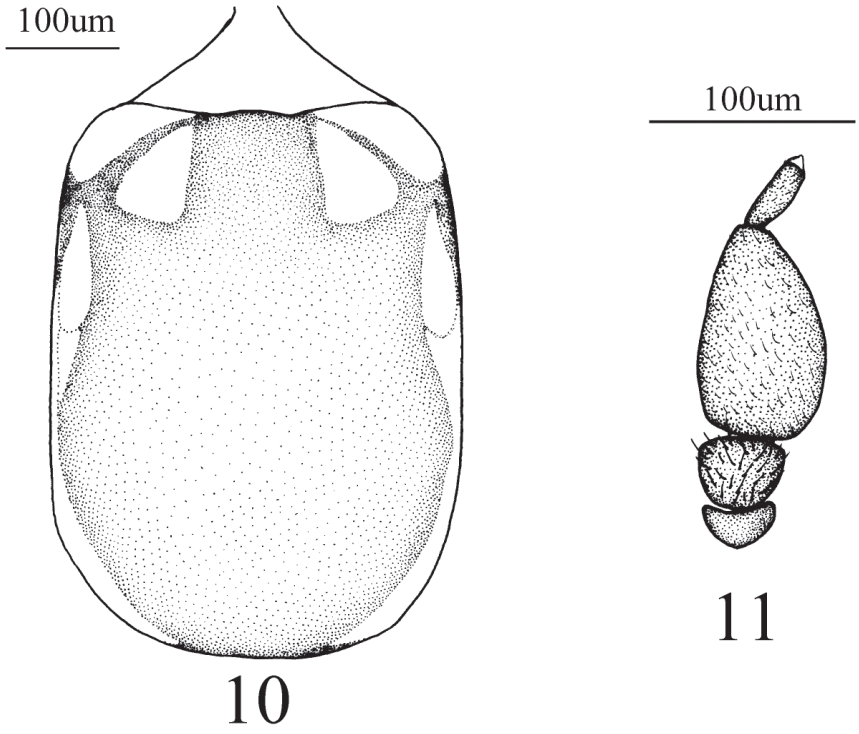

Figures 10, 11. *Empidideicus pentagonius* sp. n. **10** Thorax, dorsal view **11** Antenna, dorsal view.

Type material. Holotype male, CHINA: Yunnan Deqin Benzilan (28°21'18.91"N, 99°12'52.20"E), 08–18. XI. 2017, Yan Qin; Paratype female, CHINA: Yunnan Deqin Benzilan (28°21'18.91"N, 99°12'52.20"E), 08–18. XI. 2017, Yan Qin; 29 males 12 females, CHINA: Yunnan Deqin Benzilan (28°21'18.91"N, 99°12'52.20"E), 08–18. XI. 2017, Yan Qin.

Distribution. China (Yunnan).

Etymology. The specific name refers to the epiphallus pentagonal in dorsal view.

Remarks. The new species is similar to *E. legulicoxa* Gharali & Evenhuis, 2010 (Iran), but it can be separated from the latter by the following features: the frons and face are yellowish, except a cup-shaped brown area between frons and face; the katepisternum mostly black except for the upper 1/3, which is yellow; the abdomen with all tergites is dark brown, except the posterior margin, which has a pale brown narrow band, and laterally, which is yellow posteriorly. In *E. legulicoxa*, the frons is yellowish white, and slightly depressed medially with a large squarish brown spot medially, and the lower 3/4 of the katepisternum is yellowish white; the abdomen is predominantly yellow and with medial brown color dorsally, tergites I–III are brown with undulating posterior margins (Babak et al. 2010).

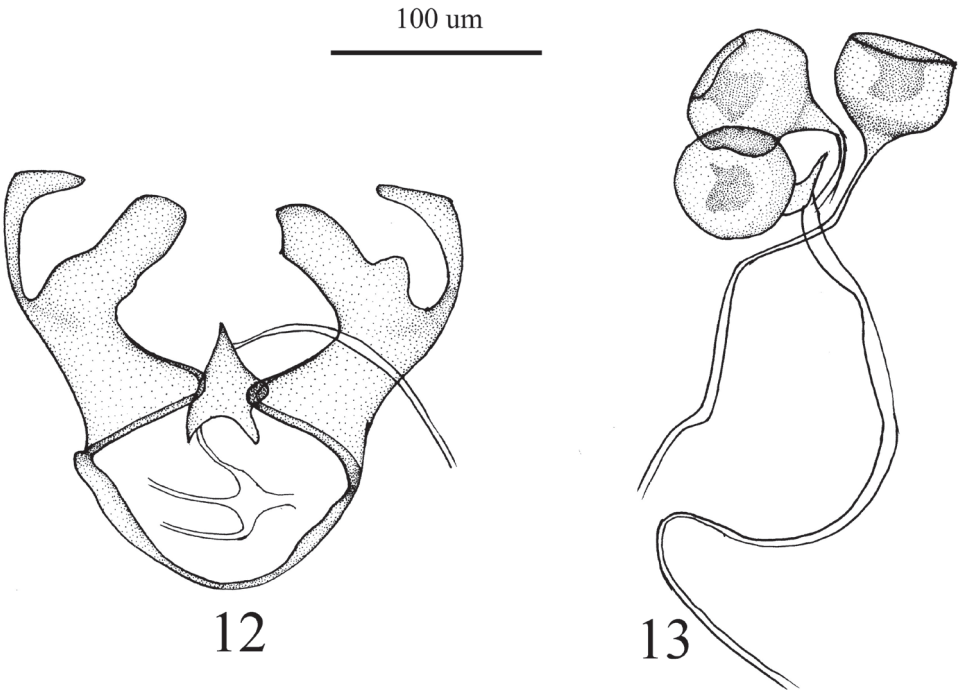

Figures 12, 13. Female genitalia of *Empidideicus pentagonius* sp. n. **12** Female genitalia **13** spermathecal bulb.

Observations

Empidideicus pentagonius sp. n. is one of the most important pollinators for *Stemona mairei* (Levl.) Krause in southwestern China (Fig. 1) (Yan Qin personal observation). During the collection of the specimens, the following observations were made by Yan Qin (Yan Qin 2018): (1) *E. pentagonius* sp. n. rests on the flowers of *Stemona mairei* for a few minutes to half an hour, apparently feeding pollen or nectar. (2) After visiting a flower, much pollen was observed on the body of flies, which visited one flower after another. (3) *E. pentagonius* sp. n. is considered an important pollinator of *S. mairei* in June, but this species is rare in July, and beetles became the dominant visitors of *S. mairei* instead. (4). Different from other species of *Stemona*, *S. mairei* has a faint fragrance instead of a rotting smell (Chen et. al. 2017), which might attract *E. pentagonius*. (5) The eggs and larvae of the flies were not found in the flower, and the life history of *E. pentagonius* is unknown (Figs 2–5).

Acknowledgements

We are very grateful to Yan Qin (Kunming) for collecting the specimens. Our thanks also go to Dr Babak Gharali (Tehran) and Dr Neal Evenhuis (Honolulu) for provid-

ing important references and for their great help in the study. Thanks to Xuankun Li (Canberra) for comments on a draft of the paper, as well as Allan Cabrero (Berkeley) and Xuankun Li (Canberra) for suggestions and comments on a draft of the paper. Support for this study was provided by grants from the NSFC-Yunnan joint fund to support key projects to G. Chen (grant no. U1602264) and National Natural Science Foundation of China (no. 31301670) as well as China Postdoctoral Science Foundation to Gang Yao (no. 2015M581205).

References

Becker T (1907) Die Ergebnisse meiner dipterologischen Frühjahrsreise nach Algier und Tunis. 1906 [part]. Zeitschrift für Systematische Hymenopterologie und Dipterologie 7: 97–128. https://biodiversitylibrary.org/page/33765928

Becker T (1914) Diptères nouveaux récoltés par MM. Ch. Alluaud et R. Jeannel en Afrique orientale. Annales de la Société entomologique de France 83: 121–131.

Chen G, Gong WC, Ge J, Schinnerl J, Wang B, Sun WB (2017) Variation in floral characters, particularly floral scent, in sapromyophilous *Stemona* species. Journal of Integrative Plant Biology 59: 825–839. https://doi.org/10.1111/jipb.12580

Efflatoun HC (1945) A monograph of Egyptian Diptera. Part VI. Family Bombyliidae. Section I: Subfamily Bombyliidae Homeophthalmae. Bulletin de la Société Fouad 1er d'Entomologie. 29: 1–483.

Engel EO (1933) Bombyliidae. In: Lindner E (Ed.) *Die Fliegen der palaearktischen Region*. Vol. 4, pt. 3. E. Schweizerbart, Stuttgart, 97–144.

Evenhuis NL (2002) A new 'microbombyliid' genus from the Brandberg massif of Namibia (Diptera: Mythicomyiidae). Cimbebasia 17: 137–141.

Evenhuis NL (2007) A remarkable new species of *Empidideicus* (Diptera: Mythicomyiidae) from Madagascar. Zootaxa 1474: 55–62. https://doi.org/10.11646/zootaxa.1474.1.2

Evenhuis NL (2009) Order Diptera, family Mythicomyiidae. In: Van Harten A (Ed.) Arthropod Fauna of the UAE. Vol. 2. Abu Dhabi, UAE: Dar Al Ummah, 714–740.

Gharali B, Evenhuis NL, Lotfalizadeh H (2011) Two new species of the genus *Empidideicus* Becker, 1907 from northern Iran (Diptera: Mythicomyiidae: Empidideicinae). Zoology in the Middle East 54: 113–120. https://doi.org/10.1080/09397140.2011.10648883

Gharali B, Jahromi BM, Evenhuis NL, Fallahzadeh M (2015) First record of the genus *Empidideicus* Becker (Diptera: Mythicomyiidae, Empidideicinae) from southern Iran with description of a new species. Entomologist's Monthly Magazine 151: 27–34.

Gharali B, Kamali K, Evenhuis NL (2010) First record of the genus *Empidideicus* (Diptera: Bombylioidea: Mythicomyiidae) from Iran, with description of six new species. Zootaxa 2627: 1–19. https://doi.org/10.11646/zootaxa.2627.1.1

Greathead DJ, Evenhuis NL (2001) Bombylioidea (Diptera: Bombyliidae; Mythicomyiidae) from the island of Sokotra. Zootaxa 14: 1–11. https://doi.org/10.11646/zotaxa.14.1.1

Hakimian S, Talebi AA, Gharali B, Evenhuis NL (2014) A study of the genus *Empidideicus* Becker, 1907 (Diptera: Mythicomyiidae) in northern Iran, with description of a new species. Turkish Journal of Zoology 38: 257–262. https://doi.org/10.3906/zoo-1209-7

Hall JC, Evenhuis NL (1986) Family Bombyliidae. Griffiths GCD (Ed.) Flies of the Nearctic Region. Vol. V, Part 13, No. 5. E. Schweizerbart, Stuttgart, 321–592.

Hesse AJ (1938) A revision of the Bombyliidae (Diptera) of Southern Africa. [I.] Annals of the South African Museum 34: 1–1053. https://biodiversitylibrary.org/page/40845178

Hesse AJ (1965) Diptera (Brachycera) Bombyliidae, Cyrtosiinae. *Euanthobates*, a remarkable new genus. South African Animal Life 11: 482–484.

Hesse AJ (1967) Additions to the Cyrtosiinae (Bombyliidae) of South Africa. Annals of the South African Museum 50: 89–130. https://biodiversitylibrary.org/page/40910681

Hull FM (1973) Bee flies of the world. The genera of the family Bombyliidae. Bulletin of the United States National Museum 286: 1–687. https://doi.org/10.5962/bhl.title.48406

Loew H (1844) Beschreibung einiger neuen Gattungen der europäischen Dipterenfauna. Stettiner Entomologische Zeitung 5: 114–130, 154–173.

Qin Y (2018) Endangerment mechanism and conservation tactics of *Stemona mairei* (Stemonaceae), an endemic to the valleys of Jinsha River in China. M.Sc. thesis, Yunnan University, Kunming.

Zaitzev VF (1992) On the phylogeny and systematics of the dipteran superfamily Bombylioidea (Diptera). Entomological Obozrenie 70: 716–736.

ZooKeys 846: 75–116 (2019)
doi: 10.3897/zookeys.846.31953
http://zookeys.pensoft.net

RESEARCH ARTICLE

A peer-reviewed open-access journal
ZooKeys
Launched to accelerate biodiversity research

A Revision of North American *Lactura* (Lepidoptera, Zygaenoidea, Lacturidae)

Tanner A. Matson[1], David L. Wagner[1], Scott E. Miller[2]

1 *Department of Ecology and Evolutionary Biology, University of Connecticut, Storrs, Connecticut 06269-3043, USA* **2** *Department of Entomology, National Museum of Natural History, Smithsonian Institution, Washington DC 20013-7012, USA*

Corresponding author: *Tanner A. Matson* (tanner.matson@uconn.edu)

Academic editor: *C. Schmidt* | Received 2 December 2018 | Accepted 26 March 2019 | Published 16 May 2019

http://zoobank.org/60B30A09-7905-4C60-BE43-ED0DD76D746E

Citation: Matson TA, Wagner DL, Miller SE (2019) A Revision of North American *Lactura* (Lepidoptera, Zygaenoidea, Lacturidae). ZooKeys 846: 75–116. https://doi.org/10.3897/zookeys.846.31953

Abstract

The *Lactura* Walker, 1854 fauna north of Mexico is revised. Six species are documented, one new species *Lactura nalli* Matson & Wagner, **sp. n.** is described, and two new synonymies are proposed: *Lactura psammitis* (Zeller, 1872), **syn. n.** and *L. rhodocentra* (Meyrick, 1913), **syn. n.** One new subspecies *Lactura subfervens sapeloensis* Matson & Wagner, **ssp. n.** is also described. Adult and larval stages, male and female genitalia, are illustrated, a preliminary phylogeny is presented based on nuclear and mitochondrial data, distribution records provided for verified specimens, and the biology and life history for each species is briefly characterized. Phylogenetic analyses, larval phenotypes, and life history information reveal that much of the historic taxonomic confusion rampant across this group in North America traces to the phenotypic variation in just one species, *L. subfervens* (Walker, 1854).

Keywords

CO1, DNA barcodes, gum bully, subspiracular gland, Sapotaceae, Sideroxylon, tropical burnet moths

Introduction

Lacturidae (tropical burnet moths) are a tropical and sub-tropical family of Zygaenoidea. Prior to the family description by Heppner (1995), members of this group had been classified in Plutellidae, Zygaenidae, and Yponomeutidae (Epstein et al. 1998). Although

Copyright *Tanner A. Matson et al.* This is an open access article distributed under the terms of the Creative Commons Attribution License (CC BY 4.0), which permits unrestricted use, distribution, and reproduction in any medium, provided the original author and source are credited.

the current global diversity is around 140 species, Heppner (2008) estimates the world fauna to be in excess of 250 species. This disparity traces to large numbers of undescribed tropical species. In North America, taxonomic understanding of the family has been hamstrung by confounding phenotypic overlap in color and pattern among many species (Heppner 2008, Matson and Wagner 2017).

The most recent checklist of North American Lepidoptera (found north of Mexico) recognizes six species of *Lactura* (Heppner and Duckworth 1983): *Lactura pupula* (Hübner, [1831]), *Lactura subfervens* (Walker, 1854), *Lactura psammitis* (Zeller, 1872), *Lactura basistriga* (Barnes and McDunnough, 1913), *Lactura atrolinea* (Barnes and McDunnough, 1913), and *L. rhodocentra* (Meyrick, 1913). To this set, we add *Lactura rubritegula* (Matson & Wagner, 2017) from the southern Hill Country of central Texas; *L. nalli* sp. n. from the Rio Grande Valley of southern Texas; and *Lactura subfervens sapeloensis* ssp. n. from Florida and coastal Georgia. The taxonomic identity and validity of Nearctic *Lactura* names – long conflated in literature, institutional collections, and digital databases – are resolved. Much of the confused species-level taxonomy of the genus traces to *L. subfervens,* a widespread and phenotypically variable entity whose forewings range from mottled smoky red to almost entirely white, with variously developed rows of antemedial and postmedial spots (Matson and Wagner 2017).

Our collections of wild *Lactura* caterpillars and reared ex-ova cohorts from across the southeastern US and Texas have revealed six distinct larval phenotypes. These were found to align with CO1 haplotype clusters (Matson and Wagner 2017) and are now additionally supported by nuclear data presented here. Using larvae, life history information, and molecular data, we redescribe five species, describe one new species and one new subspecies, and synonymize *L. psammitis* and *L. rhodocentra*. We provide redescriptions and diagnoses for adults, brief descriptions of living larvae, and life history notes for each species; taxonomic keys and images for both larvae and adults, keys for male and female genitalia; and a phylogeny based on seven nuclear loci and two mitochondrial CO1 loci.

Materials and methods

Morphology

Fresh adult collections were obtained by light trapping with UV and mercury-vapor lights. Larvae were collected from *Sideroxylon* (Sapotaceae). Additional larval specimens were reared from ova deposited by gravid females. We examined the Nearctic *Lactura* holdings of the following museums:

CC	College of Charleston, Charleston, SC
ECK	Edward C Knudson, personal collection, Houston, TX
FEM	Frost Entomological Museum, Penn State University, State College, PA

FMNH	McGuire Center for Lepidoptera and Biodiversity, Florida Museum of Natural History, Gainesville, FL
JKA	James K Adams, personal collection, Dalton, GA
JRM	James R McDermott, personal collection, College Station, TX
KSU-MEPAR	Kansas State University–Museum of Entomological and Prairie Arthropod Research, Manhattan, KS
MEM	Mississippi Entomological Museum, Mississippi State, MS
NHMUK	The Natural History Museum London, London, UK
TAMUIC	Texas A&M University Insect Collection, College Station, TX
UCMS	Biodiversity Research Collections, University of Connecticut, Storrs, CT
USNM	National Museum of Natural History, Washington DC (including primary types)

Photographs from BugGuide, iNaturalist, Moth Photographers Group, and Barcode of Life Database (Ratnasingham and Hebert 2007), through June of 2018, were examined and occurrence data added to an Excel file (Suppl. material 1). Images of types in the NHMUK were provided by Maia Vaswani. Adult redescriptions are based on 986 specimens: *L. pupula* (n = 231), *L. atrolinea* (n = 138), *L. basistriga* (n = 97), *L. subfervens* (n = 474), *L. subfervens sapeloensis* (n = 21), and *L. rubritegula* (n = 25). Several paratypes of *L. subfervens sapeloensis* were added late and are not reflected in the phenology and distribution figures. Forty-two genitalic slides of *Lactura* were examined: 29 from the USNM and 13 prepared by Tony Thomas for this study. SimpleMappr (http://www.simplemappr.net) was used to generate the geographic distribution point map (Shorthouse 2010). Types for *L. nalli* are deposited at TAMUIC, UCMS, and USNM. Types for *L. subfervens sapeloensis* are deposited at CC, FMNH, UCMS, USNM, and JKA.

Barcoding

CO1 barcodes for North American *Lactura* were compiled from holdings in the following institutions and personal collections: (CNC) Canadian National Collection of Insects, Arachnids, and Nematodes, FMNH, JRM, MEM, TAMUIC, UCMS, and USNM. We had access to 116 North American *Lactura* COI barcode submissions: for each of these, we examined the associated voucher specimen or image. 93 of the 116 CO1 barcodes were used (failed sequences excluded) to generate a neighbor-joining tree, using the default Kimura-2P model in the Barcode of Life Project (BOLD) (http://www.boldsystems.org) (Ratnasingham and Hebert 2007). DNA extraction, PCR amplification, and CO1 barcode sequencing were performed at the Canadian Centre for DNA Barcoding (Centre for Biodiversity Genomics – University of Guelph) using their standard Sanger sequencing protocols (Wilson 2012). Data for 93 sequences representing ten barcode clusters (putative species) have been released on GenBank

(accession numbers MK505610-MK505668), and more data, including images, are available on BOLD, (accessible in the dataset LACTURA1 using a DOI (dx.doi.org/10.5883/DS-LACTURA1)).

Multi-gene analysis

Seven single-copy genes capable of resolving phylogenetic relationships of Lepidoptera were sampled (5508 bp total): cytochrome c oxidase subunit 1 (CO1) from the mitochondrial genome and elongation factor–1 α (EF–1α), glyceraldehyde–3–phosphate dehydrogenase (GAPDH), isocitrate dehydrogenase (IDH), cytosolic malate dehydrogenase (MDH), sorting nexin–9–like protein (Nex9), and ribosomal protein S5 (RpS5) from the nuclear genome (Cho et al. 1995, Fang et al. 1997, Mitchell et al. 2006, Wahlberg and Wheat 2008, Zahiri et al. 2011, Rota et al. 2016, Regier et al. 2017). Both CO1 and EF–1α were sequenced in two parts making for a total of nine loci. All DNA extractions were performed using the protocol and material from Macherey Nagel's NucleoSpin Tissue 250 kit. A single leg was taken from each specimen. Once extracted, DNA was stored in a ~4 °C refrigerator until needed for PCR. The PCR profiles and primers outlined in Wahlberg and Wheat (2008) were used. PCR products were sent to Macrogen USA Inc. (Rockville, Maryland) for sequencing. Sequence chromatograms were visually inspected for base call errors and heterozygous loci in Geneious v. 8.1.9 (Kearse et al. 2012). Sequences were then exported to FASTA files and visually aligned to reference lepidopteran sequences for each locus using AliView v. 1.18 (Larsson 2014). GenBank accession numbers and voucher codes for all sequences used in the molecular analysis are given in Table 1.

Phylogenetic analysis

Outgroup Zygaenoidea included *Adscita statices* Linnaeus (Zygaenidae), *Strigivenifera venata* Aurivillius (Limacodidae), and *Dalcerides gugelmanni* Dyar (Dalceridae), as well as another lacturid, *Anticrates* Meyrick. Sequences were partitioned by locus and codon position. The best-fit model of nucleotide substitution for each partition was found using the Akaike Information Criterion in PARTITIONFINDER2 (Lanfear et al. 2016) on the CIPRES web server (Miller et al. 2010). IQTREE v. 1.6.6 (Nguyen et al. 2014) was used to infer the likelihood trees and calculate bootstrap values (1,000 replicates). MRBAYES v. 3.2.6 (Huelsenbeck and Ronquist 2001, Ronquist and Huelsenbeck 2003) was used for the Bayesian analyses. Bayesian analyses were run for 10 million generations, with every 1000th generation sampled. Clade robustness was estimated by posterior probabilities in MrBayes. Stationarity of MCMC parameters were assessed with TRACER v 1.6.0 (Rambaut et al. 2014).

Results

Generic diagnosis and description

***Lactura* Walker, 1854: 485**
Figs 1–14, 50–53, 63, Table 1

Type-species. *Lactura dives* Walker, 1854: 485.

Heppner (1997) successfully applied to conserve the widely used name *Lactura* Walker, 1854 and suppress the generic names *Eustixis* Hübner, [1827–31] and *Mieza* Walker, 1854 (ICZN 1999). Heppner's justification is discussed below, in the treatment for *Lactura pupula*. Generic synonyms can be found in Nye and Fletcher (1991) and Heppner (1995).

Generic description for adult Nearctic *Lactura*. Medium-sized (wingspan 17–26 mm) with respect to other members of the family. Body salmon red. **Head.** Antenna filiform in both sexes; labial palpus porrect, maxillary palpus small. **Thorax.** Adult forewing elongate and subquadrangular, widest at 2/3, and typically satin white or white with speckled brown or red maculation. Oblique antemedial and postmedial rows of red or black spots often present. Apex broadly rounded and little differentiated from outer margin, bounded within R4 and R5; likewise, tornus poorly differentiated. Forewing discal cell with areole; R, M, and Cu veins sessile; CuA veins running to tornus; A1 and A2 fused from basal quarter to inner margin; A3 absent. Hindwing oval quadrate and uniformly pink-red or red-orange with elongate fringe scales. Frenulum 1/5 the size of hindwing length; wing apex poorly defined, bounded within Rs and M1; R, M, and Cu veins sessile; vannal area greatly enlarged; distinct fold between A1+A2 and A3. Venation as in Fig. 3. Tibial spur formula 0–2–4. **Abdomen.** Orange-red, midventer paler, often rusty white. One to two sets of androconial hairpencils within intersegmental folds between A7 and A8 (*L. pupula*, some *L. subfervens*), or A6 and A7 and A7 and A8 (*L. atrolinea*, *L. basistriga*, *L. nalli*, *L. rubritegula*, some *L. subfervens*). Cluster of elliptic scales anterior to spiracle and dorsad of hairpencil. At rest, the hairpencil overlays this scale cluster (presumably loading pheromone onto the hairpencil). **Male genitalia** (Figs 23–30). Uncus narrow, strongly down-curved and cylindrical, ending in apical spine. Tegumen pulmonate with strong medial crease. Valva elongate-oval (2.0–2.5 × longer than wide); costa covered in long setae, concave at distal third with broadly rounded apex; outer margin with shorter, thicker scales; lateral lobe of juxta with spiniform setae (more sclerotized and robust with thicker setae in *L. subfervens*, *L. basistriga*, and *L. rubritegula*). Vinculum narrow, U-shaped, subquadrangular. Aedeagus exceeding length of valva (~4.5 × longer than wide) with broadly rounded base and gaping concave aperture at apex. Aperture oblique in *L. subfervens*, *L. basistriga*, *L. nalli*, and *L. rubritegula*. Apical thumb-like process present in *L. pupula* and *L. atrolinea*. **Female genitalia** (Figs 37–43). Papillae anales ca. 4 × times longer than broad with dorsal sclerotized rim conjoined with posterior apophyses. Apophyses

Table 1. Specimen voucher data and GenBank accession numbers for samples used in phylogenetic analysis. Dash indicates DNA markers that did not amplify.

Voucher Code	Genus Species	CO1 Begin	CO1 End	EF1-a Begin	EF1-a End	RpS5	MDH	Nex9	IDH	GAPDH
TAM0012	*Lactura rubritegula*	MH536189	MH536189	MH553373	MH553373	MH545982	MH545969	–	MH545979	MH545966
TAM0006	*Lactura rubritegula*	MH536196	MH536196	MH553372	MH553372	MH545989	MH545978	–	–	–
TAM0013	*Lactura basistriga*	MH543321	–	MH553366	–	MH545986	MH545973	–	–	–
TAM0005	*Lactura basistriga*	–	–	MH553365	–	MH545985	MH545972	–	–	–
TAM0011	*Lactura nalli*	MH536192	MH536192	MH553371	MH553371	MH545987	MH545974	–	MH545980	MH545967
TAM0007	*Lactura subfervens*	MH536190	MH536190	MH553370	MH553370	MH545983	MH545970	MH545991	–	–
TAM0003	*Lactura subfervens sapeloensis*	MH536193	MH536193	MH553367	–	–	MH545975	MH545993	–	–
TAM0010	*Lactura subfervens sapeloensis*	MH536194	MH536194	MH553368	–	MH545988	MH545976	–	–	–
TAM0004	*Lactura atrolinea*	MH536188	MH536188	MH553363	–	MH545981	MH545968	MH545990	–	–
TAM0008	*Lactura atrolinea*	MH536191	MH536191	MH553364	–	MH545984	MH545971	MH545992	–	–
TAM0009	*Lactura pupula*	MH536195	MH536195	MH553369	–	–	MH545977	MH545994	–	–
MM00180	*Anticrates* sp.	GU828624	GU828422	GU828959	–	GU830631	GU830332	–	–	–
SEM-06-5644	*Strigivenifera venata*	GU828864	–	GU829167	GU829429	GU830811	GU830556	–	GU830242	–
MM00312	*Adscita statices*	GU828630	GU828428	GU828965	GU829251	GU830634	GU830338	–	GU830017	GU829769
06-srnp-33730	*Dalcerides gugelmanni*	GU828533	GU828335	GU828879	–	–	GU830257	–	GU829924	–

Figures 1, 2. *Lactura* resting posture. **1** *Lactura rubritegula* dorsal view **2** *Lactura nalli* lateral view.

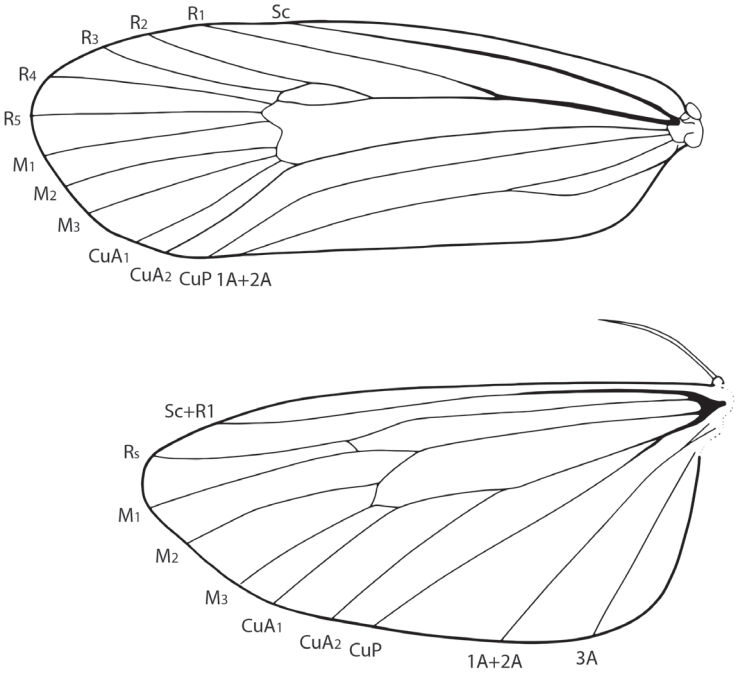

Figure 3. *Lactura* venation (based on venation of *L. pupula*).

rod-like; posterior apophysis ca. three times longer than anterior apophysis. Antrum modestly differentiated, weakly sclerotized, hat-shaped to quadrangular. Ductus bursae distally linear and then variously drawn into series of coils (the number of which is species specific), without accessory diverticula; diameter gradually increasing to corpus bursae and coils becoming more closely drawn together anteriorly. Ductus seminalis attached proximate to antrum. Corpus bursae longer than broad with signa arranged in four hemispherical lobes with dentate interior projections. Signa positioned in two transverse groups; posterior signa half again the size of anterior signa. Accessory pouch sometimes present at anterior end of corpus bursae (*L. atrolinea*, *L. basistriga*, *L. nalli*).

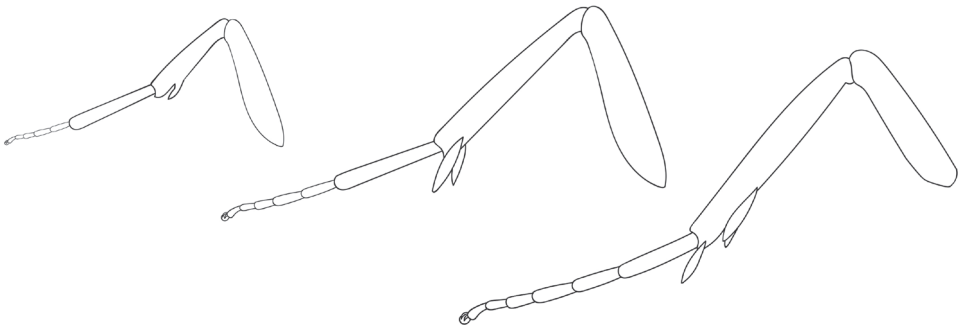

Figure 4. Adult *Lactura* legs (based on *L. pupula*).

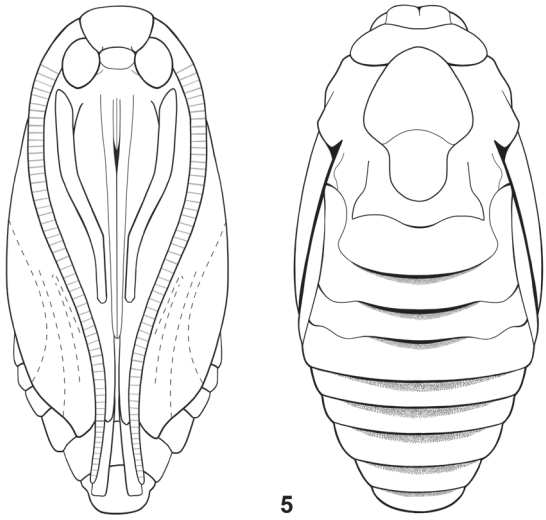

Figures 5, 6. *Lactura* pupa (based on *L. nalli*). **5** Ventral view **6** dorsal view.

Color and habitus of living final instar larva (Figs 44–49). Caterpillar shiny, usually brightly colored, somewhat tacky to the touch, and resembling small limacodids but with short, crochet-bearing prolegs and greater degree of translucence. Ground color green, with brown, black, or green dorsum. Dorsal and subdorsal setae borne from yellow, orange, black, and in some cases blue (*L. atrolinea*) translucent warts. Prothoracic plate well differentiated, divided medially; head partially retracted into thorax. Head dark brown or black, strongly sclerotized with long antennae.

Final instar larva (Figs 7, 8). Description based on *L. pupula*. **Head.** Somewhat prognathous; anterior half more strongly sclerotized; darkly melanized patches to either side and through frons; larger patch, that includes stemmata, extending to level of P1 seta; labrum (0.2 mm long x 0.4 mm wide) with margins rounded and a medial notch; clypeus bulging; antenna longer than labial palpus; head setae generally short except for anteriormost seta of AF, A, S, and SS groups. **Thorax** (Fig. 7). **T1:** Protho-

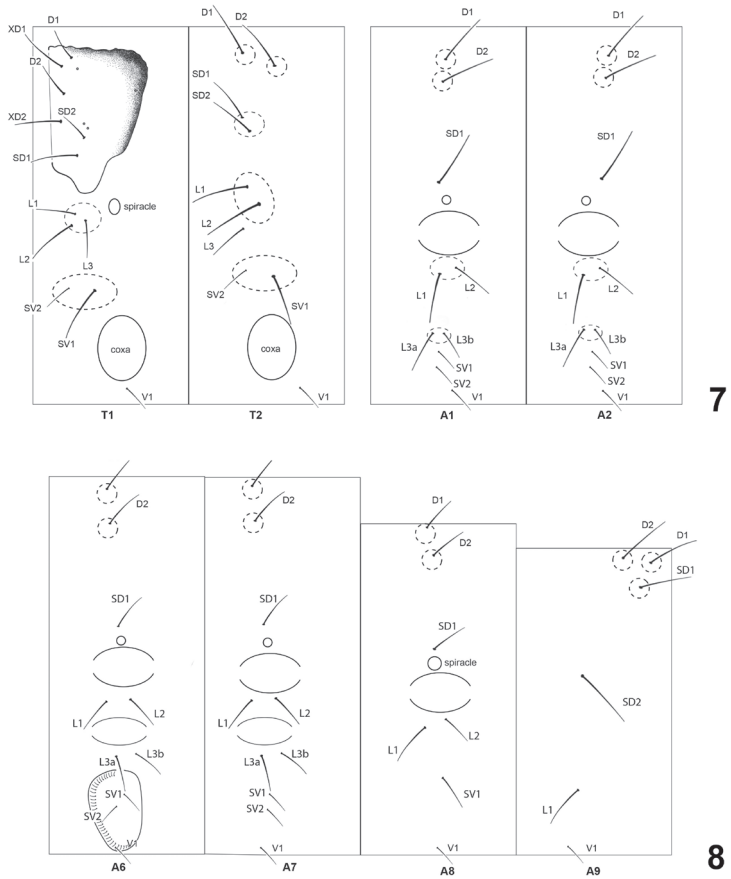

Figures 7, 8. *Lactura* chaetotaxy (based on *L. pupula*). **7** Segments T1–T2, A1–A2 **8** segments A6–A9.

racic shield well developed and strongly sclerotized along mesal and posterior edges; XD1, XD2, SD1, and D2 longest setae on prothorax; D1 and D2 shifted near anterior edge of pronotum, D2 nearly twice as long as D1 and arising midway between and just posteriad of XD1 and XD2; MXD1 included on prothoracic shield directly posterior to D2. Three pits on prothoracic shield; uppermost posteriad of XD1, and two closely set pits dorsad of SD2. Prothoracic spiracle ovate, diameter 0.3 × larger than anterior abdominal spiracles. L group trisetose on raised fleshy wart ventroanteriad to spiracle; two SV setae aligned horizontally, each borne from fleshy wart. **T2:** All setae borne from raised fleshy warts that become increasingly sclerotized to point where seta issues, with size of wart and degree of sclerotization decreasing ventrad. D1, D2, and SD2 nearly in line; D1 and D2 subequal in length and sharing common ridge; SD1 and SD2 also sharing common ridge. Two dorsal L setae sharing a common fleshy wart and lower L seta positioned midway between upper L setae and SV setae. SV1 and SV2 on shared lateral swelling. **T3:** As in T2 except with only two L setae; uppermost L seta shifted upward and sharing protuberance with SD setae. **Abdomen** (Figs 7, 8).

First eight segments with elliptical subspiracular gland and smaller subventral swelling (that may also be glandular). Setae mostly aligned along spiracular meridian and borne from clear, raised, wart-like fleshy swellings. **A1:** D1 and D2 on common swelling, transversely aligned with SD1 and spiracle; SD1 above spiracle; SD2 not observed (presumably microscopic); spiracle circular. L1 and L2 on same swelling below subspiracular gland; L2 (evidently) two-thirds length of L1 and located dorsoposteriad; L3 paired on separate swelling; SV1, SV2, and V1 in line, SV2 less than half size of SV1; V1 seta directed mesad. **A2:** Same as A1. **A3–A6:** D1, D2, SD1, L1, and L2 as on A1 and A2. L3 setae horizontally positioned beneath subventral swelling. Proleg with SV and V setae; 32–35 crochets in biordinal, mesal semi-circle along inner and posterior margin. **A7:** As in previous segments. SD1 dorsoposteriad to spiracle. V1 reduced or concealed in fold of subventral swelling. **A8:** D2 posteriolaterad to D1; both lightly sclerotized; spiracle nearly circular, 0.12 mm in diameter; 3 L setae. **A9:** D2 anterior to D1; D1, D2, and SD2 on enlarged wart; D1 pinaculum sclerotized; single L seta. **A10:** modestly sclerotized; four pairs of setae along caudal margin; 28–30 crochets; anal plate with melanized patch to either side of midline.

Pupa (Figs 5, 6, 14). Subobtect, broadest through abdominal segments and modestly dorsoventrally flattened; antennae, legs, and wings loosely fused to body; setae very short and inconspicuous. Labial palpi visible; proboscis ending beyond protibia; caudal margin of metathorax curved upward and forming low ridge over dorsum of first abdominal tergite. Forewing apex distinctly falcate; hindwing exposed with vannal lobe extended upward toward spiracles. Pro-, meso-, and metatarsus fully visible; mesotibia ending between anterior of A5 to caudal margin of A7; metatibia and antenna subequal, and of variable length, extending to caudal margin of A7 to exceeding A10. Abdomen swollen through spiracular and subspiracular areas (perhaps as a consequence of larval subspiracular glands and subventral swellings); A2–A8 with supraspiracular recess and narrow band of rearward-directed teeth along anterior margin extending from midline nearly to supraspiracular area (presumably assisting in eclosion). A10 smooth with slight cleft and posterolateral protrusions; cocoon cutter, cremaster, and pseudocremaster absent.

Cocoon (Fig. 13). Parchment-like, upper 4/5 of cocoon thick, tough, and carapace-like. Outer edge of cocoon with darkly stained, irregular, reticulate skirt which serves to anchor cocoon to substrate. Floor of cocoon tan, parchment-like; U-shaped operculum at one end tears free at eclosion. Pupa not extruded at eclosion.

Distribution and biology (Figs 9–14, 50–53). North American *Lactura* are found in woodlands, scrublands, and thicket communities from Kansas, Missouri, Illinois, and Kentucky, south through Texas and the Gulf States, east to coastal South Carolina, Georgia, and the whole of Florida, continuing into the Caribbean and Mexico (Figs 52, 53). All species treated here feed exclusively on *Sideroxylon* spp. (Sapotaceae) and overwinter as prepupae inside a tough reddish to brownish cocoon spun in leaf litter (Fig. 13). Across much of their range in the United States, *Lactura* are primarily univoltine, tied to new growth as larvae. Species of the Rio Grande Valley and southern Florida occur nearly year-round, at least in small numbers, if new leaves are present. In captivity larvae typically feed from leaf undersides, with the head partially retracted

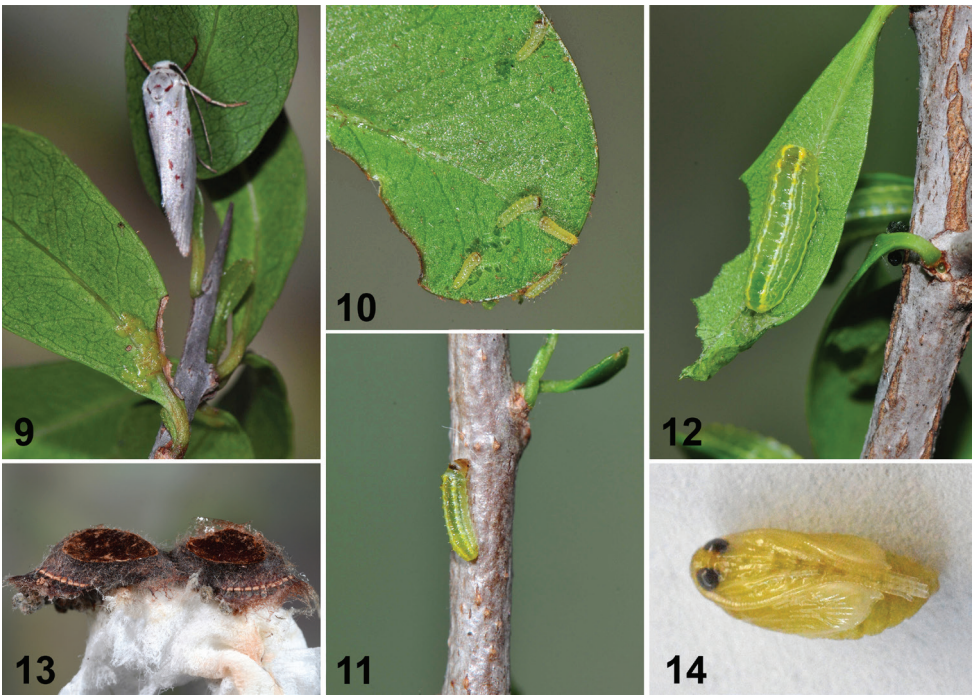

Figures 9–14. Life history of *Lactura nalli*. **9** Egg cluster (near petiole of leaf below resting female) **10** first instar **11** second instar **12** penultimate instar **13** cocoons **14** pupa.

into the prothorax. The fecal pellets are characteristically spherical, lacking any hint of the concave depression common to the pellets of limacodids and megalopygids.

Lactura are difficult to rear, often molding or desiccating as prepupae. We have had modest success rearing larvae in vials with a deep (3–5 cm), occasionally moistened, layer of peat or coir.

Larvae secrete a tacky exudate from their integument to which feculae adhere and often remain attached until the next molt. We suspect the exudate is a deterrent to ants and other invertebrates, as such sticky secretions have been shown to be in the caterpillars of the related Dalceridae (Epstein et al. 1994). When *Lactura* caterpillars are threatened, they evert transparent, balloon-like vesicles from the side of their body (Figs 50, 51) that secrete a sticky, mucilaginous fluid. As far as known, these structures are present in all Nearctic species, but especially apparent in *L. pupula*. It is unclear how prevalent these subspiracular glands and associated behaviors are among other lacturids because the life histories for most species remain unknown.

We suspect adult *Lactura* sometimes disperse from their natal colonies, given that several collection records appear to be out of range, e.g., a single *L. rubritegula* from Houston, Texas (Fig. 52) (Matson and Wagner 2017). Individuals have also been taken or photographed outside the range of their respective *Sideroxylon* hosts. Adults have a well-developed proboscis, but we have no records of adults feeding at flowers. Despite their bright, seemingly aposematic coloration, the adults of Nearctic species are thought to be exclusively nocturnal.

Key to *Lactura* adults found north of Mexico

1 White forewing with black dashes, spots, or streaks; light red scales on vertex **2**

– White forewing with series of red or brown dashes, spots, or streaks; white scales one vertex **3**

2 Forewing with black scaling over veins in upper half of forewing extending around the apex and terminating about tornus; two oblong antemedial spots and three oblong postmedial spots; absent from southern Texas ..... ***Lactura pupula*** **(Fig. 22)**

– Forewing without black scaling over veins; contiguous series of black antemedial and postmedial spots and black subcostal dash; from southern Texas ..... ***Lactura atrolinea*** **(Fig. 18)**

3. Tegula with inconspicuous red scale patch at base (below plane of forewing), otherwise white; forewing entirely white (apart from antemedial and postmedial spots); red subcostal dash often present at base of FW; from southern Texas ..... ***Lactura basistriga*** **(Fig. 20),** ***L. nalli*** **(Figs 2, 21)**

– Tegula basally and medially red (extending well above plane of forewing); forewing with or without scattered red or brown scales (apart from antemedial and postmedial spots); subcostal dash absent at base of FW; absent from extreme southern Texas **4**

4 Forewing with scattered red/brown scales (variable in density); antemedial and postmedial spots present but sometimes reduced; patagium white; widespread across portions of Midwest and southeastern US ..... ***Lactura subfervens*** **(Figs 15–17)**

– Forewing without scattered red/brown scales; antemedial and postmedial spots present; patagium with red scales near collar; west central Texas ..... ***Lactura rubritegula*** **(Figs 1, 19)**

Key to late instars of *Lactura* found north of Mexico

1 Dorsum darkly pigmented: gray, black, or brown **2**

– Dorsum without gray, black, or brown pigmentation **3**

2 From extreme southern Texas (Hidalgo and Cameron Counties) **4**

– Absent from extreme southern Texas **5**

3 Ground color green, green semitransparent dorsum; from western end of Rio Grande Valley of Texas ..... ***Lactura nalli*** **(Figs 48, 51)**

– Ground color frosty, white stripes over dorsum; widespread across southern Midwest and southeast US, absent from Rio Grande Valley of Texas ..... ***Lactura subfervens*** **(Fig. 45)**

4 Dorsum with yellow middorsal stripe and green addorsal stripe; conspicuous metallic blue warts ..... ***Lactura atrolinea*** **(Fig. 47)**

– Variable dark coloration over dorsum interrupted by wavy, white addorsal stripe; conspicuous yellow warts..... ***Lactura basistriga*** **(Fig. 49)**

5 Prominent, white to orange addorsal stripes with embedded orange warts; widespread across Midwest and southeastern US.....***Lactura pupula*** **(Figs 44, 50)**

– No orange stripping or warts; broad, cinnamon-brown middorsum outwardly edged by black addorsal stripes; from west central Texas..... .....***Lactura rubritegula*** **(Fig. 46)**

Key to male genitalia of *Lactura* found north of Mexico

1 Lateral lobe of juxta lightly sclerotized with 20–30+ spiniform setae; aedeagus with large, broadly concave aperture and thumb-like distal process.....**2**

– Lateral lobe of juxta heavily sclerotized with 10–20+ thickened spiniform setae; aedeagus with obliquely concave aperture, thumb-like distal process absent **3**

2 Uncus with strong medial constriction in basal third; broadly cylindrical to apex .....***L. atrolinea*** **(Fig. 25)**

– Uncus robust and tapering with slight medial constriction in basal third; narrowly cylindrical to apex ..... ***L. pupula*** **(Fig. 26)**

3 Uncus basally quadrangular .....***L. subfervens*** **(Fig. 24, 27)**

– Uncus basally cordiform .... ***L. basistriga*** **(Fig. 28),** ***L. rubritegula*** **(Figs 29, 30),** ***L. nalli*** **(Fig. 23)**

Key to female genitalia of *Lactura* found north of Mexico

1 Anterior accessory pouch present on corpus bursae; 4–6 coils in ductus bursae; signa ca. half diameter of corpus bursa **2**

– Anterior accessory pouch absent on corpus bursae; 6–12 coils in ductus bursae; signa ca. quarter diameter of corpus bursae.....**3**

2 Diameter of ductus bursae coils subequal throughout; anterior accessory pouch connected to corpus bursae by broad opening...***L. atrolinea*** **(Fig. 39)**

– Diameter of ductus bursae coils increasing in size anteriorly, anteriormost coil ca. 3× diameter that of posteriormost; anterior accessory pouch connected to corpus bursae by narrow opening...***L. basistriga*** **(Fig. 37),** ***L. nalli*** **(Fig. 38)**

3 Six to eight coils in ductus bursa..... ***L. rubritegula*** **(Fig. 41)**

– Nine to twelve coils in ductus bursa..... .....***L. subfervens*** **(Fig. 42–43),** ***L. pupula*** **(Fig. 40)**

***Lactura pupula* (Hübner)**
Figs 22, 26, 31, 40, 44, 50, 52, 54–56, 63, Table 1

Eustixis pupula Hübner, [1831]: 24.
Type locality: Georgia, USA
Type material: presumably lost
Eustixis leata Geyer, 1832: 5.
Type locality: Unknown
Type material: not examined
Mieza igninix Walker 1854: 527.
Type locality: St. John's Bluff, E. Florida, USA
Type material: not examined
Enaemia crassivenella Zeller 1872: 563.
Type locality: Texas, USA
Type material: not examined for this study, but seen earlier by Miller (Miller and Hodges 1990)
Enaemia crassinervella Slosson, 1896: 86; misspelling

Notes. *Lactura pupula* was first described as *Eustixis pupula* in vol. 3 of Hübner's Zuträge zur Sammlung exotischer Schmetterlinge (1827–1831). The original description was published subsequent to Hübner's death, and the approximate date of description has been inferred to be 1831 (Heppner 1997). The original description is vague, weakly informative, and the taxonomy confusing. The type is presumably lost; however, the illustration in Hübner's manuscript is unambiguous, and assignable to *L. pupula* as recognized in this work. Years prior, Hübner (1823) gave the name *Eustixia pupula* to the spotted peppergrass moth, a well-known crambid. Both *Eustixia pupula* and *Eustixis pupula* were described from North America, spelled similarly, and both of their descriptions contain the Latin phrase, "*Phalaena vera*, *Lithosia geometriformis*." It is debated to what extent this is intentional and whether Hübner considered the two congeners. Whatever the case, *Eustixia pupula* and *Eustixis pupula* are entirely different moths (representing two different superfamilies) and each name remains available.

A few decades later Walker (1854), established the generic names *Lactura* and *Mieza*. Both *Mieza igninix* and *Eustixis laeta* were placed in the latter genus and considered subjective synonyms of *Eustixis pupula* (Walsingham 1914) (Nye and Fletcher 1991). In literature, *Eustixis* is largely ignored, perhaps because of its near homonymy with *Eustixia*; *Mieza* as well became infrequently used. All authors after Walsingham (1914) used *Lactura*, by reason of page priority in Walker (1854) and *Mieza* has since been suppressed (Heppner 1997) (ICZN 1999).

Enaemia crassivenella (Zeller, 1872) and *Enaemia crassinervella* (Slosson, 1896) are both synonyms of *L. pupula*—Slosson (1896) was undoubtedly referring to "*crassivenella*" and "*crassinervella*" was simply a lapse in spelling.

Diagnosis. Forewing pattern instantly distinguishes this species from its congeners. The most notable difference is the black streaking along the veins of the forewing,

and two oblong antemedial spots and three oblong postmedial spots in the lower half of the forewing. The postmedial spots are arranged in a triangular pattern with the lower distal spot touching the inner margin. Female genitalia have 9–10 distal spirals in the ductus bursae. The larva's orange verrucae on white to orange addorsal stripes distinguishes it from all other Nearctic *Lactura*.

Description adult (Fig. 22). Forewing length: 9–13 mm (n = 231). **Head.** Light red to orange over vertex transitioning to white over frons. Labial palpus slightly porrect to straight, brick red at base and black apically, length subequal to eye diameter. Antenna filiform, 0.6 length of forewing; shiny, white above, fuscous below. **Thorax.** Patagium mostly white, with black basal scales forming contrasting collar behind head. Tegula with small ventral black basal patch; white medially and shiny black apically. Large medial mesothoracic and metathoracic black spots. Coxa and femur with red dorsal surface and light red to pale white ventral and lateral surfaces; procoxa with basal mixture of red and black scales; pro- and mesotibia and pro- and mesotarsus black or fuscous dorsally and fuscous red ventrally. Metatibia light red; metatarsus fuscous red. **Forewing.** White with black scales over veins; black scaling extending around apex and terminating about tornus; variable in thickness. Two oblong antemedial spots and three oblong postmedial spots in lower half. Postmedial spots arranged in triangular pattern with lower distal spot elongate and touching inner margin. Costal margin black along basal 1/3 of wing. Underside light red. Fringe scales light red, rarely with admixture of black scales. **Hindwing.** Uniformly light red to dark orange, above and below, with concolorous fringe scales. **Abdomen.** Dorsum and sides brick red; venter rusty white. One pair of subventral intersegmental hair-pencils (consisting of 40–60 androconial scales) between A7 and A8 (Fig. 31). **Male Genitalia** (Fig. 26) (n = 7). Uncus strongly down-curved; basally quadrangular and medially constricted through basal third; cylindrical, tapering to apex, ending in apical spine. Valva elongate-oval, ca. 2 × longer than wide, concave along distal third of costal margin; broadly rounded at apex; lateral lobe of juxta with 20–30+ setae, similar to *L. atrolinea*, but setae shorter and bearing less robust spiniform setae than those of other congeners. Vinculum narrow, U-shaped, subquadrangular. Aedeagus cylindrical, exceeding length of valva; base broadly rounded; apex with broad concave aperture and thumb-like process twice as long as wide. **Female genitalia** (Fig. 40) (n = 3). Papillae anales ca. 3.5 × times longer than broad with dorsal sclerotized rim fused with posterior apophyses. Ductus bursae with 9–11 coils, posterior two coils more open and extended than anterior coils; diameter mostly uniform; coil diameters more or less uniform with anteriormost coil slightly larger than others. Quadrate signa reduced in size compared to other species treated here; lobes fused in two of three preps. Corpus bursae without anterior accessory pouch.

Description of living final instar (Figs 44, 50). Ground color pale and mostly unpigmented to mint green, translucent below spiracles. Thin, white to orange middorsal stripe, edged with thick addorsal stripe; prominent white to orange dorsal stripe with orange verrucae that bear D1 and D2 setae; verrucae on A8 more pronounced than others. Thick black dorsolateral stripe divided by white pinstripe on T2–A8.

Thick, white supraspiracular stripe best developed on T3–A8. Spiracular stripe thin and white; interrupted by light orange spiracles. The extent of orange coloration is reduced in larvae from Texas, where orange is mostly restricted to the thorax and A7-A9, and the stripe running through the dorsal verrucae is more given to white than orange.

Distribution and biology. *Lactura pupula* occurs in woodlands, thickets, scrublands, back dune and coastal strand communities, and along forest edges of central Texas northward in Midwest to Nebraska and Illinois, and eastward to South Carolina and the whole of Florida (Fig. 52). The moth flies from February to October (southward) and is often abundant during its peak flight in March and April in Florida. Southward it is multivoltine, especially in southern Florida where it flies nearly year-round (Figs 54–56). Our host plant records are from gum bully (*Sideroxylon lanuginosum*) and tough bully (*Sideroxylon tenax*); Kimball (1965) also lists saffron plum (*Sideroxylon celastrinum*). Larvae co-occur on the same hostplants with those of *L. subfervens* over much of its range.

In central and west-central Texas, larvae show a reduction in the amount of dorsal orange maculation. A close relative of *L. pupula*, based on CO1 data in BOLD (BOLD: ACN5528), occurs in Tamaulipas, Mexico. It would be worthwhile to do more sampling in south Texas and northern Tamaulipas to better delineate the ranges of the two moths. *Lactura pupula* is rapidly expanding its range westward in Texas. In 2019, the first records of adults were made in Austin (Travis County), Boerne (Kendall County), and Camp Wood (Edwards County)—all at sites that have been regularly sampled over the past decade. Larvae were found in great numbers in the first two of these counties in April of this year.

Lactura subfervens Walker

Figs 15–17, 24, 27, 33, 36, 42–43, 45, 53, 58, 59, 63, Table 1

Mieza subfervens Walker 1854: 527.
Type locality: Texas, USA
Type material: NHMUK, TYPE – BMNH(E) 819792
Lactura psammitis, Zeller 1872: 562; syn. n.
Type locality: Texas, USA
Type material: NHMUK, TYPE – BMNH(E) 1377410
Lactura rhodocentra, Meyrick 1913: 142; syn. n.
Type Locality: Texas, USA
Type material: not found at NHMUK

Notes. Zeller described *Enaemia psammitis* from Texas in 1872. As early as 1874, Grote synonymized *L. psammitis* with *L. subfervens*; a decision followed subsequently by Barnes and McDunnough (1913, 1917). Heppner and Duckworth (1983) gave *L. psammitis* species status in their checklist without explanation. Perhaps, *L. psammitis* has persisted because phenotypes of *L. subfervens*, mostly from Oklahoma and Texas, with reduced forewing speckling were thought to represent a species independent from *L. subfervens*. Based on extensive barcode and phylogenetic data, multiple larval collections, and genitalic dissections, we see no evidence to suggest *L. psammitis* is a valid species. The origi-

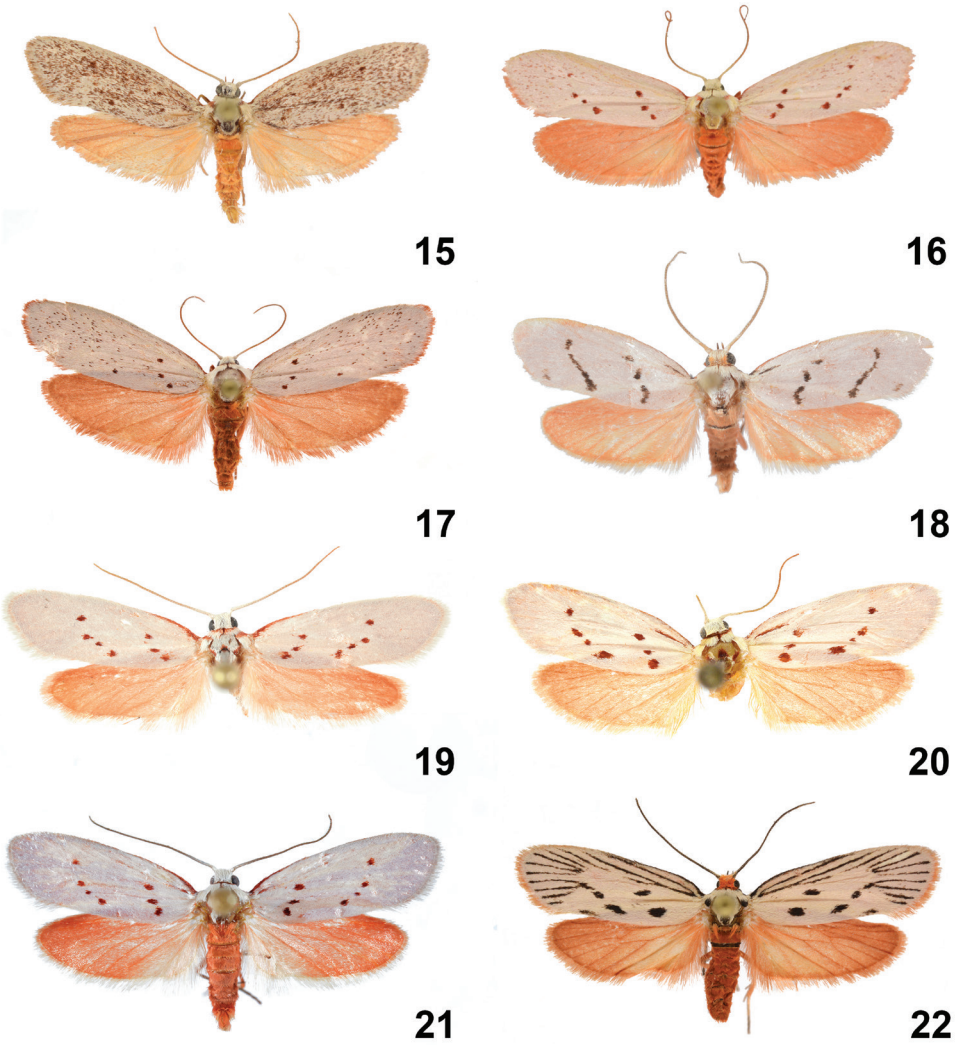

Figures 15–22. Adult *Lactura*. **15** *Lactura subfervens* (heavy maculation), TX: Kaufman Co., Becker, 18 February 2011, J. McDermott coll., CO1 Barcode DLW-000111 **16** *Lactura subfervens* (light maculation), TX: Harrison Co., Caddo Lake St. Pk., 14 June 1998, E. Knudson coll., CO1 Barcode DLW-000509 **17** *Lactura subfervens sapeloensis*, FL: Marion Co., Hopkins Prairie (29.275N, 81.692W), 18 March 2013, J. Vargo coll **18** *Lactura atrolinea*, TX: Cameron Co., Sabal Palm Grove Sanctuary, 16–17 November 1998, E. Knudson coll., genitalia slide #TAM-2017-015, CO1 Barcode DLW-000510 **19** *Lactura rubritegula* [HOLOTYPE], TX: Kendall Co., Boerne, D. Cain Home (29°52'51"N, 98°36'51"W), 27 April 2015, David Wagner & Delmar Cain colls., genitalia slide #TAM-2017-002, CO1 Barcode DLW-000816 **20** *Lactura basistriga*, TX: Cameron Co., Sabal Palm Grove (25°51'9"N, 97°25'3.8"W), BBN15#27a, larva collected 25 April 2015, emerged 21 May 2015, Berry Nall coll., host: *Sideroxylon celastrinum*, genitalia slide #TAM-2017-005 **21** *Lactura nalli* [PARATYPE], TX: Starr Co., Falcon Heights (26.5585N, 99.1220W), 19 March 2018, Berry Nall coll **22** *Lactura pupula*, FL: Nassau Co., Fort Clinch State Park, Ft. Clinch Fernandina Beach, DLW Lot: 2014D136, larva: 28 April 2014, emerged: 22 May 2014, host: *Sideroxlon tenax*, Richard Owen coll.

nal description of *L. psammitis* and type specimen in the NHMUK agree in detail with forms of *L. subfervens*, so we follow others and return the name to synonymy.

Lactura rhodocentra (*Mieza rhodocentra*) was described from Texas by Meyrick in 1913. Shortly thereafter, it was designated as a synonym of *L. basistriga* by Barnes and McDunnough (1917) without explanation. Meyrick's description which mentions "with a few scattered red [forewing] scales," unambiguously places it as a form of *L. subfervens.* While the type of *L. rhodocentra* cannot be located at the Natural History Museum in London, we are not convinced that it no longer exists, because there are random pockets of Meyrick specimens spread throughout the large accumulation of "accessions" of unsorted microlepidoptera. Clarke (1955) did not include a depository for this species, suggesting the type was not present at the NHMUK at that time. Furthermore, it is unlikely that Meyrick would have had access to specimens of *L. basistriga*, *L. nalli*, or *L. rubritegula*, given that all three are geographically restricted to south Texas, and distant from major population centers or travel routes of the early 1900s. We have collected *Lactura* larvae and adults from various locales in eastern Texas, the likely source of the types for both names, examined the *Lactura* collections of Texas A&M University and the private collections of the late Edward Knudson (Houston) and James McDermott (Dallas area), checked barcodes for all US specimens, and see no evidence for the existence of a species that differs from the six treated species in this work. Like *L. psammitis*, we regard this name to be a synonym of *Lactura subfervens*.

Diagnosis. *Lactura subfervens* adults can be immediately distinguished by the presence of scattered smoky red scales (although highly variable in density) over the forewing. The forewing lacks the basal subcostal red or black dash usually present in *L. atrolinea*, *L. basistriga*, and *L. nalli*. This species can also be separated from *L. basistriga*, *L. nalli*, and *L. rubritegula* by the absence of red scaling at the base of the patagium. Female genitalia differ from those of other *Lactura* in having 11 or 12 coils along the ductus bursae. The caterpillar is among the most distinct of the North America *Lactura*: it is the only species whose ground color is predominately white; seven pairs of pale stripes run the length of the body, giving the larva a frosted appearance. The darker stripes are due to the larva's internal coloration showing through its transparent body wall; with the exception of the prothoracic shield, there is essentially no black pigmentation dorsally or laterally along the trunk.

Description adult (Figs 15–17). Forewing length: 9–13 mm (n = 495). **Head.** Shiny, white decumbent scales over vertex and frons. Labial palpus slightly porrect to straight, brick red, subequal to diameter of eye. Antenna filiform, 2/3 length of forewing; shiny, white above, fuscous below. **Thorax.** Predominantly white. Patagium white; tegula with conspicuous basal band of red scales, similar to *L. rubritegula*. Medial mesothoracic red spot flanked posterolaterally by red ellipsoid to bar-like spots. Coxae, femora, and tibiae with red dorsal surface, and white or admixture of white- and red-scaled ventral surface; tarsi fuscous to red. **Forewing.** Mostly white, variable. Typically with seven crimson- to russet-red spots in antemedial and postmedial oblique series. Spotting sometimes reduced, but generally antemedial series with three spots and postmedial series with four spots. Varying degrees of scattered red to brown

scales throughout. Some individuals with speckling so thick as to obscure antemedial and postmedial spots; other forms with only a few red or fuscous scales. Basal red scaling along costa narrows and then ends before antemedial spots. Fringe scales usually matching white forewing, although some individuals with red fringe. Underside light red with matching or slightly paler fringe scales. **Hindwing.** Uniformly light red above and below. **Abdomen.** Dorsum and sides brick red; venter rusty white. Ventral intersegmental hairpencils (with 40–60 androconial scales) inserted between A7 and A8. A second set of brushes between A6 and A7 was found in three preparations (Figs 33, 36). **Male Genitalia** (Figs 24, 27) (n = 6). Uncus strongly down-curved; medially constricted in basal third; distal part cylindrical and tapered (usually longer than congeners), terminating in reduced thorn-like apical spine. Valva elongate-oval, 2.5 × longer than wide, costa slightly concave along distal third; apex broadly rounded; lateral lobe of juxta with 15–20+ thickened spiniform setae. Vinculum narrow, U-shaped, subquadrangular. Aedeagus cylindrical, exceeding length of valva; base broadly rounded, gradually narrowing to apex; apex with concave oblique aperture; subapical thumb-like process absent. **Female genitalia** (Figs 42, 43) (n = 3). Papillae anales ca. 4 × longer than broad with dorsal sclerotized rim fused with posterior apophyses. Ductus bursae with 11 or 12 coils, posterior two coils more open; coil diameters more or less uniform with anteriormost coil slightly larger than others. Corpus bursae longer than broad with quadrate signa reduced; arms fused; lightly sclerotized in one preparation (USNM 76686). Corpus bursae without anterior accessory pouch.

Description of living final instar (Fig. 45). Appearing frosty or pale green or exceptionally yellowish; seven pairs of whitish stripes run length of body; without black pigment dorsally or laterally. D2 on elevated yellow verrucae connected by thick yellow to white subdorsal stripe. Prothoracic shield well differentiated, medially divided, with much less black dorsal pigmentation relative to congeners. Head brown, partially retracted into prothorax.

Distribution and biology. *Lactura subfervens* is found in woodlands, bottomlands, and thickets of central Texas northward to southeast Kansas, Missouri, and Illinois, and east through Gulf States to coastal Georgia (Fig. 53). Its range is largely sympatric with *L. pupula*, with both species mirroring the distribution of one of their shared host plants, *Sideroxylon lanuginosum*. *Lactura subfervens* is not found in southern Florida, unlike *L. pupula*. The species is essentially univoltine, typically flying very early in season (January to April) (Figs 58, 59), when *Sideroxylon* is producing new leaves, although there are smaller, facultative broods across the southern portions of its range, with captures into June and occasionally into the fall. We suspect that larvae from these adults commonly fail due to lack of appropriate foliage. From at least the Dallas area west into the Hill Country region of Texas, *L. subfervens* can reach larval densities high enough to severely damage or completely defoliate *Sideroxylon lanuginosum*.

Remarks. For decades, less speckled forms of *L. subfervens* have been misidentified as *L. basistriga* in collections, literature (Heppner 2003), and on commonly used internet sites, e.g., BugGuide, iNaturalist, and Moth Photographers Group. Much of this confusion was avoidable and speaks to the merit (and necessity) of revisiting original de-

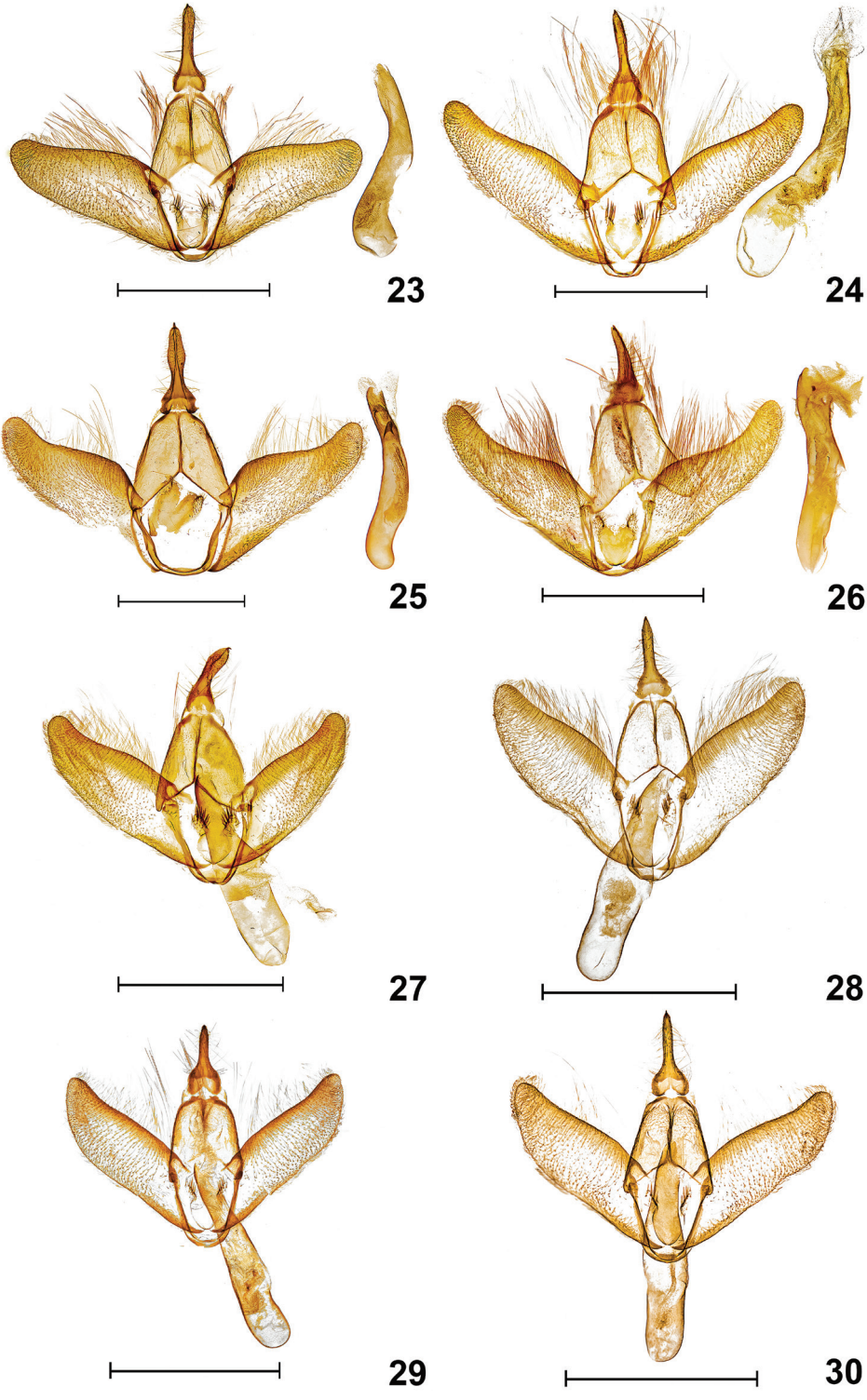
23
24
25
26
27
28
29
30

scriptions and examining types. Barnes and McDunnough's (1913) original description of *L. basistriga* provides clear diagnostic characters that unambiguously distinguished the adult from *L. subfervens*: "lacking the brown streaks on the forewings and in having a red basal streak below the costa," although the latter character is sometimes absent.

***Lactura subfervens sapeloensis* Matson & Wagner, ssp. n.**
http://zoobank.org/A187618D-1434-4FA4-BFDC-1F2C9400EC65
Figs 17, 24, 33, 36, 43, 59, 63, Table 1

Notes. *Lactura subfervens* collections from central and coastal Florida, and coastal Georgia show modest genetic differentiation (pairwise distance ~0.02) (Fig. 63) from *L. subfervens* populations found further west, i.e., from Alabama to Texas north into the Great Plains. We describe this geographic segregate as a new subspecies: *Lactura subfervens sapeloensis*. It is possible that the phylogeographic structure arose when central Florida was separated from the mainland during interglacial rises in sea level (Neill 1957). In early May of 2017, Brian Scholtens and James Adams collected females of *Lactura subfervens sapeloenisis* from Sapelo Island, Georgia. While the neonates established on *Sideroxylon celastrinum*, mortality was high because there was little new growth on the plants: most larvae failed in the penultimate instar with only one making it into the final instar. The single final instar larva displayed a darker green dorsum (no photograph available) than the *L. subfervens* that we have imaged or reared from Texas. Given the large role that larval differences played in this work, it would be valuable if wild larvae from Sapelo Island, Georgia, or Florida, could be collected and evaluated to

Figures 23–30. Male genitalia. **23** *Lactura nalli* [PARATYPE], TX: Starr Co., Falcon Heights (26.5337N, 99.1059W), larva: 30 March 2014, pupated: 05 May 2014, emerged: 06 November 2014, host: *Sideroxylon celestrinum*, Berry Nall coll., BBN14#06c, genitalia slide #TAM-2017-014, CO1 Barcode DLW-000486 **24** *Lactura subfervens sapeloensis* [PARATYPE], GA: McIntosh Co., Sapelo Island, Lighthouse Rd. Salt marsh edge habitat (31°23'25.7"N, 81°16'55"W), 11–12 March 2016, James Adams and Brian Scholtens colls., genitalia slide #TAM-2017-018, Voucher Code TAM0010 **25** *Lactura atrolinea*, TX: Cameron Co., Sabal Palm Grove Sanctuary, 16–17 November 1998, E. Knudson coll., genitalia slide #TAM-2017-015, CO1 Barcode DLW-000510 **26** *Lactura pupula*, FL: Nassau Co., Fort Clinch St. Pk. Ferdinanda Beach, larva: 28 April 2014, emerged: 24 May 2014, host: *Sideroxylon tenax*, Richard Owen coll., DLW Lot: 2014D136, Genitalia slide #TAM-2017-016, CO1 Barcode DLW-000282, Voucher Code TAM0009 **27** *Lactura subfervens*, TX: Uvalde Co., Neil's Lodges, Rio Frio, larva: 17 April 2014, emerged: 16 April 2015, host: *Sideroxylon lanuginosum*, David L. Wagner coll., DLW Lot: 2014D45, genitalia slide #TAM-2017-019, Voucher Code TAM0007 **28** *Lactura basistriga*, TX: Hidalgo Co., Bentsen St. Pk., 30 April 1995, E. Knudson coll., genitalia slide #TAM-2017-003, CO1 Barcode DLW-000513 **29** *Lactura rubritegula* [PARATYPE], TX: Kendall Co., Boerne (29°52'51"N, 98°36'50"W), 27 April 2015, David Wagner and Delmar Cain colls., genitalia slide #TAM-2017-004 **30** *Lactura rubritegula* [HOLOTYPE], TX: Kendall Co., Boerne, D. Cain Home (29°52'51N, 98°36'51"W), 27 April 2015, David Wagner & Delmar Cain colls., genitalia slide #TAM-2017-002, CO1 Barcode DLW-000816. Scale bar: 1mm. Dissections and images prepared by Tony Thomas.

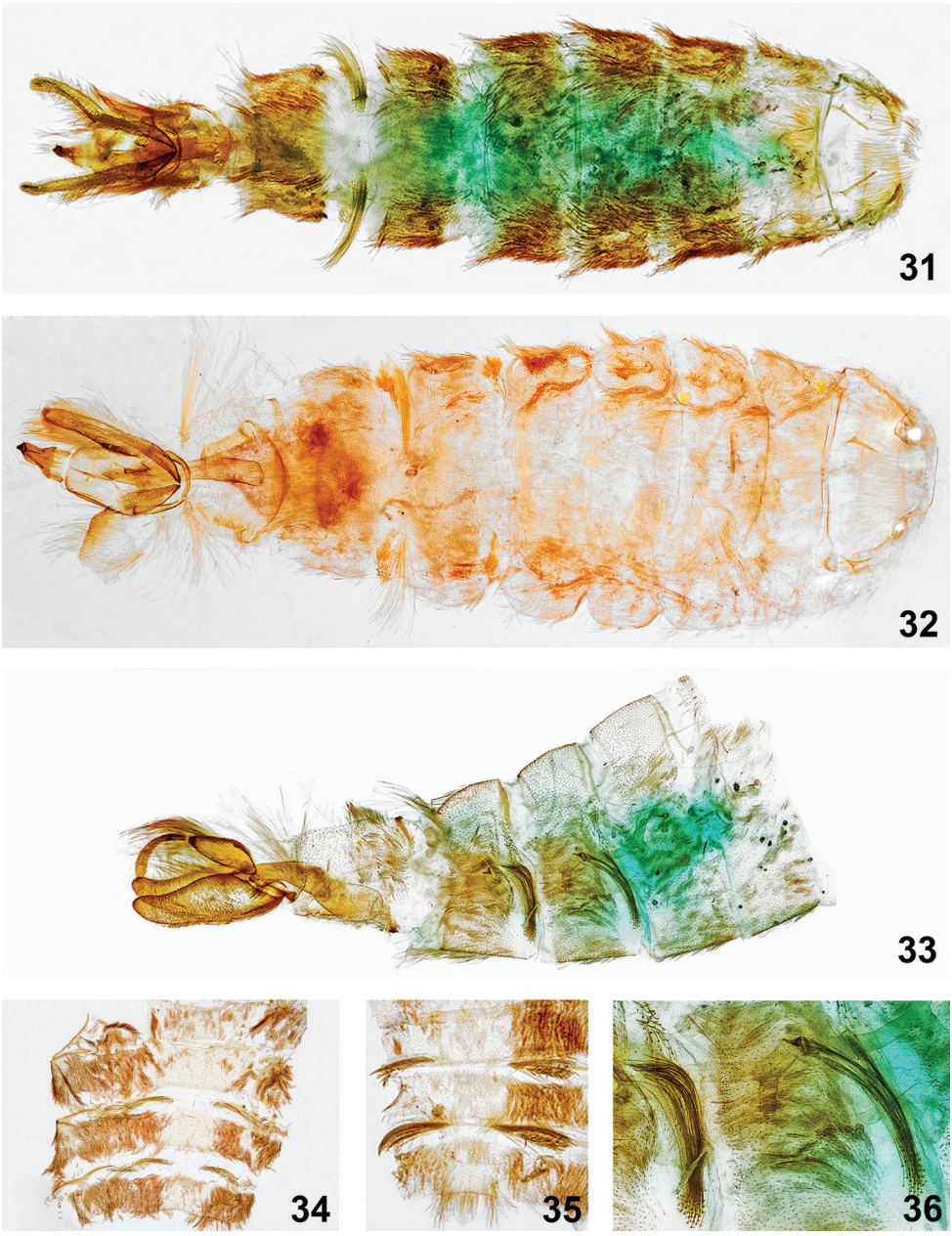

Figures 31–36. Male abdomens with scent-emitting androconial structures. **31** *Lactura pupula,* FL: Nassau Co., Fort Clinch St. Pk. Ferdinanda Beach, DLW Lot: 2014D136, larva: 28 April 2014, emerged: 24 May 2014, host: *Sideroxylon tenax*, Richard Owen coll., Genitalia slide # TAM-2017-016, CO1 Barcode DLW-000282, Voucher Code TAM0009 **32** *Lactura atrolinea*, TX: Cameron Co., Sabal Palm Sanctuary (25°51'3"N, 97°25'1"W), ex-ova: female 25 November 2014, DLW Lot: 2014L121b, emerged: 17 February 2015, host: *Sideroxylon celastrinum*, genitalia slide #TAM-2017-006, Voucher Code TAM0008

assess the larval features of these southeastern populations. As noted above, many have long misidentified some forms of this moth as *L. basistriga* (see *L. subfervens* Remarks).

Diagnosis. *Lactura subfervens sapeloensis* is most easily identified by its Florida/Georgia distribution. We have not found consistent diagnostic characters that will distinguish it from *L. subfervens* in adult pattern or male genitalia. Female genitalia do show modest differentiation: there are 12 or13 coils in the ductus bursae of *L. subfervens* and nine or ten coils in our preparations of *L. subfervens sapeloensis*.

Etymology. We derived this trinomen from Sapelo Island, Georgia, where the moth is particularly common, and from which most of the paratype series was collected.

Distribution and biology. *Lactura subfervens sapeloensis* is found in coastal strand communities, mesic woodlands, thickets, flatwoods, scrublands, and edges of wetlands from central Florida, north into southeast Georgia (Fig. 53). The moth has been collected south to the Archbold Biological Station in Highlands Co., Florida, although recent collections from this area are modest in number. Its range overlaps with southeastern populations of *L. pupula*. We suspect that a primary hostplant for the larva will prove to be *Sideroxylon tenax* (a dominant *Sideroxylon* in Florida) instead of the more widely distributed *Sideroxylon lanuginosum*, which is used by *L. pupula*, *L. rubritegula*, and *L. subfervens* to the west. As far as known, there is one principle spring brood (Fig. 59).

Type material. Holotype male, dry pinned, GA: McIntosh Co., Sapelo Island, Lighthouse Rd., salt marsh edge habitat (31°23'25.7"N, 81°16'55"W), 11–12 March 2016, light trap, James Adams & Brian Scholtens coll., genitalia slide #TAM–2017–017, CO1 Barcode DLW–000570, Voucher Code TAM0003, Deposited at USNM, Washington D.C., USA. **Paratypes adults** (14♂, 14♀): GA: McIntosh Co., Sapelo Island, Beach Rd nr. greenhouse (31.397436N, 81.274092W), 21–22 April 2017, MV light, Tanner A. Matson coll. (1♀) (FMNH); GA: McIntosh Co., Sapelo Island, Lighthouse Rd., salt marsh edge habitat (31°23'25.7"N, 81°16'55"W), 11–12 March 2016, light trap, James Adams & Brian Scholtens coll., genitalia slide #TAM–2017– 018, Voucher Code TAM0010 (1♂) (UCMS); GA: Camden Co., Little Cumberland Island (30°58'N, 81°25'W), 15–19 March 1997, W. E. Steiner et al. coll., CO1 Barcode LNAUV110-16, LNAUV174-16, Voucher Code USNMENT 01237375, 01237311 (1♂, 2♀) (USNM); FL: [Highlands Co.], Lake Placid, Archbold Bio. Sta., 27 March 1959, Ronald W. Hodges coll., genitalia slide 827, CO1

Figures 31–36. Continued. 33 *Lactura subfervens sapeloensis* [PARATYPE], GA: McIntosh Co., Sapelo Island, Lighthouse Rd. salt marsh edge habitat (31°23'25.7"N, 81°16'55"W), 11–12 March 2016, James Adams and Brian Scholtens coll., genitalia slide #TAM-2017-018, Voucher Code TAM0010 **34** *Lactura nalli* [PARATYPE], TX: Starr Co., Falcon Heights (26.5337N, 99.1059W), larva: 30 March 2014, pupated: 05 May 2014, emerged: 06 November 2014, host: *Sideroxylon celastrinum*, Berry Nall coll., BBN14#06c, genitalia slide #TAM-2017-014, CO1 Barcode DLW-000486 **35** *Lactura atrolinea*, TX: Cameron Co., Audubon Sabal Palm Grove Sanctuary, 16–17 November 1998, E. Knudson coll., genitalia slide # TAM-2017-015, CO1 Barcode DLW-000510 **36** *Lactura subfervens sapeloensis*, see 33 above. Dissections and images prepared by Tony Thomas.


37
38
39
40
41
42
43

Barcode LNAUS279-12, Voucher Code USNMENT 00831263 (1♀) (USNM); FL: Marion Co., Hopkins Prairie (29.275N, 81.692W), 18 March 2013, Jim Vargo coll. (2♀) (FMNH); FL: Martin Co., Hopkins Prairie (27.00N, 80.142W), 05 February 2014, Jim Vargo coll. (1♂) (UCMS); GA: McIntosh Co., Sapelo Island, Lighthouse (31.391500N, 81.285703W), 17 July 2015, UV light trap, Lance Durden coll., BGS collection #BGSGA05096 (1♂) (CC); GA: McIntosh Co., Sapelo Island, Nannygoat Beach dunes (31.390N, 81.265W), 10 May 2012, UV light trap, Lance Durden coll., BGS collection #BGSGA02307 (1♂) (CC); GA: McIntosh Co., Sapelo Island, Old Beach Rd. (31.4064N, 81.2592W), 21 May 2014, UV light trap, John Hyatt coll., BGS collection #BGSGA02318 (1♂) (CC); GA: McIntosh Co., Sapelo Island, Lighthouse Rd., salt marsh edge habitat (31°23'25.7"N, 81°16'55"W), 11–12 March 2016, light trap, James Adams and Brian Scholtens coll., BGS collection #BGSGA02636, #BGSGA02637, #BGSGA02638, #BGSGA02639 (1♂, 3♀) (CC); GA: McIntosh Co., Sapelo Island, trailer opening (31.399N, 81.281W), 10 Mar 2016, MV light, Brian Scholtens coll., BGS collection #BGSGA02640 (1♀) (CC); GA, McIntosh Co., Sapelo Island, dune ca. bridge (31.3917N, 81.2685W), 11 March 2016, UV light trap, Brian Scholtens coll., BGS collection #BGSGA02641 (1♂) (CC); GA, McIntosh Co., Sapelo Island, Nannygoat Beach dunes (31.390N, 81.265W), 10 Mar 2016, UV light trap, Brian Scholtens coll., BGS collection #BGSGA02642 (1♂) (CC); GA: McIntosh Co., Sapelo Island, Lighthouse Rd., salt marsh edge habitat (31°23'25.7"N, 81°16'55"W), 11–12 March 2016, light trap, James Adams & Brian Scholtens coll., (3♂, 2♀) (JKA); GA: McIntosh Co., Sapelo Island, beach habitat, end of Beach Rd. light trap (31°23'26.5"N, 81°15'54.5"W), 10–12 March 2016, James K. Adams & Brian Scholtens coll., (1♂) (JKA); same locality, 8–10 March 2017, James K. Adams & Brian Scholtens coll. (1♂, 1♀) (JKA); GA: McIntosh Co., Sapelo Island, near UGA dorms (31°23'54"N, 81°16'51"W), 12 March 2016, at light trap, James Adams coll. (1♀)(JKA).

Figures 37–43. Female genitalia. **37** *Lactura basistriga*, TX: Cameron Co., Sabal Palm Sanctuary (25°51'9"N, 97°25'3.8"W), larva: 25 April 2015, pupated: 29 April 2015, emerged: 21 May 2015, host: *Sideroxylon celestrinum*, Berry Nall coll., BBN15#27a, genitalia slide #TAM-2017-005, Voucher Code TAM0005 **38** *Lactura nalli* [PARATYPE], TX: Starr Co., Falcon Heights (26.5337N, 99.1059W), genitalia slide #TAM-2017-013, CO1 Barcode DLW-000569 **39** *Lactura atrolinea*, TX: Cameron Co., Sabal Palm Sanctuary (25°51'3"N, 97°25'1"W), 25 November 2014, David L. Wagner coll., genitalia slide #TAM-2017-007 **40** *Lactura pupula*, FL: Duval Co., Little Talbot State Park, 24 March 2007, B.D. Williams coll., genitalia slide #TAM-2017-011 **41** *Lactura rubritegula* [PARATYPE], TX: Kendall Co., Boerne (29°52'51"N, 98°36'51"W), 27 April 2015, David L. Wagner coll., ♀ DLW 2015D60.2b, genitalia slide #TAM-2017-001 **42** *Lactura subfervens*, TX: Comal Co., New Braunfells off Huaco Sprgs, Loop Road, 24 March 1995, genitalia slide #TAM-2017-009 **43** *Lactura subfervens sapeloensis* [PARATYPE], GA: McIntosh Co., Sapelo Island, Lighthouse Rd. salt marsh edge habitat (31°23'25.7"N, 81°16'55"W), 11–12 March 2016, James Adams and Brian Scholtens colls., genitalia slide #TAM-2017-017, CO1 Barcode DLW-000770, Voucher Code TAM0003. Scale bar: 2 mm. Dissections and images prepared by Tony Thomas.

***Lactura atrolinea* (Barnes & McDunnough, 1913)**
Figs 18, 25, 32, 35, 39, 47, 53, 57, 63, Table 1

Mieza atrolinea Barnes and McDunnough, 1913: 142.
Type locality: San Benito, Texas, USA
Type material: USNM

Diagnosis. *Lactura atrolinea* is easily distinguished by its larger size and nearly continuous series of black antemedial and postmedial spots. The tegula is black apically as are the spots over the thorax; the forewing has a thin black subcostal dash. In females the ductus bursae has five or six coils anteriorly. The larva displays attractive, metallic blue, dorsal warts that unmistakably separate this species from its co-occurring Texas congeners.

Description adult. (Fig. 18) Forewing length: 9–13 mm (n = 138). **Head.** Vertex white with paired, addorsal, salmon scale patches; frons with shiny white decumbent scales. Labial palpus slightly porrect, brick red at base and black at terminus, subequal to diameter of eye. Antenna filiform, 0.6 length of forewing; shiny, white decumbent scales over scape and basal 2/5, transitioning to fuscous with scattered whitish scales; distal 1/5 brick red. **Thorax.** Predominantly white. Patagium white with a few red basal scales. Tegula with small ventral black basal patch; white medially and shiny black apically. Prothorax with lateral pair of black spots, but these sometimes obscured by patagium. Coxa and femur with red dorsal surface and light red to pale white outer and ventral surfaces; procoxa with basal mixture of red and black scales; pro- and mesotibia and pro- and mesotarsus black or fuscous dorsally and fuscous red ventrally; metatibia light red; metatarsus fuscous red. **Forewing.** Pearly white, with oblique series of black antemedial and postmedial spots. Spots nearly contiguous to fused. Antemedial row with three spots; lower spot largest and rendering row convex with respect to base of forewing. Postmedial series with heavy black dash approximately 1/2 width of forewing (continuous but narrowing anteriorly); smaller spot above. Inconspicuous black spot near tornus. Black, basal, subcostal dash similar in size and placement to red subcostal dash in *L. basistriga*. Basal black scaling along costa narrows and ends before antemedial spots. Fringe scales white. Underside red. **Hindwing.** Uniformly light red to orange with white fringe scales. Underside of hindwing paler than those of underside of forewing. **Abdomen.** Dorsum and sides brick red; venter rusty white. Two pairs of subventral intersegmental hairpencils (with 40–60 androconial scales) inserted between A6 and A7, and A7 and A8 (Figs 32, 35). Roseate cluster of elliptic scales, 5 × longer than broad, located anterior to spiracle in intersegmental folds, much more pronounced than in other Texas congeners. Hairpencils and roseate scale clusters more extensive between A7 and A8 than between A6 and A7. **Male Genitalia** (Fig. 25) (n = 6). Uncus more robust than congeners, strongly down-curved and tapering, strong medial constriction in basal third, ending in short thorn-like apical spine. Valva elongate-oval, 2× longer than wide, costa concave along distal third; broadly rounded at apex; outer margin with shorter, thicker scales; lateral lobe of juxta similar to *L. pupula*, but more sclerotized and prominent, with 20–30+ spiniform setae. Vinculum narrow, U-

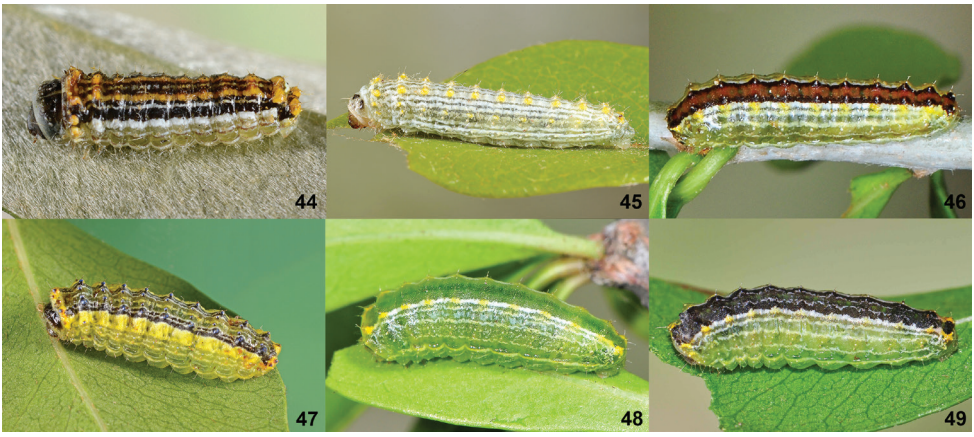

Figures 44–49. *Lactura* last instars. **44** *Lactura pupula* **45** *Lactura subfervens* **46** *Lactura rubritegula* **47** *Lactura atrolinea* **48** *Lactura nalli* **49** *Lactura basistriga*.

Figures 50, 51. When threatened, *Lactura* caterpillars evert transparent, balloon-like vesicles from the side of their body that secrete a sticky, mucilaginous fluid. **50** *Lactura pupula* larval defense response **51** *Lactura nalli* larval defense response.

shaped, subquadrangular. Aedeagus cylindrical, exceeding length of valva; base broadly rounded; apex with gaping concave aperture and subapical thumb-like process twice as long as wide. **Female genitalia** (Fig. 39) (n = 4). Papillae anales ca. 4 × longer than broad with dorsal sclerotized rim fused with posterior apophyses. Ductus bursae with five or six coils; coils more open than other treated species; posterior two coils more open and extended, with corrugated surface; remaining (anterior) coils tightly bound with little to no surface corrugation. Corpus bursae longer than broad; four lobes of signa large with dentate interior projections; teeth widely spaced (similar to those of *L. basistriga*). Corpus bursae with anterior accessory pouch with broad opening.

Description of living final instar. (Fig. 47) Ground color yellow to lime green. D1 and D2 setae borne from metallic blue warts. Middorsum with yellow middorsal stripe; green addorsal stripe running through D1 wart; the latter bound laterally by

white pinstripe. Doubled, black dorsal/subdorsal stripe running through larger D2 wart. Supraspiracular area broadly yellow, transitioning to green through spiracular region. Light blue SD1 pinacula positioned directly above spiracles on A1–A8; these connected by thin, wavy, often broken lateral yellow line. A thicker, continuous, stripe runs just below the tan-yellow spiracles.

Distribution and biology. *Lactura atrolinea* inhabits the mesic woodlands, coastal scrub, and palm forests of south Texas, southward into Mexico. Breeding populations are known from coastal areas of Texas from Fort Bend to Cameron counties (Fig. 53). What may represent strays have also been taken from the south-central Texas counties of Medina, Live Oak, and Duval. Multiple generations each year with peak activity tied to early spring (March to May) and the fall rainy periods (September into November) (Fig. 57). Larvae feed on saffron plum (*Sideroxylon celastrinum*); caterpillars and adults are sometimes common in the Sabal Palm Sanctuary near Brownsville, Texas.

Lactura basistriga (Barnes & McDunnough, 1913)

Figs 20, 28, 37, 49, 52, 61, 63, Table 1

Mieza basistriga Barnes and McDunnough, 1913: 142.
Type locality: San Benito, Texas, USA
Type material: USNM

Diagnosis. *Lactura basistriga* can be distinguished from *L. rubritegula* by the absence of dorsal red scales on the tegula. Most forms exhibit a basal, red, subcostal dash on the forewing, and all individuals lack the scattered flecking of red or brown scales characteristic of *L. subfervens*. Many, but not all individuals can be distinguished from *L. rubritegula* by a reduced upper postmedial spot and the convex arcing of the three lower postmedial spots, due to a more basal placement on the lowermost spot. Adults are exceedingly close to and often indistinguishable from those of *L. nalli*; see comments under that species. With the exception of *L. nalli* and *L. atrolinea*, female genitalia differ from other *Lactura* in having four or five coils in ductus bursae. Larvae with a dark dorsum that ranges from smoky gray-green to nearly black, and without the metallic blue dorsal pinacula of *L. atrolinea*; larvae of *L. nalli* are lime green above and lack any hint of white striping or black fill between the subdorsal stripes that are present in *L. basistriga*.

Description adult. (Fig. 20) Forewing length: 9–11 mm (n = 97). **Head.** Shiny, white decumbent scales over vertex and frons. Labial palpi fuscous red, straight or slightly porrect. Antenna filiform, 0.6 length of forewing; shiny, white decumbent scales over scape and basal 1/3, transitioning to shiny, orange to fuscous orange scales; fuscous beneath. **Thorax.** Patagium mostly white; red basally, most apparent around perimeter of eye. Tegula white with small, ventral, red basal patch. Subtriangular, medial, mesothoracic red spot flanked posterolaterally by ellipsoid to bar-like red spots. Coxa and femur with reddish mesal surface, distal and ventral surfaces with admixture of both white and red scaling; tibia given more to white scaling; protarsus mostly red,

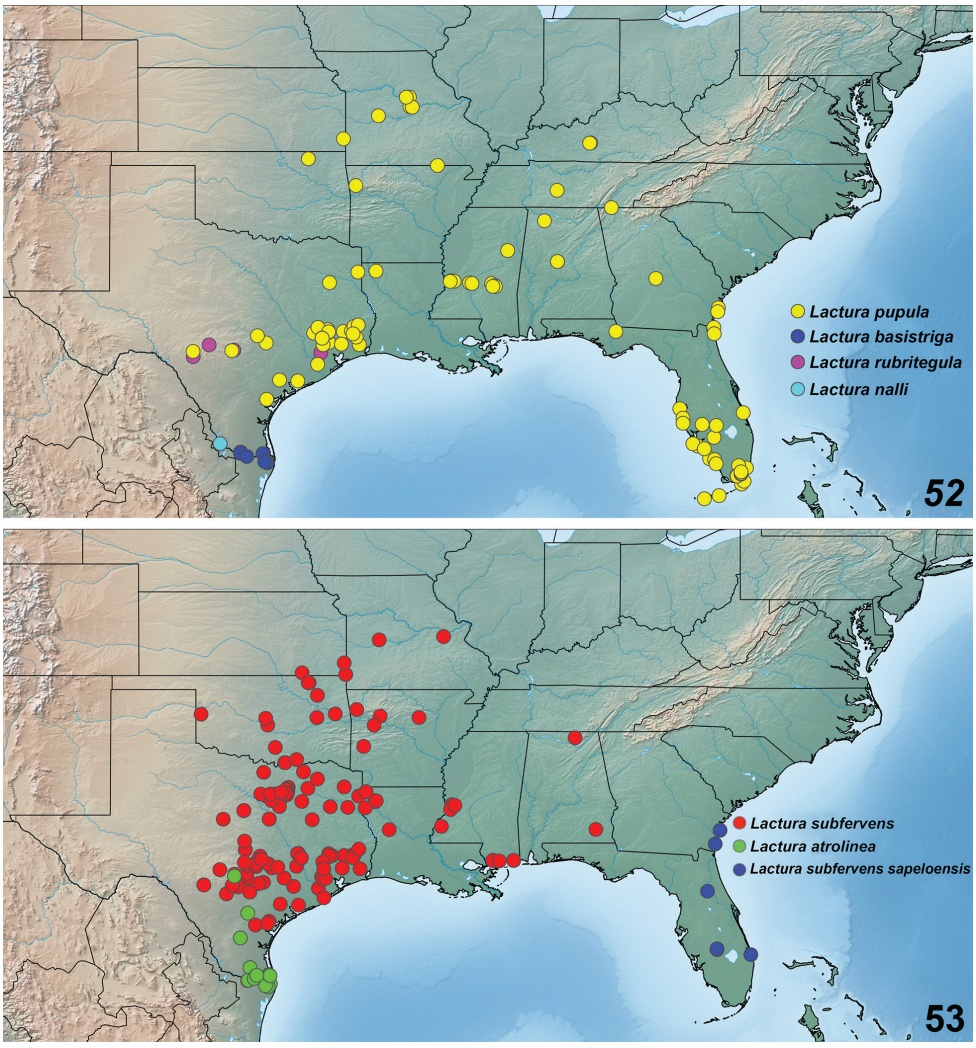

Figures 52, 53. Geographic distribution of *Lactura* north of Mexico. Single dots may represent >1 individuals. **52** *Lactura pupula* (n = 231), *Lactura basistriga* (n = 93), *Lactura rubritegula* (n = 13), and *Lactura nalli* (n = 11) **53** *Lactura subfervens* (n = 472), *Lactura atrolinea* (n = 138), and *Lactura subfervens sapeloensis* (n = 20).

meso- and metatarsus given to more white scaling. **Forewing.** Pearly white, with seven blood- to mahogany-red spots in oblique antemedial and postmedial series; without scattered dark scales (of *L. subfervens*). Antemedial row with three spots; lower and upper spots often larger than middle spot; postmedial series with four spots: uppermost usually smaller or subequal to that below it; lower three forming straight line or, more commonly, a convex arc facing the termen. (These same three spots often form a concave arc open to termen in *L. rubritegula* due to a more distal placement of the lowermost spot.) Basal subcostal red dash from which the species derives its specific epithet,

typically ending before the uppermost antemedial spot; subcostal dash always present in males, but its development (length and thickness varying among individuals); basal red subcostal dash frequently absent in females. Basal red scaling along costa narrows and ends before antemedial spots. Underside red with white fringe scales. **Hindwing.** Uniformly light orange-red above; light orange-red below, becoming paler along inner margin. **Abdomen.** Dorsum and sides brick red; venter rusty white. Two pairs of subventral intersegmental hairpencils (with 40–60 androconial scales) inserted between A6 and A7, and A7 and A8. **Male Genitalia** (Fig. 28) (n = 3). Male genitalic characters overlap with those of *L. nalli* and *L. rubritegula*. **Female genitalia** (Fig. 37) (n = 2). Papillae anales ca. 4 × longer than broad with dorsal sclerotized rim anastomosed with posterior apophyses. Ductus bursae with four or five coils, posterior half sublinear, transitioning to strongly coiled anterior half; diameter of coils increasing to corpus bursae, anteriormost coil 3 × greater in diameter than posteriormost coil (subequal to width of corpus bursae). Corpus bursae longer than broad; signa consisting of four, large hemispherical lobes with dentate interior projections; teeth widely spaced (similar to *L. atrolinea*). Corpus bursae with anterior accessory pouch narrowed at its opening.

Description of living final instar. (Fig. 49) Ground color glossy yellow, pale, or smoky green with variable black coloration over dorsum interrupted by wavy, white addorsal stripe. D2 seta borne from slightly elevated yellow wart connected by thick yellow to white subdorsal stripe; yellow warts less evident through midabdominal segments. Enlarged dorsal verrucae on A8 (bearing D1, D2, and SD1 setae), usually yellow or yellow-orange and black over mesal surface. Two pale, wavy supraspiracular stripes extending from T1–A8.

Distribution and biology. *Lactura basistriga* inhabits the woodlands, thickets, palm forests, and scrublands of the lower Rio Grande Valley; presumably the core of its range is in Mexico. Breeding populations are known from the extreme southern Texas counties of Hidalgo and Cameron (Fig. 52). This species is sympatric with *L. atrolinea* in the United States; the moths are active at the same time of year and both feed on new foliage of saffron plum (*Sideroxylon celastrinum*). Peak activity is tied to early spring (March to May) and the fall rainy seasons (September into November) (Fig. 61).

Lactura rubritegula Matson & Wagner, 2017

Figs 1, 19, 29, 30, 41, 46, 52, 62, 63, Table 1

Lactura rubritegula Matson & Wagner, 2017: 141.
Type locality: Kendall Co., Texas, USA
Type material: USNM, UCMS, TAMUIC

Diagnosis. *Lactura rubritegula* can be distinguished from its relative *L. basistriga* by the prominence of red dorsal scales on the tegula. It lacks the red subcostal dash that can be found in most forms of *L. basistriga* and *L. nalli*, and the scattered flecking of red or brown scales characteristic of *L. subfervens*. Many, but not all, individuals can be distin-

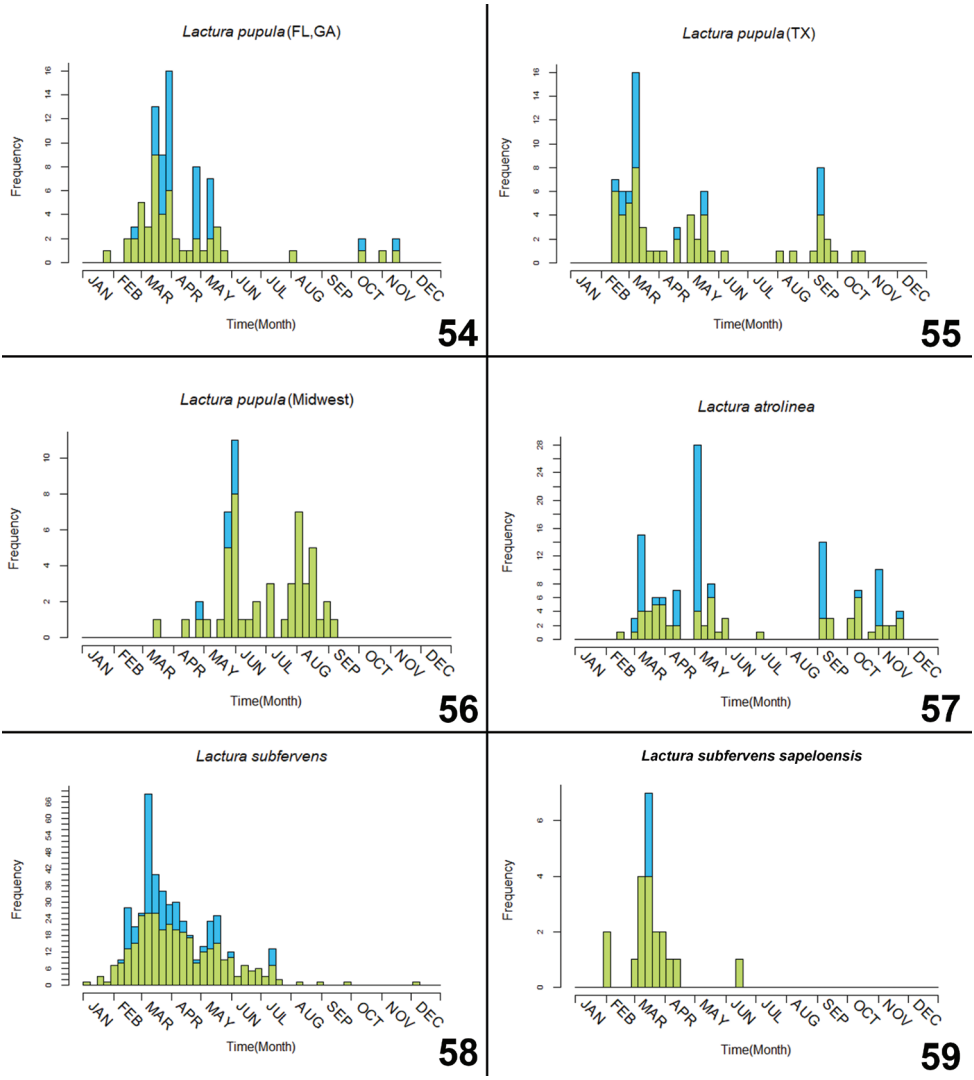

Figures 54–59. Phenology of North American *Lactura*, ■ all specimen records, ■ records representing a unique collecting event (multiple individuals from the same collecting event represent a single data point). **54** *L. pupula* from Florida/Georgia (n = 82) **55** *L. pupula* from Texas (n = 74) **56** *L. pupula* from Midwest, U.S. (n = 54) **57** *L. atrolinea* (n = 138) **58** *L. subfervens* (n = 474) **59** L. subfervens sapeloensis (n = 21).

guished by the basal displacement of the lowermost antemedial spot, somewhat enlarged upper postmedial spot, and the concave arc (open to termen) of the three lower postmedial spots. Female genitalia differ from other *Lactura* in this treatment in having six or seven coils in the ductus bursae. Unique to the larva of this species is the rusty brown dorsum.

Description adult. (Figs 1, 19) Forewing length: 9–11 mm (n = 25). **Head.** Shiny, white decumbent scales over vertex and frons; lower frons sometimes with scattered pink scales. Labial palpus slightly porrect to straight, brick red, subequal to diameter

of eye. Antenna filiform, 0.6 length of forewing; shiny, white decumbent scales over scape and basal 2/5, transitioning to admixture of white and red scales; distal 1/5 brick red. **Thorax.** Predominantly white. Patagium mostly white, but red basally. Tegula with conspicuous basal and medial red scales, similar to *L. subfervens*. Medial mesothoracic red spot flanked posterolaterally by ellipsoid to bar-like red spots. Coxa and femur with reddish mesal and dorsal surfaces, distal and ventral surfaces mostly white with mixture of both white and red scaling; tibia given more to white scaling; protarsus mostly red, meso- and metatarsus given to more white scaling. **Forewing.** Pearly white, with seven blood- to mahogany-red spots in oblique antemedial and postmedial series; without scattered dark scales (of *L. subfervens*). Antemedial row with three spots; lower spot usually displaced basally and often smaller than middle spot; postmedial series with four spots: uppermost usually larger or subequal to that below it; lower three forming straight line or (more commonly) slightly concave arc open to termen. (These same three spots often form convex arc in *L. basistriga* and *L. nalli* due to basal displacement of lowermost spot.) Basal red scaling along costa narrows and ends before antemedial spots. Underside red with white fringe scales. **Hindwing.** Uniformly light red, above and below, with elongate white fringe scales. **Abdomen.** Dorsum and sides brick-red; venter rusty white. Two pairs of subventral intersegmental hairpencils (with 40–60 androconial scales) inserted between A6 and A7, and A7 and A8. **Male Genitalia** (Figs 29, 30) (n = 2). Uncus strongly down-curved; medially constricted in basal third; distal part cylindrical and tapered, terminating in thorn-like apical spine. Valva elongate-oval, 2.5 × longer than wide, costa concave at distal third; apex broadly rounded; lateral lobe of juxta with 10–20+ thickened spiniform setae. Vinculum narrow, U-shaped, subquadrangular. Aedeagus exceeding length of valva; thickest at midlength; base broadly rounded; apex ca. half width of middle section, ending in concave oblique aperture, subapical thumb-like process absent. **Female genitalia** (Fig. 41) (n = 2). Papillae anales ca. 4 × longer than broad with dorsal sclerotized rim fused with posterior apophyses. Ductus bursae with 6–8 coils; coil diameter gradually increasing to corpus bursae; anteriormost coil 2 × diameter of posteriormost coil, and subequal to diameter of bursa. Corpus bursae longer than broad with large four-lobed signa; without anterior accessory pouch.

Description of living final instar. (Fig. 46) Glossy pale green with broad cinnamon-brown middorsal stripe outwardly edged with black that runs through the D1 pinacula; white dorsal/subdorsal stripe running through yellow D2 warts; two, wavy-edged, pale supraspiracular stripes, subequal in width to subdorsal stripe, that extend from T1–A8. Larger primary setae borne from minute white spots (~pinacula). Dorsum with vague, black, transverse intersegmental lines. White D1 pinacula borne from apex of otherwise black warts. D2 seta from white pinaculum at apex of yellow wart with yellow extending down to SD seta. Thin, vague, wavy, pale spiracular stripe immediately ventral to light-orange spiracles, as well as single, white, straight-edged subventral stripe equal in width to supraspiracular stripes.

Distribution and biology. *Lactura rubritegula* is known from the Hill Country around San Antonio, Texas, westward to Edwards and Uvalde counties, but its range remains unclarified due to previous taxonomic confusion with *L. basistriga* and other

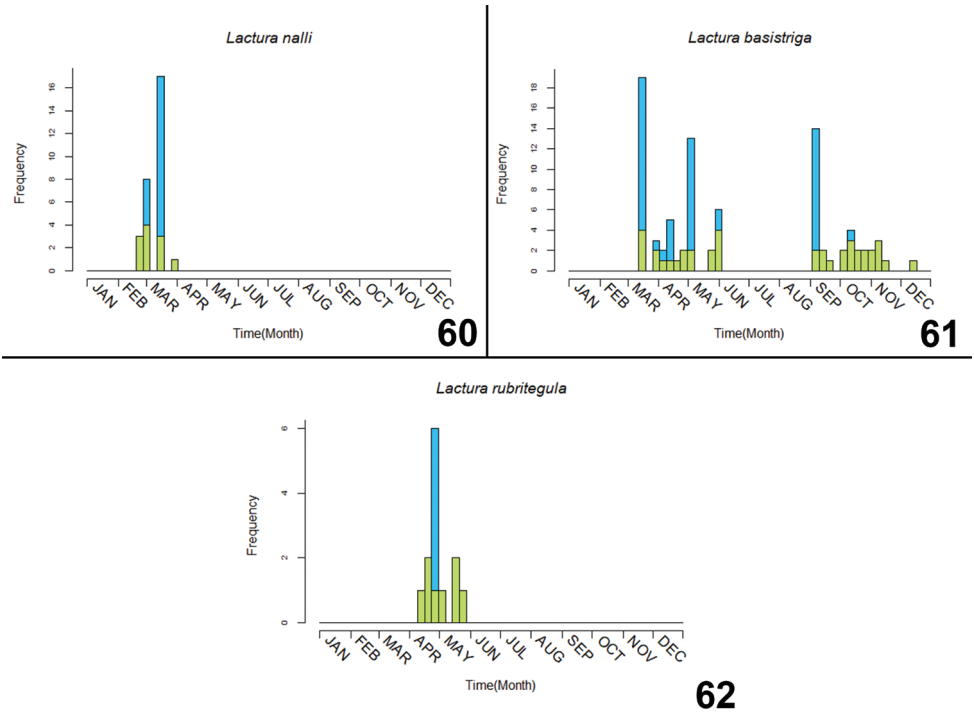

Figures 60–62. Phenology of North American *Lactura*, ■ all specimen records, ■ records representing a unique collecting event (multiple individuals from the same collecting event represent a single data point). **60** *L. nalli* (n = 29) **61** *L. basistriga* (n = 87) **62** *L. rubritegula* (n = 13).

Lactura (Fig. 52). Its range likely extends into Mexico. Delmar Cain has found larvae feeding on *Sideroxylon lanuginosum* (this is the only *Sideroxylon* that occurs at the three known localities for the species). Peak flight of *L. rubritegula* appears to be tied to spring rains and the availability of new foliage. The moth begins flying, late for a *Lactura*, i.e., in the second half of April into May, following the flights of *L. subfervens* and *L. pupula* at the type locality (Fig. 62).

Remarks. A comparative assessment of *L. rubritegula* relative to *L. basistriga* is provided in Matson and Wagner (2017).

***Lactura nalli* Matson & Wagner, sp. n.**
http://zoobank.org/D25568AD-1682-4C9F-8198-A403AC074DFE
Figs 2, 9–14, 21, 23, 34, 38, 48, 51, 52, 60, 63, Table 1

Diagnosis. Adult *Lactura nalli* are similar to *L. basistriga*, and in some cases indistinguishable. The following generalizations can be made when comparing series of adults: when the red basal streak is present, it is almost always shorter, usually ending before the most basal antemedial spot; the antemedial wing spots tend to be more reduced;

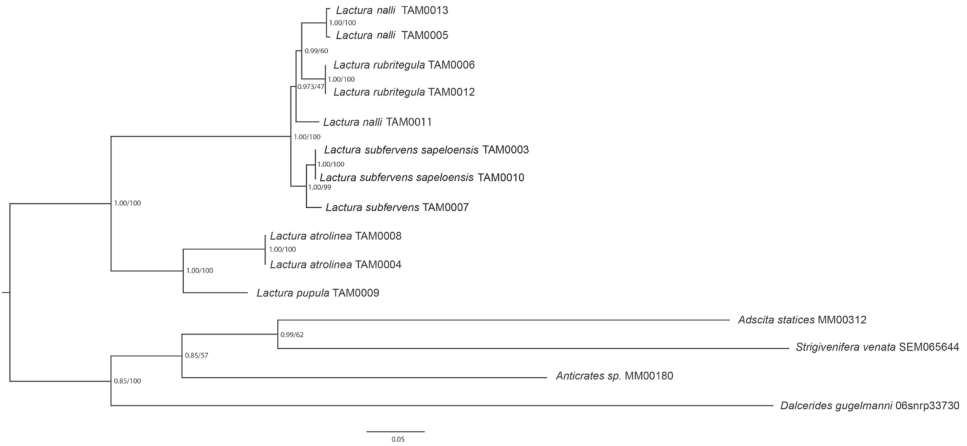

Figure 63. Likelihood tree for *Lactura* found north of Mexico with four outgroup zygaenoids based on nine gene regions – see Methods. Bayesian posterior probabilities (left) and bootstrap support values (right) for internal branches.

and the hindwings are more roseate and given to pink, while those of *L. basistriga* are more orange-red in hue. *L. nalli* can be distinguished from *L. rubritegula* by the absence of red tegular scales (that are visible in dorsal view). Like *L. basistriga*, many individuals can be differentiated from *L. rubritegula* by a reduced upper postmedial spot and the convex arc facing the termen of the three lower postmedial spots. *L. nalli* can be separated from *L. subfervens* by the absence of the scattered flecking of red or brown scales over the forewing. Female genitalia overlap with *L. basistriga* but differ from other *Lactura* in having 4–5 anterior whirls present in the spiraled ductus bursae. Larvae can be immediately distinguished from those of other North American *Lactura* by their green semitransparent dorsum lacking any black or white markings, which is in stark contrast to the dark dorsum of *L. basistriga*.

Description adult. (Figs 2, 21) Forewing length: male: 8.5–9.5 mm (n = 21); female: 9–10 mm (n = 8). Body salmon red. **Head.** Shiny, white decumbent scales over vertex and frons. Labial palpi fuscous red, straight or slightly porrect. Antenna filiform, 0.6 length of forewing; shiny, white decumbent scales over scape and basal 1/3, transitioning to fuscous to orange scales; fuscous beneath. **Thorax**. Patagium mostly white; red basally, most apparent around perimeter of eye. Tegula white with small ventral red basal patch. Subtriangular medial mesothoracic red spot flanked posterolaterally by ellipsoid to bar-like red spots. Coxa and femur with reddish mesal surfaces, distal and ventral surfaces with admixture of white and red scaling; tibia given more to white scaling; protarsus mostly red, meso- and metatarsus given to more white scaling. **Forewing.** Pearly white, with seven blood- to mahogany-red spots in oblique antemedial and postmedial series; without scattered dark scales (of *L. subfervens*); antemedial row with three spots, postmedial row with four spots. Lower three spots of postmedial row forming straight line or more commonly a convex arc (closed to termen); on average,

spots more reduced than those of *L. basistriga* (when comparing series). (These same three spots often form concave arc, open to termen, in *L. rubritegula* due to a more distal displacement of the lowermost spot.) Basal, subcostal red dash, typically ending before basal antemedial spot; this dash always present in males but usually absent in females. Basal red scaling along costa often narrows and ends before antemedial spots. Underside light red with pale fringe scales. **Hindwing.** Pinkish red in fresh individuals; dull red below but paler along inner margin. **Abdomen.** Dorsum and sides dull orange-red; venter rusty white. Two pairs of subventral intersegmental hairpencils (with 40–60 androconial scales) inserted between A6 and A7, and A7 and A8 (Fig. 34). **Male Genitalia** (Fig. 23) (n = 1). As in *L. basistriga*. **Female Genitalia** (Fig. 38) (n = 1). As in *L. basistriga*.

Description of living final instar. (Figs 48, 51) Ground color glossy green with green semitransparent dorsum, lacking pale addorsal stripes and black dorsal pigmentation of *L. basistriga*, and brick-red to black dorsal coloration of *L. rubritegula*. Alimentary canal visible as a pseudo-middorsal stripe (viewed through transparent heart). Thick white subdorsal stripe punctuated by raised yellow warts with D2 setae borne from apex. Subdorsal warts on A9 yellow, never orange-yellow as in *L. basistriga* or black as in *L. rubritegula*. Two, wavy-edged, pale, supraspiracular stripes extending from T1–A8. Prothoracic shield well differentiated, medially divided, partially melanized, with little pigment deposition along its anterior and lateral margins. Head brown, partially retracted into prothorax.

Type material. Holotype male, dry pinned, TX: Starr Co., Falcon Heights (26.5585N, 99.1220W), 05 March 2018, Berry Nall coll., Deposited at USNM, Washington D.C., USA. **Paratypes adults** (18♂, 8♀): TX: Starr Co., Falcon Heights (26.5585N, 99.1220W), 25 February 2018 – 19 March 2018, Berry Nall coll., BBN18#01, BBN18#05, BBN18#06 (6♂, 5♀) (UCMS); TX: Starr Co., Falcon Heights (26.5337N, 99.1059W), Berry Nall coll., BBN14#06c, (ex-ova; 30 March 2014) emerged 11 June 2014, reared on *Sideroxylon celastrinum*, genitalia slide #TAM–2017–014, CO1 Barcode DLW–000486 (1♂) (UCMS); TX: Starr Co., Falcon Heights (26.5337N, 99.1059W), Berry Nall coll., BBN14#06a, (ex-ova; 30 March 2014) emerged 27 May 2014, reared on *Sideroxylon celastrinum*, Voucher Code TAM0011 (1♀) (UCMS); TX: Starr Co., Falcon Heights (26.5337N, 99.1059W), 19 March 2014, Berry Nall coll., genitalia slide #TAM–2017–013, CO1 Barcode DLW–000569 (1♀) (UCMS); TX: Starr Co., Falcon Lk. (26.559N, 99.125W), 19 March 2018, Jim Vargo coll. (11♂,1♀) (USNM) (TAMUIC).

Other material examined. Adults. TX: Starr Co., Falcon Heights (26.5585N, 99.1220W), 27 February 2018, Berry Nall coll. (1♂); TX: Starr Co., Falcon Heights (26.5585N, 99.1220W), 06 March 2018, Berry Nall coll., BBN18#07 (1♂) **Larvae.** TX: Starr Co., Falcon Heights (26.5337N, 99.1059W), ex-ova from female 25 February 2018 – 6 March 2018, BBN18#01, BBN18#05, BBN18#06, BBN18#07, Berry Nall coll., (n~60) (UCMS).

Etymology. We name this new species after our colleague Berry Nall who provided the majority of type material, reared four clutches of larvae, and first photographed the larva.

Distribution and biology. So far as known, *L. nalli* and *L. basistriga* are allopatric in south Texas, with *L. basistriga* being limited to Tamualipan communities of the lower eastern Rio Grande Valley, and *L. nalli* restricted to the Chihuahuan scrub areas of the western end of the Valley (Fig. 52). The east and west ends of the Rio Grande Valley differ substantially in habitat: the east end is subtropical with palm forests and dry to mesic scrub thickets, while the west end (e.g., Starr County) is drier and more typical of Chihuahuan desert communities. Many species of plants and animals occur at one end of the Valley and not the other. While our collections are limited for *L. nalli*, peak activity of *L. nalli* appears to be from February through March when spring rains are frequent and *Sideroxylon celastrinum* is flushing new leaves (Fig. 60).

Molecular Data

Our phylogenetic analyses of a multi-gene dataset based on seven genes (Fig. 63) suggest that the six species resident north of Mexico fall into two well supported groups with *L. atrolinea* and *L. pupula* forming a group sister to the remainder: *L. basistriga*, *L. nalli*, *L. rubritegula*, and *L. subfervens*. The latter clade, in turn, divides into two groups with *L. subfervens* sister to the three other Nearctic members of the genus (*L. basistriga*, *L. nalli*, and *L. rubritegula*). Relationships among these remain unresolved with (uncorrected) pairwise distances among the three cryptic taxa averaging ~4.5 percent. Average pairwise distance among all sister taxa in the phylogeny was ~5.9 percent. We caution that our phylogenetic analyses consider only US species, and that many relevant Mexican sister taxa (including apparent sister species, based on barcode data in BOLD) were not represented. For example, the omission of the apparent Mexican sister taxa of *L. pupula* and *L. atrolinea*, inflates the average distance between sister taxa that we report. While a few loci did not amplify (Table 1), phylogenetic resolution improved when loci without full coverage were included (Wiens and Morrill 2011).

Discussion

Lactura has challenged some of North America's top systematic microlepidopterists, including August Busck, Harrison Dyar, and Ronald Hodges. Our contributions to the biosystematics of this group were kick-started by larval material and CO1 data for initial sorting. Both data sources were quintessentially important for *L. nalli*, for which no definitive adult characters are yet known. The nuclear data presented here were the last data to be added, and thus acted as a corroboratory data source, affirming the taxonomic decisions that we made based on larvae, life history information, CO1 data, genitalic characters, and distributional data.

As the taxonomic understanding of this group is untangled, it is likely that North American members of *Lactura* will be relegated to a new or different genus. The type-species *Lactura dives* (Walker, 1854) is a striking orange and black Australian moth

with greater than ten percent (uncorrected) barcode dissimilarity from North American members of the genus. Presently, more than 80 species of *Lactura* are distributed worldwide and include an array of seemingly unrelated phenotypes (Heppner 1995, Roskov et al. 2018). Global barcode data suggest that current *Lactura* classification is unnatural and in need of a modern revisionary treatment.

All known species of North American *Lactura* are specialists on the host-plant genus *Sideroxylon* (Sapotaceae). *L. pupula*, *L. rubritegula*, and *L. subfervens* occur in sympatry in central Texas where they use *Sideroxylon lanuginosum*. We have found caterpillars of *L. pupula* and *L. subfervens* feeding alongside one another on early spring foliage; *L. rubritegula* occurs later, flying only at the tail-end of the flights of its congeners (Matson and Wagner 2017). *L. pupula* and *L. subfervens* co-occur widely through the Gulf States, where they share the same host species. In southern Texas, *L. basistriga* and *L. atrolinea* share *Sideroxylon celastrinum* in sympatry. Both moths appear to share the same niche and are active synchronically – a common phenomenon among lepidopterans (Wagner 2005, Wagner et al. 2002, 2011, Nakadai and Murakami 2015, Nakadai and Kawakita 2017, Matson unpubl. data) that appears to challenge the generality of Gause's competitive exclusion principle as a fundamental paradigm in the organization of lepidopteran communities.

Phelan and Baker (1987) hypothesized that male scent-emitting structures in moths are more likely to evolve among closely related sympatric Lepidoptera species that share a common host (because of a higher probability of mating mistakes) than closely related taxa with different hosts. A phylogenetically rigorous example supporting their hypothesis, drawn from a revisionary study of *Atlides* (Lycaenidae) butterflies, was recently published by Martins et al. (2018). Our finding of abdominal male-scent emitting organs in sympatric host-sharing *Lactura* (Figs 31–36) is also consistent with their thesis. It would be telling if tropical burnet moths feeding on novel hostplants or taxonomically (or geographically) isolated lacturids occurring elsewhere were shown to lack abdominal hairpencils or other androconial structures.

CO1 data were valuable in unmasking misidentifications, disambiguating cryptic lineages, and helping guide our fieldwork and genitalic dissections. Given our new understanding of this genus, the records in Barcodes of Life Database (BOLD) were in dire need of curation due to the confusion of *L. subfervens* and its phenotypic overlap with *L. basistriga* and *L. rubritegula*; as well as its failure to treat *L. psammitis* and *L. rhodocentra* as synonyms. Forty-six percent of the 116 North American *Lactura* specimens in BOLD were misidentified prior to the submission of Matson and Wagner (2017).

Evolution advances at different rates across the various behavioral, ecological, molecular, and morphological axes used to adjudicate taxonomic decisions (e.g., adult color/pattern, male and female genitalia, larval morphology, DNA, courtship behaviors, etc.). This revision of North American *Lactura* is a case in point that speaks to the value of larvae, life history data, and molecular analyses over the set of salient adult characters commonly used by moth systematists. Given the overlapping and seemingly indistinguishable adult phenotypes and male genitalic structures in *Lactura*, our findings serve as an endorsement of the value that larvae and molecular data hold for some

lepidopteran groups. We venture that larval phenotypic and life history data will prove equally valuable in advancing our systematic understanding of the rich lacturid faunas of Mexico and the Neotropics.

Acknowledgments

We would like to thank the Biodiversity Institute of Ontario, University of Guelph, for providing DNA barcoding support through the iBOL project, funded by Genome Canada and others, as well as the National Museum of Natural History, Smithsonian Institution, for their generous contributions of genetic data. Specimen loans were provided by the late Edward C Knudson (Texas Lepidoptera Survey), James R McDermott, Richard L Brown (Mississippi Entomological Museum), and Jim Vargo. Andy Deans (Frost Entomological Museum) and Gregory Zolnerowich (KSU Museum of Entomological and Prairie Arthropod Research) provided specimen records from their respective institutions. A special thanks to Delmar Cain who helped with many aspects of this effort: collecting specimens and providing phenological data for the three species of *Lactura* on his property, egging females for ex-ova rearings, assistance with rearing, sending photographs of adults and larvae, providing lodging, and much encouragement. We are much indebted to Berry Nall for his exceptional rearing and photographic assistance and for collecting most of the type series; it was through his efforts that we could describe *L. nalli* as new. Ann Hendrickson sent photographs and collected specimens of *Lactura* from her ranch in Camp Wood, Texas. We thank Brian Scholtens and James Adams for sending material from Sapelo Island, GA, and Lance Durden and Rachel Guy for assisting TAM while on Sapelo Island. Jimmy Paz and Seth Patterson assisted with visits to the Sabal Palm Sanctuary in Brownsville. We are especially grateful to Tony Thomas who prepared most of the genitalic preparations and the (stacked) photographs used in this work (Figs 23–43). Kennedy Marshall assisted with figure illustrations and prepared many of the figures. Marc Epstein, Jean-Francois Landry, and Chris Schmidt provided helpful suggestions that improved earlier versions of this manuscript. Finally, we thank the University of Connecticut's Ecology and Evolutionary Biology Department for funding TAM's travel to collect *Lactura* in Georgia and Florida through the UConn EEB Student Award. DLW is supported by USFS Co-op Agreement 14-CA-11420004-138 and an award from the Richard P Garmany Fund (Hartford Foundation).

References

Barnes W, McDunnough JH (1913) Yponomeutidae. New N. Am. Lepidoptera with notes on described species. Contributions to the natural history of the Lepidoptera of North America. The Review Press (Decatur, Illinois) 2: 142–144.

Barnes W, McDunnough JH (1917) Yponomeutidae. Check List of the Lepidoptera of Boreal America. Herald Press, Decatur, Illinois, 1: 184. https://doi.org/10.5962/bhl.title.29466

Cho S, Mitchell A, Regier JC, Mitter C, Poole RW, Friedlander TP, Zhao S (1995) A highly conserved nuclear gene for low-level phylogenetics: elongation factor-1a recovers morphology-based tree for heliothine moths. Molecular Biology and Evolution 12: 650–656.

Clarke JFG (1955) Catalogue of the type specimens of Microlepidoptera in the British Museum (Natural History) described by Edward Meyrick. Volume II. Stenomidae, Xyloryctidae, Copromorphidae. British Museum (Natural History), London, 531 pp.

Epstein ME, Smedley SR, Eisner T (1994) Sticky integumental coating of a dalcerid caterpillar: a deterrent to ants. Journal of the Lepidopterists Society 48: 381–386.

Epstein ME, Geertsema H, Naumann CM, Tarmann GE (1998) The Zygaenoidea. In: Kristensen NP (Ed.) Lepidoptera, Moths and Butterflies, 1: Evolution, Systematics, and Biogeography. Handbook of Zoology 4. Walter de Gruyter, Berlin, 169–170.

Fang QQ, Cho S, Regier JC, Mitter C, Matthews M, Poole RW, Friedlander TP, Zhao S (1997) A new nuclear gene for insect phylogenetics: dopa decarboxylase is informative of relationships within Heliothinae (Lepidoptera: Noctuidae). Systematic Biology 46: 269–283. https://doi.org/10.1093/sysbio/46.2.269

Heppner JB, Duckworth WD (1983) Yponomeutoidea. In: Hodges RW (Ed.) Check List of the Lepidoptera of America North of Mexico. EW Classey Ltd. & The Wedge Entomological Research Foundation, London, 26–28.

Heppner JB (1995) Lacturidae, new family (Lepidoptera: Zygaenoidea). Tropical Lepidoptera 6: 146–148.

Heppner JB (1997) Case 3001. *Lactura* Walker, 1854 (Insecta, Lepidoptera): Proposed conservation, and proposed conservation of the specific name of *Eustixis pupula* Hübner, [1831] (Currently *Lactura pupula*). Bulletin of Zoological Nomenclature 54: 159–161. https://doi.org/10.5962/bhl.part.100

Heppner JB (2003) Lepidoptera of Florida, Part 1, Introduction and Catalog, Arthropods of Florida and Neighboring Land Areas. Florida Department of Agriculture and Consumer Services, Gainesville, Florida, 312 pp.

Heppner JB (2008) Tropical burnet moths (Lepidoptera: Lacturidae). In: Capinera J (Ed.) Encyclopedia of Entomology. Springer, Dordrecht, 3925 pp. https://doi.org/10.1007/978-1-4020-6359-6_2561

Hübner J (1831) Zuträge zur Sammlung exotischer Schmettlinge. Augsburg, Germany, 1: 24.

Hübner J (1823) Zuträge zur Sammlung exotischer Schmettlinge. Augsburg, Germany, 2: 24.

Huelsenbeck JP, Ronquist F (2001) MRBAYES: Bayesian inference of phylogeny. Bioinformatics 17: 754–755. https://doi.org/10.1093/bioinformatics/17.8.754

ICZN (1999) Opinion 1927. *Lactura* Walker, 1854 (Insecta, Lepidoptera): conserved, and the specific name of *Eustixis pupula* Hübner, (1831) (currently *Lactura pupula*): conserved. The Bulletin of Zoological Nomenclature 56: 158–159.

Kearse M, Moir R, Wilson A, Stones-Havas S, Cheung M, Sturrock S, Buxton S, Cooper A, Markowitz S, Duran C, Thierer T, Ashton B, Mentjies P, Drummond A (2012) Geneious Basic: an integrated and extendable desktop software platform for the organization and analysis of sequence data. Bioinformatics 28: 1647–1649. https://doi.org/10.1093/bioinformatics/bts199

Kimball CP (1965) Arthropods of Florida and neighboring land areas. 1. Lepidoptera of Florida. Division of Plant Industry, State of Florida Department of Agriculture, 292 pp.

Lanfear R, Frandsen PB, Wright AM, Senfeld T, Calcott B (2016) PartitionFinder 2: new methods for selecting partitioned models of evolution for molecular and morphological phylogenetic analyses. Molecular Biology and Evolution 34: 772–773. https://doi.org/10.1093/molbev/msw260

Larsson A (2014) AliView: a fast and lightweight alignment viewer and editor for large datasets. Bioinformatics 30: 3276–3278. https://doi.org/10.1093/bioinformatics/btu531

Martins ARP, Duarte M, Robbins R (2018) Hairstreak butterflies (Lepidoptera, Lycaenidae) and evolution of their male secondary sexual organs. Cladistics 34: 1–25. https://doi.org/10.1111/cla.12355

Matson T, Wagner DL (2017) A new cryptic *Lactura* from Texas (Lepidoptera, Zygaenoidea, Lacturidae). ZooKeys 711: 141–150. https://doi.org/10.3897/zookeys.711.17766

Miller MA, Pfeiffer W, Schwartz T (2010) Creating the CIPRES Science Gateway for inference of large phylogenetic trees. Proceedings of the Gateway Computing Environments Workshop (GCE), New Orleans, 1–8. https://doi.org/10.1109/GCE.2010.5676129

Miller SE, Hodges RW (1990) Primary types of Microlepidoptera in the Museum of Comparative Zoology (with a discursion on V.T. Chambers' work). Bulletin of the Museum of Comparative Zoology 152: 45–87.

Mitchell A, Mitter C, Regier JC (2006) Systematics and evolution of the cutworm moths (Lepidoptera: Noctuidae): evidence from two protein-coding nuclear genes: molecular systematics of Noctuidae. Systematic Entomology 31: 21–46. https://doi.org/10.1111/j.1365-3113.2005.00306.x

Nakadai R, Kawakita A (2017) Patterns of temporal and enemy niche use by a community of leaf cone moths (*Caloptilia*) coexisting on maples (*Acer*) as revealed by metabarcoding. Molecular Ecology 26: 3309–3319. https://doi.org/10.1111/mec.14105

Nakadai R, Murakami M (2015) Patterns of host utilisation by herbivore assemblages of the genus *Caloptilia* (Lepidoptera; Gracillariidae) on congeneric maple tree (*Acer*) species. Ecological Entomology 40: 14–21. https://doi.org/10.1111/een.12148

Neill WT (1957) Historical biogeography of present-day Florida. Bulletin of the Florida State Museum 2: 180–200.

Nguyen LT, Schmidt HA, von Haeseler A, Minh BQ (2014) IQ–TREE: a fast and effective stochastic algorithm for estimating maximum-likelihood phylogenies. Molecular Biology and Evolution 32: 268–274. https://doi.org/10.1093/molbev/msu300

Nye IWB, Fletcher DS (1991) The Generic Names of Moths of the World. Microlepidoptera. London: National History Museum Publications 6: 368. https://doi.org/10.5962/bhl.title.119516

Shorthouse DP (2010) SimpleMappr, an online tool to produce publication-quality point maps. http://www.simplemappr.net [accessed on 1 March 2018]

Slosson AT (1896) Note on *Enæmia crassinervella* Zell (*Mieza igninix* Walk.). Journal of the New York Entomological Society 4: 86–87.

Phelan PL, Baker TC (1987) Evolution of male pheromones in moths: reproductive isolation through sexual selection? Science 235: 205–207. https://doi.org/10.1126/science.235.4785.205

Rambaut A, Suchard MA, Xie D, Drummond AJ (2014) Tracer v1.6. http://beast.bio.ed.ac.uk/Tracer

Ratnasingham S, Hebert PD (2007) BOLD: The Barcode of Life Data System [http://www.barcodinglife. org]. Molecular Ecology Resources 7: 355–364. https://doi.org/10.1111/j.1471-8286.2007.01678.x

Regier JC, Mitter C, Mitter K, Cummings MP, Bazinet AL, Hallwachs W, Janzen DH, Zwick A (2017) Further progress on the phylogeny of Noctuoidea (Insecta: Lepidoptera) using an expanded gene sample. Systematic Entomology 42: 82–93. https://doi.org/10.1111/syen.12199

Ronquist F, Huelsenbeck JP (2003). MRBAYES 3: Bayesian phylogenetic inference under mixed models. Bioinformatics 19: 1572–1574. https://doi.org/10.1093/bioinformatics/btg180

Roskov Y, Abucay L, Orrell T, Nicolson D, Bailly N, Kirk PM, Bourgoin T, DeWalt RE, Decock W, De Wever A, Nieukerken E, Zarucchi J, Penev L (2018) Species 2000 & ITIS Catalogue of Life, 2018 Annual Checklist. Digital resource at www.catalogueoflife.org/annual-checklist/2018. Species 2000: Naturalis, Leiden, the Netherlands.

Rota J, Zacharczenko BV, Wahlberg N, Zahiri R, Schmidt BC, Wagner D (2016) Phylogenetic relationships of Acronictinae with discussion of the abdominal courtship brush in Noctuidae (Lepidoptera). Systematic Entomology 41: 416–429. https://doi.org/10.1111/syen.12162

Wagner DL (2005) Caterpillars of Eastern North America: A Guide to Identification and Natural History. Princeton University Press, Princeton, New Jersey, 512 pp.

Wagner DL, Ferguson DC, McCabe TL, Reardon RC (2001) Geometrid caterpillars of northeastern and Appalachian forests. US Department of Agriculture, Forest Service, publication FHTET–2001–10, 237 pp. https://doi.org/10.5962/bhl.title.150204

Wagner DL, Schweitzer DF, Sullivan JB, Reardon RC (2011) Owlet Caterpillars of Eastern North America (Lepidoptera: Noctuidae). Princeton University Press, Princeton, New Jersey, 576 pp.

Walker F (1854) List of the specimens of lepidopterous insects in the collection of the British Museum. British Museum (Natural History). Department of Zoology 2: 527–528.

Walsingham T (1914) Fam. 18. Hyponomeutidae 321–326. In: Biologia Centrali-Americana. Insecta: Lepidoptera–Heterocera. London 4: 482.

Wahlberg N, Wheat CW (2008) Genomic outposts serve the phylogenomic pioneers: designing novel nuclear markers for genomic DNA extractions of Lepidoptera. Systematic Biology 57: 231–242. https://doi.org/10.1080/10635150802033006

Wiens JJ, Morrill MC (2011) Missing data in phylogenetic analysis: reconciling results from simulations and empirical data. Systematic Biology 60: 719–731. https://doi.org/10.1093/sysbio/syr025

Wilson JJ (2012) DNA barcodes for insects. In: Kress W, Erickson D (Eds) DNA Barcodes: Methods and Protocols. Totowa, New Jersey, 17–46. https://doi.org/10.1007/978-1-61779-591-6_3

Zahiri R, Kitching IJ, Lafontaine JD, Mutanen M, Kaila L, Holloway JD, Wahlberg N (2011) A new molecular phylogeny offers hope for a stable family level classification of the Noctuoidea (Lepidoptera). Zoologica Scripta 40: 158–173. https://doi.org/10.1111/j.1463-6409.2010.00459.x

Zeller PC (1872) Contributions to the knowledge of North American moths, especially the microlepidoptera. Verhandlungen der Zoologisch-Botanischen Gesellschaft in Wien. Selbstverlag 22: 562–563.

Supplementary material 1

Table of localities

Authors: Tanner A. Matson, David L. Wagner, Scott E. Miller

Data type: occurrence

Copyright notice: This dataset is made available under the Open Database License (http://opendatacommons.org/licenses/odbl/1.0/). The Open Database License (ODbL) is a license agreement intended to allow users to freely share, modify, and use this Dataset while maintaining this same freedom for others, provided that the original source and author(s) are credited.

Link: https://doi.org/10.3897/zookeys.846.31953.suppl1

ZooKeys 846: 117–132 (2019)
doi: 10.3897/zookeys.846.31944
http://zookeys.pensoft.net

CHECKLIST

A peer-reviewed open-access journal
ZooKeys
Launched to accelerate biodiversity research

Ichthyofaunal list of the continental slope of the southern Gulf of Mexico

José Martín Ramírez[1], Ana Rosa Vázquez-Bader[2], Adolfo Gracia[3]

1 *Posgrado en Ciencias del Mar y Limnología, Universidad Nacional Autónoma de México* **2** *Posdoc. Unidad Académica de Ecología y Biodiversidad Acuática, Instituto de Ciencias del Mar y Limnología, Universidad Nacional Autónoma de México* **3** *Unidad Académica de Ecología y Biodiversidad Acuática, Instituto de Ciencias del Mar y Limnología, Universidad Nacional Autónoma de México, A.P.70-305, Ciudad de México, 04510, México*

Corresponding author: *José Martín Ramírez* (montevivo100@gmail.com)

Academic editor: *M. Elina Bichuette* | Received 26 November 2018 | Accepted 3 January 2019 | Published 16 May 2019

http://zoobank.org/D1A66290-1018-490B-9832-2E51ED42D66B

Citation: Ramírez JM, Vázquez-Bader AR, Gracia A (2019) Ichthyofaunal list of the continental slope of the southern Gulf of Mexico. ZooKeys 846: 117–132. https://doi.org/10.3897/zookeys.846.31944

Abstract

Four oceanographic cruises were carried out between April 2011 and May 2013 on the continental slope of the southern Gulf of Mexico (GoM) in a depth range of 290 to 1200 m on board the R/V JUSTO SIERRA. A total of 91 trawls covered a total swept area of 170.49 hectares. We recorded 177 fish species belonging to 80 families. Fifteen species extended their distribution into the south of the gulf and 37 increased their depth ranges. Five species could have commercial importance: *Aphanopus carbo* Lowe, 1839; *Hydrolagus mirabilis* (Collett, 1904); *Helicolenus dactylopterus* (Delaroche, 1809); *Lophius gastrophysus* Miranda Ribeiro, 1915, and *Merluccius albidus* (Mitchill, 1818). The most abundant species were *Polymixia lowei* Günther, 1859; *Parasudis truculenta* (Goode & Bean, 1896); *M. albidus*, *Chlorophthalmus agassizi* Bonaparte, 1840; *Dibranchus atlanticus* Peters, 1876; *Nezumia aequalis* (Günther, 1878); *Yarrella blackfordi* Goode & Bean, 1896; and *Laemonema barbatulum* Goode & Bean, 1883. High values of fish species richness, diversity, and evenness were registered throughout the study area. A high percentage of the fish species (97%) collected during this project are distributed in the entire GoM. Most of the species showed a wide depth distribution; however, a vertical zonation of species can be observed.

Keywords

Deep water, fishes, new records, species richness

Copyright *José Martín Ramírez et al.* This is an open access article distributed under the terms of the Creative Commons Attribution License (CC BY 4.0), which permits unrestricted use, distribution, and reproduction in any medium, provided the original author and source are credited.

Introduction

The Gulf of Mexico (GoM) is one of the most productive and economically important ecosystems in the world (Cato 2009, Tunnell 2009), and its large biodiversity makes it one of the most diverse seawater bodies (Felder et al. 2009). Due to its ecological and economic importance, ichthyofauna studies initially focused on commercial species. Research on fish biodiversity in the GoM, which began in 1850 (Darnell and Defenbaugh 1990), became more systematic and extensive since 1950. A total of 1541 species has been reported in the GoM in the different types of habitats that exist in this large ecosystem (McEachran 2009). Nevertheless, more emphasis has been placed on coastal regions because they are more accessible and economical to survey compared to deeper areas and the open sea.

Few investigations about fish biodiversity have been conducted on the continental slope, and most have focused on different ecological aspects of demersal fish communities in the northern part of the GoM (Pequegnat et al. 1990, Powell et al. 2003). More than 126 mesopelagic fish species were found in this region by Ross et al. (2010), who compared the composition of mesopelagic fishes in three different habitats located at depths between surface and 1000 m. Sulak et al. (2007) documented 53 benthic fishes associated with deep water coral habitats in the north-central gulf. McEachran and Fechhelm (1998) produced one of the most complete ichthyological inventories for the GoM and for the Caribbean Sea's continental slope. In addition, Anderson et al. (1985), Saavedra-Díaz et al. (2004) and Paramo et al. (2015) issued complementary reports of 44 species in this region. Others studies of the deep-water fishes in the Caribbean, but concerning to deep reef fishes have been conducted by Colin (1974); Thresher and Colin (1986); Baldwin and Robertson (2014); Baldwin et al. (2016) and Quattrini et al. (2017).

Since there were not studies of fish communities in the southern deep-water of the GoM, the ichthyological inventory of this ecosystem is not yet completed. The Mexican portion of the GoM deep water has recently become an area of interest because of its oil extraction potential (PEMEX 2016) and its potential fishing resources, where at least three important shrimp species have recently been discovered (Gracia et al. 2010). In a potential scenario of exploitation of both living and non-living resources of deep waters of the GoM, it is crucial to acquire more knowledge about this ecosystem. Biodiversity inventories need to be developed to understand, manage, and conserve these resources.

In this study we present information of the fish biodiversity of the scarce explored continental slope of the southern GoM. Our study is the first one that systematically analyzes the deep-water fish fauna in this region.

Materials and methods

The GoM is in a subtropical region that measures 1600 km from east-to-west and 1300 km from north-to-south. It is influenced by the Caribbean Sea due to the transport of water masses via the Loop Current flowing into the gulf through the Yucatan

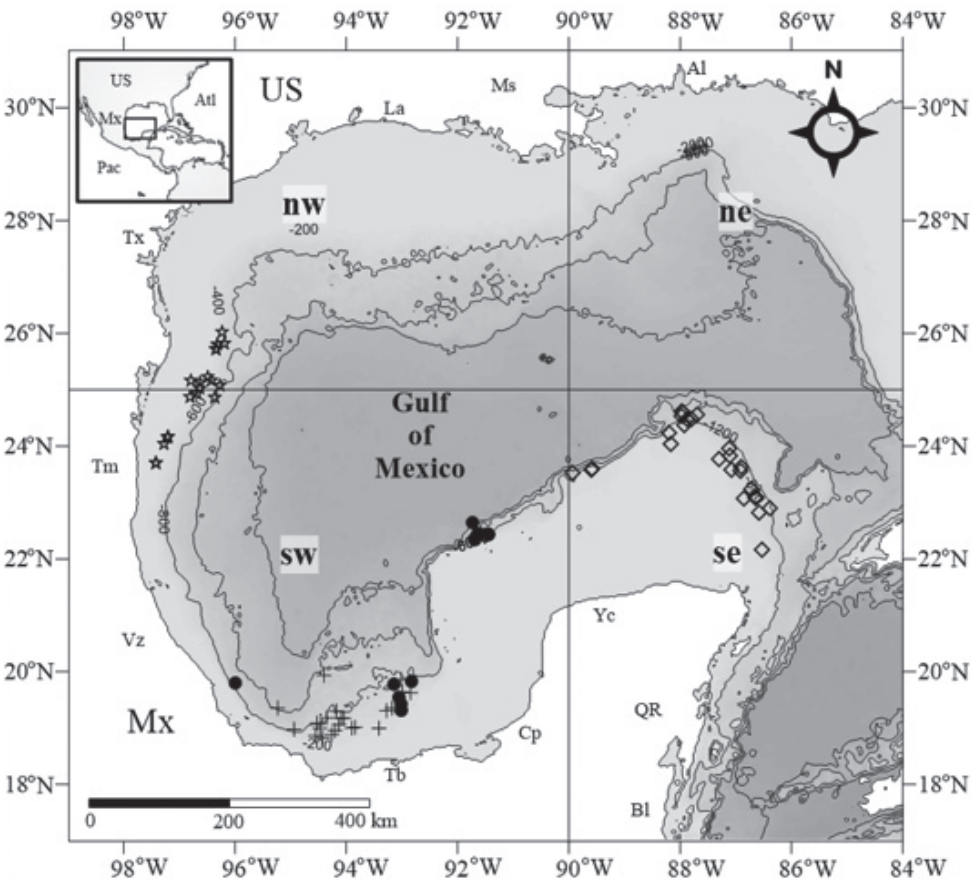

Figure 1. Locations of the oceanographic cruises: COBERPES 2; COBERPES 3; COBERPES 4; and COBERPES 5. Abbreviations: ne: north-east; nw: north-west; se: south-east; sw: south-west; Al: Alabama; Atl: Atlantic; Bl: Belize; Cp: Campeche; La: Louisiana; Ms: Mississippi; Mx: Mexico; Pac: Pacific; QR: Quintana Roo; Tb: Tabasco; Tm: Tamaulipas; Tx: Texas; US: United States; Vz: Veracruz; Yc: Yucatan. Gulf of Mexico division taken from Felder et al. (2009).

Channel and out of the gulf through the Straits of Florida. Winds, especially in winter also impact gulf circulation (Monreal-Gómez et al. 2004) (Fig. 1).

This research forms part of the project "Biodiversity and Potential Fishing Resources in Deep waters of the Gulf of Mexico," through which oceanographic cruises (Benthic communities and potential fishing resources in the Gulf of Mexico deep waters, COBERPES) were conducted on the Mexican continental slope of the GoM on board the R/VJUSTO SIERRA of the Universidad Nacional Autónoma de México.

Four oceanographic cruises were carried out from April 2011 to May 2013: COBERPES 2 and COBERPES 3 on the Yucatan Slope; COBERPES 4, off the coast of Tamaulipas and COBERPES 5 on the Campeche Bank (Table 1). The benthic megafauna of soft bottom substrates was sampled in a depth range of 290–1200 m, using

Table 1. Geographic location and data on oceanographic cruises.

Cruise	Date	Geographic locations				Number of samples	Area (ha)
COBERPES 2	07–15 Apr 2011	23°02'46"N, 86°26'34"W	23°30'98"N, 89°49'42"W	24°22'60"N, 87°42'98"W	22°53'05"N, 86°15'49"W	28	46.79
COBERPES 3	13–19 Nov 2011	22°25'65"N, 91°26'49"W	19°19'38"N, 93°02'54"W	22°23'93"N, 91°37'41"W	19°33'82"N, 93°01'46"W	20	34.87
COBERPES 4	23–30 Aug 2012	23°30'73"N, 97°12'79"W	25°47'30"N, 96°14'83"W	24°54'93"N, 96°36'91"W	25°45'97"N, 96°13'05"W	20	38.58
COBERPES 5	22–31 May 2013	19°03'92"N, 94°05'53"W	18°45'66"N, 94°22'13"W	19°00'80"N, 93°50'35"W	19°48'22"N, 92°59'11"W	23	50.25

a semi-commercial shrimp trawling net with an 18m mouth, a 4.5cm mesh and a 1.5cm cod-end opening. Since information about sea bottom was lacking, sea bed was previously explored using a Multihaz EM 300 echo sounder and a Topas PS-18 sub-bottom profiler. After finding adequate substrate, 30-minute trawls were performed at an average velocity of 77.16 m/min. The distance of each tow was determined by GPS readings. Fauna samples were sorted by taxonomic groups, weighed, and preserved in 10% formalin on board.

In the laboratory, fishes were identified to species level. The names, authorities, and years of the descriptions were cross-referenced against the Eschmeyer database (2017), as well as the geographic and bathymetric distribution of the species was consulted in different web sites: Ocean Biogeographic Information System (OBIS 2018); Smithsonian National Museum of Natural History; Biodiversity of the Gulf of Mexico Database (Moretzsohn et al. 2017); Texas A & M University Corpus Christi, Harte Research Institute for Gulf of Mexico Studies (2017); FishNet 2 (2013); World Register of Marine Species (WoRMS 2017) and FishBase (Froese and Pauly 2017). Each individual was measured, weighed, preserved in 70% alcohol, and retained in the Reference Collection of the Laboratorio de Ecología Pesquera de Crustáceos del Instituto de Ciencias del Mar y Limnología, UNAM. Number of fish species vs. sampling effort was analyzed to determine sample size using the Clench model (Jiménez-Valverde and Hortal 2003) and the freeware Stimates v8 (Colwell 2006). With the biological data was examined the abundance (individuals/ha), richness (number of species), diversity (Shannon and Wiener 1963), and evenness (Pielou 1977) of the fish communities in different sampling areas. The bathymetric distribution of the species was recorded considering the average depth of each trawl.

Results

Ninety-one trawls covering a 290–1200 m depth range were done in the different regions of the southern GoM during the four oceanographic cruises. The numbers of successful trawls at each depth stratum were 300 m: 17; 400 m: 11; 500 m: 16; 600 m: 8; 700 m:

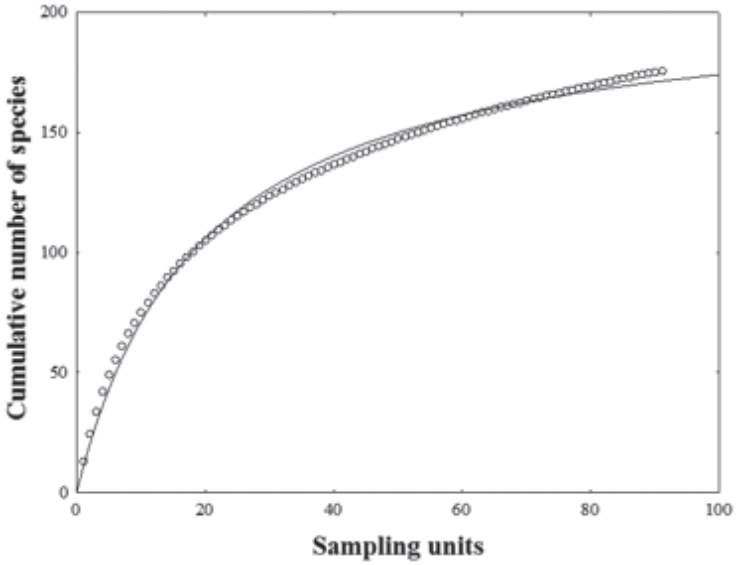

Figure 2. Plot for fish species accumulation for the total sample. Key: circles, random curve; continuous line, fit curve of Clench function ($Sn = (10.79*n)/(1+(0.0520*n)$. Each sample unit consisted of 30 minutes trawl at an average speed of 77.16 m/min (2.5 knots).

11; 800 m: 11; 900 m: 6; and 1000 m: 4, corresponding to 170 hectares total swept area. Seven trawls failed (Table 1). A total of 9781 fishes was caught, belonging to 80 families and 177 species (Table 2). The species accumulation curve related to the number of samples did not reach a clear asymptote; however, data adjusted with a Clench model suggests that 91% species richness of the southern GoM continental slope was recorded (Fig. 2).

The most abundant species were *P. lowei* (1206 individuals), *P. truculenta*, *M. albidus*, *C. agassizi*, *D. atlanticus*, *N. aequalis*, *Y. blackfordi*, and *L. barbatulum*. Among these, *P. lowei* and *C. agassizi* are outstanding, with a relative abundance greater than 10%, and *D. atlanticus*, and *M. albidus* with a relative frequency of more than 50% (Fig. 3).

The lowest richness was found in the Yucatan slope area near the Caribbean Sea (COBERPES 2), with a total of 27 species and a mean of 11.81 ± 5.71 (SD) species per trawl, whereas, the highest one was registered in the Campeche Bay (COBERPES 5) with 39 species (17.26 ± 9.06 species per trawl), however, a high fish species richness (>30 species) was recorded at different sites throughout the GoM (Fig. 4a). The highest fish abundance was registered in the Yucatan continental slope, close to the Caribbean Sea (COERPES 2), with 412.46 individuals/ha recorded and a sample mean of 76.83 ± 19.18 individuals/ha (Fig. 4b). High fish diversity (Fig. 4c) and evenness (Fig. 4d) were recorded in several locations along the entire gulf, except in the area close to the Caribbean Sea (COBERPES 2).

Fifteen species extended their distribution into the continental slope of the southern GoM: *Eptatretus caribbeaus* Fernholm, 1982; *Ventrifossa mucocephalus* Marshall, 1973; *L. barbatulum*; *Brotulotaenia nigra* Parr, 1933; *Lophiodes beroe* Caruso, 1981;

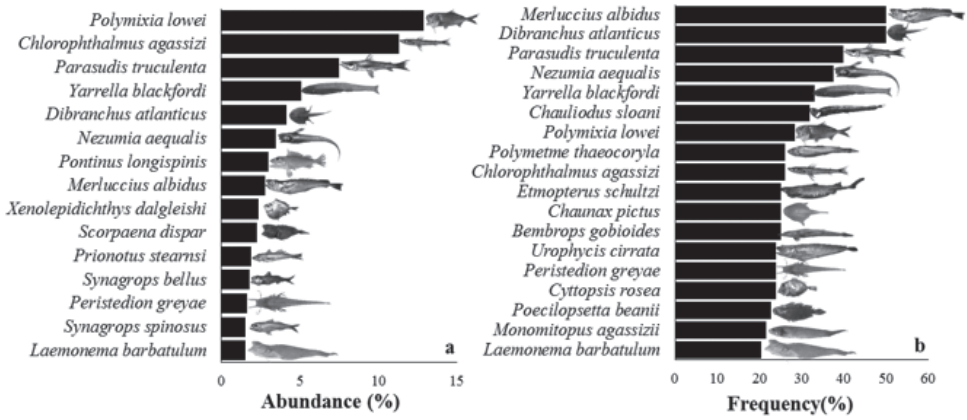

Figure 3. Abundance and frequency of the fish species: **a** Abundance (%) and **b** Frequency (%).

Table 2. List of the fish community. Presence and depth distribution ranges of fish species in the different cruises and literature reported (McEachran 2009, Ocean Biogeographic Information System (OBIS), Eschmeyer 2017, Moretzsohn et al. 2017, FishNet 2 2013, World Register of Marine Species 2017, and Froese and Pauly 2017). Key: * species which extended their distribution into the south of the Gulf of Mexico; ne: north-east; nw: north-west; se: south-east; sw: south-west; Al: Alabama; Atl: Atlantic; Bh: Bahamas; Bl: Belize; Cp: Campeche; Cb: Caribbean; Cu: Cuba; La: Louisiana; Ms: Mississippi; Mx: Mexico; QR: Quintana Roo; Tb: Tabasco; Tx: Texas; Tm: Tamaulipas; US: United States; Vz: Veracruz; Yc: Yucatan. ** Species which extended their depth ranges.

Specie	COBERPES cruises				Species depth range (m)	Reported distribution and depth range (m)
	2	3	4	5		
Antigonia capros Lowe, 1843		X			296	entire/50–900
Antigonia combatia Berry & Rathjen, 1959	X				308	Fl, Al, Bl/68–585
Aphanopus carbo Lowe, 1839			X		823	Atl, Vz/200–2300
Apristurus laurussonii (Saemundsson, 1922)	X				562–937	Ms, Al, Tx, Fl, Mx/500–1000
Argentina georgei Cohen & Atsaides, 1969**	X	X	X	X	300–825	entire/220–457
Argyropelecus aculeatus Valenciennes, 1850	X		X	X	436–825	entire/100–2056
Aristostomias tittmanni Welsh, 1923	X				974	entire/100–2000
Astronesthes similus Parr, 1927				X	611	entire/0–800
Atractodenchelys phrix Robins & Robins, 1970**	X			X	534–600	Cb, Fl, Cu, Vz/385–425
Baldwinella aureorubens (Longley, 1935)		X		X	300–611	Mx/91–610
Baldwinella vivanus (Jordan & Swain, 1885)	X		X	X	300	Mx/20–610
Barathronus bicolor Goode & Bean, 1886					846	entire/366–1561
Barbantus curvifrons (Roule & Angel, 1931)			X		953	ne, nw, Fl/0–4500
Bathyclupea argentea Goode & Bean, 1896**	X		X	X	300–677	entire/366–677
Bathycongrus dubius (Breder, 1927)				X	327	entire/120–886
Bathycongrus vicinalis (Garman, 1899)	X				477	Mx, US, Cb/101–503
Bathygadus favosus Goode & Bean, 1886	X	X			904–1068	entire/770–2745
Bathygadus macrops Goode & Bean, 1885**	X	X	X	X	494–1068	entire/200–777
Bathygadus melanobranchus Vaillant, 1888	X	X	X	X	602–1071	entire/400–2600
Bathypterois bigelowi Mead, 1958	X		X		534–780	entire/377–986
Bathypterois grallator (Goode & Bean, 1886)		X			953	entire/878–4720
Bathypterois quadrifilis Günther, 1878	X				865	entire/462–1408

Specie	COBERPES cruises 2	3	4	5	Species depth range (m)	Reported distribution and depth range (m)
Bathypterois viridensis (Roule, 1916)	X		X	X	593–904	entire/476–1477
Bathyuroconger vicinus (Vaillant, 1888)	X	X			477	ne, nw, Tm/100>1000
Bembrops anatirostris Ginsburg, 1955**	X	X	X	X	300–611	entire/82–538
Bembrops gobioides (Goode, 1880)**	X	X	X	X	300–825	entire/82–740
Benthodesmus simonyi (Steindachner, 1891)*	X			X	436–500	ne/200–900
Benthodesmus tenuis (Günther, 1877)	X	X	X	X	300–825	nw, ne, Mx/200–850
Bolinichthys supralateralis (Parr, 1928)	X		X	X	599–677	entire/40–850
Bregmaceros atlanticus Goode & Bean, 1886				X	300–462	entire/50–2000
Bregmaceros cantori Milliken & Houde, 1984***	X				812	ne/0–475
Bregmaceros houdei Saksena & Richards, 1986***	X		X		346–611	ne/>50
Brotulotaenia nigra Parr, 1933***			X	X	800–953	Atl/1000–1100
Caulolatilus cyanops Poey, 1866		X			300–500	entire/45–459
Chascanopsetta lugubris Alcock, 1894	X				358–426	entire/60–3210
Chauliodus sloani Bloch & Schneider, 1801	X	X	X	X	300–953	entire/0–4700
Chaunax pictus Lowe, 1846	X	X	X	X	321–865	ne, nw, Tb/200–978
Chiasmodon sp.				X	780	ne, Tb, QR
Chlorophthalmus agassizi Bonaparte, 1840	X	X	X	X	300–825	entire/50–3000
Citharichthys dinoceros Goode & Bean, 1886	X				336–423	ne, QR, Bl, Cu/180–2000
Coccorella atlantica (Parr, 1928)			X		995	entire/50–1000
Coelorinchus caribbaeus (Goode & Bean, 1885)**		X	X	X	300–825	entire/200–700
Coelorinchus caelorhincus (Risso, 1810)	X		X	X	436–800	entire/90–1485
Coelorinchus occa (Goode & Bean, 1885)	X	X		X	321–820	entire/400–2220
Coelorinchus ventrilux Marshall & Iwamoto, 1973	X	X	X	X	300–534	se, sw/300>500
Coloconger meadi Kanazawa, 1957		X	X		494–846	Tm, Vz, ne, nw/366–925
Conocara macropterum (Vaillant, 1888)**	X	X		X	354–1071	Mx/800–2200
Coryphaenoides alateralis Marsahll & Iwamoto, 1973	X				904	Mx/1035–1116
Coryphaenoides mexicanus (Parr, 1946)	X				534–937	Mx/110–1600
Coryphaenoides zaniophorus (Vaillant, 1888)	X		X	X	677–1065	entire/400–2775
Cruriraja rugosa Bigelow & Schroeder, 1958	X	X	X		321–825	Mx/366–1007
Cyttopsis rosea (Lowe, 1843)	X	X	X	X	300–825	Mx/100>1000
Dactylobatus clarkii (Bigelow & Schroeder, 1958)	X				626	Mx/366–1000
Diaphus dumerilii (Bleeker, 1856)	X		X		423–823	entire/0–850
Diaphus fragilis (Tåning, 1928)			X		823	entire/15–1313
Dibranchus atlanticus Peters, 1876	X	X	X	X	300–1071	entire/22–1300
Dicrolene introniger Goode & Bean, 1883		X	X	X	321–1071	entire/200–1785
Diplacanthopoma brachysoma Günther, 1887	X		X		494–766	entire/439–1670
Dipturus oregoni (Bigelow & Schroeder, 1958)		X			611	Mx/369–1079
Dipturus teevani (Bigelow & Schroeder, 1951)				X	540–800	Cp/311–940
Diretmoides pauciradiatus (Woods, 1973)**	X	X	X	X	321–800	entire/0–600
Epigonus denticulatus Dieuzeide, 1950	X	X		X	354–800	Mx/130–830
Epigonus macrops (Brauer, 1906)			X		766–823	entire/550–1300
Epigonus occidentalis Goode & Bean, 1896	X			X	573–700	Vz, Tm/360–737
Epigonus oligolepis Mayer, 1974	X				540–619	Mx/380–660
Epigonus pandionis (Goode & Bean, 1881)		X	X	X	419–494	Cp/200–600
Epigonus pectinifer Mayer, 1974			X		346–677	Mx/100–1200
Eptatretus caribbeaus Fernholm, 1982***	X				597	Cb/300–400
Espringeria folirostris Bigelow & Schroeder, 1951		X	X	X	354–800	ne, nw, se, sw/50–1052
Etmopterus schultzi Bigelow, Schroeder & Springer, 1953	X	X	X	X	300–852	entire/200–1000
Etmopterus virens Bigelow, Schroeder & Springer, 1953	X	X	X	X	392–800	Mx/100–1000
Gadella imberbis (Vaillant, 1888)	X	X	X	X	300–974	Mx, Cb, Cu/70>900
Gadomus arcuatus (Goode & Bean, 1886)**	X	X	X	X	321–1068	entire/610–1370
Gadomus dispar (Vaillant, 1888)		X	X		611–677	Tm/548–1105
Gadomus longifilis (Goode & Bean, 1885)**	X	X	X	X	321–1071	entire/630–2168

Specie	COBERPES cruises				Species depth range (m)	Reported distribution and depth range (m)
	2	3	4	5		
Galeus arae (Nichols, 1927)	X	X			358–780	Mx/250–750
Gibberichthys pumilus Parr, 1933	X				746	entire/300–1100
Gigantura chuni Brauer, 1901	X				540	entire/0–1830
Gymothorax kolpos Böhlke & Böhlke, 1980	X				336	entire/30–300
Halieutichthys aculeatus (Mitchill, 1818)		X			611	entire/8–820
Halosaurus ovenii Johnson, 1864	X	X	X	X	321–1068	entire/300>2000
Helicolenus dactylopterus (Delaroche, 1809)	X				426	Mx/50–1100
Hemantias leptus (Ginsburg, 1952)		X			611	entire/35–640
Heptranchias perlo (Bonnaterre, 1788)				X	436	entire/0–1000
Hollardia hollardi Poey, 1861	X	X		X	300–800	Mx/230–915
Hoplostethus mediterraneus Cuvier, 1829*	X		X	X	354–800	ne/100–1750
Hoplunnis tenuis Ginsburg, 1951**		X		X	302–611	entire/30>400
Hydrolagus alberti Bigelow & Schroeder, 1951		X	X	X	494–1068	entire/348–1470
Hydrolagus mirabilis (Collett, 1904)	X		X	X	462–812	entire/450–1933
Hygophum reinhardtii (Lütken, 1892)	X				611	entire/0–1100
Hymenocephalus aterrimus Gilbert, 1905		X			354–540	entire/340–1348
Hymenocephalus billsam Marshall & Iwamoto, 1973	X				573–711	entire/400–900
Hymenocephalus italicus Giglioli, 1884	X	X	X	X	428–800	entire/100–1400
Ijimaia antillarum Howell Rivero, 1935**	X	X	X	X	462–1068	entrire/439>700
Laemonema barbatulum Goode & Bean, 1883*	X	X	X	X	426–937	QR/50–1620
Leptoderma macrops Vaillant, 1886	X	X	X	X	700–1065	Mx/500–2000
Leucoraja garmani (Whitley, 1939)**	X	X	X	X	300–800	Mx/37–530
Leucoraja lentiginosa (Bigelow & Schroeder, 1951)**	X	X	X	X	346–852	entire/53–538
Lophiodes beroe Caruso, 1981*	X	X		X	462–735	ne/347–860
Lophiodes monodi (Le Danois , 1971)**	X	X		X	419–800	ne, se/366–549
Lophiodes reticulatus Caruso & Suttkus, 1979	X				590–619	entire/64–820
Lophius gastrophysus Miranda Ribeiro, 1915	X				599	entire/40–700
Luciobrotula corethromycter Cohen, 1964	X	X			606–846	Mx/220–1830
Macroramphosus scolopax (Linnaeus, 1758)*	X				308	ne, nw, Cu/25–600
Malacocephalus laevis (Lowe, 1843)	X	X	X	X	300–800	entire/200–1000
Malacocephalus occidentalis Goode & Bean, 1885	X	X	X	X	308–800	entire/140–1495
Merluccius albidus (Mitchill, 1818)	X	X	X	X	300–852	entire/80–1170
Monolene sessilicauda Goode, 1880	X	X			336–1046	ne, nw, sw/0>3000
Monomitopus agassizii (Goode & Bean, 1896)	X	X	X	X	300–1071	entire/48–1125
Myctophum nitidulum Garman, 1899			X		823	entire/0–1537
Nemichthys scolopaceus Richardson, 1848		X			321	ne, nw, Yc, Cu/100–4337
Neoepinnula americana (Grey, 1953)			X	X	300–370	Yc/0–600
Neoscopelus macrolepidotus Johnson, 1863*	X	X	X	X	300–852	ne, nw, Cu, Tb/300–1180
Neoscopelus microchir Matsubara, 1943*	X			X	300–814	ne, nw, Cu, Bh/60>900
Nettastoma melanurum Rafinesque, 1810	X	X	X	X	300–852	entire/37–1647
Nezumia aequalis (Günther, 1878)	X	X	X	X	321–973	entire/200–2320
Nezumia cyrano Marshall & Iwamoto, 1973**	X	X	X	X	321–1071	entire/400–1324
Nezumia suilla Marsahll & Iwamoto, 1973	X				904–1046	entire/860–1500
Oxinotus caribbaeus Cervigón, 1961**				X	800	Yc/402–457
Parasudis truculenta (Goode & Bean, 1896)	X	X	X	X	300–846	entire/0>1000
Parazen pacificus Kamohara, 1935	X				300	Cp, Cu/145–512
Peristedion ecuadorense Teague, 1961*	X	X			392–814	ne, nw/324–910
Peristedion greyae Miller, 1967**	X	X	X	X	300–1071	entire/60–914
Peristedion longispatha Goode & Bean, 1886	X			X	302–553	entire/101–787
Peristedion miniatum Goode, 1880		X	X	X	300–500	entire/64–910
Peristedion thompsoni Fowler, 1952*	X				358–423	ne, nw, Cu/115–475

Specie	COBERPES cruises 2	3	4	5	Species depth range (m)	Reported distribution and depth range (m)
Peristedion truncatum (Günther, 1880)	X	X	X		336–852	Vz, Yc/155–910
Photostomias guernei Collett, 1889	X				540–772	entire/500–3100
Poecilopsetta beanii (Goode, 1881)	X	X	X	X	300–825	entire/155–1636
Polyipnus asteroides Schultz, 1938*	X			X	300–820	ne, nw/0>1000
Polymetme thaeocoryla Parin & Borodulina, 1990	X	X	X	X	300–953	entire/165–1400
Polymixia lowei Günther, 1859	X	X	X	X	300–825	entire/0>2000
Pontinus longispinis Goode & Bean, 1896**	X	X		X	300–611	entire/50–440
Prionotus alatus Goode & Bean, 1883**		X			611	Yc/35–457
Prionotus stearnsi Jordan & Swain, 1885	X	X	X		308–346	entire/11–549
Pristipomoides macrophthalmus (Müller & Jelks, 1848)**		X			611	ne, nw, Cp/110–550
Promethichthys prometheus (Cuvier, 1832)	X			X	540–609	ne, Cu, Yc/80–800
Pseudomyrophis frio (Jordan & Davis, 1891)**		X			494	sw, Atl, Yc/0–180
Pseudoraja fischeri Bigelow & Schroeder, 1954	X				534–580	Yc/412–576
Rinoctes nasutus (Koefoed, 1927)		X			1068	ne, nw, Yc/1000–4337
Rouleinia maderensis Maul, 1948	X	X	X		852–1068	ne, Cu/595–1450
Saurida caribbaea Breder, 1927	X		X		308–422	entire/4–460
Saurida normani Longley, 1935	X	X		X	300–611	entire/25–550
Scopelosaurus smithii Bean, 1925			X		953	ne, Vz/50>3000
Scorpaena dispar Longley & Hildebrand, 1940**	X	X	X	X	300–812	entire/0>500
Scyliorhinus retifer (Garman, 1881)	X			X	300–812	entire/36–750
Setarches guentheri Johnson, 1862	X				392	ne, nw, Yc, QR/150–780
Sigmops elongatum (Günther, 1878)	X	X	X	X	494–1068	entire/25–1463
Sphagemacrurus grenadae (Parr, 1946)**	X	X	X	X	820–1071	entire/1000–1960
Squalogadus modificatus Gilbert & Hubbs, 1916	X		X		865–995	entire/50–1740
Squalus cubensis Howell Rivero, 1936**	X	X	X	X	300–608	entire/60>500
Squatina dumeril Lesueur, 1818			X		354–370	entire/0–1375
Steindachneria argentea Goode & Bean, 1886			X	X	300–370	entire/350–550
Stephanoberyx monae Gill, 1883	X	X	X		628–953	entire/945–4777
Sternoptyx diaphana Hermann, 1781	X	X	X		577–1065	entire/300–3676
Sternoptyx pseudobscura Baird, 1971	X		X		628–953	entire/0>3000
Stomias affinis Günther, 1887	X	X			611–772	entire/0–3180
Symbolophorus rufinus (Tåning, 1928)				X	327	entire/0–3000
Synagrops bellus (Goode & Bean, 1896)	X	X	X	X	300–974	entire/00>900
Synagrops spinosus Schultz, 1940**	X	X	X	X	300–825	entire/0–544
Synaphobranchus affinis Günther, 1877					820	entire/290–2400
Synaphobranchus oregoni Castle, 1960	X	X	X	X	377–1071	entire/45–1900
Synchiropus agassizii (Goode & Bean, 1888)	X	X			336–426	Mx, Cb, Cp/0–500
Tetronarce nobiliana (Bonaparte, 1835)				X	540	ne, nw, Cp, Yc/0–530
Thaumatichthys binghami Parr, 1927**	X				820	ne, nw, Cb/1100–4032
Trachonurus sulcatus (Goode & Bean, 1885)**	X	X	X	X	626–1068	entire/700–1500
Trachyscorpia cristulata (Goode & Bean, 1896)					619–628	ne, Cb, Mx/130–1100
Urophycis cirrata (Goode & Bean, 1896)**		X	X	X	300–825	entire/27>700
Venefica procera (Goode & Bean, 1883)	X		X	X	327–953	ne, nw, Tm, Vz/326–2340
Ventrifossa macropogon Marshall, 1973**	X	X	X		300–846	Tm, Yc/439–1000
Ventrifossa mucocephalus Marshall, 1973***	X	X	X	X	300–814	ne, Cb/450–732
Xenocephalus egregius (Jordan & Thompson, 1905)	X		X		370–423	entire/180–440
Xenodermichthys copei (Gill, 1884)	X			X	590–865	ne, nw, Vz, Tb/100–2650
Xenolepidichthys dalgleishi Gilchrist, 1922	X		X		346–547	Tm, Cp/90–900
Yarrella blackfordi Goode & Bean, 1896	X	X	X	X	321–1071	entire/350–1000
Zalieutes mcgintyi (Fowler, 1952)	X				300–394	entire/70–500
Zenion hololepis (Goode & Bean, 1896)**	X	X	X	X	300–825	Cp, Tb/180–700

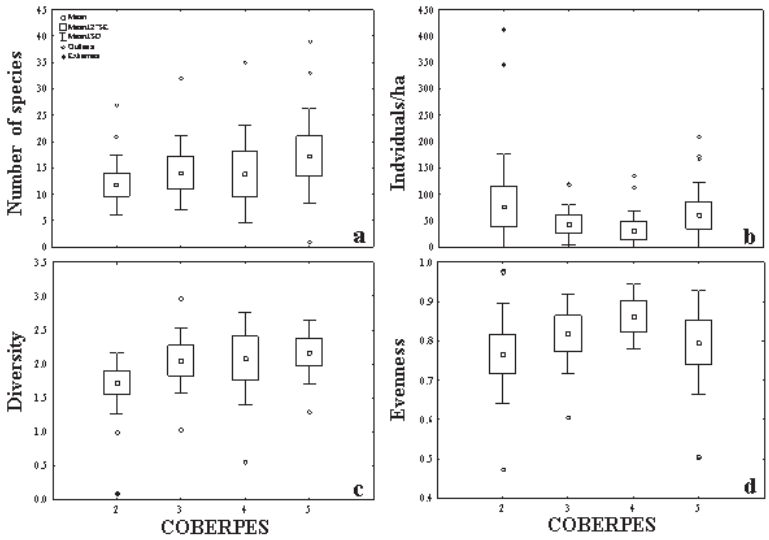

Figure 4. Community parameters for each cruise (COBERPES): **a** Species richness (number of species); **b** Abundance (individuals/ha); **c** Diversity (Shannon-Wiener); **d** Evenness (Pielou).

Hoplostethus mediterraneus Cuvier, 1829; *Benthodesmus simonyi* (Steindachner, 1891); *Macroramphosus scolopax* (Linnaeus, 1758); *Bregmaceros cantori* Milliken & Houde, 1984; *Bregmaceros houdei* Saksena & Richards, 1986; *Peristedion ecuadorense* Teague, 196; *Peristedion thompsoni* Fowler, 1952; *Polyipnus asteroides* Schultz, 1938; *Neoscopelus microchir* Johnson, 1863, and *Neoscopelus macrolepidotus* Matsubara, 1943 (Table 2).

Thirty seven species increased its depth range distribution (Table 2). Three of the most abundant species recorded an average depth lower than 400 m (Fig. 3): *Prionotus stearnsi* Jordan & Swain, 1885 (318 ± 24.57 m); *Xenolepidichthys dalgleishi* Gilchrist, 1922 (379 ± 33.05 m) and *Pontinus longispinis* Goode & Bean, 1896 (376 ± 114.03 m). Many of the species showed a wide depth range distribution (400>800); however, only two of them presented the highest average depth: *Monomitopus agassizii* (Goode & Bean, 1896) and *Y. blackfordi* (743 ± 223.92 m and 749 ± 172.95 m, respectively) (Fig. 5).

Discussion

The species accumulation curve suggests that we registered most of the fish species found on soft bottoms of the continental slope of the southern GoM. Nevertheless, since the species accumulation curve continued to increase, the inventory still appears to be inconclusive. This situation is congruent with the fact that the sampling effort in the GoM deep waters has been low, particularly in the south. We identified 177 species which represent 12% of the total fish species (1541) reported for all habitats in continental shelf and deep waters including demersal and pelagic fishes of the GoM

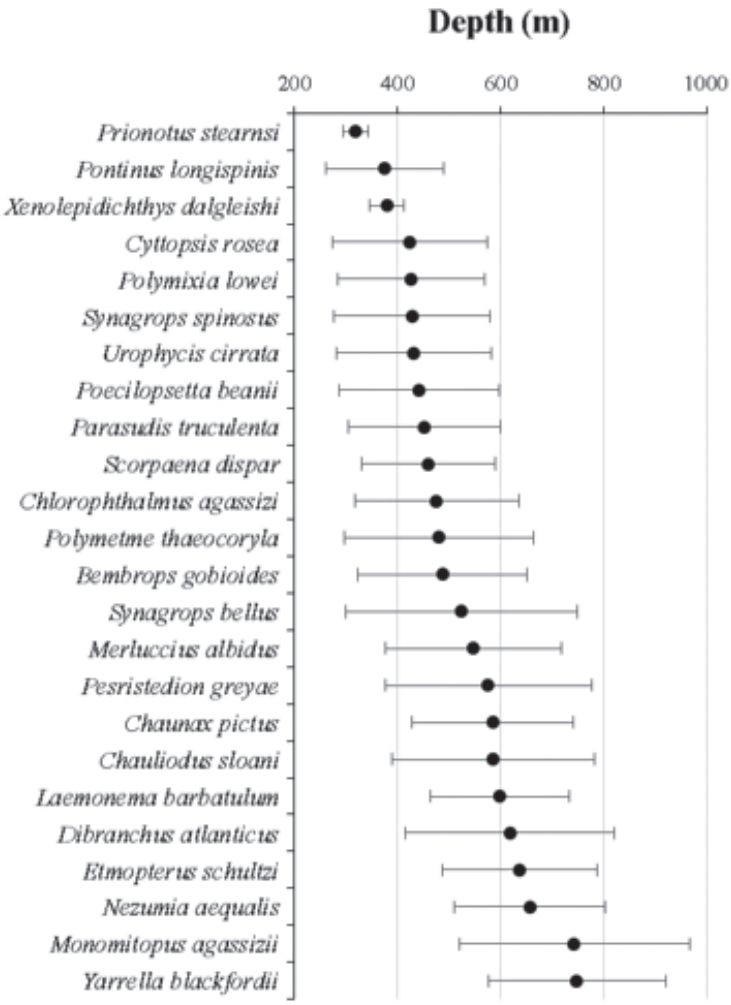

Figure 5. Depth of occurrence of the most abundant fish species: average depth ± standard deviation (SD).

(McEachran 2009). The only previous systematic study using a similar sampling gear was conducted in the northern GoM by Powell et al. (2003) who recorded 93 demersal fish species for the upper (315–785 m) and mid slope (686–1369 m).

Based on the fish list elaborated by McEachran (2009) we counted 335 benthic and demersal fishes for the continental slope of the GoM. This number is 30 % higher than the 235 summed from this paper and Powell et al. (2003) study. It must be noted that McEachran list includes fishes collected with other gears and also in other habitats, like hard bottoms. Nonetheless, three fish species can be added to McEachran list: *Kali indica* Lloyd, 1909, following Powell et al. (2003) and two species found in this research *E. caribbeaus* and *B. nigra*. In this way, a total compilation of 338 species of benthic and demersal

fishes can be listed for this ecosystem. Additionally, 15 species extended their distribution into the south of the GoM (Table 2). It must also be noted that 37 species extended their depth ranges, nine of them were recorded in deeper ranges and 28 species in shallower depths than previously reported in literature. Most of the species showed a wide distribution depth range which is consistent with the distribution pattern of deep water fishes.

The highest species richness recorded in the continental slope of the Campeche Bay (COBERPES 5), is probably influenced by the high freshwater discharge of the largest hydrological system in the southern GoM: Grijalva-Usumacinta during summer, which inputs 62% of the total freshwater to the mexican GoM (Day et al. 2004), similar to what Powell et al. (2003) found in the northern GoM, near the mouth of the Mississippi River. Likewise, the upwelling produced by cyclonic gyres in the Campeche Bank (De la Lanza-Espino and Gómez-Rojas 2004, Durán-Campos et al. 2017), could be playing an important ecological role. These factors together incorporate large concentrations of nutrients which may trigger local productivity, and subsequently the diversity of demersal fishes on the continental slope in this region. Fish richness and diversity difference between COBERPES 3 and COBERPES 5 could also be influenced by seasonal productivity variations due to current pattern change in the area.

Five species captured in this survey are of commercial importance in other parts of the world. *M. albidus* was one of the second most frequent species (50%) which accounted greatly to total biomass (72.296 kg) and presented relatively large sizes (total length = 103–555 mm). This species could have a fishing potential in the GoM, as it was an important fishing resource in the US Atlantic in the early 1990s, but its production decreased significantly over a 10-year period of exploitation (Traver et al. 2012). Other taxa of commercial interest in the Atlantic such as *H. mirabilis*, *H. dactylopterus* and particularly *A. carbo* (one individual), are important fishing resources in the central and northern regions of the eastern Atlantic Ocean (Bensch et al. 2009, Pajuelo et al. 2010). Another species registered in the present study was *L. gastrophysus*, which was a significant deep water fishing resource in Brazil from 2000 to 2007 (Álvarez et al. 2009). However, the fishing potential of these species in the GoM is still to be defined with further studies.

Compiling data of fish species of this study as well as from the literature (McEachran and Fechhelm 1998, Powell et al. 2003 and McEachran 2009), we found that the north and south parts of the GoM share 97% of the species recorded on soft bottoms of the continental slope of the whole gulf. On the other hand, more than 63% of the species (n = 44) recorded for the Caribbean Sea (n = 69) (Anderson et al. 1985, Saavedra-Díaz et al. 2004, Paramo et al. 2015) also occur in the GoM. McEachran (2009) pointed out that this fish similarity is influenced by fauna from the central Atlantic (the region between North Carolina and the Great and Lesser Antilles, including The Bahamas, Bermuda islands, and South America) due to the Loop Current effect that connects the Yucatan and Florida currents (Monreal-Gómez et al. 2004, NOAA 2016).

This result is consistent with the distribution of deep water fishes inhabiting large bathymetric areas due to more stable environmental conditions in these habitats (Clark et al. 2010). A similar distribution pattern has been recorded in several studies done in the world, for example in the Mediterranean Sea (Moranta et al.1998), in the Atlantic (Menezes et al. 2006, 2015; Magnussen 2002; Bergstad et al. 2012; Koslow 1993;

Quattrini et al. 2015); in the Caribbean (Quattrini et al. 2017), and in the northern of the GoM (Powell et al. 2003).

Our results suggest that a high number of species dwelling on the continental slope are shared between the north and south of the GoM. We recorded an extension in distribution into the south of the GoM and also bathymetrically of several fish species. New records are highly likely to be increased if sampling effort continues both geographically and bathymetrically, since the species cumulative curve did not reach an asymptote. This research contributes to the knowledge of the deep water fish community of the GoM, never studied before in the southern region. However, information needs to be enhanced since deep water natural resources of the southern GoM could be subject to increasing human pressures in the near future.

Acknowledgements

Our acknowledgements are due to Programa de Apoyo a Proyectos de Investigación e Innovación Tecnológica (PAPIIT), Proyecto IN223109-3 of the Universidad Nacional Autónoma de México (UNAM) and to the crew of the R/V *Justo Sierra* for their support in conducting the cruises. The Consejo Nacional de Ciencia y Tecnología (CONACyT) is greatly appreciated for the PhD scholarship. Particularly, we extended thanks to our colleagues of the laboratory of Ecología Pesquera de Crustáceos, ICML, UNAM: Rosa María Hernández Díaz, Diana Torres Galíndez, Magaly Galván Palmerín, Linda Trejo Torres, Sandra Antonio Bueno, Andrea Yazmín López Chávez, León Felipe González Morales, and Iván Martínez Romero. Thanks also to the staff of the Department of Hidrobiología of the Universidad Autónoma Metropolitana-Iztapalapa (UAM-I): Verónica Escobar Morales, Araceli Soto Ávila, Obeth Ayala Medina, Luis Arturo Ponza Ramos, and David Herrera Olayo.

References

Álvarez JAP, Pezzuto PR, Wahrlich R, Souza ALS (2009) Deep-water fisheries: History, status and perspectives. Latin American Journal of Aquatic Research 37(3): 513–541. https://doi.org/10.3856/vol37-issue3-fulltext-18

Anderson ME, Crabtree RE, Carter HJ, Sulak KJ, Richardson MD (1985) Distribution of demersal fishes of the Caribbean Sea found below 2,000 meters. Bulletin of Marine Science 37: 749–807.

Baldwin CC, Robertson DR (2014) A new *Liopropoma* sea bass (Serranidae, Epinephelinae, Liopropomini) from deep reefs off Curaçao, southern Caribbean, with comments on depth distribution of western Atlantic liopropomins. ZooKeys 409: 71–92. https://doi: 10.3897/zookeys.409.7249

Baldwin CC, Robertson DR, Nonaka A, Tornabene (2016) Two new deep-reef basslets (Teleostei, Grammatidae, Lipogramma), with comments on the ecoevolutionary relationship of the genus. Zookeys 638: 45–82. https://doi.org/10.3897/zookeys.638.10455

Bensch A, Gianni M, Gréboval D, Sanders JS, Hjort A (2009) Worldwide review of bottom fisheries in the high seas. FAO Fisheries and Aquaculture Technical Paper No. 522, Rev. 1, Roma, 145 pp.

Bergstad OD, Menezes GMM, Høines ÅS, Gordon JDM, Galbraith JK (2012) Patterns of distribution of deepwater demersal fishes of the North Atlantic mid-ocean ridge, continental slopes, islands and seamounts. Deep-Sea Research I 61: 74–83. https://doi.org/10.1016/j.dsr.2011.12.002

Cato JC (2009) Gulf of Mexico Origin, Waters and Biota: Ocean and Coastal Economy (Vol. 2). Texas A & M University Press, College Station, 136 pp.

Clark MR, Althaus F, Williams A, Niklitsheck E, Menezes G, et al. (2010) Are deep-sea fish assemblages globally homogeneous? Insights from seamounts. Marine Ecology 31(Suppl. 1): 39–51. https://doi.org/10.1111/j.1439-0485.2010.00384.x

Colin PL (1974) Observation and collection of deep-reef fishes off the coast of Jamaica and British Honduras (Belize). Marine Biology 24(1): 29–38.

Colwell RK (2006) Statistical estimation of species richness and shared species from samples. Version 8. http://pulr.oclc.org/estimates

Darnell MR, Defenbaugh ER (1990) Gulf of Mexico: Environmental overview and history of environmental research. American Zoologist 30: 3–6. https://doi.org/10.1093/icb/30.1.3

Day WJ, Díaz de León A, González-Sansón G, Moreno-Casasola P, Yáñez-Arancibia A (2004) Diagnóstico Ambiental del Golfo de México. Resumen ejecutivo. In: Caso M, Pisanty I, Ezcurra E (Eds) Diagnóstico Ambiental del Golfo de México. SEMARNAT, Ciudad de México, 15–46.

De la Lanza-Espino G, Gómez-Rojas JE (2004) Características físicas del Golfo de México. In: Caso M, Pisanty I, Ezcurra E (Eds) Diagnóstico Ambiental del Golfo de México. SEMARNAT, Ciudad de México, 103–132.

Durán-Campos E, Salas de León DA, Monreal-Gómez MA, Coria-Monter E (2017) Patterns of chlorophyll-a distribution linked to mesoscale structure in two contrasting areas Campeche Canyon and Bank, Southern Gulf of Mexico. Journal of Sea Research 123: 30–38. https://doi.org/10.1016/j.seares.2017.03.013

Eschmeyer WN (2017) Catalog of fishes. Catalog databases of CAS. https://www.calacademy.org/scientists/projects/catalog-of-fishes [accessed April 2017]

Felder DL, Camp D, Tunnell Jr JW (2009) An Introduction to Gulf of Mexico Biodiversity Assessment. In: Felder DL, Camp DK (Eds) Gulf of Mexico: Origin, Waters, and Biota. Texas A & M University Press, 1–13.

Fishnet 2 (2013) Fishnet 2. http://www.fishnet2.net/search.aspx [accessed April 2017]

Froese R, Pauly D (2017) FishBase. http://www.fishbase.org [accessed August 2018]

Gracia A, Vázquez-Bader AR, Lozano-Álvarez E, Biones-Fourzán P (2010) Deep water shrimp (Crustacea: Penaeoidea) off the Yucatan Peninsula (southern Gulf of Mexico) a potential fishing resource? Journal of Shellfish Research 29(1): 37–43. https://doi.org/10.2983/035.029.0124

Jiménez-Valverde A, Hortal J (2003) Las curvas de acumulación de especies y la necesidad de evaluar la calidad de los inventarios biológicos. Revista Ibérica de Aracnología 31(8): 151–161.

Koslow JA (1993) Community structure in the North Atlantic deep-sea fishes. Progress in Oceanography 31: 321–338. https://doi.org/10.1016/0079-6611(93)90005-X

Magnussen E (2002) Demersal fish assemblages of Faroe Bank: species composition, distribution, biomass spectrum and diversity. Marine Ecology Progress Series 238: 211–225. https://doi.org/10.3354/meps238211

McEachran JD (2009) Fishes (Vertebrata: Pisces) of the Gulf of Mexico. In: Felder DL, Camp DK (Eds) Gulf of Mexico: Origin, Waters, and Biota. Texas A & M University Press, USA, 1223–1316.

McEachran JD, Fechhelm JD (1998) Fishes of the Gulf of Mexico. (Vol. 1) Myxiniformes to Asterosteiformes. University of Texas Press, USA, 1004 pp.

Menezes GM, Sigler M, Silva HM, Pinho MR (2006) Structure and zonation of demersal fish assemblages off the Azores Archipelago (Mid-Atlantic). Marine Ecology Progress Series 324: 241–260. https://doi.org/10.3354/meps324241

Menezes GM, Tariche O, Pinho MR, Sigler MF, Silva HM (2015) Structure and zonation of demersal fish assemblages off the Cabo Verde archipelago, (northeast-Atlantic) as sampled by baited longlines. Deep-Sea Research I 102: 118–134. https://doi.org/10.1016/j.dsr.2015.04.013

Monreal-Gómez MA, Salas de León DA, Velasco-Mendoza H (2004) La hidrodinámica del Golfo de México. In: Caso M, Pisanty I, Ezcurra E (Eds) Diagnóstico Ambiental del Golfo de México. SEMARNAT, Ciudad de México, 47–68.

Moretzsohn F, Brenner J, Michaud P, Tunnell Jr JW, Shirley T (2017) Biodiversity of the Gulf of Mexico Database (BioGoMx). Version 1.0. Harte Research Institute for Gulf of Mexico Studies (HRI), Texas A & M University-Corpus Christi (TAMUCC), Corpus Christi, Texas. http://www.e-gulf.org [accessed May 2017]

Moranta J, Stefanescus C, Massuti E, Morales-Nin B, Lloris D (1998) Fish community structure and depth related trends on the continental slope of the Balearic Islands (Algerian Basin, western Mediterranean). Marine Ecology Progress Series 171: 247–259. https://doi.org/10.3354/meps171247

NOAA (2016) Gulf of Mexico Regional Action Plan. https://www.cakex.org/documents/gulf-mexico-regional-action-plan [accessed 13 June 2018]

OBIS [Ocean Biogeographic Information System] (2018) Ocean Biogeographic Information System. http://www.iobis.org [accessed August 2018]

Pajuelo JG, González JA, Santana JI (2010) Bycatch and incidental catch of the black scabbardfish (*Aphanopus* spp.) fishery off the Canary Islands. Fisheries Research 106: 448-453. https://doi.org/10.1016/j.fishres.2010.09.019

Paramo J, Pérez D, Acero A (2015) Estructura y distribución de los condrictios de aguas profundas en el Caribe colombiano. Latin American Journal of Aquatic Research 43(4): 691–699. https://doi.org/10.3856/vol43-issue4-fulltext-8

PEMEX (2016) Reporte de resultados de PEMEX al 31 de diciembre de 2015. http://www.pemex.com/ri/finanzas/Reporte%20de%20Resultados%20no%20Dictaminados/Reporte_4T15.pdf [accessed 28 June 2018]

Pequegnat WE, Gallaway BJ, Pequegnat LH (1990) Aspects of the ecology of the deep-water fauna of the Gulf of Mexico. American Zoologist 30: 45–64. https://doi.org/10.1093/icb/30.1.45

Pielou EC (1977) Mathemathical Ecology. Wiley, New York, 385 pp.

Powell MS, Haedrich RL, McEachran JD (2003) The deep-sea demersal fish fauna of the northern Gulf of Mexico. Journal of Northwest Atlantic Fisheries Science 31: 19–33. https://doi.org/10.2960/J.v31.a2

Quattrini AM, Nizinsky MS, Chaytor JD, Demopoulos AW, Roak EB, France SC, Moore JA, Heyl T, Auster PJ, Kinlan B, Ruppel C, Elliott K P, Kennedy BRC, Lobecker E, Skarke A, Shank TM (2015) Exploration of the canyon-incised continental margin of the northeastern United States reveals dynamics habitats and diverse community. PLos ONE 10(10): e0139904. https://doi.org/10.1371/journal.pone.0139904

Quattrini AM, Demopoulos AEJ, Randal S, Roa-Varón A, Chaytor JD (2017) Demersal fish assemblages on seamounts and other features in the northeastern Caribbean. Deep-Sea Research I 123: 90–104. https://doi.org/10.1016/j.dsr.2017.03.009

Ross WS, Quattrini MA, Roa-Varón A, Mc Clain PJ (2010) Species composition and distribution of mesopelagic fishes over the slope of the north-central Gulf of Mexico. Deep Sea Research II 57: 1926–1956. https://doi.org/10.1016/j.dsr2.2010.05.008

Saavedra-Díaz LM, Roa-Varón A, Acero PA, Mejía LS (2004) Nuevos Registros ícticos en el talud superior del Caribe Colombiano (Órdenes: Albuliformes, Anguilliformes, Osmeriformes, Stomiiformes, Atelopodiformes, Aulopiformes y Pleuronectiformes). Boletín de Investigaciones Marinas y Costeras 33: 181–207.

Shannon CE, Wiener W (1963) The mathematical theory of communication. University of Illinois, Urbana, 117 pp.

Smithsonian National Museum of Natural History (2017) Search the Division of Fishes Collection. http://collections.nmnh.si.edu/search/fishes/ [accessed August 2018]

Sulak KJ, Brooks RA, Luke KE, Norem AD, Randall M, Quaid AJ, Yeargin GE, Miller JM, Harden WM, Caruso JH, Ross SW (2007) Demersal fishes associated with *Lophelia pertusa* coral and hard-substrate biotopes on the continental slope, northern Gulf of Mexico. In: George RY, Cairns SD (Eds) Conservation and adaptive management of seamount and deep-sea coral ecosystems. University of Miami, 65–92.

Texas A & M University Corpus Christi, Harte Research Institute for Gulf of Mexico Studies (2017) Biodiversity of the Gulf of Mexico Database. http://www.e-gulf [accessed April 2017]

Traver ML, Alade L, Sosebee KA (2012) Population biology of a data poor species, offshore hake (*Merluccius albidus*) in the northwest Atlantic, United States. Fisheries Research 114: 42–51. https://doi.org/10.1016/j.fishres.2011.08.004

Thresher RE, Colin PL (1986) Trophic structure, diversity and abundance of fishes of the deep reef (30–300 m) at Enewetak, Marshall Island. Bulletin of Marine Science 38(1): 253–272.

Tunnell Jr JW (2009) Gulf of Mexico. In: Earle SA, Glover LK (Eds) Ocean: An Illustrated Atlas. National Geographic Society, Washington DC, 136–137.

WoRMS Editorial Board (2017) World Register of Marine Species. http://www.marinespecies.org [accessed April 2017]

ZooKeys 846: 133–156 (2019)
doi: 10.3897/zookeys.846.33200
http://zookeys.pensoft.net

RESEARCH ARTICLE

A peer-reviewed open-access journal
ZooKeys
Launched to accelerate biodiversity research

A new caruncle-bearing fanged frog (*Limnonectes*, Dicroglossidae) from Laos and Thailand

Somphouthone Phimmachak[1], Stephen J. Richards[2], Niane Sivongxay[1], Sengvilay Seateun[1,3], Yodchaiy Chuaynkern[4], Sunchai Makchai[5], Hannah E. Som[6], Bryan L. Stuart[6]

1 *National University of Laos, Faculty of Natural Sciences, Department of Biology, P.O. Box 2273, Dong Dok Campus, Vientiane, Laos* **2** *South Australia Museum, Herpetology Department, Adelaide, South Australia 5000, Australia* **3** *Kasetsart University, Faculty of Science, Department of Zoology, Chatuchak, Bangkok, 10900, Thailand* **4** *Khon Kaen University, Faculty of Science, Department of Biology, Khon Kaen, 40002, Thailand* **5** *Natural History Museum, National Science Museum, Thailand, Technopolis, Khlong 5, Khlong Luang, Pathum Thani 12120 Thailand* **6** *North Carolina Museum of Natural Sciences, 11 West Jones Street, Raleigh, North Carolina 27601, USA*

Corresponding author: *Bryan L. Stuart* (bryan.stuart@naturalsciences.org)

Academic editor: *Angelica Crottini* | Received 18 January 2019 | Accepted 6 April 2019 | Published 16 May 2019

http://zoobank.org/90EE7041-0DC2-4519-9E0D-24C524D1CEB4

Citation: Phimmachak S, Richards SJ, Sivongxay N, Seateun S, Chuaynkern Y, Makchai S, Som HE, Stuart BL (2019) A new caruncle-bearing fanged frog (*Limnonectes*, Dicroglossidae) from Laos and Thailand. ZooKeys 846: 133–156. https://doi.org/10.3897/zookeys.846.33200

Abstract

A new species of the dicroglossid frog genus *Limnonectes* is described from recent and historical museum specimens collected in central and southern Laos and northeastern Thailand. *Limnonectes savan* **sp. nov.** has males that bear a caruncle on top of the head, and most closely resembles *L. dabanus* from adjacent southern Vietnam and eastern Cambodia. However, the new species is readily distinguished from *L. dabanus*, and all other caruncle-bearing species of *Limnonectes* in mainland Southeast Asia, by its adult and larval morphology, mitochondrial DNA, and advertisement call. Its description brings the total number of caruncle-bearing species of *Limnonectes* to six.

Keywords

Amphibia; bioacoustics; larval morphology; *Limnonectes dabanus*; mitochondrial DNA; Southeast Asia

Copyright *Somphouthone Phimmachak et al.* This is an open access article distributed under the terms of the Creative Commons Attribution License (CC BY 4.0), which permits unrestricted use, distribution, and reproduction in any medium, provided the original author and source are credited.

Introduction

The dicroglossid frog genus *Limnonectes* Fitzinger, 1843 currently contains 73 species that are distributed from southern China and the Ryukyu Islands of Japan south and eastward to Papua New Guinea (Frost 2019). Most species in the genus exhibit remarkable sexual dimorphism by having males with hypertrophied heads and enlarged odontoid processes on the lower jaw (Lambertz et al. 2014; Rowley et al. 2014; Aowphol et al. 2015), with the latter character earning the genus their colloquial name of "fanged frogs." Additionally, males of five species in the *Limnonectes* subgenus *Elachyglossa* Andersson, 1916 bear a swollen or cap-like structure ("caruncle") on top of their head that consists of a dense pad of connective tissue on the frontoparietal bones (Lambertz et al. 2014): *L. dabanus* (Smith, 1922), *L. gyldenstolpei* (Andersson, 1916), *L. lauhachindai* Aowphol et al., 2015, *L. macrognathus* (Boulenger, 1917) and *L. plicatellus* (Stoliczka, 1873). Caruncle morphology is species-specific (Lambertz et al. 2014; Aowphol et al. 2015), and may be involved in male-male combat (Lambertz et al. 2014; Rowley et al. 2014). Females of most of these species are difficult to distinguish solely from morphology (Aowphol et al. 2015; Phimmachak et al. 2018).

Our collective fieldwork during 1998–2016 at multiple localities in central and southern Laos and northeastern Thailand, and examination of historical museum specimens and the literature (Chan-ard 2003), revealed the presence of a caruncle-bearing *Limnonectes* that could not be assigned to any named species. Males of these "Lao-Thai" specimens generally resemble *L. dabanus*, a species from southern Vietnam and eastern Cambodia (Smith 1922; Stuart et al. 2006; Rowley et al. 2014), but differ in several morphological characters. Herein, we examine adult and larval morphology, mitochondrial DNA, and advertisement calls to test the hypothesis that the "Lao-Thai" specimens represent a distinct species from all other caruncle-bearing *Limnonectes*.

Materials and methods

Sampling

Specimens collected in the field were humanely euthanized by immersion in tricaine methanesulfonate (MS-222; Simmons 2015) and fixed in 10% buffered formalin after preserving liver (adults) or the tail (representative larvae) in 20% DMSO-salt saturated storage buffer, RNAlater (Invitrogen), or 95% ethanol. Adult specimens were later transferred to 70% ethanol for permanent storage. Specimens and tissue samples were deposited at the National University of Laos, Faculty of Natural Sciences, Department of Biology (**NUOL**), North Carolina Museum of Natural Sciences (**NCSM**), South Australian Museum (**SAMA**), and Field Museum of Natural History (**FMNH**). Comparative material was examined in the holdings of these institutions and the American Museum of Natural History (**AMNH**), Natural History Museum, London (**NHMUK**), California Academy of Sciences (**CAS**), Muséum national d'Histoire

naturelle, Paris (**MNHN**), Museum of Vertebrate Zoology, University of California, Berkeley (**MVZ**), and Zoological Museum Kasetsart University, Bangkok, Thailand (**ZMKU**; Appendix 1). Data for larvae of *L. dabanus* were taken from Rowley et al. [(2014); the larvae of *L. gyldenstolpei*, *L. macrognathus* and *L. lauhachindai* remain unknown (Aowphol et al. 2015)].

Morphological analyses

Measurements were taken to the nearest 0.1 mm using dial calipers under an ocular microscope. Adult measurements followed Aowphol et al. (2015):

EYE eye diameter;
FTL pes length from tip of fourth toe to base of inner metatarsal tubercle;
HDL head length from tip of snout to rear of jaws;
HDW maximum head width;
HND manus length from tip of third digit to base of palmar tubercle;
IML inner metatarsal tubercle length;
IMW inner metatarsal tubercle width;
IND internasal distance;
IOD interorbital distance, measured as minimum distance between eyes on top of head;
LAL forearm length, from elbow to base of palmar tubercle;
SHK shank length;
SNT snout length from tip of snout to anterior margin of eye;
SVL snout-vent length;
TGH thigh length, from knee to midline of vent;
TMP horizontal diameter of tympanum.

Terminology for the cap-like structure, "caruncle," followed Lambertz et al. (2014). Specimens were sexed by internal examination of gonads. Staging of eggs and larvae followed Gosner (1960). Larval measurements of body length (BL), tail length (TAL), and total length (TL), and labial tooth row formulae, followed Altig and McDiarmid (1999). Measurements are presented as mean ± standard deviation (SD).

Phylogenetic analyses

Total genomic DNA was extracted from liver or muscle samples from 53 individuals of *Limnonectes* (Appendix 2) using the ArchivePure DNA Cell/Tissue Kit (5 Prime) or the DNeasy Blood and Tissue Kit (Qiagen). An 551–1,949 nucleotide base pair (bp) fragment of mitochondrial (mt) DNA that encodes parts of the 12S rRNA, tRNA valine, and 16S rRNA genes was amplified by the polymerase chain reaction (PCR; 94–95° C 45s, 53–60° C 30s, 72° C 1 min) for 35 cycles using at least one of four

primer combinations: (i) 12L1 (Moriarty and Cannatella 2004) and 16Sbr-3' (Palumbi 1996), (ii) 16S3L (Chen et al. 2005) and 16Sbr-3', (iii) 16S3L and H-16SRana (5'-ACAAACGAACCATTAGTAGCG-3'; this study), and/or (iv) 16Sar-5' (Palumbi 1996) and 16Sbr-3'. Most samples were amplified using the third primer combination. PCR products were sequenced in both directions by direct double strand cycle sequencing using the BigDye Terminator version 3.1 Cycle Sequencing Kit (Applied Biosystems) and the amplifying primers. The internal sequencing primers 16Sar-5' (Palumbi 1996) and H16SRana-int (Phimmachak et al. 2018) were also used when sequencing the first three primer combinations. Cycle sequencing products were sequenced with a 3130 or 3730 DNA Analyzer (Applied Biosystems). Sequences were edited using Sequencher version 5.4.6 (Gene Codes) and deposited in GenBank under accession numbers MK688558–MK688610. GenBank accession numbers GU934329–31 and GU934337, originally provided by Inger and Stuart (2010), were updated with longer sequences for use in this study.

Newly generated sequences were aligned to the same homologous sequences used by Aowphol et al. (2015) and Phimmachak et al. (2018; Appendix 2). Sequences were aligned using the default parameters in MAFFT v. 7 (Katoh and Standley 2013). The dataset contained representatives of all major clades of *Limnonectes* (based on Evans et al. 2003; Pyron and Wiens 2011), dense sampling of species that are closely related to *L. dabanus*, and the outgroups *Fejervarya limnocharis* and *Quasipaa spinosa* (based on Pyron and Wiens 2011; Appendix 2). The model of sequence evolution that best described the data (GTR+I+G) was inferred using the Akaike Information Criterion as implemented in jModelTest 2.1.5 (Darriba et al. 2012). Four independent Bayesian analyses were performed using MrBayes 3.2 (Ronquist et al. 2012). In each analysis, four chains were run for 20 million generations using the default priors, the chain temperature was set to 0.1, trees were sampled every 4,000 generations, and the first 25% of trees were discarded as 'burn-in'. The resulting trace plots were viewed using Tracer v.1.6 (Rambaut et al. 2014). A 50% majority-rule consensus of the post burn-in trees was constructed to calculate the posterior probabilities of nodes. Nodes with posterior probabilities ≥ 0.95 were considered to be statistically supported. Uncorrected pairwise distances were calculated using PAUP* 4.0a (Swofford 2003).

Bioacoustic analyses

Advertisement calls were recorded from one male (NCSM 76299) at 1935 h on 28 June 2009 that was calling from a wet gully under roots and dead leaves in semi-evergreen forest among a chorus of of approximately 6–10 other males. Calls were recorded under natural conditions at a distance of approximately 0.2 m from the frog using an Edirol R-09 WAVE/MP3 Recorder (96 kHz sampling rate and 24-bit encoding) with a Røde NTG-2 condenser shotgun microphone. Ambient air temperature, relative humidity, and atmospheric pressure were taken immediately after the recording using a Kestrel 3500 hand-held weather meter. Calls were analyzed using Avisoft-SASLab Pro software (Avisoft Bioacous-

tics). Temporal and spectral parameters of calls, including call duration (ms), inter-call interval (ms), and dominant frequency (kHz), were measured following Köhler et al. (2017).

Results

Morphological analyses

Comparisons of "Lao-Thai" specimens to all other *Limnonectes* species having males that bear a caruncle on top of the head revealed consistent differences in body size, shape and position of the head caruncle, shape and length of odontoid processes, dorsal skin texture, toe length, and larval tooth rows.

Phylogenetic analyses

The aligned dataset contained 2,533 characters. The standard deviation of split frequencies was 0.005711 among the four Bayesian runs, and the Estimated Sample Sizes (ESS) of parameters were ≥ 1,092. The "Lao-Thai" specimens were recovered as a well-supported monophyletic group (Fig. 1) within a clade containing *L. dabanus, L. gyldenstolpei*, and *L. lauhachindai*, but the exact sister taxon relationship of the "Lao-Thai" clade was not resolved (Fig. 1). Thirteen "Lao-Thai" specimens from localities throughout its known range have an uncorrected pairwise divergence of 0–1.05% from each other, but 6.49–7.49% from *L. dabanus* (*n*=24), the species to which it is phenotypically most similar, and to which it was recovered as sister taxon, but without statistical support (Fig. 1).

Bioacoustic analyses

Nine advertisement calls from the "Lao-Thai" male specimen NCSM 76299 were recorded at an ambient air temperature of 26.3° C, 100% relative humidity, and atmospheric pressure of 1086.3 hPa. Calls were a single, low-pitched, unmelodic note lasting 57–76 ms (Fig. 2). Notes were finely pulsed, and pulses were not distinguishable to the human ear, but the number of pulses could be determined for four calls. These calls contained 19–21 pulses produced at a rate of 295–312 pulses/s. Calls were amplitude modulated, with amplitude increasing relatively slowly for the first 2/3–3/4 of the call before decreasing rapidly. During several calls, amplitude stabilized or decreased in the middle of the call before increasing again near the end (Fig. 2). The dominant frequency (also the fundamental frequency) was 0.55–0.64 kHz and harmonics were not evident. Calls were repeated relatively slowly and at highly variable intervals, with inter-call intervals (*n*=8) ranging from 5.5–26.8 s. Background calls recorded from other males in the same chorus were of insufficient quality for analysis.

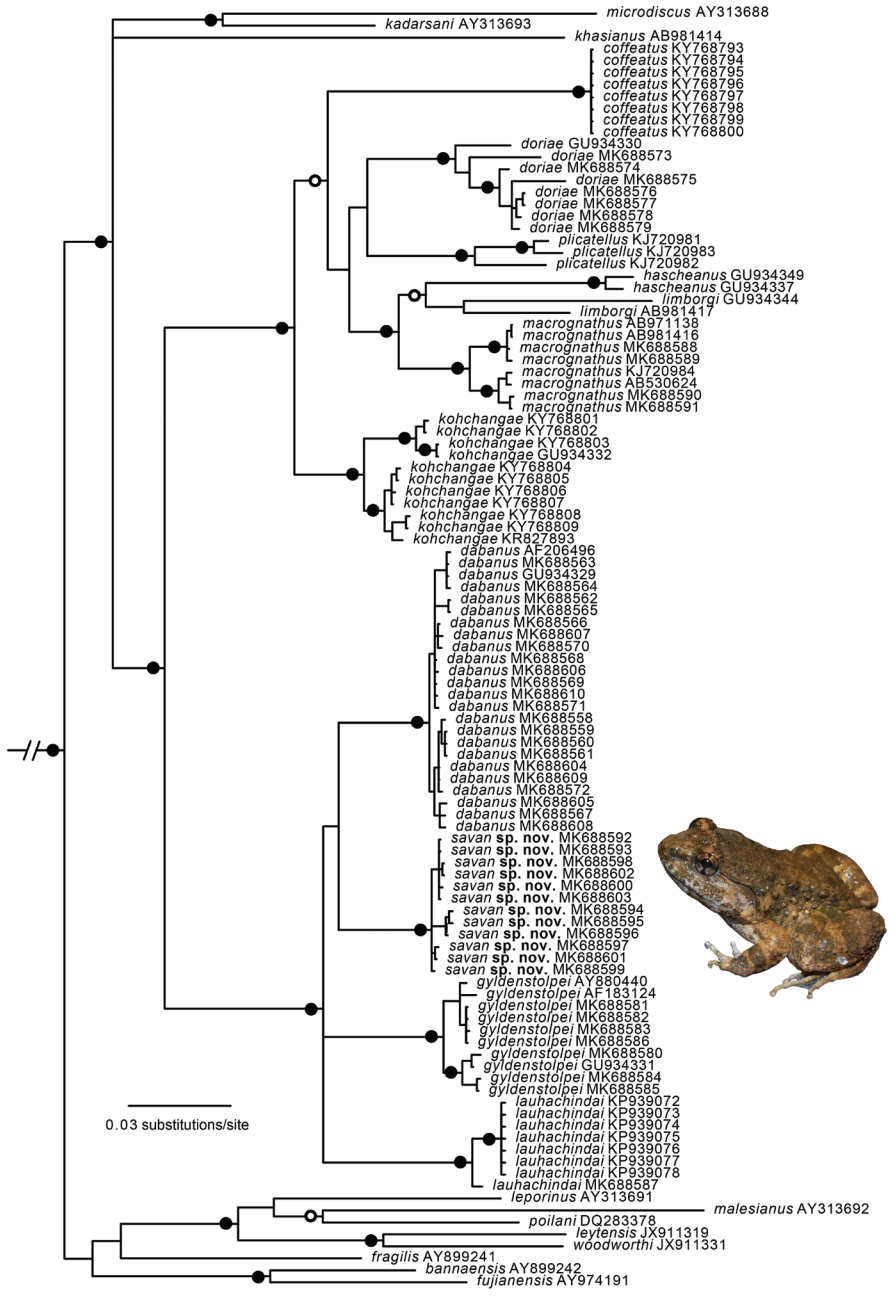

Figure 1. Fifty percent majority-rule consensus phylogram resulting from Bayesian analysis of 2,533 aligned characters of mitochondrial DNA from dicroglossid frogs in the genus *Limnonectes*, and the outgroup taxa *Fejervarya limnocharis* and *Quasipaa spinosa* (not shown). Black circles at nodes indicate Bayesian posterior probabilities ≥ 0.99, and open circles at nodes indicate Bayesian posterior probabilities ≥ 0.95. Numbers at terminal tips are GenBank accession numbers. Voucher and locality data for sequenced samples are provided in Appendix 2.

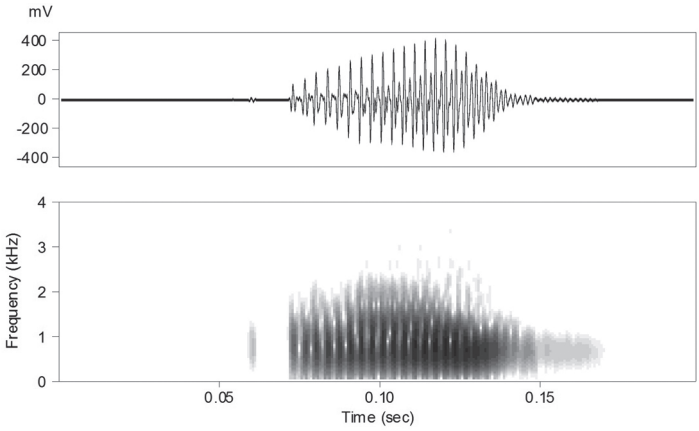

Figure 2. Spectrogram of the advertisement call of an adult male paratype (NCSM 76299) of *Limnonectes savan* sp. nov. from Savannakhet Province, Laos, recorded at an ambient air temperature of 26.3°C.

Species description

On the basis of these corroborated lines of evidence from multiple, independent datasets (larval morphology, adult male morphology, mitochondrial DNA, and male advertisement calls), we hypothesize that the "Lao-Thai" specimens represent a distinct evolutionary lineage that should be recognized as a species, described herein as:

***Limnonectes* (*Elachyglossa*) *savan* sp. nov.**
http://zoobank.org/673B5D88-212D-40C4-BB8A-3598A1A9E1AD
Figures 3–6

Limnonectes sp. Chan-ard, 2003: 120.

Holotype. NCSM 76288 (field tag BLS 12395), adult male (Figs 3, 4), **Laos**, Savannakhet Province, Vilabouli District, Sepon Mining Tenement, Ban Houay Hong Village, Houay Hong Stream, 17.04444°N, 106.12622°E, 254 m elev., under boulder in shallow water of 1–3 m wide swift, rocky stream in semi-evergreen forest, coll.15 November 2008 at 2220 h by Bryan L. Stuart, Somphouthone Phimmachak, Stephen J. Richards, and Niane Sivongxay.

Paratypes. Laos, Savannakhet Province, Vilabouli District: NCSM 76287 (one adult male), SAMA R64243 (one juvenile), same data as holotype. NCSM 76294 (one adult female), NCSM 76295, SAMA R64251 (two juveniles), same data as holotype except coll. 04 December 2008. NCSM 76289 (one adult male), SAMA R64244 (one adult female), same data as holotype except Houay Po Stream, 17.04297°N, 106.12503°E, 278 m elev., coll. 18–20 November 2008. SAMA R64245 (one adult male), NCSM 76290, SAMA R64249 (two juveniles), same data as holotype except

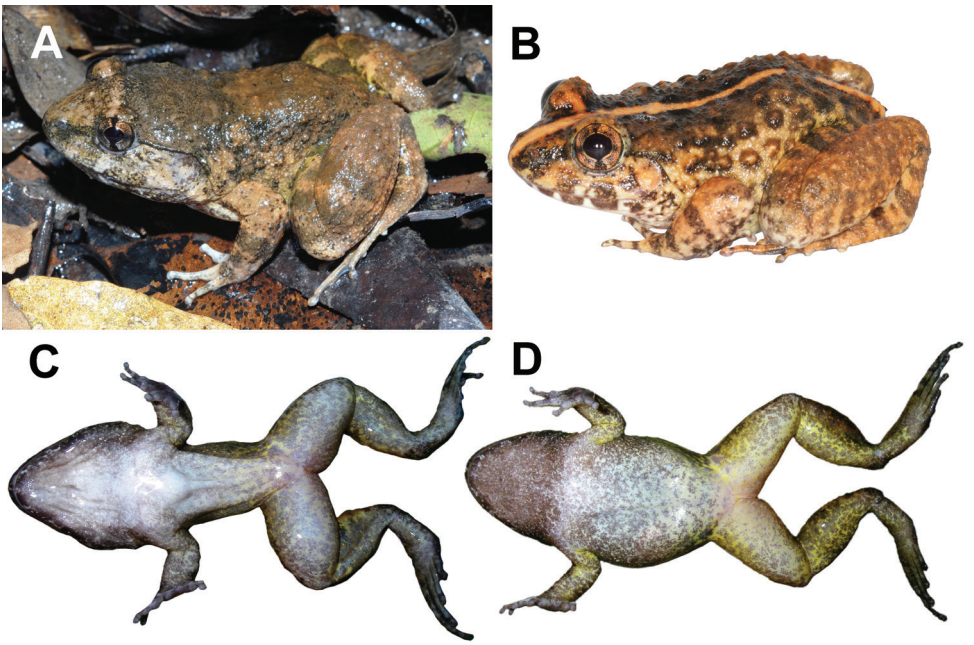

Figure 3. *Limnonectes savan* sp. nov. in life **A** lateral view of holotype male (NCSM 76288) **B** lateral view of paratype female (NUOL 00061) **C** ventral view immediately prior to preservation of paratype male (NCSM 76303) **D** ventral view immediately prior to preservation of paratype female (NCSM 76301).

Ban Nam Pa Village, Houay Hua Tad Stream, 16.96317°N, 106.04661°E, 326 m elev., coll. 22–25 November 2008. SAMA R64246–47 (two adult males), SAMA R64248, NCSM 76291–93 (four juveniles), same data as holotype except Houay Lavi Stream, 16.95653°N, 106.06767°E, 303 m elev., coll. 26 November 2008. SAMA R64250 (one adult female), same data as holotype except Houay Nam Pa Stream, 16.95944°N, 106.04661°E, 280 m elev., coll. 29 November 2008. NCSM 76308 (one adult male), NCSM 76309 (one juvenile), same data as holotype except 17.04120°N, 106.12889°E, 315 m elev., coll. 6 July 2009 by Bryan L. Stuart, Somphouthone Phimmachak, and Niane Sivongxay. NUOL 00092 [formerly NCSM 76298], NCSM 76296, NCSM 76300 (Fig. 4), NCSM 76301 (Fig. 3), NCSM 76304 (five adult females), NUOL 00091 [formerly NCSM 76297], NCSM 76299, NCSM 76302, NCSM 76303 (Fig. 3), NCSM 76305–06 (six adult males), NCSM 76307 (one juvenile), same data as holotype except Nam Sangi River Drainage Basin, 17.02073°N, 106.28625°E, 454 m elev., coll. 25 June–1 July 2009 by Bryan L. Stuart, Somphouthone Phimmachak, and Niane Sivongxay. NCSM 84943 (one adult male), same data as holotype except Ban Namalou Village, 16.93401°N, 105.90562°E, coll. 28 September 2014 by Bryan L. Stuart, Sengvilay Seateun, Niane Sivongxay, Derin Henderson, and Singthong Sanvixay. NUOL 00061 (one adult female; Fig. 3), same data as holotype except Phou Thaeng-

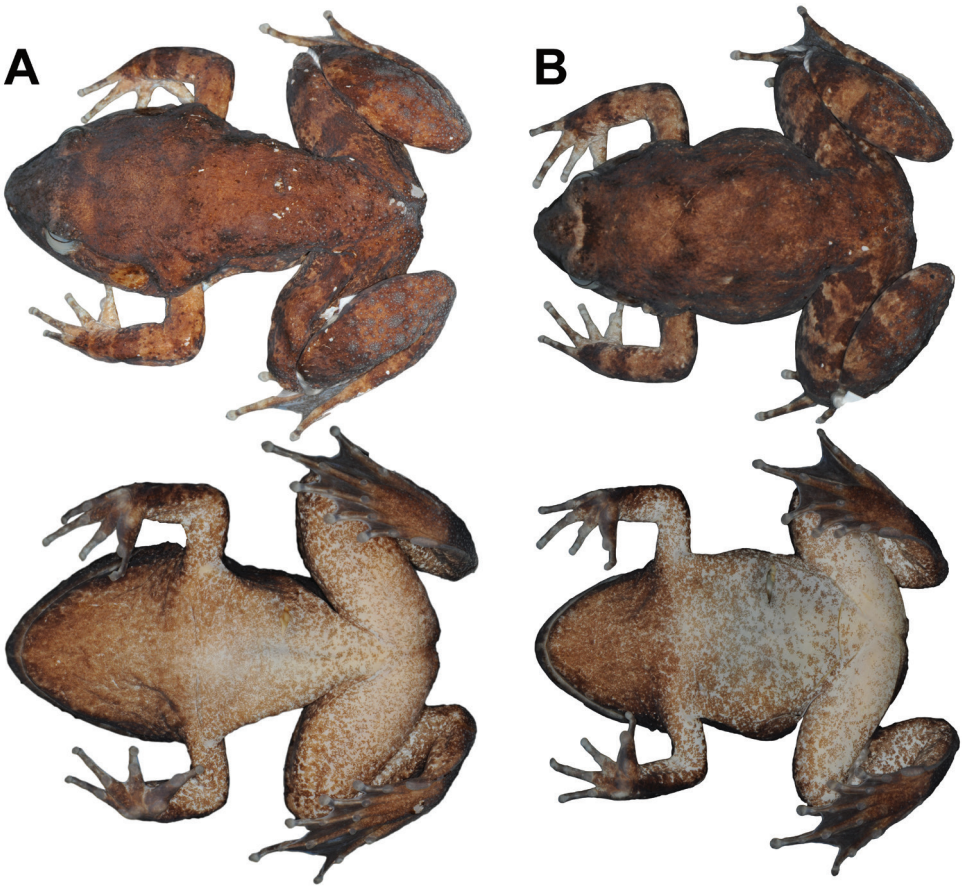

Figure 4. Sexual dimorphism of *Limnonectes savan* sp. nov. in preservative: Dorsal (above) and ventral (below) views of **A** holotype male (NCSM 76288) and **B** paratype female (NCSM 76300).

kham Mountain, 16.95279°N, 105.92284°E, coll. 28 September 2014 by Bryan L. Stuart, Sengvilay Seateun, Niane Sivongxay, Derin Henderson, and Singthong Sanvixay.

Laos, Khammouan Province, Boualapha District: NCSM 80962 (one juvenile), Xe Bangfay River, 6 km upstream of Ban Pakphanang Village, 17.39972°N, 105.77278°E, coll. 17 March 2002 by Maurice Kottelat. FMNH 255385 (one adult male), FMNH 255386–87 (two juveniles), Hin Nam No National Protected Area, Phou Khaonok Mountain, 17.38333°N, 105.75000°E, 545 m elev., coll. 19–21 February 1998 by Bryan L. Stuart. FMNH 255388 (one adult female), FMNH 255389–90 (two juveniles), same data as FMNH 255385 except 17.33333°N, 105.68333°E, 500 m elev., coll. 23–24 February 1998.

Laos, Champasak Province, Pakxong District: NUOL 01151 (one adult female), NUOL 01152–55 (four adult males), Ban Nong Theuam Village, Phou Katam Moun-

tain, Houay Hongkhimin Stream, 15.14461°N, 106.61658°E, 790 m elev., coll. 3 April 2016 by Somphouthone Phimmachak and Sengvilay Seateun. NUOL 01156 (one juvenile), Ban Nam Tuad, downstream of Houay Hongkhimin Stream near road to Attapeu Province, 15.12535°N, 106.63216°E, 503 m elev., coll. 6 April 2016 by Somphouthone Phimmachak and Sengvilay Seateun. NUOL 01157 (one adult male), same data as NUOL 01156 except Xe Katam Waterfall, 15.12355°N, 106.63779°E, 350 m elev.

Thailand, Ubon Ratchatani Province, Na Chaluai District: FMNH 266149 (one adult male), Phu Jong-Na Yoi National Park, Huay Luang Noi Stream, 14.43775°N, 105.28006°E, 360 m elev., coll. 15 September 2004 by Bryan L. Stuart, Yodchaiy Chuaynkern, Chatchay Chuechat, and Sunchai Makchai. FMNH 266155 (one adult male), FMNH 266156 (one adult female), same data as FMNH 266149 except hill evergreen forest along road, 14.43850°N, 105.26792°E, 325 m elev., coll. 13 September 2004.

Thailand, Ubon Ratchatani Province, Buntharik District: FMNH 266157–58 (two adult females), Phu Jong-Na Yoi National Park, evergreen forest along dirt road, 14.44186°N, 105.30753°E, 400 m elev., coll. 16 September 2004 by Bryan L. Stuart, Yodchaiy Chuaynkern, Chatchay Chuechat, and Sunchai Makchai.

Thailand, Ubon Ratchatani Province, Sirindhorn District: FMNH 173514–15 (two juveniles), Forestry Station, Sai Noi River, coll. 23 March 1958 by Edward H. Taylor.

Referred specimens. NCSM 76491 (13 larvae), same data as NUOL 00091. NCSM 76492 (28 larvae), NCSM 76493 (43 larvae), NCSM 76494 (one clutch of 70 eggs), same data as NCSM 76305.

Etymology. The specific epithet *savan* means paradise in the Lao language, and is a commonly used, truncated form of the name for Savannakhet Province, Laos, that contains the holotype and most paratype localities of the new species. The specific epithet *savan* is a noun in apposition.

Suggested common names. Savan Fanged Frog (English), Kop Hone Savan (Lao), Kop Panomdongrak (Thai).

Diagnosis. Assigned to the genus *Limnonectes* on the basis of its inferred phylogenetic position (Fig. 1), the presence of fang-like odontoid processes on the lower jaw (Emerson et al. 2000; Lambertz et al. 2014), and having males with hypertrophied heads (Lambertz et al. 2014). Assigned to the subgenus *Elachyglossa* (following Ohler and Dubois 1999; Lambertz et al. 2014) on the basis of its close phylogenetic position to the subgenerotype *L. gyldenstolpei* (Fig. 1). A medium-sized *Limnonectes* having the combination of adult males with SVL 39.0–56.2, adult females with SVL 38.9–55.2; males with hypertrophied head; males with interorbital caruncle consisting of low-profile swelling without a free posterior margin, extending from level of anterior margin of eye to level midway between posterior margin of eye and tympanum; odontoid processes on anterior margin of lower jaw larger in males than in females; horizontal diameter of tympanum equal to eye in adult males, ¾ of eye diameter in subadult males, immature males, and females; enlarged, rounded, tubercles on dorsum, becoming more elongated dorsolaterally; dark brown or gray spotting on throat, belly, and ventral surfaces of forelimbs and hindlimbs; and ova with pigmented poles.

Description of holotype. Habitus moderately stocky; body broad anteriorly, tapering to narrow groin. Head broad and depressed, head width equal to head length. Snout obtusely pointed in dorsal view; round, projecting well beyond lower jaw in profile; nostril dorsolateral, much closer to tip of snout than to eye, below canthus; internarial distance 72% of interorbital distance; canthus rostralis indistinct, rounded, slightly constricted behind nostrils; lores concave, oblique; eye diameter 59% of snout length, upper eyelid width 50% of interorbital distance; pineal ocellus visible; tympanum imperfectly circular, not elevated from side of head, annulus visible, tympanum diameter equal to eye diameter and greater than distance between tympanum and eye; small, slit-like vocal sac openings on floor of mouth near lateral margin of tongue; vomerine teeth on two oblique ridges, equidistant to each other as to choanae; two large odontoid processes at front of mandible, triangular, tapered, length subequal to depth of mandible at base of process; median triangular symphysial knob at mandibular symphysis.

Forelimbs robust. Fingers relatively slender, without webbing, with fringe of skin on preaxial and postaxial sides of all fingers, fringes on Fingers II-III movable; tips of fingers rounded, expanded into discs; relative finger lengths II < I < IV < III; distinct, rounded subarticular tubercles, one on Fingers I–II, two on Fingers III–IV; distinct thenar tubercle; two palmar tubercles in contact at base of Fingers II–IV; nuptial pad absent.

Hindlimbs robust. Toes relatively slender; tips of toes rounded, expanded into small discs; relative toe lengths I<II<III=V<IV on right foot, I<II<V<III<IV on left foot; webbing on Toe I to base of disc, on preaxial side of Toe II to level midway between subarticular tubercle and disc and continuing as fringe to base of tip, on postaxial side of Toe II to base of disc, on preaxial side of Toe III to level of distal subarticular tubercle and continuing as fringe to base of disc, on postaxial side of Toe III to base of disc, on preaxial and postaxial sides of Toe IV to level of distal subarticular tubercle and continuing as fringe to base of disc, and on Toe V to base of disc; moveable fringe of skin on outer margins of Toes I and V; distinct fold on distal two-thirds of tarsus; distinct, elongate, oval, inner metatarsal tubercle, length approximately 59% distance between tip of toe I and tubercle; no outer metatarsal tubercle.

Skin on dorsum and flank shagreened with large, irregular, scattered tubercles; tubercles tipped with single, whitish spinule on loreal region, eyelid, lower back near groin, around vent, and ventral surfaces of tibiotarsus and foot; dense clusters of warts (enlarged tubercles), each tipped with numerous whitish spinules, on dorsal surfaces of shank; interorbital caruncle consisting of low-profile swelling without free posterior margin, extending from level of anterior margin of eye to level midway between posterior margin of eye and tympanum, with highest point between eyes; hypertrophied jaw musculature forming two low postorbital swellings on top of head at level of tympanum; distinct supratympanic fold from posterior corner of eye to axilla; rictal gland absent; dorsolateral fold absent; aberrant, triangular skin tag near midline of back; skin on throat with weak longitudinal wrinkles, that on remaining ventral surfaces smooth.

Color of holotype in life. Dorsum tan. Loreal region, tympanic region, and dorsal surfaces of digits whitish gray. Back of head, dorsolateral region, under canthus and

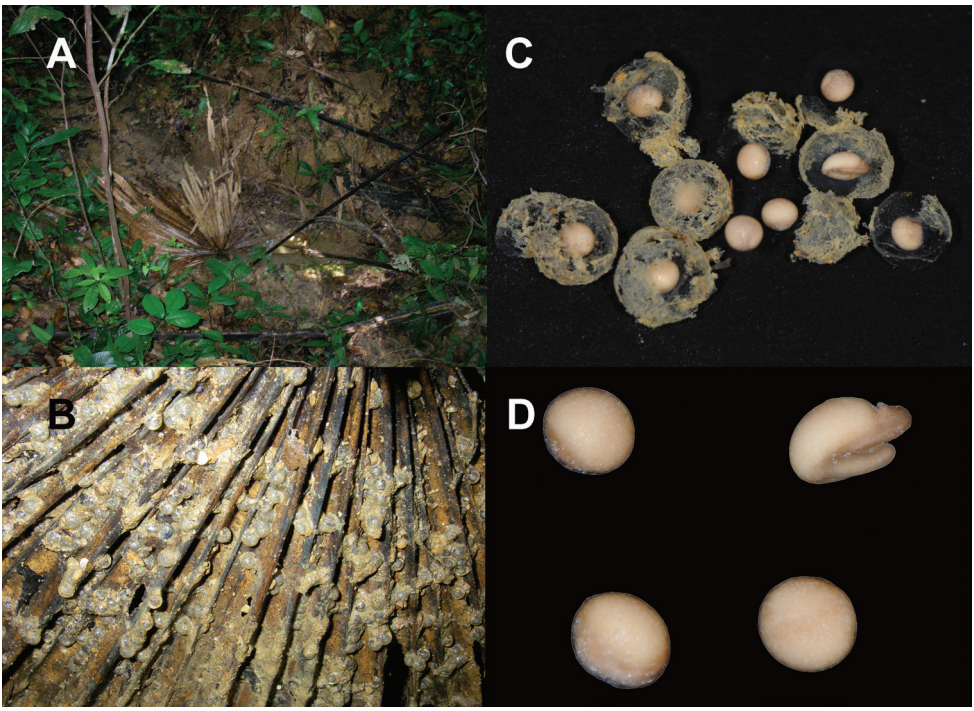

Figure 5. *Limnonectes savan* sp. nov. **A** oviposition site with dead palm frond *in situ* in Savannakhet Province, Laos **B** eggs (NCSM 76494) prior to preservation adhered to underside of dead palm frond that is visible in previous image **C** eggs (NCSM 76494) in preservative with jelly layer **D** eggs (NCSM 76494) in preservative after removal from jelly layer.

dorsoposterior region of tympanum with gray mottling. Dorsal and posterior surfaces of thigh, posterior surface of shank, and groin with yellowish wash. Lips with irregular, broad, gray bars, dorsal surfaces of limbs with cross-bands. Interorbital bar tannish yellow. Iris bronze with black vermiform mottling, black vertical and horizontal bars forming shape of a single plus sign ("+") over eye (Fig. 3). Ventral surfaces not photographed prior to preservation.

Color of paratype male in life. Based on NCSM 76303. Dorsal surfaces same as holotype except narrow yellow vertebral stripe from tip of snout to vent. Ventral surfaces very light gray with dark gray mottling, only small area near midline of chest nearly immaculate, dark gray mottling becoming denser on ventral surfaces of limbs, nearly uniformly dark gray on ventral surfaces of hands and feet. Inguinal region and ventral surfaces of shank with yellowish wash (Fig. 3).

Color of holotype in preservative. Dorsal surfaces nearly uniformly brown with indistinct, scattered, dark brown mottling, lips with indistinct dark brown bars, and dorsal surfaces of limbs with indistinct dark brown cross-bands. Tympanum and forelimbs with lighter brown than remaining dorsum. Interorbital bar indistinct. Ventral

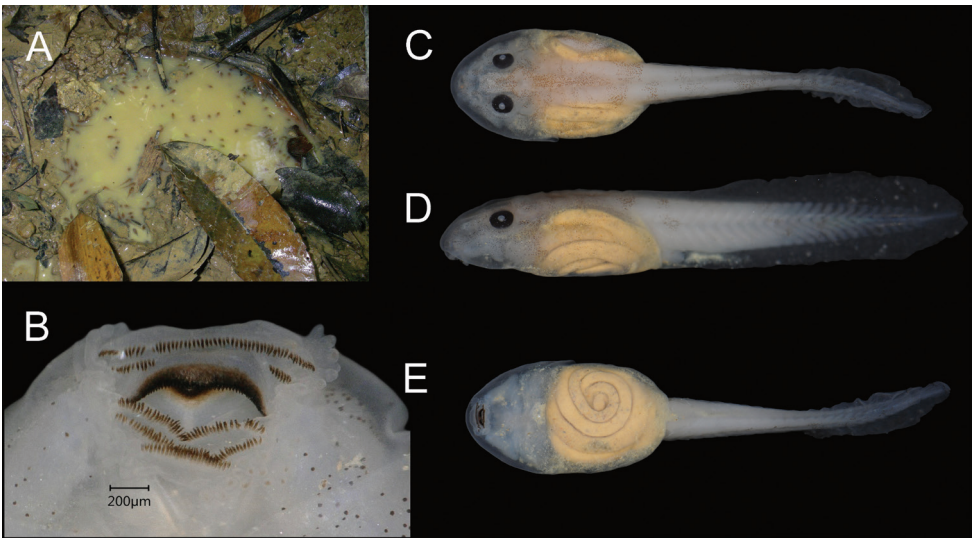

Figure 6. *Limnonectes savan* sp. nov. larvae **A** *in situ* in puddle in wet gully in semi-evergreen forest in Savannakhet Province, Laos; one exemplar larva in preservative (NCSM 76492) at Gosner Stage 31, TL 18.4 mm in **B** oral view **C** dorsal view **D** lateral view and **E** ventral view.

surfaces light brown with dark brown mottling, becoming uniformly dark brown on ventral surfaces of hands and feet (Fig. 4).

Description of eggs. Based on subsample of eggs (NCSM 76494) collected from a larger clutch *in situ* (Fig. 5). Most in Gosner Stage 14, with single jelly layer having diameter of 4.8–5.5 mm (5.1 ± 0.3, n = 13), and embryos with a darkly pigmented animal pole having diameter of 2.2–2.5 mm (2.3 ± 0.1, n = 13).

Description of larvae. Based on largest individual in series of 28 larvae (NCSM 76492; Fig. 6). Gosner Stage 31, TL 18.4 mm, BL 7.4 mm, TAL 11.0 mm. Body oval in dorsal view, slightly compressed dorsoventrally, maximum body width slightly anterior to level of spiracle. Nares dorsal, without raised rim. Eyes dorsolateral, not visible from below. Spiracular tube single, sinistral on left side, angled slightly dorsally, aperture near midline and projecting posteriorly, approximately midway between snout and end of body. Tail slender, tapering in distal one-fourth to rounded tip, origins of dorsal and ventral fins at end of body, dorsal and ventral fin widest near middle of tail, dorsal fin only slightly deeper than ventral fin. Oral disk ventral, subterminal, width about 39% maximum width of body. Anterior labium with single row of papillae on lateral margins; posterior labium with single row of papillae on lateral and posterior margins; papillae homogenous in length. Labial tooth row formula 2(2)/3(1). A-1 longer than A-2, medial gap in A-2 approximately three-fourth length of A-2. P-1 and P-2 subequal in length, P-3 approximately one-half length of P-1 and P-2. Upper and lower jaw sheaths black with serrated margins, upper sheath without median convexity. In life, dorsum light brown. In preservative, body and tail white with brown mot-

tling on dorsolateral surfaces of body, forming indistinct crossbands on tail. Intestine yellow in dorsal and ventral views. Measurements (TL) of additional larvae (NCSM 76491–93): Gosner Stage 25 11.7–13.1 mm (12.4 ± 0.4, *n* = 15), Gosner Stage 26 12.9–14.5 mm (13.6 ± 0.5, *n* = 13), Gosner Stage 27 14.2–15.8 mm (15.0 ± 0.6, *n* = 13), and Gosner Stage 28 15.5–17.0 mm (16.3 ± 0.8, *n* = 3).

Variations. Females lack caruncle and postorbital swellings (Fig. 3); have narrower heads in dorsal view than males (Table 1; Fig. 4); have relatively smaller tympana than males, with tympanum diameter less than eye diameter (Table 1; Fig. 3); have smaller and shorter odontoid processes than males; have more elongated tubercles on dorsolateral region and flank than males; and contain ova with pigmented poles (Fig. 5).

The holotype is the largest male in the type series, with the next largest male (NCSM 76299) having SVL of 53.6 mm. Two paratype males (NCSM 76299, NCSM 76303) have higher-profile caruncles, higher-profile postorbital swellings, and more distinct longitudinal wrinkles on skin of throat than holotype.

Dorsal surfaces are lighter brown, or have more gray mottling, in some specimens than in the holotype. Lip bars on lips and crossbands on dorsal surfaces of limbs more distinct in some specimens than in the holotype. Six paratypes (NCSM 76294, NCSM 76302–04, NUOL 00061, NUOL 00091, NUOL 01153, and SAMA R64247) have a narrow, pale vertebral stripe from tip of snout to vent. Measurements of adults are summarized in Table 1.

Distribution, natural history. *Limnonectes savan* is known to occur in central and southern Laos (Khammouan, Savannakhet, and Champasak Provinces), and northeastern Thailand (Ubon Ratchatani; Fig. 7). Chan-ard (2003) also reported it (as *Limnonectes* sp.) from Amnat Charoen Provinces in northeastern Thailand. The species occurs in hill and semi-evergreen forest from 254–790 m elevation, and is usually associated with small (1–3 m wide) streams (Fig. 8); based on 51 specimens sampled at night (1900h–2251h), 38 (74.5%) were found in streams (permanent streams with rocky or sandy substrates, or intermittent streams), nine (17.7%) were found in puddles, two (3.9%) were found in ponds, and two (3.9%) were found on the forest floor, away from an obvious body of water. Nineteen (37.3%) of the 51 specimens were sampled in water, with the remaining 32 individuals (62.7%) found on substrates of soil, leaf litter, rocks or logs.

Limnonectes savan breeds in puddles on the forest floor during the rainy season. A chorus of calling males, including paratype male NCSM 76299, was observed in a wet gully under roots and dead leaves in semi-evergreen forest at 1935 h on 28 June 2009. Egg clutch NCSM 76494 was found adhering to the underside of a submerged dead palm frond in a puddle in the same wet gully on 1 July 2009 (Fig. 5). Larvae NCSM 76491 (*n*=13), NCSM 76492 (*n*=28), and NCSM 76493 (*n*=43) were sampled from small puddles (0.2–1 m diameter) in the same wet gully during 28 June–1 July 2009 (Fig. 6).

Limnonectes savan occurs in sympatry with *L. lauhachindai* in Ubon Ratchathani Province in northeastern Thailand (Appendix 1), but its geographic distribution appears to be parapatric to that of *L. dabanus* in southern Laos, and to that of *L. gyldenstolpei* in central and southern Laos and northeastern Thailand (Appendix 1).

Table 1. Measurements (mm) of types of *Limnonectes savan* sp. nov. and *L. dabanus*. Abbreviations defined in the text. Values are presented as range; mean ± standard deviation (SD).

Measurement	*L. savan* Holotype male NCSM 76288	*L. savan* Paratype males *n* = 22	*L. savan* Paratype females *n* = 14	*L. dabanus* Males *n* = 24	*L. dabanus* Females *n* = 14
SVL	56.2	39.0–53.6; 45.9 ± 4.8	38.9–55.2; 47.2 ± 5.5	48.8–64.4; 56.9± 4.5	42.3–57.4; 48.2 ± 4.8
HDL	26.8	16.6–26.0; 20.4 ± 2.9	15.7–22.2; 19.2 ± 2.2	21.2–38.0; 26.8 ± 3.5	17.3–24.1; 20.0 ± 1.9
HDW	26.9	17.0–26.1; 20.8 ± 2.7	16.1–22.1; 19.8 ± 2.3	20.8–35.4; 26.5 ± 3.2	17.1–23.9; 19.8 ± 1.8
SNT	9.9	6.1–9.9; 7.8 ± 1.1	6.1–9.2; 7.6 ± 0.9	8.9–14.3; 11.0 ± 1.1	7.0–9.8; 8.2 ± 0.8
EYE	5.8	4.5–6.9; 5.4 ± 0.7	4.4–6.8; 5.5 ± 0.8	5.4–7.3; 6.2 ± 0.5	5.1–7.1; 5.9 ± 0.6
IOD	7.6	3.0–7.5; 5.1 ± 1.2	3.1–4.9; 4.2 ± 0.4	5.2–7.9; 6.4 ± 0.7	3.8–5.3; 4.3 ± 0.3
TMP	5.8	3.4–6.3; 4.7 ± 0.8	3.4–5.5; 4.3 ± 0.7	5.0–9.5; 6.5 ± 1.3	3.7–5.3; 4.4 ± 0.6
IND	5.5	3.6–6.0; 4.6 ± 0.6	3.9–5.6; 4.6 ± 0.5	4.6–7.7; 5.7 ± 0.6	4.1–5.9; 4.7 ± 0.5
SHK	26.9	18.6–25.8; 22.2 ± 2.1	18.9–25.4; 22.5 ± 2.4	23.0–31.1; 27.8 ± 2.7	21.9–29.3; 24.5 ± 2.1
TGH	28.9	18.4–29.1; 23.9 ± 2.8	20.0–28.0; 24.3 ± 3.2	22.0–33.1; 29.1± 3.1	21.9–31.1; 24.8 ± 2.3
LAL	11.0	7.1–10.4; 8.8 ± 0.9	7.7–10.8; 9.2 ± 1.2	8.5–14.1; 11.6 ± 1.3	8.2–11.6; 9.8 ± 0.9
HND	13.8	9.7–14.6; 12.1± 1.3	9.3–14.0; 12.2 ± 1.4	12.4–16.6; 15.1 ± 1.3	11.1–14.1; 12.5 ± 1.0
FTL	26.6	18.8–25.7; 22.3 ± 2.1	18.0–25.4; 22.5± 2.4	22.4–31.4; 27.3 ± 2.7	21.8–27.0; 23.8 ± 1.6
IML	4.1	2.3–4.0; 3.2 ± 0.4	2.9–4.0; 3.4± 0.4	3.0–4.6; 3.8 ± 0.4	2.8–4.2; 3.3 ± 0.4
IMW	1.3	1.0–2.1; 1.3 ± 0.3	0.8–1.6; 1.3 ± 0.2	1.1–2.0; 1.5 ± 0.2	0.9–1.6; 1.1 ± 0.2
TMP:EYE	1.0	0.7–1.1; 0.9 ± 0.1	0.7–0.9; 0.8 ± 0.1	0.8–1.5; 1.0 ± 0.2	0.7–0.8; 0.8 ± 0.1
TMP:SVL	0.1	0.1–0.1; 0.1 ± 0.0	0.1–0.1; 0.1 ± 0.0	0.1–0.2; 0.1 ± 0.0	0.1–0.1; 0.1 ± 0.0

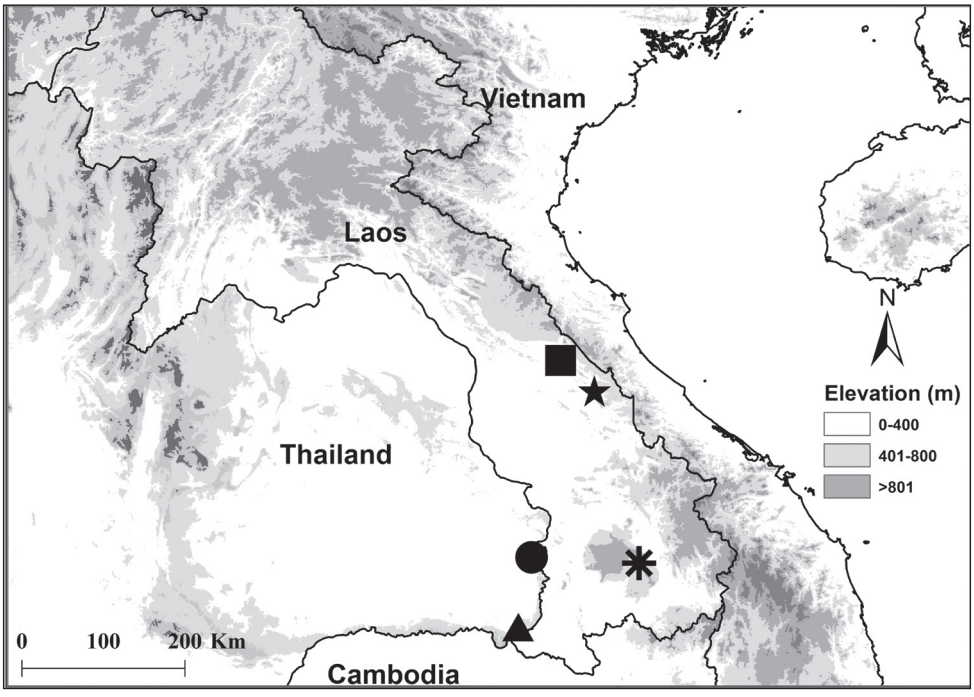

Figure 7. Localities of studied specimens of *Limnonectes savan* sp. nov. at the holotype locality at Savannakhet Province, Vilabouli District, Laos (star) and the paratype localities at Khammouan Province, Boualapha District, Laos (square), Champasak Province, Pakxong District, Laos (asterisk), Ubon Ratchathani Province, Sirindhorn District, Thailand (circle), and Ubon Ratchathani Province, Na Chaluai and Buntharik Districts, Thailand (triangle).

Comparisons. *Limnonectes savan* differs from all other species of mainland Southeast Asian *Limnonectes*, except *L. gyldenstolpei*, *L. lauhachindai*, *L. dabanus*, *L. macrognathus,* and *L. plicatellus,* by having mature males with an interorbital caruncle (sensu Lambertz et al. 2014). *Limnonectes savan* differs from these five species by having mature males with interorbital caruncle consisting of low-profile swelling without free posterior margin, with highest point at level between eyes (vs. caruncle U-shaped with free posterior margin in *L. gyldenstolpei* and *L. lauhachindai*, caruncle high-profiled in *L. dabanus*, caruncle high-profiled and horned in *L. plicatellus*, and caruncle with highest point posterior to level of eyes in *L. macrognathus*); and by having dark spotting on ventral surfaces of chest, belly, and limbs in preserved specimens of adults and juveniles of both sexes (vs. these surfaces mostly immaculate in *L. gyldenstolpei*, *L. lauhachindai*, *L. dabanus*, *L. macrognathus,* and *L. plicatellus*; Figs 9, 10).

Limnonectes savan further differs from *L. gyldenstolpei*, *L. lauhachindai*, *L. dabanus*, and *L. macrognathus* by having relative toe lengths I<II<III=V<IV, with the tips of Toes III and V reaching the base of the distal subarticular tubercle on Toe IV (vs. relative toe lengths I<II<V<III<IV, with the tip of Toe III shorter not reaching the distal subarticular tubercle on Toe IV in *L. gyldenstolpei*, *L. lauhachindai*, *L. dabanus*, and *L. macrognathus*). *Limnonectes savan* further differs from *L. plicatellus* by having males with much larger body size (SVL ≤ 43.0 in *L. plicatellus*; Boulenger 1920; Taylor 1962; Chan-ard 2003; Lambertz et al. 2014) and by lacking dorsal rugosities arranged in distinct, longitudinal rows parallel to the body axis (vs. present in *L. plicatellus*).

Limnonectes savan is phenotypically most similar and phylogenetically most closely related (Fig. 1), to *L. dabanus*. The new species further differs from *L. dabanus* by having mature males with two large, tapered odontoid processes of length subequal to depth of mandible at base of process (vs. odontoid processes much less tapered and with length less than one-half depth of mandible at base of process in *L. dabanus*; Fig. 11); by having mature males with TMP = EYE (vs. TMP > EYE in *L. dabanus*); by having the dorsal surfaces of shank with dense clusters of warts, each tipped with numerous whitish spinules (vs. warts and tubercles less distinct and lower in profile, with more homogeneous distributions of whitish spinules in *L. dabanus*); by having larvae with A-1 longer than A-2 (vs. A-1 and A-2 subequal in length in *L. dabanus*), with medial gap in A-2 approximately three-fourths length of A-2 (vs. approximately one-half length of A-2 in *L. dabanus*), and having P-1 and P-2 subequal in length (vs. P-1 longer than P-2 in *L. dabanus*); and by having much shorter calls of 57–74 ms (vs. 141–197 ms in *L. dabanus*; Rowley et al. 2014).

Male secondary sexual characters are unknown in *L. khammonensis* (Smith 1929), which is known only from the female holotype, but females of *L. savan* differ by having a distinct tympanum (indistinct in *L. khammonensis*); having larger body size, with SVL 38.9–55.2 (vs. gravid holotype female SVL 37.5 in *L. khammonensis*); and less toe webbing (vs. Toe IV webbed to distal subarticular tubercle, continuing as fringe to base of disc, and all remaining toes webbed to base of disc in *L. khammonensis*).

Figure 8. Habitat of *Limnonectes savan* sp. nov. in Savannakhet Province, Vilabouli District, Laos in December 2008 at **A** Houay Khalai Stream, Ban Khalai Village, and **B** Houay Hong Stream, Ban Houay Hong Village.

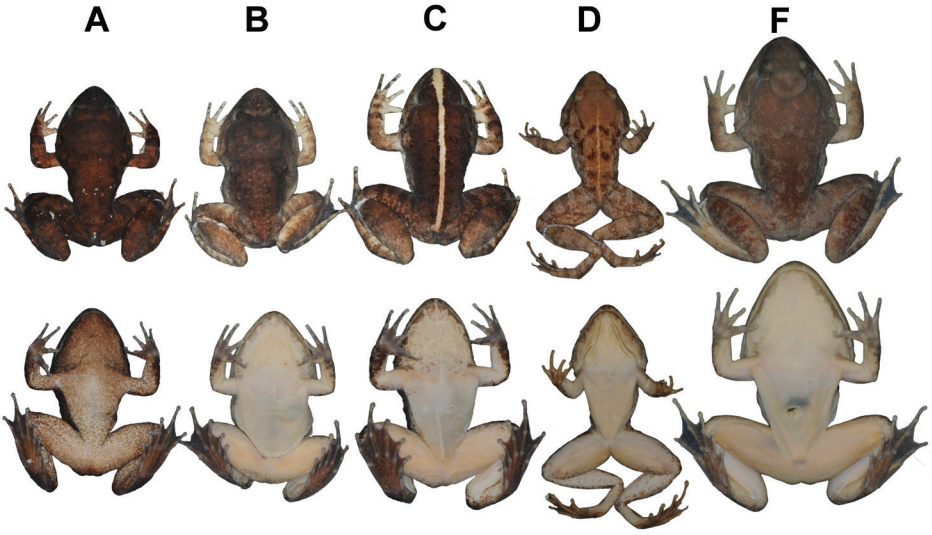

Figure 9. Comparisons of males of four similar, caruncle-bearing species of *Limnonectes* in preservative: Dorsal (above) and ventral (below) views of **A** *L. savan* sp. nov. holotype male (NCSM 76288) **B** *L. dabanus* (MVZ 258200) with high-profiled caruncle from Ratanakiri Province, Cambodia **C** *L. dabanus* (MVZ 258202) with low-profiled caruncle from Ratanakiri Province, Cambodia **D** *L. macrognathus* (FMNH 174526) from Nakhon Si Thammarat Province, Thailand **E** *L. gyldenstolpei* topotype (ZMKU AM 01143) from Lampang Province, Thailand.

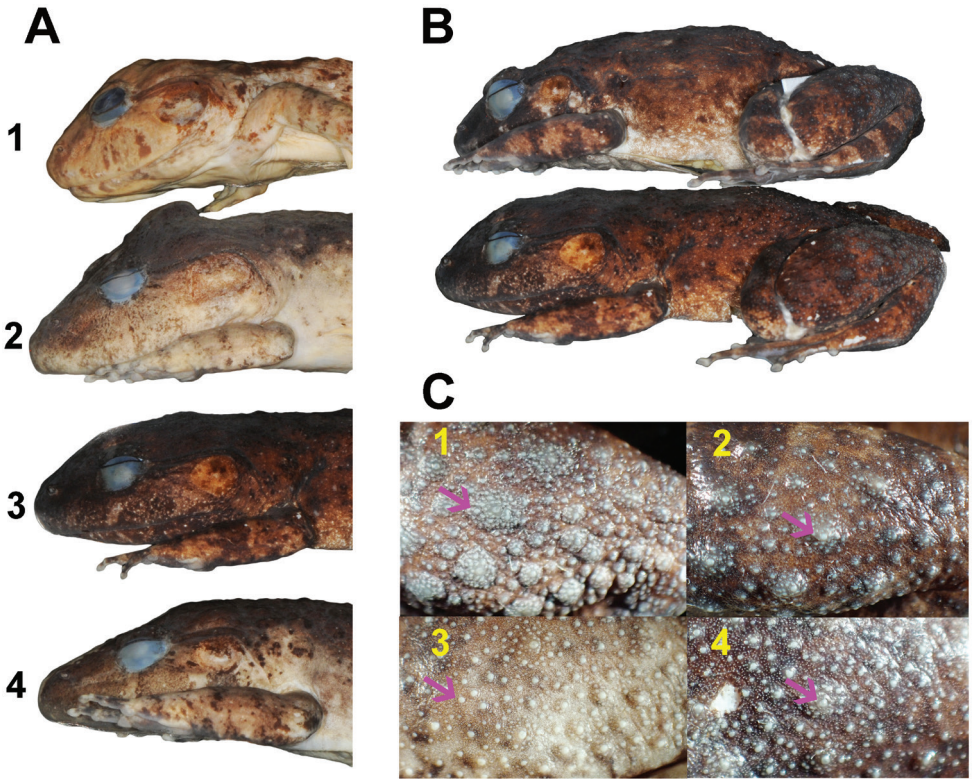

Figure 10. Comparisons of *Limnonectes dabanus* and *L. savan* sp. nov. in preservative **A** lateral view of head of males **A1** *L. macrognathus* (FMNH 174526) from Nakhon Si Thammarat Province, Thailand; **A2** *L. dabanus* (MVZ 258200) with high-profiled caruncle from Ratanakiri Province, Cambodia **A3** *L. savan* sp. nov. holotype (NCSM 76288) **A4** *L. dabanus* (MVZ 258202) with low-profiled caruncle from Ratanakiri Province, Cambodia **B** lateral body view of *L. savan* sp. nov. illustrating flank: paratype female (NCSM 76300) above; holotype male (NCSM 76288) below **C** dorsoposterior views of thigh illustrating tubercles (arrows) of **C1** *L. savan* sp. nov. holotype male (NCSM 76288) **C2** *L. savan* sp. nov. paratype female (NCSM 76300) **C3** *L. dabanus* male (MVZ 258200) from Ratanakiri Province, Cambodia **C4** *L. dabanus* female (MVZ 258235) from Ratanakiri Province, Cambodia.

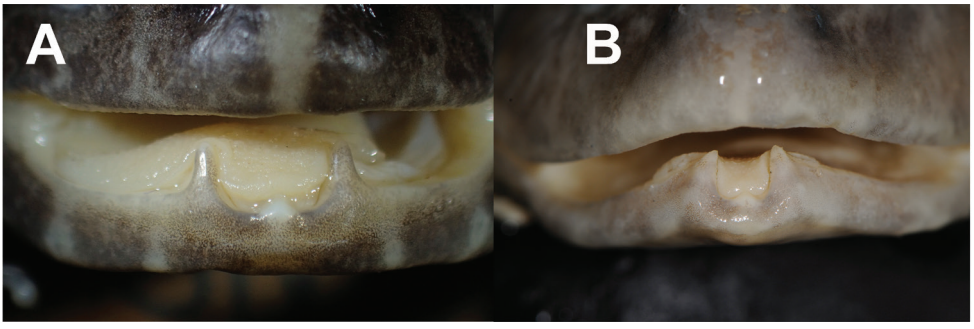

Figure 11. Comparisons of adult male odontoid processes in **A** *L. savan* sp. nov. (NUOL 01153) from Champasak Province, Laos, and **B** *L. dabanus* (NCSM 80375) from Binh Thuan Province, Vietnam.

Discussion

New species of *Limnonectes* continue to be discovered and described in mainland Southeast Asia (e.g. Matsui et al. 2010; McLeod et al. 2012; Aowphol et al. 2015; Pham et al. 2018; Phimmachak et al. 2018), and the description of *L. savan* brings the number of named, caruncle-bearing *Limnonectes* species to six. Additional fieldwork is needed to clarify the geographic distribution of the new species, in particular, any co-occurrence with the morphologically-similar (and, potentially, sister taxon) *L. dabanus* in southern Laos.

This study found that *L. savan* is phylogenetically related to the caruncle-bearing species *L. dabanus*, *L. gyldenstolpei*, and *L. lauhachindai* (Fig. 1), but the exact relationships among those species remained unresolved owing to a lack of statistical support (Fig. 1). Ohler and Dubois (1999) recognized *Elachyglossa* Andersson, 1916 at the subgenus rank for eight species of *Limnonectes*, including *L. dabanus*, *L. gyldenstolpei* (the subgenerotype species), and *L. lauhachindai*, the three closest relatives to *L. savan* (Fig. 1). Lambertz et al. (2014) restricted the subgenus *Elachyglossa* to the four caruncle-bearing species of *Limnonectes* that were recognized at the time (*L. dabanus*, *L. gyldenstolpei*, *L. macrognathus*, and *L. plicatellus*), but they did not study the caruncle-lacking species *L. hascheanus* (Stoliczka, 1870), *L. limborgi* (Sclater, 1892), and *L. doriae* (Boulenger, 1887) that render the caruncle-bearing species to be non-monophyletic (Fig. 1; Aowphol et al. 2015; Phimmachak et al. 2018). Hence, we are confident in placing *L. savan* in the subgenus *Elachyglossa*, but recognize that determining the full taxonomic content of the subgenus requires additional study. The generation of a larger (ideally, multi-locus) molecular dataset would likely resolve the sister relationship of *L. savan* and the conflicting hypotheses of relationships among the caruncle-bearing *Limnonectes* species that have been generated in recent studies (Lambertz et al. 2014; Aowphol et al. 2015; Phimmachak et al. 2018), including the taxonomic content of the subgenus *Elachyglossa*.

Finally, the taxonomic identity of the Lao-endemic *L. khammonensis*, known only from the female holotype specimen taken near Ban Na Pe ("Napé; Smith 1929) in Bolikhamxay Province, ca. 125 air-km north of the northernmost known locality of *L. savan* in Khammouan Province, Laos, needs to be resolved. It is clear on the basis of adult female morphology that *L. khammonensis* is not conspecific with *L. savan*. However, the lack of known males precludes knowing if *L. khammonensis* also bears a caruncle, and might be phylogenetically closely related to *L. savan*. Fieldwork at the type locality of *L. khammonensis* to obtain additional material of this taxon is warranted to facilitate future biodiversity research on *Limnonectes* in the region.

Acknowledgments

Fieldwork in Laos was conducted with permission of the Ministry of Agriculture and Forestry, Vientiane, Laos; Bounnhot Namsena, Deputy Head of the Forestry Section, Savannakhet Province; and Phonekham Sayasombath, District Governor of Vilabouli District. Fieldwork in Thailand was conducted under the auspices of the

Thailand Natural History Museum, the National Research Council of Thailand, and the head of Phu Jong-Na Yoi National Park. The Wildlife Conservation Society Laos Program, Lane Xang Minerals Ltd. (Sepon), and MMG Ltd. (Sepon) provided invaluable logistical support. Chatchay Chuechat, Derin Henderson, and Singthong Sanvixay assisted with fieldwork. David Kizirian and Lauren Vonnahme (AMNH), Barry Clarke and David Gower (NHMUK), Jens Vindum and Lauren Scheinberg (CAS), Alan Resetar (FMNH), Annemarie Ohler (MNHN), Jim McGuire and Carol Spencer (MVZ), Carolyn Kovach and Mark Hutchinson (SAMA), and Anchalee Aowphol (ZMKU) kindly provided access to specimens and tissues in their care. Jeff Streicher, George Zug, and Jennifer Sheridan provided photographs of NHMUK specimens. David McLeod and Jiang Jianping improved the manuscript. This research was funded by consulting agreements from Lane Xang Minerals Ltd. (Sepon) and MMG Ltd. (Sepon) to the Wildlife Conservation Society Laos Program, a consulting agreement from the Wildlife Conservation Association (WCA), the National Geographic Society (grants 6247-98 and WW-236R-17), the John D. and Catherine T. MacArthur Foundation (grant 03-75621 to the Field Museum of Natural History and grant 92482-0 to the North Carolina Museum of Natural Sciences), the US National Science Foundation (grant DEB-1145922), a Professional Development Grant from the World Wildlife Fund's Russell E. Train Education for Nature Program to SP, a US-ASEAN Fulbright Scholarship to SP, and the Partnerships for Enhanced Engagement in Research (PEER) Science program (grant PGA-2000003545), which is a partnership between the US Agency for International Development (USAID) and the US National Science Foundation.

References

Altig R, McDiarmid RW (1999) Body plan: development and morphology. In: McDiarmid RW, Altig R (Eds) Tadpoles: The Biology of Anuran Larvae, University of Chicago Press, Chicago and London, 24–51.

Andersson LG (1916) Zoological results of the Swedish zoological expeditions to Siam 1911–1912 and 1914. 3. Batrachians. Kungliga Svenska Vetenskapsakademiens Handlingar 55: 13–17.

Aowphol A, Rujirawan A, Taksintum W, Chuaynkern Y, Stuart BL (2015) A new caruncle-bearing *Limnonectes* (Anura: Dicroglossidae) from northeastern Thailand. Zootaxa 3956: 258–270. https://doi.org/10.11646/zootaxa.3956.2.6

Boulenger GA (1887) An account of the reptiles and batrachians obtained in Tenasserim by M. L. Fea, of the Genoa Civic Museum. Annali del Museo civico di storia naturale di Genova, Ser. 2, 5: 474–486.

Boulenger GA (1917) Descriptions of new frogs of the genus *Rana*. Annals and Magazine of Natural History, Series 8, 20: 413–418. https://doi.org/10.1080/00222931709487029

Boulenger GA (1920) A monograph of the South Asian, Papuan, Melanesian and Australian frogs of the genus *Rana*. Records of the Indian Museum 20: 1–226. https://doi.org/10.5962/bhl.title.12471

Chan-ard T (2003) A Photographic Guide to Amphibians in Thailand. Darnsutha Press Co., Bangkok, 175 pp.

Chen L., Murphy RW, Lathrop A, Ngo A, Orlov NL, Ho CT, Somorjai ILM (2005) Taxonomic chaos in Asian ranid frogs: an initial phylogenetic resolution. Herpetological Journal 15: 231–243.

Darriba D, Taboada GL, Doallo R, Posada D (2012) jModelTest 2: more models, new heuristics and parallel computing. Nature Methods 9: 772. https://doi.org/10.1038/nmeth.2109

Delorme M, Dubois A, Kosuch J, Vences M (2004) Molecular phylogenetic relationships of *Lankanectes corrugatus* from Sri Lanka: endemism of South Asian frogs and the concept of monophyly in phylogenetic studies. Alytes 22: 53–64.

Emerson SB, Inger RF, Iskandar D (2000) Molecular systematics and biogeography of the fanged frogs of Southeast Asia. Molecular Phylogenetics and Evolution 16: 131–142. https://doi.org/10.1006/mpev.2000.0778

Evans BJ, Brown RM, McGuire JA, Supriatna J, Andayani N, Diesmos A, Iskandar D, Melnick DJ, Cannatella DC (2003) Phylogenetics of fanged frogs: testing biogeographical hypotheses at the interface of the Asian and Australian faunal zones. Systematic Biology 52: 794–819. https://doi.org/10.1080/10635150390251063

Fitzinger LJFJ (1843) Systema Reptilium. Fasciculus Primus. Amblygossae. Braumüller et Seidel, Vindobonae, 3 pp.

Frost DR (2019) Amphibian Species of the World: an Online Reference. Version 6.0. American Museum of Natural History, New York, USA. http://research.amnh.org/vz/herpetology/amphibia/ [Last accessed 10 January 2019].

Frost DR, Grant T, Faivovich J, Bain RH, Haas A, Haddad CFB, de Sá RO, Channing A, Wilkinson M, Donnellan SC, Raxworthy CJ, Campbell JA, Blotto BL, Moler P, Drewes RC, Nussbaum RA, Lynch JD, Green DM, Wheeler WC (2006) The amphibian tree of life. Bulletin of the American Museum of Natural History 297: 1–370. https://doi.org/10.1206/0003-0090(2006)297[0001:TATOL]2.0.CO;2

Gosner KL (1960) A simplified table for staging anuran embryos and larvae with notes on identification. Herpetologica 16: 183–190.

Grosjean S, Ohler A, Chuaynkern Y, Cruaud C, Hassanin A (2015) Improving biodiversity assessment of anuran amphibians using DNA barcoding of tadpoles. Case studies from Southeast Asia. Comptes Rendus Biologies 338: 351–361. https://doi.org/10.1016/j.crvi.2015.03.015

Hasan M, Islam MM, Khan MMR, Igawa T, Alam MS, Djong HT, Kurniawan N, Joshy H, Sen YH, Belabut DM, Kurabayashi A, Kuramoto M, Sumida M (2014) Genetic divergences of South and Southeast Asian frogs: a case study of several taxa based on 16S ribosomal RNA gene data with notes on the generic name *Fejervarya*. Turkish Journal of Zoology 38: 389–411. https://doi.org/10.3906/zoo-1308-36

Inger RF, Stuart BL (2010) Systematics of *Limnonectes* (*Taylorana*) Dubois. Current Herpetology 29: 51–68. https://doi.org/10.3105/018.029.0201

Katoh K, Standley DM (2013) MAFFT Multiple Sequence Alignment software version 7: improvements in performance and stability. Molecular Biology and Evolution 30: 772–780. https://doi.org/10.1093/molbev/mst010

Köhler J., Jansen M, Rodríguez A, Kok PJR, Toledo LF, Emmrich M, Glaw F, Haddad CFB, Rödel M.-O., Vences M (2017) The use of bioacoustics in anuran taxonomy: theory, terminology, methods and recommendations for best practice. Zootaxa 4251: 1–124. https://doi.org/10.11646/zootaxa.4251.1.1

Lambertz M, Hartmann T, Walsh S, Geissler P, McLeod DS (2014) Anatomy, histology, and systematic implications of the head ornamentation in the males of four species of *Limnonectes* (Anura: Dicroglossidae). Zoological Journal of the Linnean Society 172: 117–132. https://doi.org/10.1111/zoj.12171

Liu ZQ, Wang YQ, Su B (2005) The mitochondrial genome organization of the rice frog, *Fejervarya limnocharis* (Amphibia: Anura): a new gene order in the vertebrate mtDNA. Gene 346: 145–151. https://doi.org/10.1016/j.gene.2004.10.013

McLeod DS, Kelly JK, Barley A (2012) "Same-same but different": another new species of the *Limnonectes kuhlii* complex from Thailand (Anura: Dicroglossidae). Russian Journal of Herpetology 19: 261–274.

Matsui M, Panha S, Khonsue W, Kuraishi N (2010) Two new species of the "*kuhlii*" complex of the genus *Limnonectes* from Thailand (Anura: Dicroglossidae). Zootaxa 2615: 1–22. https://doi.org/10.11646/zootaxa.2615.1.1

Matsui M, Nishikawa K (2014) Description of a new species of *Limnonectes* from Sarawak, Malaysian Borneo (Dicroglossidae, Anura). Current Herpetology 33: 135–147. https://doi.org/10.5358/hsj.33.135

Matsui M, Nishikawa K, Eto K (2014) A new burrow-utilising fanged frog from Sarawak, East Malaysia (Anura: Dicroglossidae). Raffles Bulletin of Zoology 62: 679–687.

Moriarty EC, Cannatella DC (2004). Phylogenetic relationships of the North American chorus frogs (*Pseudacris*: Hylidae). Molecular Phylogenetics and Evolution 30: 409–420. https://doi.org/10.1016/S1055-7903(03)00186-6

Oaks JR, Sukumaran J, Esselstyn JA, Linkem CW, Siler CD, Holder MT, Brown RM (2013) Evidence for climate-driven diversification? A caution for interpreting ABC inferences of simultaneous historical events. Evolution 67: 991–1010. https://doi.org/10.1111/j.1558-5646.2012.01840.x

Ohler A, Dubois A (1999) The identity of *Elachyglossa gyldenstolpei* Andersson, 1916 (Amphibia, Ranidae), with comments on some aspects of statistical taxonomy. Zoologica Scripta 28: 269–279. https://doi.org/10.1046/j.1463-6409.1999.00002.x

Palumbi SR (1996) Nucleic acids II: the polymerase chain reaction. In Hillis DM, Moritz C, Mable BK (Eds) Molecular Systematics. Second edition. Sinauer Associates, Inc., Sunderland, 205–247.

Pham CT, Le MD, Ngo HT, Ziegler T, Nguyen TQ (2018) A new species of *Limnonectes* (Amphibia: Anura: Dicroglossidae) from Vietnam. Zootaxa 4508: 115–130. https://doi.org/10.11646/zootaxa.4508.1.7

Phimmachak S., Sivongxay N, Seateun S, Yodthong S, Rujirawan A, Neang T, Aowphol A, Stuart BL (2018) A new *Limnonectes* (Anura: Dicroglossidae) from southern Laos. Zootaxa 4375: 325–340. https://doi.org/10.11646/zootaxa.4375.3.2

Pyron RA, Wiens JJ (2011) A large-scale phylogeny of Amphibia including over 2800 species, and a revised classification of extant frogs, salamanders, and caecilians. Molecular Phylogenetics and Evolution 61: 543–583. https://doi.org/10.1016/j.ympev.2011.06.012

Rambaut A, Suchard MA, Xie D, Drummond AJ (2014) Tracer v1.6. http://beast.bio.ed.ac.uk/Tracer

Ronquist F., Teslenko M, van der Mark P, Ayres DL, Darling A, Höhna S, Larget B, Liu L, Suchard MA, Huelsenbeck JP (2012) MrBayes 3.2: efficient Bayesian phylogenetic inference and model choice across a large model spaces. Systematic Biology 61: 1–4. https://doi.org/10.1093/sysbio/sys029

Rowley JJL, Le DTT, Hoang HD, Altig R (2014) The breeding behaviour, advertisement call and tadpole of *Limnonectes dabanus* (Anura: Dicroglossidae). Zootaxa 3881: 195–200. https://doi.org/10.11646/zootaxa.3881.2.8

Sabaj-Pérez MH (2016) Standard Symbolic Codes for Institutional Resource Collections in Herpetology and Ichthyology: an Online Reference. Version 6.5. American Society of Ichthyologists and Herpetologists, Washington, DC, USA. http://www.asih.org/ [Last accessed 10 January 2019].

Sclater WL (1892) On some specimens of frogs in the Indian Museum, Calcutta, with descriptions of several new species. Proceedings of the Zoological Society of London 1892: 341–348.

Simmons JE (2015) Herpetological collecting and collections management. Society for the Study of Amphibians and Reptiles Herpetological Circular 42: 1–191.

Smith, MA (1922) The frogs allied to *Rana doriae*. The Journal of the Natural History Society of Siam 4: 215–229.

Smith MA (1929) Descriptions of a new skink from Christmas Island and a new frog from Annam. Annals and Magazine of Natural History, Series 10, 3: 294–297. https://doi.org/10.1080/00222932908672972

Stoliczka F (1870) Observations on some Indian and Malayan Amphibia and Reptilia. Journal of the Asiatic Society of Bengal 39: 134–228. https://doi.org/10.1080/00222937008696209

Stoliczka F (1873) Notes on some species of Malayan Amphibia and Reptilia. Journal of the Asiatic Society of Bengal 42: 111–126.

Stuart BL, Sok K, Neang T (2006) A collection of amphibians and reptiles from hilly eastern Cambodia. Raffles Bulletin of Zoology 54: 129–155.

Swofford DL (2003) PAUP*: Phylogenetic Analysis Using Parsimony *(and Other Methods). Version 4. Sinauer Associates, Sunderland.

Taylor EH (1962) The amphibian fauna of Thailand. The University of Kansas Science Bulletin 43: 265–599. https://doi.org/10.5962/bhl.part.13347

Zhang JF, Nie LW, Wang Y, Hu LL (2009) The complete mitochondrial genome of the large-headed frog, *Limnonectes bannaensis* (Amphibia: Anura), and a novel gene organization in the vertebrate mtDNA. Gene 442: 119–127. https://doi.org/10.1016/j.gene.2009.04.018

Zhou Y, Zhang, JY, Zheng RQ, Yu BG, Yang G (2009) Complete nucleotide sequence and gene organization of the mitochondrial genome of *Paa spinosa* (Anura: Ranoidae (*sic*)). Gene 447: 86–96. https://doi.org/10.1016/j.gene.2009.07.009

Supplementary material 1

Appendix 1. Comparative specimens examined

Authors: Somphouthone Phimmachak, Stephen J. Richards, Niane Sivongxay, Sengvilay Seateun, Yodchaiy Chuaynkern, Sunchai Makchai, Hannah E. Som, Bryan L. Stuart

Data type: species data

Copyright notice: This dataset is made available under the Open Database License (http://opendatacommons.org/licenses/odbl/1.0/). The Open Database License (ODbL) is a license agreement intended to allow users to freely share, modify, and use this Dataset while maintaining this same freedom for others, provided that the original source and author(s) are credited.

Link: https://doi.org/10.3897/zookeys.846.33200.suppl1

Supplementary material 2

Appendix 2. *Fejervarya*, *Quasipaa*, and *Limnonectes* 16S sequences used in the phylogenetic analysis

Authors: Somphouthone Phimmachak, Stephen J. Richards, Niane Sivongxay, Sengvilay Seateun, Yodchaiy Chuaynkern, Sunchai Makchai, Hannah E. Som, Bryan L. Stuart

Data type: phylogenetic analysis

Copyright notice: This dataset is made available under the Open Database License (http://opendatacommons.org/licenses/odbl/1.0/). The Open Database License (ODbL) is a license agreement intended to allow users to freely share, modify, and use this Dataset while maintaining this same freedom for others, provided that the original source and author(s) are credited.

Link: https://doi.org/10.3897/zookeys.846.33200.suppl2